SYNTHESIS AND CHARACTERIZATION OF DNA OLIGOMERS CONTAINING THE PROMUTAGEN O4-ALKYLTHYMINE

BY

GARRY WALTER BUCHKO, B.Sc., M.Sc.

A Thesis
Submitted to the Faculty of Graduate Studies
in Partial Fulfilment of the Requirements
for the Degree of

DOCTOR OF PHILOSOPHY

Department of Chemistry
University of Manitoba
Winnipeg, Manitoba

ISBN 0-315-71871-4

SYNTHESIS AND CHARACTERIZATION OF DNA OLIGOMERS CONTAINING THE PROMUTAGEN O4-ALKYLTHYMINE

BY

GARRY WALTER BUCHKO

A thesis submitted to the Faculty of Graduate Studies of
the University of Manitoba in partial fulfillment of the requirements
of the degree of

DOCTOR OF PHILOSOPHY

ABSTRACT

O4-Alkylthymine, r^4T, is a promutagen. To better understand the biological consequences of the O4-alkylation of DNA, the following oligomers were synthesized using a modified phosphotriester approach: 1) $d(r^4TpT)$ with r equal to methyl (m), ethyl (e), propyl (p), butyl (b), isopropyl (i), and isobutyl (ib); 2) $d(r^4TpX)$ with r equal to e and i and X equal to adenine (A), guanine (G), cytosine (C) and thymine (T); 3) $d(Xpr^4T)$ with r equal to e or i and X equal to A and T; 4) $d(Tpr^4TpT)$ with r equal to m, e, and i; 5) $d(Ape^4TpA)$ and $d(ApTpA)$; 6) $d(e^4TpApe^4TpA)$, $d(e^4TpApTpA)$, and $d(TpApe^4TpA)$. These molecules were identified and characterized by ^1H and ^{13}C Nuclear Magnetic Resonance (NMR), Fast Atom Bombardment mass spectrometry (FAB-MS), and circular dichroism (CD).

The $[M - H]^-$ ions as well as some $[2M - H]^-$ aggregates are easily detected by FAB-MS operating in the negative ion mode, illustrating the usefulness of the technique for the structural analysis of DNA oligomers containing a r^4T base. The CD spectra of the alkylated oligomers differed from their non-alkylated counterparts, with the most prominent difference being a reduction in the magnitude of the negative CD band. In the ^1H NMR spectra, the α-methylene protons of the O4-ethyl, -propyl, -butyl, and -isobutyl groups, and the methyl protons of the O4-isopropyl group are magnetically nonequivalent at most temperatures, in contrast to the corresponding nucleosides, r^4dT. Furthermore, the chemical shift difference of these α-methylene protons (Δδ) usually increased with decreasing temperature and this has been related to intramolecular base stacking. Vicinal proton coupling constants of the deoxyribose sugars reveal a shift towards the 3'-endo *conformation of a r^4dT unit relative to a dT unit. The 3'*-endo *population of the r^4dT sugar generally increased with decreasing temperature, the magnitude of the increase depending on the sequence. Variable temperature profiles of base protons suggest that O4-alkylation does not disrupt base stacking in terms of the formation of right handed/*χ-anti *stacks.*

TABLE OF CONTENTS

ACKNOWLEDGEMENTS

I would like to acknowledge the support of the following: Mr. K. Marat and T. Wolowiec for assistance in acquiring the NMR spectra; Dr. D. Hughes and Mr. B. Sayer at McMaster University for acquiring some 500 MHz spectra; Mr. W. Buchannon for acquiring the FAB-MS spectra; Dr. J.B. Westmore and Mr. F. Lafortune for discussions regarding the FAB-MS spectra; Dr. C.C. Bigelow for access to his CD spectropolarimeter and Dr. B. Reid for help in acquiring the CD spectra; Mr. A. Silvanovich for assistance with the HPLC system; Dr. H.W. Duckworth for allowing me access to his laboratory; Drs. A.S. Secco and J.L. Charlton for discussions; Dr. P.C. Loewen for being on my advisory committee; Dr. L.-S. Kan for serving as my external examiner; Mr. R. Sebastian for help with computer programs; and the University of Manitoba for a Manitoba Graduate Studies Fellowship for myself.

Special acknowledge goes out to: Dr. K.L. Sadana for helping me get started with the organic syntheses; Dr. F.E. Hruska, not only for the financial aspects, but for putting up with my many "bad habits", (running, finger tapping, pencil tapping, toe tapping, coin juggling, and so on); my mom, for doing my laundry and making the porogies; my dad, for encouraging me to finish quickly ("you're still going to school!"); and lastly, the Vancouver Canucks, whose style of play was always an inspiration (especially in the summers).

LIST OF FIGURES

LIST OF TABLES

LIST OF ABBREVIATIONS

1D	*one dimensional*
2D	*two dimensional*
A	*absorbance*
A	*adenine*
b	n-*butyl*
c	*concentration*
C	*cytosine*
^{13}C	*carbon*
CD	*circular dichroism*
COSY	*2D correlated spectroscopy*
δ	*chemical shift*
$\Delta\delta$	*difference in chemical shifts (downfield - upfield)*
$\Delta\delta^{o}$	*high temperture* δ *- low temperature* δ
dA	*deoxyadenosine*
dC	*deoxycytidine*
dG	*deoxyguanosine*
DCFC	*dry column flash chromatography*
DMF	*dimethylformamide*
DMTCl	*4,4'-dimethoxytrityl chloride*
DNA	*deoxyribonucleic acid*
D_2O	*deuterium oxide*
dT	*deoxythymidine*
dr^4T	*deoxy-O4-alkylthymidine*
DSS	*4,4-dimethyl-4-silapentan-1-sulfonate*
ε	*molar extinction coefficient*
e	*ethyl*
EDTA	*ethylenediaminetetraacetic acid*
EtOAc	*ethyl acetate*
EtOH	*ethanol*
f	*fraction*
FAB-MS	*fast atom bombardment mass spectrometry*
FID	*free induction decay*
g	*gauche*
G	*guanine*
^1H	*proton*
HD	*homo-decoupling*
HG	*homogated decoupling*
HPLC	*high performance liquid chromatography*
H_R	*pro-R*
H_S	*pro-S*
Hz	*Hertz*
i	*isopropyl*
ib	*isobutyl*
IsoOH	*isopropanol*
J	*coupling constant*
λ	*wavelength*
m	*methyl*
m^6G	*O6-methylguanine*
m^7G	*N7-methylguanine*
MeCl	*methylene chloride*
MeOH	*methanol*
MST	*1-(2-mesitylenesulfonyl)-tetrazole*
N	*3'*-endo
NaOR	*sodium alkoxide*

NMR	*nuclear magnetic resonance*
NOE	*nuclear Overhauser enhancement*
NOESY	*2D nuclear Overhauser enhancement spectroscopy*
p	n-*propyl*
P	*phase angle*
^{31}P	*phosphorus*
ppm	*parts per million*
PU	*purine*
PY	*pyrimidine*
r^2C	*O2-alkylcytosine*
RELAY	*2D relay coherence transfer spectroscopy*
RNA	*ribonucleic acid*
r^2T	*O2-alkylthymine*
r^4T	*O4-alkylthymine*
Σ	$^3J_{5'\text{-}P} + {}^3J_{5''\text{-}P}$
$\Sigma 1'$	$^3J_{1'\text{-}2'} + {}^3J_{1'\text{-}2''}$
S	2'-endo
Θ	*torsion angle*
$[\Theta]$	*molar ellipticity*
τ_m	*amplitude of pucker*
t	*trans*
T	*thymine*
TBAF	tetra-*N-butylammonium fluoride*
TBDMSCl	tetra-*butyldimethylsilyl chloride*
TEA	*triethylamine*
THF	*tetrahydrofuran*
tlc	*thin layer chromatography*
T_m	*melting temperature*
TOCSY	*2D total correlation spectroscopy*
TPSCL	*triisopropylsulfonyl chloride*
U	*uracil*
UV	*ultra-violet*

*NOTE: **Bold** molecules in text indicate compounds that were synthesized or analyzed by G.W.B..*

SYNTHESIS AND CHARACTERIZATION OF DNA OLIGOMERS CONTAINING THE PROMUTAGEN O4-ALKYLTHYMIDINE

CHAPTER 1

INTRODUCTION. DNA Alkylation

Alkylating agents are known to play a role in mutagenesis and carcinogenesis (Singer and Grunberger, 1983; Saffhill et al., *1985). These compounds can modify all oxygens and nitrogens in DNA except the nitrogen involved in the glycosidic bond and the oxygens involved in the phosphodiester bonds (Lindahl* et al., *1988). Such compounds are widely found in the environment from both natural and unnatural sources (Bartsch and Montesano, 1984). Some are even generated in the digestive system (Singer and Grunberger, 1983). Among the most potent are N-nitroso compounds like N-methyl-N-nitrosourea, N-ethyl-N-nitrosourea, N-methyl-N'-nitro-N-nitrosoguanidine, and N-ethyl-N'-nitro-N-nitrosoguanidine (Singer, 1975).*

One adduct of DNA alkylation is O4-alkylthymine (r^4T) (Figure 1.1). This residue in DNA leads to mutations, specifically A:T--->G:C transitions (Preston et al., *1986), and is recognized by DNA repair enzymes. To explain, and perhaps predict, the biological consequences of O4-alkylation of thymine on DNA, it is useful to study the effects that this residue has on DNA structure. Short oligodeoxynucleotides have been used as models for conformational investigations of DNA (Patel,* et al., *1982; Kearns, 1984). Nuclear magnetic resonance (NMR) and circular dichroism (CD) spectroscopy can then be used to probe the conformation and dynamics of DNA at the individual base level (Cantor* et al., *1970; Kondo* et al., *1970; Cheng and Sarma, 1977). It is this approach that was used to explore the structural effects of O4-alkylation of thymine on DNA (Chapters 3 and 4) after developing a synthetic strategy to make the molecules (Chapter 2). However, before describing these results a short review of DNA alkylation will be useful.*

In DNA, in vivo *and* in vitro, *the majority of the total alkylation found after exposure to a N-nitroso agent is on the phosphates (Sun and Singer, 1975; Singer and Fraenkel-Conrat, 1975). This finding is not surprising since the phosphate backbone is the most exposed surface of the DNA double helix. Furthermore, the alkyl phosphotriesters are the most persistent type of DNA alkylation (Brent* et al., *1988) with a half life of over a*

month (Den Engelese et al., *1986). Enzymatic studies with synthetic DNA oligomers containing alkylated phosphates show gene transcription to be affected* in vitro *(Miller* et al., *1982). However, NMR and CD studies with synthetic DNA oligomers containing a single site of phosphate alkylation suggest that phosphate alkylation does not disrupt the intrastrand Watson-Crick hydrogen bonds of the double helix but does slightly perturb the helix backbone (Pramanik and Kan, 1987; Kan* et al., *1987; Lawrence* et al., *1987). In conclusion, alkyl phosphotriesters appear to hinder enzymes that bind to the surface of DNA but probably are not promutagenic as no miscoding has yet been demonstrated (Jensen, 1986).*

The first, and most prominent, nucleoside adduct isolated after treatment with N-nitroso and other alkylating agents was N7-methylguanine (m^7G). This residue was originally believed to be an important carcinogenic adduct. However, later studies indicated that ethylating agents produced the same carcinogenic effects in animals as methylating agents with the isolation of <u>less</u> *N7-ethylguanine (Singer, 1975). m^7G was eventually shown not to lead to miscoding (Abbott and Saffhill, 1979). Instead it is now believed that the high mutagenic and carcinogenic activity of the N-nitroso compounds is due to their ability to alkylate oxygens on DNA bases (Loveless, 1969; Singer, 1976).*

The first oxygen alkylated base isolated was O6-methylguanine (m^6G) (Friedman et al., *1965). O6-Alkylation of dG deprotonates the N1 position, destroying a hydrogen donating site in a normal Watson-Crick G:C base pair. Furthermore, an alkyl group at the O6 position of G may sterically hinder the formation of other potential hydrogen bonds as suggested by X-ray crystallographic studies with monomers which indicate that the O6-alkyl group is in the* syn-*periplanar position (Figure 1.1) (Parthasarathy and Fridey, 1986; Yamagata* et al., *1988).* In vitro *studies suggest that r^6G acts as an A, base pairing preferably with T (or U) (Abbott and Saffhill, 1979; Gerchman and Ludlum. 1973). This contrasts with solution state optical melting studies with self-complementary dodecamers involving m^6G opposite to A, C, G or T. The lowest melting temperature (T_m) was noted for*

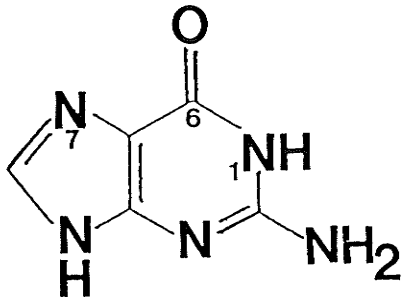

guanine

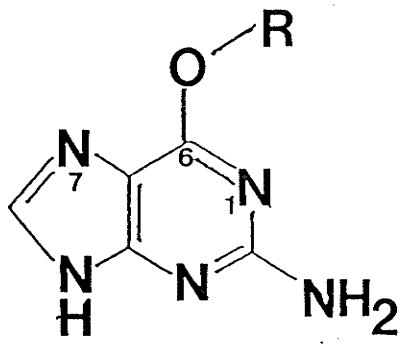

O6-alkylguanine (r^6G)

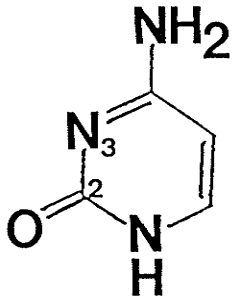

cytosine

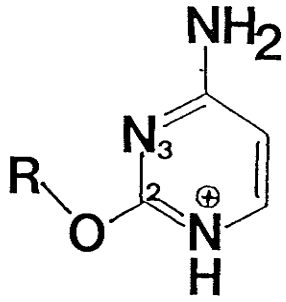

O2-alkylcytosine (r^2C)

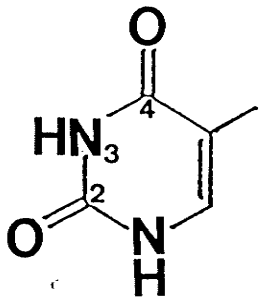

thymine

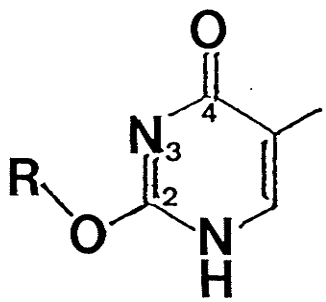

O2-alkylthymine (r^2T)

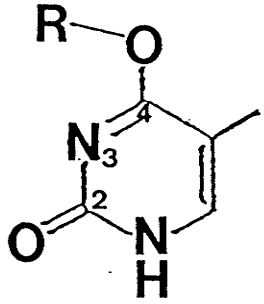

O4-alkylthymine (r^4T)

Figure 1.1: Chemical structures of some major bases and their O-alkylated derivatives. The R groups are oriented in the syn-periplanar position relative to N1 (guanine) and N3 (thymine and cytosine).

the sequence with an m^6G:T base pair and the highest for the sequence with a m^6G:C base pair (Gaffney et al., *1984), in line with later NMR studies of these sequences (Patel* et al., *1986), recent molecular orbital calculations (Yamagata,* et al., *1988) and other optical melting studies (Gaffney and Jones, 1989). This suggests that factors other than base-pair stabilization energies are involved in replication (Loeb and Kunkel, 1982; Parthasarathy and Fridey, 1986; Loeb* et al., *1986).*

Eventually O4-methylthymidine (m^4dT) was detected in vivo *(Lawley* et al., *1973) followed by O2-alkyluridine, O4-alkyluridine (Kusmierek and Singer, 1976), O2-alkyldeoxy-cytidine (r^2dC), and O2-alkylthymidine (r^2dT) (Singer, 1976). The major reason for the delays in isolating the O-alkylpyrimidines is the lability of the alkyl group, in acid and in base (Singer* et al., *1978; Allore* et al., *1983). Of the O-alkylated deoxypyrimidines, r^2dC is the most unstable (Singer* et al., *1978) because not only is the alkyl group labile but the glycosidic bond is prone to cleavage. In fact the latter event, depyrimidination, may be the major reason for the mutagenic properties of r^2dC as abasic sites lead to deletion mutations (Singer, 1976).*

Alkylation at the O2 position of thymidine results in the deprotonation of N1 and the introduction of a bulky group on the base (Figure 1.1). The only X-ray crystallographic study on such a molecule, O2-isopropylthymidine (i^2dT), shows that the alkyl group is in a syn-*periplanar position in relation to N3 (Birnbaum* et al., *1988) where it might interfere with base pairing. The glycosidic bond of r^2dT is not as susceptible to cleavage as the same bond in r^2dC, allowing the synthesis of r^2dTTPs and their incorporation by DNA Polymerase I into the alternating polymer poly [d(A-T)] (Singer* et al., *1989). This incorporation shows that DNA Polymerase I can bind and utilize r^2dTTPs and suggests that stable r^2T:A base pairs can form. Further experiments with these poly [d(A-T)] sequences, containing significant amount of r^2dTs in place of dT, have shown higher levels of dGTP incorporation during replication by DNA Polymerase I. This implies that r^2T:G base pairs are forming*

(Singer et al., *1989).*

The remaining O-alkylated deoxypyrimidine possible is O4-alkylthymidine, the adduct which is the subject of this thesis. Alkylation at the O4 position removes a proton involved in hydrogen bonding at N3 (Figure 1.1). Crystal structures of O4-methylthymidine (Brennan et al., *1986) and O4-ethylthymidine (e^4dT) (Birnbaum et al., 1986) reveal a number of important features. First, the alkyl group is in the* syn*-periplanar position in both molecules where it could interfere with hydrogen bonding. Second, O4-alkylation produces "cytosine-like" conjugation of the ring. However, the electron density at O2 is lower than in cytosine, possibly decreasing its ability to act as a hydrogen bond acceptor. Last, the deoxyribose moiety adopts unusual puckers for nucleosides, ${}_1T^2$ for m^4dT and ${}^3T_2$ for e^4dT.*

Numerous studies have been conducted to determine the biological consequences of the presence of O4-alkylthymines in DNA. Highlights of these studies are: 1) DNA Polymerase I will substitute O4-methyl dTTP, O4-ethyl dTTP, and O4-isopropyl dTTP for dTTP during the replication of the alternating polymer poly [d(A-T)] (Singer et al., *1986). Furthermore, the rate of synthesis decreases as the size of the alkyl group increases (methyl > ethyl > isopropyl), and the amount of r^4dTTP incorporated is greater than r^2dTTP (Singer* et al., *1989); 2) d(A-T) Polymers, with a number of r^4dTs substituted for dT, were shown to misincorporate a higher percentage of dGTP when replicated. Such an event would lead to an A:T--->G:C transition upon the next cycle of replication as illustrated in Figure 1.2.*

However, the strongest evidence for the promutagenic potential of O4-alkylated thymine comes from site-directed mutagenesis experiments conducted by Preston et al. *(1986). A single m^4dT residue was introduced into a specific site of a bacteriophage gene. The phage were then transfected into* E. *coli spheroplasts deficient in methylthymine-DNA methyltransferase (ada^-), an enzyme that repairs O4-alkylated DNA, where they yielded a 10-fold increase in mutant phage progeny in comparison to ada^+* E. *coli cells. Twenty mutant plaques were then individually isolated and the DNA in the region of the m^4dT adduct*

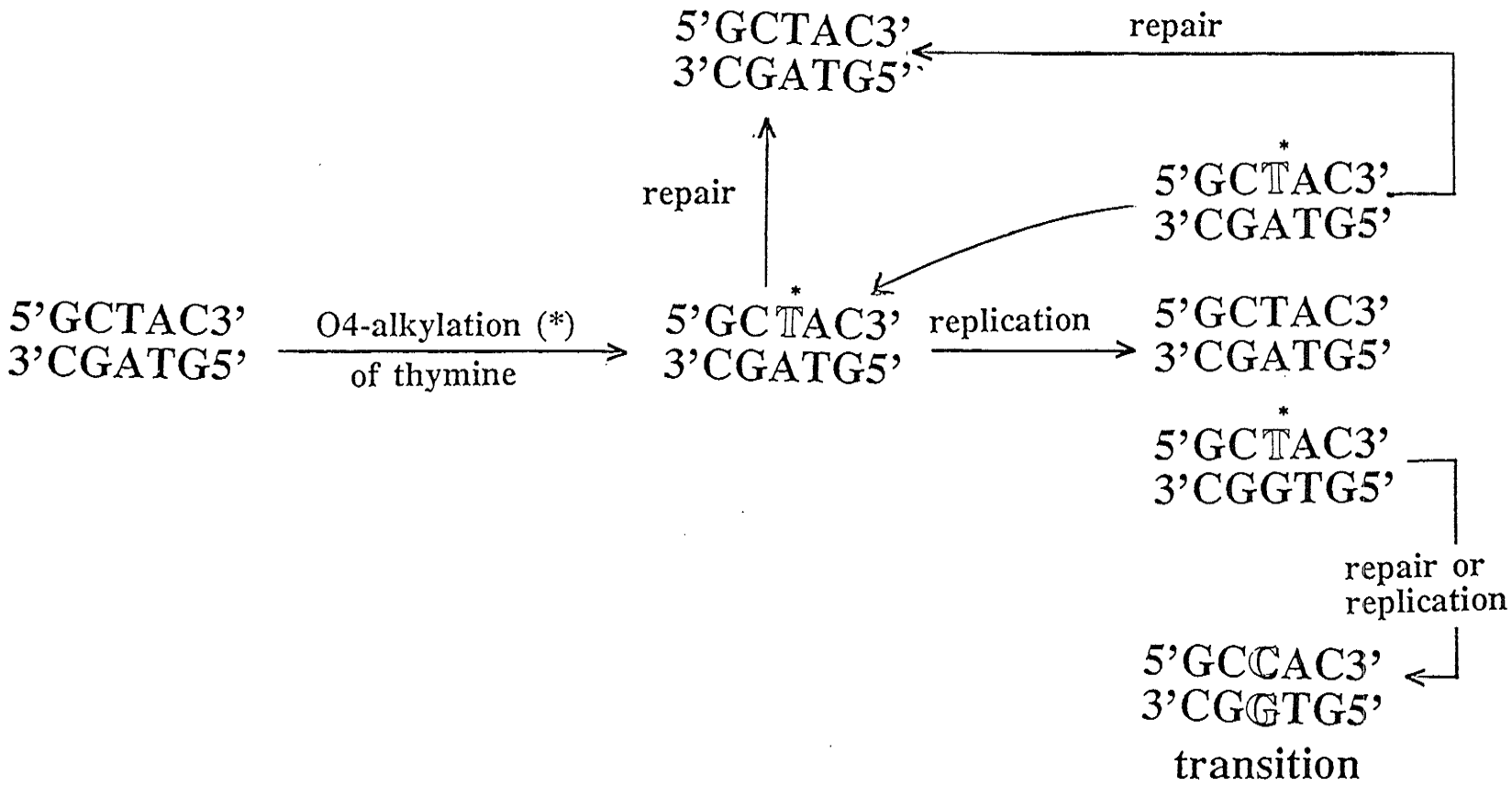

Figure 1.2: Possible pathway for the generation of an A:T-->G:C transition after O4- (or O2-) alkylation of thymine (*).

sequenced. All of these mutant phage contained an A:T --->G:C transition at the site of the original introduction of the m^4dT.

DNA oligomers containing an O4-methylthymidine have been synthesised (Li et al., *1987) to study the effect of alkylation on base pairing and on the double helical conformation. Four self-complementary dodecamers containing a G:T, G:m^4T, A:C, and A:m^4T base pair at identical positions were prepared for this study (Kalnik* et al., *1988a, b). Two-dimensional (2-D) nuclear Overhauser enhancement spectra (NOESY) of the exchangeable and nonexchangeable proton resonances were used to characterize the oligomers. The data suggested that G:T formed a wobble base pair with two hydrogen bonds (Figure 1.3A) whose protons resonate at 10.57 and 11.98 ppm (10°C). Comparatively, the only imino proton present in G:m^4T, G(H1), resonates at 8.67 ppm. The upfield position of this lone signal suggests that G(H1) is not involved in hydrogen bonding and hence, the only hydrogen bond possible is between the H2 amino position of G and the O2 carbonyl of m^4T as illustrated in Figure 1.3B. Nuclear Overhauser enhancement (NOE) experiments suggest that the alkyl group is in the* syn-*periplanar position, as in crystalline m^4dT (Brennan* et al., *1986), where it would prohibit the G imino proton from participating in hydrogen bonding. The weakness of this base pairing led Kalnik* et al., *1988a, to suggest that the enhanced lipophilicity of m^4T may be a more important factor in m^4dT's promutagenic nature than its base pairing potential because the enzymes involved in DNA replication play a large role in maintaining its fidelity and the active site containing the DNA template is in a hydrophobic cleft. Therefore the lipophilicity of the base pair may be more important than the energy of base pairing in determining the type of base pair formed (Loeb and Kunkel, 1982; Loeb* et al., *1986). Alternatively, the enzyme binding cleft appears to snugly fit correct base pairs (Petruska* et al., *1988) hence, when an unusual base is present in DNA, the preferred base pair produced during* in vivo *and* in vitro *replication may be the one which most closely resembles a Watson-Crick alignment (Eritja* et al., *1986; Fazakerley* et al., *1987;*

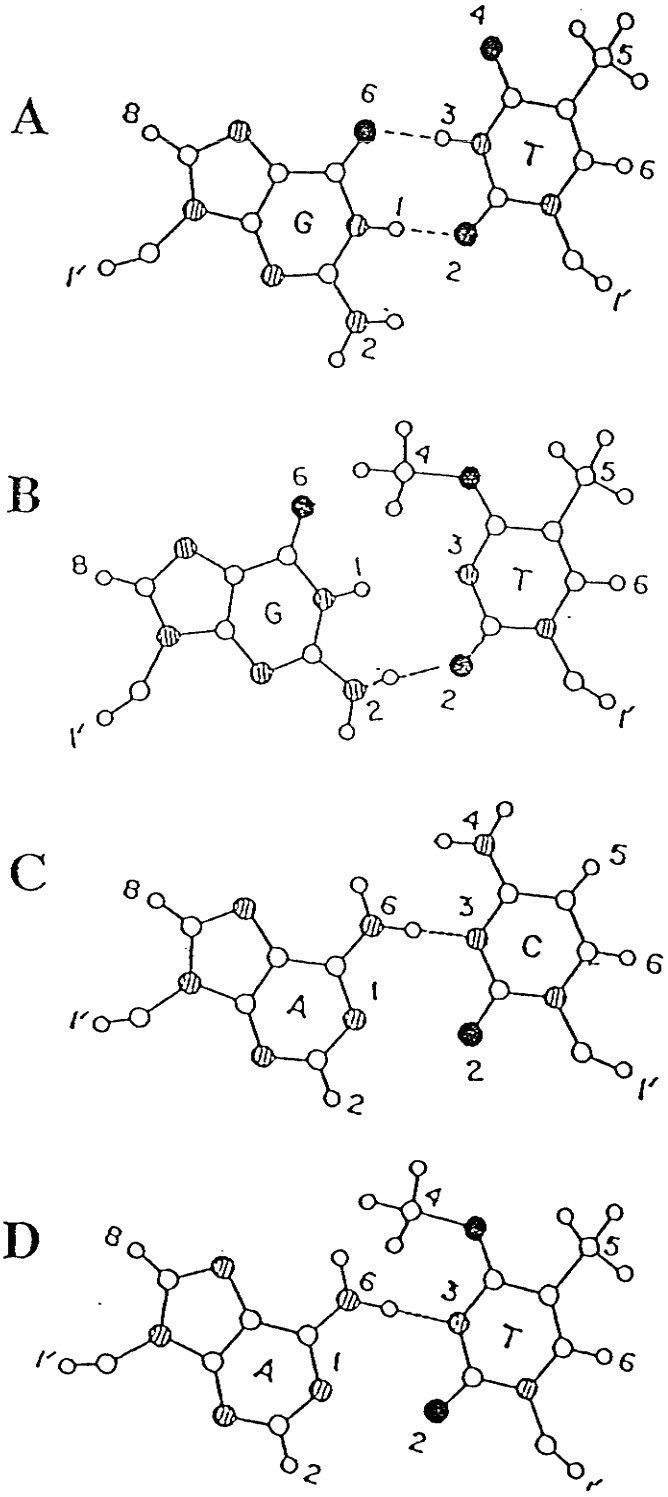

Figure 1.3: A) G:T wobble base pair, B) G:m⁴T base pair, C) A:C wobble base pair, and D) A:m⁴T base pair (Kalnik et al., *1988a, 1988b).*

Gaffney and Jones, 1989; Kalnik et al., *1989a, b).*

In contrast, the two other self-complementary dodecamers, one with an A:C and the other with an A:m⁴T base pair, both behave identically to each other over temperature. That is, identical NMR experiments, as conducted for the G:T and G:m⁴T sequences, produced similar spectra for the A:C and A:m⁴T complexes. Their data correlated with other studies (Patel et al., *1984; Hunter* et al., *1986) that suggest an A:C wobble of the type illustrated in Figure 1.3C. All the NMR data were recorded at pH 5.5 to 6.0 and there is evidence to suggest that A(N1) is protonated and a second hydrogen bond to the pyrimidine O2 carbonyl exists (not shown in Figure 1.3C). A:m⁴T appears to base pair similarly, as illustrated in Figure 1.3D, with the alkyl group located in the* syn-*periplanar position. A stable A:m⁴T base pair would explain why the presence of m⁴dT does not always lead to a transition mutation because most of the time replicating enzymes place an A opposite the m⁴T. The formation of these A:m⁴T base pairs retards strand elongation during replication (Preston* et al., *1986; Singer* et al., *1989). Stable A:m⁴T base pairs might also aid in explaining data with poly [d(A-T)] double helixes containing r⁴dT lesions which show no distortions in their helical structure as measured by UV methods (Singer* et al., *1986).*

This thesis describes the synthesis of DNA oligomers containing an O4-alkylthymidine with the goal of better understanding the effects of O4-alkylation on DNA structure. An emphasis has been placed on the construction of oligomers containing an O4-ethyl- and O4-isopropylthymidine, since these adducts may be more mutagenic (Singer et al., *1986; Richardson* et al., *1987). All molecules were purified by high performance liquid chromatography (HPLC) and identified by NMR and fast atom bombardment mass spectrometry (FAB-MS). NMR, and to a lesser extent CD, was then used to probe the conformation of these molecules in solution. Series of different sequences were synthesised to study the effect of various factors. For example, alkyl group size was examined in the sets d(r⁴TpT) and d(Tpr⁴TpT). Sequence effects were compared in the sets d(r⁴TpT) and d(Tpr⁴T), d(e⁴TpA)*

and ***d(Ape^{4}T)****, and* ***d(e^{4}TpApe^{4}TpA)****,* ***d(e^{4}TpApTpA)****, and* ***d(TpApe^{4}TpA)****. Neighbouring base effects were probed in the sets* ***r^{4}TpX*** *(with X = A, G, C, and T, r = ethyl and isopropyl), and* ***d(Ape^{4}TpA)*** *and* ***d(Tpe^{4}TpT)****. All these alkylated DNA fragments were also compared to their non-alkylated counterparts. Conformational differences may be important because sequence specific features of DNA structure may play a role in gene regulation (Rich* et al., *1984). Furthermore, such sequence specific changes may be vital for the recognition of damaged DNA segments by repair enzymes (Topal* et al., *1986).*

CHAPTER 2

***EXPERIMENTAL**. Synthesis, Purification, Sample Preparation, and Fast-Atom Bombardment Mass Spectrometry of DNA Oligomers Containing O4-Alkylthymine*

2.1 INTRODUCTION:

Oligonucleotide synthesis has been extensively reviewed (Zhdanov and Zhenodarova, 1975; Reese, 1978; Crockett, 1983) and the technology now exists to fully automate the operation (Caruthers, 1985). The major requirement is the protection of the most nucleophilic sites: the base amino groups (G, C, and A), the hydroxy functions on the sugar (3' and 5') and phosphate group. By coupling selectively protected nucleotidyl and nucleosidyl fragments, protected oligonucleotides of defined sequence can be obtained. Removal of all the protecting groups (deblocking or deprotecting) yields DNA.

Because of the vulnerability of the O4-alkyl group to both acidic and basic conditions (Singer et al., *1978; Allore* et al., *1983), a synthetic strategy favourable to the survival of the O4-alkyl group had to be developed. During the course of our work, Li* et al. *(1987) reported the first synthesis of a DNA oligomer containing an O4-methylthymidine in quantities sufficient for NMR studies. More recently Borowy-Borowski and Chambers (1989) have reported the synthesis of oligomers containing other alkyl groups at the O4 position of thymine. However, the procedures we developed differ from those of these two groups in many aspects, in terms of protecting groups, condensing reagents, and deprotection conditions.*

In general, for an oligomer larger than two nucleotides, we make use of 4,4'-dimethoxytrityl to protect the 5'-hydroxyl group, acetyl to protect the amino and 3'-hydroxyl groups, and 2-chlorophenyl to protect the phosphate. The alkyl group is introduced at the O4 position of thymine via a C4 linked 1,2,4-triazole moiety (Divakar and Reese, 1982) which can easily be displaced by sodium alkoxide (NaOR) before condensation. After coupling it was possible to exchange alkyl groups through displacement with a different sodium alkoxide during deprotection. Couplings were performed using triisopropylsulfonyl chloride (TPSCl) and tetrazole as condensing reagents, with synthesis occurring one nucleotidyl unit at a time starting with the 3'-nucleotide of the oligomer. Deprotection

involved treatment with 1) $ZnBr_2$, 2) oximate, and 3) NaOR. Crude purification by descending paper chromatography was followed by more thorough purification with reverse phase HPLC. A detailed description of all the synthetic procedures follows.

2.2 TECHNIQUES:

2.2.1 Dry Column Flash Chromatography (DCFC): For a typical 10 mmol synthesis, a 150 mL cylindrical sinter of medium porosity was packed with silica gel (Terochem, Flash Chromatography Type). Unlike standard flash chromatography, in DCFC suction instead of pressure is used to pass solvent through the gel (Harwood, 1985). The material to be purified was first evenly placed on the column using the minimal amount of solvent. A gradient of MeOH in MeCl was often used to elute the products, with tlc employed to monitor their passage off the column. The only other solvents regularly used were 100% ethyl acetate (EtOAc) or 100% ether.

2.2.2 Thin Layer Chromatography (tlc): Whatman polyester-backed silica gel plates (250 μm layer) were cut into 6.3 cm long strips of various widths and stored under Drierite (anhydrous $CaSO_4$) prior to use. Spotted plates were developed in screw-capped jars 8 cm high and 5 cm in diameter.

2.2.3 Paper Chromatography: Whatman #1 sheets (46 x 57 cm) cut in half along the long axis were used for descending paper chromatography. These sheets were folded at one end at 2 and 6 cm (to allow placement in the chromatography chamber) with a horizontal line drawn at the 10 cm point. The product, dissolved in the minimal amount of solvent (H_2O plus a drop of MeOH or EtOH), was streaked across the 10 cm mark using open end capillary tubes (0.8 - 1.10 x 100 mm, Kimax-51). The organic phase of a 5:4:1 (H_2O:n-butanol:EtOH, v:v:v) mixture was used to elute the material (solvent B'). Approximately 20 hours were necessary for the solvent front to reach the end of the paper. Once complete, the papers were removed from the tank, air dried in a fumehood, and examined under UV light. The UV absorbing areas were marked, cut out, and eluted with H_2O. The UV spectra of these samples were then recorded on a Unicam SP 800B ultraviolet spectrophotometer to identify promising fractions. These were lyophilized and prepared for either ^1H NMR or HPLC. Note that HPLC purification was dramatically facilitated by prior

paper chromatography.

2.2.4 High Performance Liquid Chromatography (HPLC): It was necessary to purify all oligomers by HPLC before any detailed NMR, CD, or mass spectral analysis could be conducted. A Perkin-Elmer system containing a Sigma 15 Chromatography Data Station, a LC Terminal, a LC-85 Spectrophotometric Detector, and a Series 4 Liquid Chromatograph was used. Both analytical (25 x 0.46 cm, CSC) and semi-preparative (25 x 1.0 cm, CSC and Phenomenex) reverse phase (5 μm Hypersil-ODS) columns were employed with a pre-column (5 μm Hypersil-ODS, 4.5 x 0.46 cm, CSC). HPLC grade MeOH (Fisher) filtered through 0.20 μm nylon filters (Whatman) was the organic solvent. The aqueous phase was a 0.1 M ammonium acetate (HPLC grade, Fisher) buffer adjusted to pH = 6.0 with acetic acid. This buffer was passed though a 0.45 μm cellulose nitrate filter (Whatman) prior to use. All material injected on to the column first passed though a 0.45 μm syringe filter (Spartan-3).

The standard gradient employed during the first purification attempt on a semi-preparative column is listed in Figure 2.1. When an analytical column was used the same gradient was employed except for a 50% reduction in the flow rates. Table 2.1 lists the retention times of some oligomers separated in this manner. If the retention times between the peaks of interest and the impurities were less than 1.5 minutes, then the gradient would be modified appropriately to meet this criterion. A sample chromatogram is reproduced in Figure 2.2 which illustrates the sensitivity of this tool for separating the oligomers ***d(e⁴TpApTpA)*** *and* ***d(TpApe⁴TpA)****. These two tetramers have identical base compositions but different base sequences yet have retention times that differ by 2 minutes when the standard gradient is used; a time sufficient for isolation.*

2.2.5 NMR Sample Preparations: After HPLC purification the solvents were removed by rotary evaporation and lyophilized three times from H_2O (approximately 1 mL volumes) to remove the ammonium acetate. The samples were then lyophilized twice from 99.8% D_2O

TIME	Flow Rate	%Aqueous	%MeOH
eq.	1.0	100	00
1.0	2.0	100	00
90.0	2.0	10	90
4.0	2.0	10	90
10.0	2.0	100	00
2.0	1.0	100	00

-TIME = minutes
-flow rate = mL/minute.
-all gradients are linear.

Figure 2.1: Standard gradient used for the hplc purification of the DNA fragments after deprotection. Organic phase: MeOH. Aqueous phase: 0.1 M ammonium acetate (pH = 6.0).

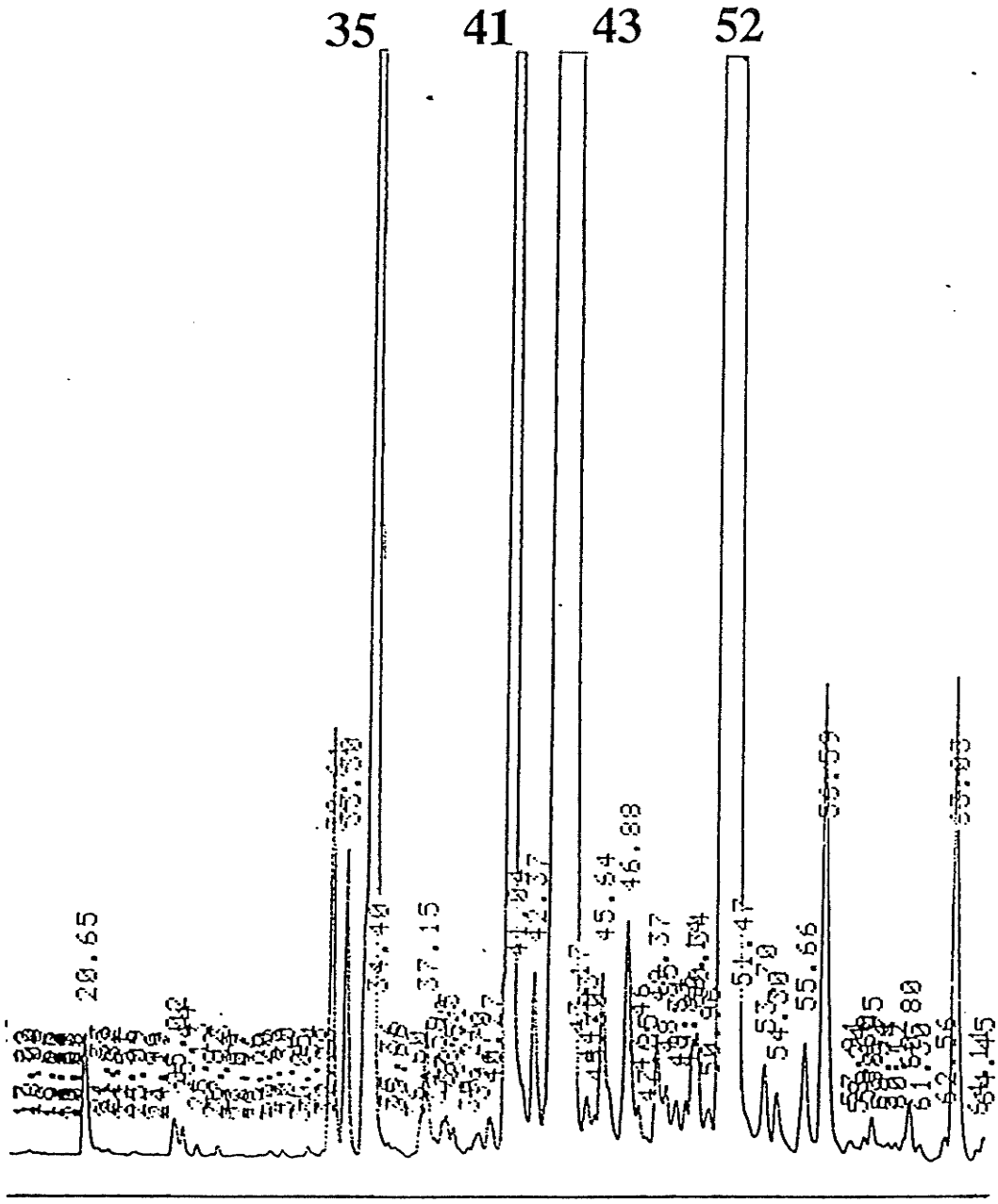

Figure 2.2: Hplc chromatogram obtained in the purification of d(e⁴TpApe⁴TpA) using the standard gradient. The bold numbers above the peaks are retention times in minutes: (35) d(ApTpA), (41) d(TpApe⁴TpA), (43) d(e⁴TpApTpA), (52) d(e⁴TpApe⁴TpA).

Table 2.1. HPLC retention times of some DNA oligomers using the standard gradient.[a]

Molecule	*retention time*
dT·	28
5'dTMP·	17
d(m^{4}TpT)	43
d(i^{4}TpT)	58
d(i^{4}TpT3'Ac)	64
d(Tpi^{4}T)	56
d(TpTpT)·	35
d(Tpm^{4}TpT)	40
d(Tpe^{4}TpT)	46
d(Tpi^{4}TpT)	58
d(Tpi^{4}TpT3'Ac)	65
d(m^{4}Tpc)	41
d(e^{4}TpC)	48
d(i^{4}TpC)	56
d(TpA)·	30
d(e^{4}TpA)	50
d(i^{4}TpA)	57
d(TpApe^{4}TpA)	41
d(e^{4}TpApTpA)	43
d(e^{4}TpApe^{4}TpA)	52

[a]Standard gradient (See Figure 2.1) with retention times in minutes.

(approximately 0.5 mL volumes, Aldrich). For ^1H NMR, 0.5 mL of NMR buffer was used to dissolve the sample before transfer to a Wilmad 528 PP (5 mm od) NMR tube. This buffer consisted of 0.1 M NaCl, 0.01 M sodium phosphate ($Na_2HPO_4 \cdot 7H_2O$) and 0.001M ethylenediaminetetraacetic acid (EDTA) adjusted to pH 7.0 with HCl (Hare et al.*; 1986, Buchko, 1986). Prior to sample preparation a small volume of the NMR buffer was measured out and lyophilized twice from 99.8% D_2O. The precipitates were then resuspended in an original volume of 99.9% D_2O (Aldrich) and added to the DNA sample. A trace of* tert*-butanol was included as an internal reference (1.231 ppm relative to sodium 4,4-dimethyl-4-silapentan-1-sulfonate (DSS), (Kan,* et al.*, 1974, Bell* et al.*, 1981). When conducting ^{13}C NMR the ^1H NMR sample would be lyophilized inside the NMR tube, redissolved in 0.4 mL of 99.9% D_2O and 10 μL of dry dioxane added as an internal reference (67.86 ppm relative to tetramethylsilane). For a detailed description of the conditions of the NMR experiments please see the Appendix.*

2.2.6 Fast Atom Bombardment Mass Spectrometry (FAB-MS): Negative ion FAB-MS spectra were obtained for many of the precursors and deprotected oligomers on a VG 7070E-HF spectrometer (glycerol matrix, 8-ke V xenon atoms). Most of the major ions have been assigned and are reported after the synthesis descriptions as m/z(relative intensity, [ionic species]$^+$). The relative intensities are normalized to the most intense peak in the spectrum.

2.2.7 Circular Dichroism (CD): CD spectra were obtained on a Jasco J-500A spectropolarimeter using a cell equipped for temperature control with a water bath. This cell had a 0.5 cm path length and held 600 μL. Solution concentrations were in the 10^{-4} M range as determined by UV absorption methods (Borer, 1975) using a 100 μL aliquot from the CD cell.

2.2.8 Concentration Determination: The quantity of product used for the CD and NMR experiments was not sufficient for direct weighing and therefore it was necessary to use the Beer-Lambert law to obtain concentrations:

$$A = \varepsilon cl$$

where A = absorbance, ε = molar extinction coefficient (L/mole cm), c = concentration (moles/L), and l = path length (cm). This equation is widely used to determine the concentration of nucleic acids in solution (Young and Krugh, 1975; Klevit et al., *1986; Kalnik et al., 1988a). The difficulty with this approach is obtaining accurate values for ε. However, it is not a problem with the monomers because enough sample can usually be obtained to accurately determine the concentration and hence, ε. Singer* et al. *(1983) have reported an* ε_{max} *at 281 nm of 6,700 (L/mole cm) for* m^4dT *and 6,800 for* i^4dT. *The absorbance ratios (260:281) calculated in our laboratory are: 0.48,* m^4dT *and* e^4dT, *0.47, O4-propylthymidine (*p^4dT*), and 0.52, O4-isobutylthymidine (*ib^4dT*) and* i^4dT. *Assuming that ε for* e^4dT *and* p^4dT *are the same as for* m^4dT, *and ε for* ib^4dT *is the same as for* i^4dT, *then* ε_{260} *for* m^4dT, e^4dT, *and* p^4dT *is 3,200, and for* ib^4dT *and* i^4dT *it is 3,500.*

For the dimers containing an O4-alkylthymidine, ε_{260} *was estimated by adding the* ε_{260} *values for the monomers,* r^4dT *plus dG, dA, dT, or dC, and multipling this figure by 0.95. (The 0.95 is the average hypochomicity effect in going from the constituent monomers to the dimers as observed for the sixteen possible combinations with dG, dA, dT and dC.) For example,* ε_{260} *for* $d(i^4TpT)$ *(rounded off to the nearest hundred) was estimated as follows:*

$\varepsilon_{260}\ i^4dT = 3{,}500$, $\varepsilon_{260}\ dT = 8{,}700$,

$\varepsilon_{260}\ d(i^4TpT) = (3{,}500 + 8{,}700)(0.95) = 11{,}600.$

To estimate ε_{260} *for oligomers greater than two bases long, equations are employed that use the* ε_{260} *values for the monomers and dimers. One such equation, for oligonucleotide DpEpFpG...KpL, is:*

$\varepsilon_{DpEpFpG...KpL} = (\varepsilon_{DpE} + \varepsilon_{EpF...} + \varepsilon_{KpL}) - \varepsilon_E - \varepsilon_{F...} - \varepsilon_K$ *(Borer, 1975).*

For example, ε_{260} *for* $d(Ape^4TpA)$ *was calculated as follows:*

$\varepsilon_{260}\ d(Ape^4T) = \varepsilon_{260}\ d(e^4TpA) = (15{,}400 + 3{,}200)(0.95) = 17{,}700,$

$\varepsilon_{260}\ d(Ape^4TpA) = ((17{,}700 + 17{,}700) - 3{,}200) = 32{,}200.$

Using ε_{260} values generated in this manner, aliquots from the NMR tube (generally 20 μL) or CD cell (100 μL) were diluted and the absorbance measured at 260 nm on a Cary-219 Varian spectrophotometer to determine the concentrations. The accuracy of such calculations depends on the value of ε. Note that even using Borer's equation to calculate ε for non-alkylated oligomers, there is still error due to sequence dependent hypochromicity effects. For our NMR solutions accurate knowledge of the concentration is not critical because we only require a concentration range to determine if interstrand aggregation might be a problem. However, for the CD solutions, the concentration is important in determining the molar ellipticities [Θ]. Until ε for our O-alkylated oligomers are determined by other methods, the accuracy of our ε estimations for these molecules remains unknown and therefore, so does the accuracy of their [Θ]s.

2.3 REAGENTS:

All solvents were purchased from Fisher Scientific except where indicated otherwise.

2.3.1 0.3 M Oximate: p-Nitrobenzaldoxime (Sigma) (0.166 g, 1.0 mmol) and 1,1,3,3-N,N,N',N'-tetramethylguandinium (Aldrich) (0.11 mL, 0.88 mmol) were dissolved in 1 mL of dry dioxane and 1 mL of dry acetonitrile prior to use. One mL of this solution was sufficient to deprotect 30 to 60 mg of a fully protected dimer, trimer, or tetramer.

2.3.2 0.3 M tetra-*N-Butylammonium fluoride (TBAF): TBAF (Sigma) (40% w/w in H_2O) (20 mL, 30 mmol) was titrated to pH 7.0 with methanol (MeOH) diluted hydrofluoric acid (Fisher) using a pH-meter. Solvents were removed under vacuum, co-distilling with 1:1 (v:v) benzene:acetonitrile. The solid was placed in a desiccator containing phosphorus pentoxide (P_2O_5) (Fisher) under reduced pressure. After a minimum of two days the solid was resuspended in 100 mL of dry tetrahydrofuran (THF).*

2.3.3 1.0 M Zinc Bromide ($ZnBr_2$): $ZnBr_2$ (Sigma) (2.25 g, 1.0 mol) was dissolved in MeCl (8.5 mL) and isopropanol (IsoOH) (1.5 mL).

2.3.4 Dry Pyridine: Between 8 - 12 mL of chlorosulfonic acid (Matheson, Coleman, & Bell) was slowly added to 1.5 L of reagent grade pyridine. After a two hour reflux the pyridine was distilled into calcium hydride (CaH_2) (Fisher) and left overnight. In the morning the solution was distilled and stored under Linde type 3A molecular sieves (Matheson, Coleman & Bell).

2.3.5 Dry Ethanol (EtOH): Magnesium (Mallinckrodt Chemical Works) (5 g, 200 mmol) and iodine (0.5 g, 2.0 mmol) were added to 75 ml of absolute EtOH (Canadian Industrial Alcohols and Chemicals Limited) and warmed until a vigorous reaction occurred, sometimes assisted with carbon tetrachloride (CCl_4). The mixture was heated until all the magnesium had reacted and then an additional 1 L of absolute ethanol was added. The solution was refluxed for one hour and distilled.

Other alcohols required for alkylation were dried similarly.

2.3.6 Dry Triethylamine (TEA): 1.5 L of TEA was refluxed with CaH_2 (ca. 5 g) for over five hours, distilled, and stored under Linde type 4A molecular sieves.

2.3.7 Dry Methylene Chloride (MeCl): 1.5 L of MeCl sat over P_2O_5 overnight and was then decanted into another vessel and distilled into a flask containing potassium carbonate (K_2CO_3) (Fisher). After again standing overnight the MeCl was decanted into a storage vessel containing Linde type 3A molecular sieves.

2.3.8 Dry Acetonitrile (CH_3CN): 1.5 L of CH_3CN was refluxed over CaH_2 for three hours, distilled, and stored under Linde type 4A molecular sieves.

2.3.9 Dry Tetrahydrofuran (THF): Approximately 0.5 L of THF was refluxed over sodium metal and benzophenone. When the solution turned blue the desired quantity was distilled for immediate use (Perrin et al., *1980).*

2.4 PRECURSORS:

The numbering scheme for the precursors and some of their intermediates are listed in Figure 2.3.

*2.4.1 5'-O-*tert*-Butyldimethylsilythymidine (2): Synthesis followed Ogilvie's procedure (1973) with slight modifications regarding purification. Thymidine (1) (Sigma) (2.42 g, 10 mmol)* tert*-butyldimethlysilyl chloride (Aldrich and Sigma) (TBDMS) (1.66 g, 11 mmol), imidazole (Sigma) (1.50 g, 22 mmol), and dimethylformamide (Aldrich) (DMF) (10 ml) were stirred at room temperature for 2.5 hours. The reaction was monitored by tlc using EtOAc as the eluent where the 5',3'-di-O-*tert*-butyldimethylsilythymidine (3), a by-product, had a greater R_f than 2 (ca. 0.7 to 0.5) with unreacted 1 remaining near the baseline. The products, 2 and 3, were worked-up by precipitation in 1 L of distilled water followed by vacuum filtration through a Buchner funnel. The white solid was scraped off the filter paper and dissolved in the minimal amount of MeCl and purified by DCFC using EtOAc as the eluting solvent (65% average yield).*

UV: λ_{max} *= 267 nm (EtOH).*

*2.4.2 5'-O-*tert*-Butyldimethylsilyl-3'-acetylthymidine (4): Pyridine-dried but not purified 2 (3.55 g, 10 mmol), pyridine (12.5 mL), and acetic anhydride (Fisher) (2.0 mL, 20 mmol) were stirred together overnight. The reaction was monitored by tlc using ether as elutant where molecule 4 had a higher R_f than 2 but a lower one than 3. Work-up involved quenching the reaction with methanol (MeOH) (10 mL) and removing the solvents by co-distilling with toluene. Molecule 4 was generally used without further purification.*

*2.4.3 5'-O-*tert*-Butyldimethylsilyl-3'-acetyl-4-(1,2,4-triazol-1-yl)-thymidine (5): Synthesis followed the procedure of Divakar and Reese (1982). Acetonitrile dried 1,2,4-triazole (Sigma) (6.2 g, 90 mmol) was dissolved in 52 mL of acetonitrile. Phosphorus oxychloride (Aldrich) ($POCl_3$) (1.8 ml, 19.2 mmol) was added after cooling the solution in an ice bath and stirred for 15 minutes. Dry TEA (12 mL, 86 mmol) was then introduced over a 15 minute period*

1) $R_1 = H, R_2 = H, B = T$
2) $R_1 = TBDMS, R_2 = H, B = T$
3) $R_1 = R_2 = TBDMS, B = T$
4) $R_1 = TBDMS, R_2 = Ac, B = T$
5) $R_1 = TBDMS, R_2 = Ac, B = T^{Tz}$
6) $R_1 = TBDMS, R_2 = H, B = T^{O4e}$
7) $R_1 = TBDMS, R_2 = H, B = T^{O4m}$
8) $R_1 = TBDMS, R_2 = H, B = T^{O4i}$
9) $R_1 = TBDMS, R_2 = H, B = T^{O4p}$
10) $R_1 = TBDMS, R_2 = H, B = T^{O4b}$
11) $R_1 = TBDMS, R_2 = H, B = T^{O4ib}$
12) $R_1 = DMT, R_2 = H, B = T$
13) $R_1 = DMT, R_2 = DMT, B = T$
14) $R_1 = DMT, R_2 = Ac, B = T$
15) $R_1 = DMT, R_2 = H, B = T^{O4e}$
16) $R_1 = DMT, R_2 = H, B = TO^{4i}$
17) $R_1 = DMT, R_2 = Ac, B = T^{Tz}$
18) $R_1 = H, R_2 = Ac, B = T^{Tz}$
19) $R_1 = H, R_2 = H, B = T^{Tz}$
20) $R_1 = H, R_2 = Ac, B = T$
21) $R_1 = H, R_2 = H, B = A$
22) $R_1 = TBDMS, R_2 = H, B = A$
23) $R_1 = TBDMS, R_2 = Ac, B = A^{Ac}$
24) $R_1 = TBDMS, R_2 = Ac, B = A^{dAc}$
25) $R_1 = H, R_2 = Ac, B = A^{Ac}$
26) $R_1 = H, R_2 = Ac, B = A^{dAc}$
27) $R_1 = TBDMS, R_2 = H, B = A^{Bz}$
28) $R_1 = DMT, R_2 = H, B = A^{Bz}$
29) $R_1 = H, R_2 = H, B = G$
30) $R_1 = TBDMS, R_2 = H, B = G$
31) $R_1 = TBDMS, R_2 = Ac, B = G^{Ac}$
32) $R_1 = H, R_2 = Ac, B = G^{Ac}$
33) $R_1 = H, R_2 = H, B = C$
34) $R_1 = H, R_2 = Ac, B = C^{Ac}$

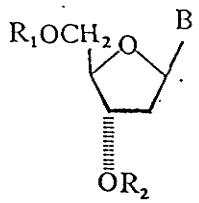

B = T = thymine
B = T^{Tz} = 4-(1,2,4-triazol-1-yl)-thymine
B = T^{O4e} = O4-ethylthymine
B = T^{O4m} = O4-methylthymine
B = T^{O4i} = O4-isopropylthymine
B = T^{O4p} = O4-propylthymine
B = T^{O4b} = O4-butylthymine
B = T^{O4ib} = O4-isobutylthymine
B = A = adenine
B = A^{Ac} = 6-N-acetyladenine
B = A^{dAc} = 6-N,N-diacetyladenine
B = A^{Bz} = 6-N-benzoyladenine
B = G = guanine
B = G^{Ac} = 2-N-acetylguanine
B = C = cytosine
B = C^{Ac} = 4-N-acetylcytosine

Figure 2.3: Numbering scheme for the precursors involved in the syntheses.

followed by molecule 4 (4.0 g, 10 mmol), suspended in 31 mL of acetonitrile, over a minimum of 30 minutes. After 10 minutes the ice was removed and the reaction left till morning. The product was detected by the EtOAc elution of a blue tlc band.

The work-up involved adding TEA (8.2 ml, 5.9 mmol) and water (2.2 mL, 12 mmol) to the reaction vessel. Solvents were removed after 10 minutes, the product dissolved in 50 mL of MeCl and an equal volumn of H_2O saturated, with sodium carbonate, was added. The organic layer was removed and the aqueous layer washed with an additional 40 mL of MeCl. The organic layers were combined and dried for 30 minutes with sodium sulphate (Fisher) (Na_2SO_4). The solvent was removed and the product purified, if necessary, by DCFC using EtOAc as the eluent.

UV: λ_{max} *= 326, 251 and 218 nm (EtOH).*

2.4.4 5'-O-tert-Butyldimethylsilyl-O4-ethylthymidine (6): Molecule 5 (4.5 g, 10 mmol) was dried, suspended in EtOH, and treated with 60 mmol of sodium ethoxide (0.3 M final concentration in EtOH) for 30 minutes at room temperature. The reaction was followed by the disappearance of the blue tlc band. The reaction was then worked up by neutralization with glacial acetic acid using Colorphast pH indicator sticks. The solvents were removed under vacuum and the material purified by DCFC using EtOAc as the eluent (Figure 2.4) (Buchko et al., *1989a).*

UV: λ_{max} *= 281 nm (EtOH).*

2.4.5 5'-O-tert-Butyldimethylsilyl-O4-alkylthymidine (7 - 11): Other O-alkyl groups were introduced to the C4 position, as described for 6, using the appropriate alcohol to prepare the alkoxide. As the chain length increased the time necessary for the displacement of the triazole group increased and therefore the propylation and butylation reactions were left overnight. While the isobutylation and isopropylation reactions were also left overnight, it was necessary to prepare these alkoxides by heating. Only the isopropylation reaction was heated continuously (ca. *40°C) to keep the isopropoxide in solution after addition of 5.*

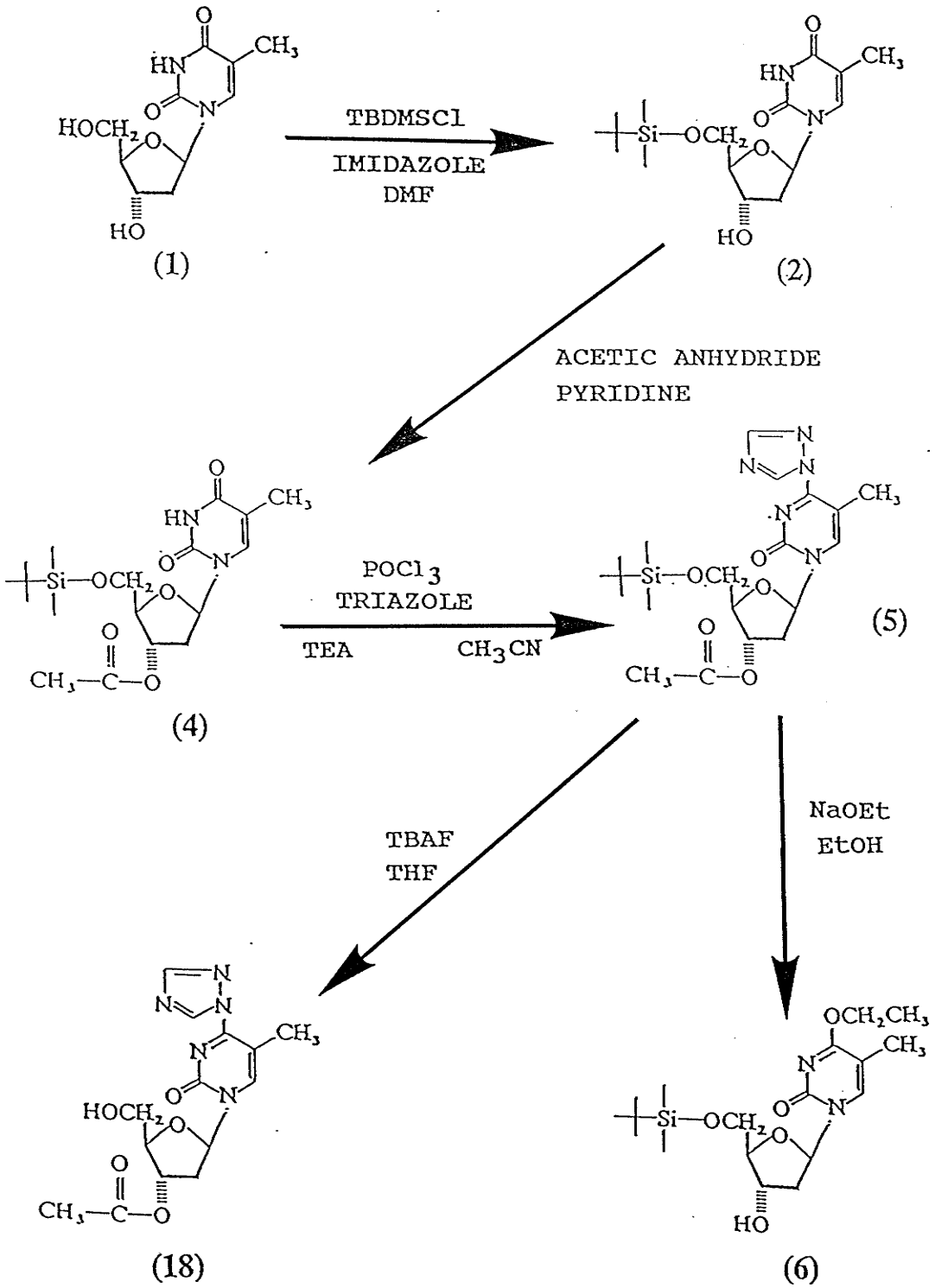

<u>Figure 2.4</u>: Strategy for the synthesis of 3'-acetyl-4-(1,2,4-triazol-1-yl)-thymidine (18) and 5'-O-tert-butyldimethylsilyl-O4-ethylthymidine (6).

2.4.6 5'-O-4,4'-Dimethoxytritylthymidine (12): Molecule 12 was prepared by stirring 1 (2.42 g, 10 mmol) and 4,4'-dimethoxytrityl chloride (Sigma) (DMTCl) (3.25 g, 10 mmol) in pyridine (25 ml) overnight (Schaller et al., *1963). The product, 12, had a tlc* R_f ca. *0.7 when developed in 9:1 MeCl:MeOH. The reaction was worked up by pouring the mixture into 600 mL of cold* H_2O *followed by extraction with MeCl (200 and 100 mL portions). The organic layer was dried over* Na_2SO_4 *before the solvent was removed by rotary evaporation (co-distilling with toluene). If 12 was to be used in a condensation it was purified by recrystallization in approximately 150 mL of benzene.*

2.4.7 5'-O-4,4'-Dimethoxytrityl-3-acetylthymidine (14): Molecule 14 was prepared as described for 4 except that 12 was substituted for 2. The product had a higher R_f *then the starting material* (ca. *0.8) when developed in 9:1 MeCl:MeOH.*

2.4.8 5'-O-4,4'-Dimethoxytrityl-3-acetyl-4-(1,2,4-triazoyl-1-yl)-thymidine (17): Molecule 17 was prepared as described for 5 with the substitution of 14 for 4.

2.4.9 5'-O-4,4'-Dimethoxytrityl-O4-ethylthymidine (15) and 5'-O-4,4'-dimethoxytrityl-O4-isopropylthymidine (16): Molecules 15 and 16 were prepared as described for 6 and 7 using 17 instead of 5.

2.4.10 3'-Acetyl-4-(1,2,4-triazol-1-yl)-thymidine (18): Two procedures were used to prepare 18 with #1 illustrated in Figure 2.4.

#1) Molecule 5 (4.5 g, 10 mmol) was dissolved in THF and stirred for 10 minutes with TBAF suspended in THF (16.7 ml, 10 mmol) to remove the silyl group (Corey and Venkateswarlu, 1972). (Cautionary note: longer treatment leads to a gradual removal of the C4 triazole group). The reaction was followed on tlc plates developed in EtOAc. The desilylated product had a R_f *that was about 0.1 smaller than the starting material. Dowex-50* (Na^+ *form) (Aldrich) was added, stirred for 15 minutes, and then filtered off. The product was immediately purified by DCFC using EtOAc (which also served to remove the THF). If a substantial amount of 19 was present it would be removed from 18 by DCFC using a*

gradient of MeOH in MeCl.

#2) Compound 17 (6.4 g, 10 mmol) was detritylated by the addition of 100 mL of 1.0 M zinc bromide ($ZnBr_2$) (8.5:1.5 MeCl:isopropanol v:v) (Kierzek et al., *1981). The reaction was followed on tlc plates developed first in ether then EtOAc. The product had a lower R_f than the starting material. The solvents were removed by rotary evaporation and the products redissolved in MeCl. This was washed with the minimal amount of H_2O to remove the $ZnBr_2$ (which was assumed to be complete when the color of the solution changed from red to an off-white). The organic layer was then dried over Na_2SO_4. The product was concentrated by removing some of the solvent and purified by DCFC using a gradient of MeOH in MeCl.*

2.4.11 3'-Acetylthymidine (20): Molecule 14 (5.9 g, 10 mmol) was treated with 1.0 M $ZnBr_2$ (100 mL, 100 mmol). The reaction was followed on tlc plates developed first in ether followed by EtOAc. The band for the detritylated product had a lower R_f than the starting material and failed to turn yellow upon heating. Molecule 20 was worked up and purified as described for 18 in procedure #2.

2.4.12 5'-O-tert-Butyldimethylsilyl-2'-deoxyadenosine (22): Pyridine-dried 2'-deoxyadenosine (21) (Sigma) (2.52 g, 10 mmol), TBDMSCl (1.66 g, 11 mmol), imidazole (1.5 g, 22 mmol) and DMF (10 mL) were stirred for 3 hours (Ogilvie, 1973). Tlc plates, developed first in ether and then 9:1 MeCl:MeOH, revealed a single product with an R_f around 0.3. The reaction was worked up by adding approximately 300 mL of H_2O and extracting the product with MeCl. The organic layer was dried over Na_2SO_4 and the solvents were removed by rotary evaporation (co-distilling with toluene).

2.4.13 3'-Acetyl-6-N-acetyl-2'-deoxyadenosine (25) and 3'-Acetyl-6-N,N-diacetyl-2'-deoxyadenosine (26): The synthesis of molecules 25 and 26 is described in Figure 2.5. Compound 22 (3.7 g, 10 mmol) was pyridine-dried three times before suspension in 20 mL of pyridine. Acetic anhydride (6 mL, 60 mmol) was added and the solution stirred for 48

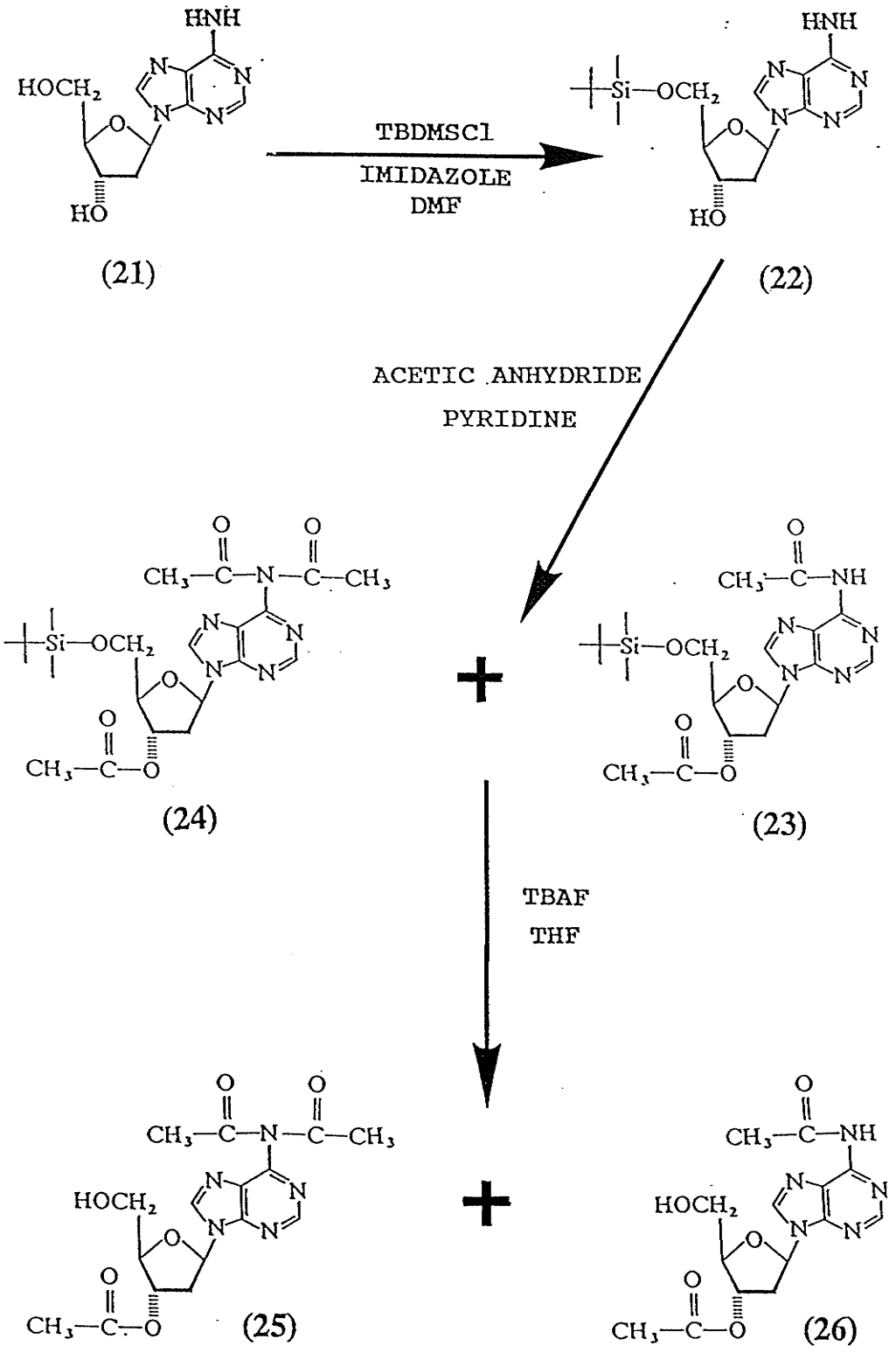

Figure 2.5: Strategy for the synthesis of 3'-acetyl-6-N-acetyl-2'-deoxyadenosine (25) and 3'-acetyl-6-N,N-diacetyl-2'-deoxyadenosine (26).

*hours. Two major tlc bands with R_f values of 0.5 (**23**) and 0.6 (**24**) appeared when developed in ether followed by 9:1 MeCl:MeOH. The reaction was quenched with 30 mL of MeOH and the solvents were removed by rotary evaporation.*

*Molecules **23** and **24** were dissolving in TBAF (0.3 M in THF, 16.7 mL, 10 mmol) to remove the silyl groups. After 24 hours two major tlc bands appeared with R_f values lower than the bands for the starting material after development in ether followed by 9:1 MeCl:MeOH. Dowex-50 (Na^+ form) was added, stirred for 30 minutes, and filtered off. The two products were separated by DCFC using a gradient of MeOH in MeCl. Proton NMR and FAB-MS (Figure 2.6) identified the upper tlc band as **25** and the lower one as **26**.*

***FAB-MS** (-ve ion): (25): MW = 335; 334(100, [M - H]$^-$); 292(8.1, [M - acetyl]$^-$); 176(66, [6-N-acetyladenine - H]$^-$).*

(26): MW = 377; 376(95, [M - H]$^-$); 334(12, [M - acetyl]$^-$); 176(100,[6-N-acetyladenine - H]$^-$).

***2.4.14 5'-O-tert-Butyldimethylsilyl-2'-deoxyguanosine** (30): 2'-Deoxyguanosine (Cruachem) (29) (2.67 g, 10 mmol) was pyridine-dried three times and dissolved in 10 mL of DMF together with TBDMSCl (1.66 g, 11 mmol) and imidazole (1.50 g, 22 mmol). After two hours the reaction was worked up as described for **2**. The product had a tlc R_f of about 0.6 when developed in 4:1 MeCl:MeOH.*

***2.4.15 5'-O-tert-Butyldimethylsilyl-3'-acetyl-2-N-acetyl-2-deoxyguanosine** (31): Molecule **30** (3.82 g, 10mmol) was pyridine-dried three times, dissolved in pyridine (20 mL) and acetic anhydride (6 mL, 60 mmol), and refluxed overnight. The major product had a tlc R_f of 0.8 (4:1 MeCl:MeOH). The reaction was quenched with 30 mL of MeOH and the solvents removed by rotary evaporation. Note that this method was more successful than that using 4-dimethylaminopyridine to catalyze the acetylation as it led to fewer side products and the solution's color did not turn brown.*

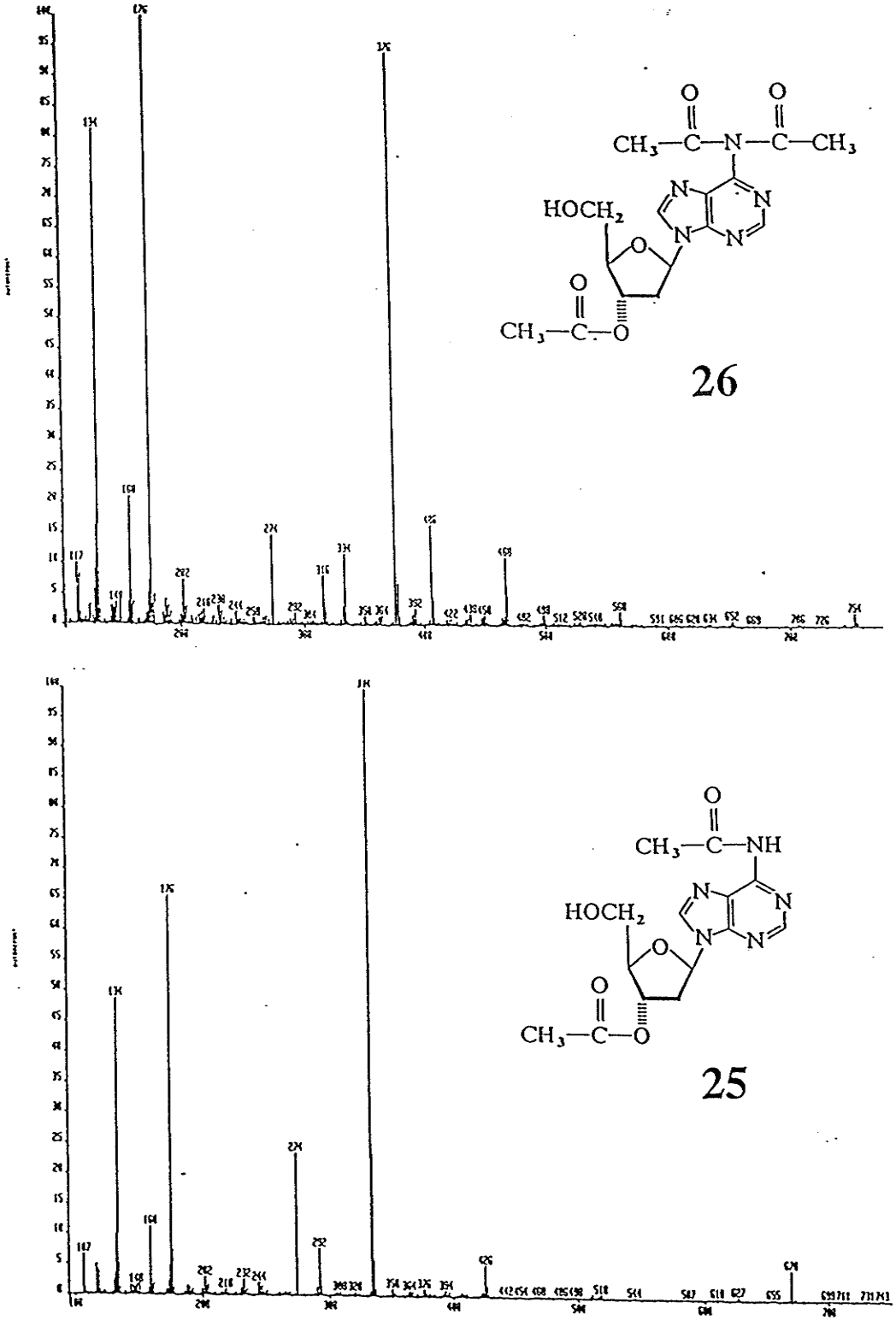

Figure 2.6: FAB-MS (-ve ion) spectra of 3'-acetyl-6-N-acetyl-2'-deoxyadenosine (25) and 3'-acetyl-6-N,N-diacetyl-2'-deoxyadenosine (26).

2.4.16 3'-Acetyl-2-N-acetyl-2'-deoxyguanosine (32): Molecule 32 was prepared from 31 as described for 25 and 26 using TBAF to remove the silyl group. The major product, 32, had a tlc R_f of about 0.4 when developed in ether followed by 9:1 MeCl:MeOH. The product was purified by DCFC using a MeOH gradient in MeCl and identified by NMR and FAB-MS.

***FAB-MS** (-ve ion): MW = 351; 350(100, [M - H]$^-$); 701(6.4, [2M - H]$^-$); 1052(0.6, [3M - H]$^-$).*

2.4.17 5'-O-tert-Butyldimethylsilyl-6-N-benzoyl-2'-deoxyadenosine (27): Molecule 27 was synthesised by Dr. Krish Sadana following Ogilvie's procedure (1973).

2.4.18 5'-O-4,4'-Dimethoxytrityl-6-N-benzoyl-2'-deoxyadenosine (28): Molecule 28 was purchased from Cruachem Inc.

2.5 COUPLINGS AND DEPROTECTIONS:

*2.5.1 d(e^4TpT): The strategy for the synthesis of fully protected d(e^4TpT) is illustrated in Figure 2.7. Pyridine-dried **6** (0.43 g, 1.1 mmol) was dissolved in pyridine and phosphorylated by stirring overnight with p-chlorophenyl phosphate (0.39 g, 1.3 mmol) and 2,4,6-triisopropylbenzenesulfonyl chloride (Sigma) (TPSCl) (0.83 g, 2.8 mmol). The reaction was followed on tlc plates by the appearance of a band at or near the origin after developing the plates in ether followed by 9:1 MeCl:MeOH. Pyridine-dried **20** (0.62 g, 2.2 mmol) and 1-(2-mesitylenesulfonyl)-tetrazole (Sigma) (MST) (0.83 g, 3.3 mmol) were added and stirred overnight. Four tlc bands were eluted with 9:1 MeCl:MeOH. Only the upper two possessed UV maxima in the range expected for such a dimer (> 267 nm and < 281 nm). The reaction was worked up by cooling the mixture in an ice bath and adding 1 mL of H_2O. After 30 minutes about half of the pyridine was removed by rotary evaporation and 40 mL of H_2O was added. Extraction with MeCl followed with the organic layer dried over Na_2SO_4 and decanted. Two of the four tlc bands were co-isolated by DCFC using a MeOH gradient in MeCl. Various deblocking procedures were attempted on these products with the method described in Deprotection Scheme #1 (Figure 2.8) being most successful.*

*Molecule **35** (30 mg, 0.036 mmol) was treated overnight with oximate reagent (1 mL, 0.3 M). The reaction was followed on tlc plates by the appearance of a band at the origin after developing the plates in ether followed by 9:1 MeCl:MeOH. The solution was purified by small scale DCFC (15 mL cylindrical sinter) using ether to remove the oximate reagent followed by MeOH to free the product. The MeOH was removed and the product treated overnight with TBAF dissolved in THF (0.23 mL, 0.14 mmol). Dowex-50 (Na^+ form) was added and stirred for 15 minutes. The solid was filtered out; the filtrate was completely dried and then treated for 1 hour with 0.3 M ethanolic NaOEt (0.7 mL, 0.22 mmol). The material was resuspended in a few drops of H_2O, streaked on Whatman No. 1 chromatography papers, and developed in solvent B' using the descending paper technique.*

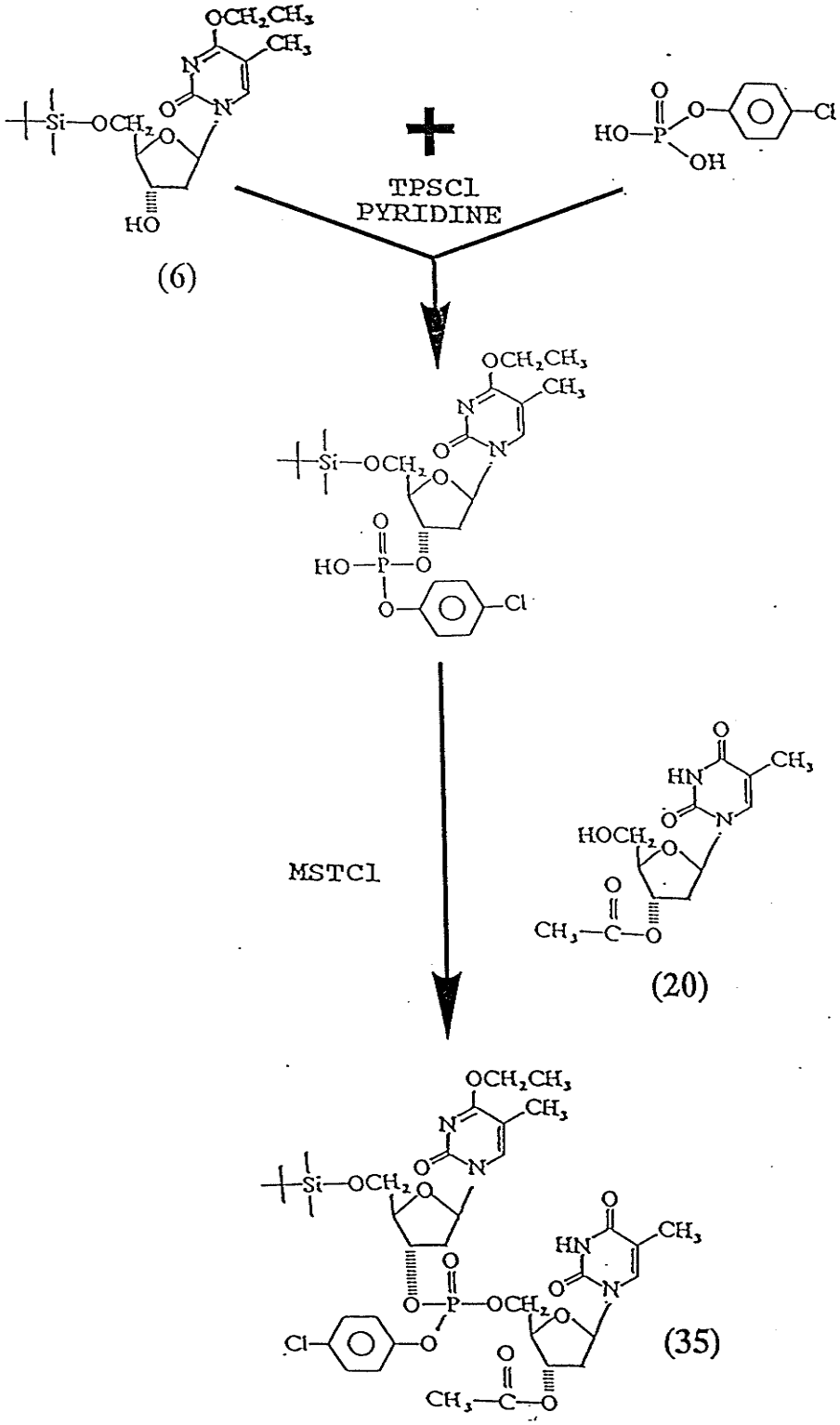

Figure 2.7: *Strategy for the synthesis of fully protected d(e⁴TpT) (35).*

DEPROTECTION SCHEMES

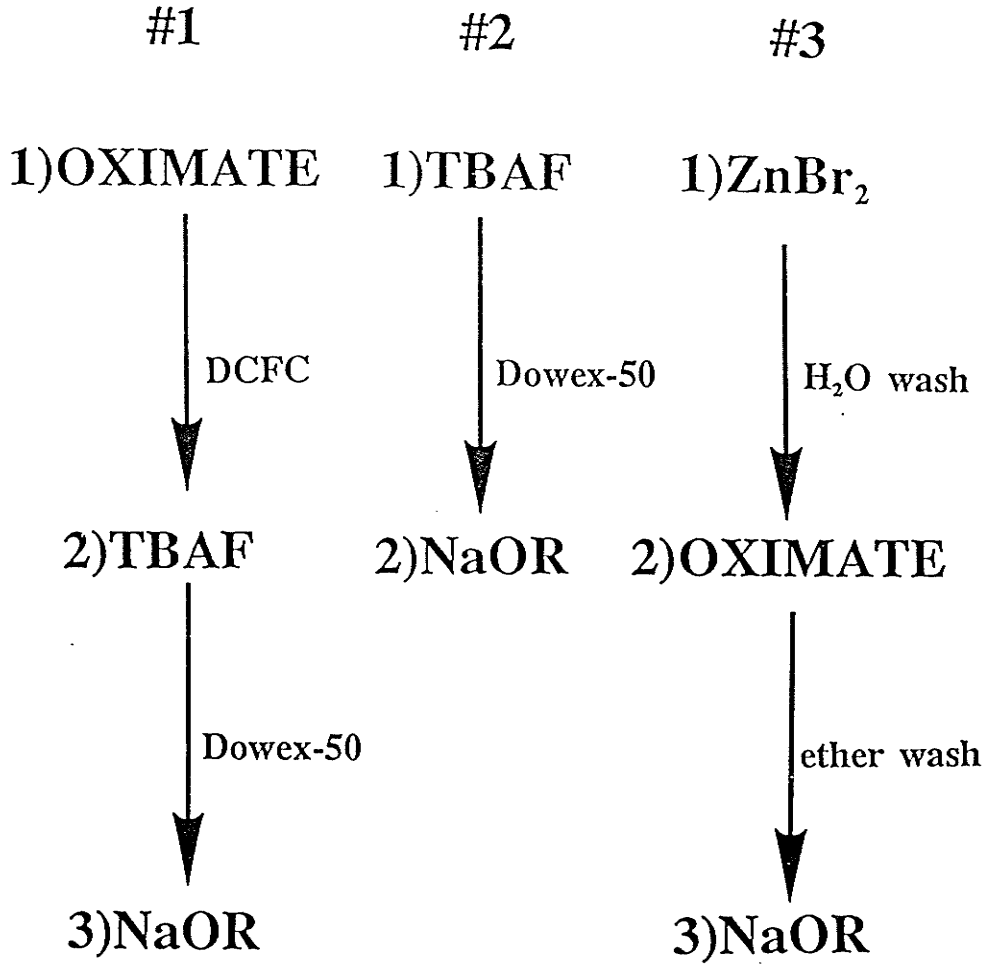

Figure 2.8: Deprotection schemes for the removal of all the protecting groups from fully blocked oligomers.

UV detectable bands were cut out, eluted with H_2O and lyophilized. Appropriate bands, based on UV absorption maxima, were prepared for 300 MHz ^1H NMR spectroscopy. Samples with promising spectra were further purified by HPLC and pure d(e⁴TpT) was obtained as determined by NMR and FAB-MS (Figure 2.9).

UV: λ_{max} = 273 nm; λ_{min} = 239 nm (H_2O).

***FAB-MS** (-ve ion): MW = 574; 573(100, [M - H]⁻); 1147(3.4, [2M - H]⁻); 1721(0.05, [3M - H]⁻); 125(27, [thymine - H]⁻); 153(25, [O4-ethylthymine - H]⁻); 321(17, [5'dTMP - H]⁻); 349(23, [3'e⁴dTMP - H]⁻).*

<u>2.5.2 d(Tpe⁴T)</u>: In all the subsequent condensations, initial phosphorylation was performed using o-chlorophenyl phosphodichloridate instead of p-chlorophenyl phosphate because it was faster and just as efficient. The details are described below for d(Tpe⁴T) (Figure 2.10). The ratios used are expressed as equivalents (eq) relative to the molecule first phosphorylated.

Molecule 2 (0.19 g, 0.5 mmol, 1.0 eq) was pyridine-dried three times and added to newly prepared phosphorylating agent, (o-chlorophenyl phosphodichloridate (Aldrich) (0.091 mL, 0.55 mmol, 1.1 eq)), and 1,2,4-triazole (0.14 g, 2.0 mmol, 4 eq) dissolved in 2-3 mL of pyridine). The reaction was verified after 15 minutes by developing a tlc plate in ether followed by 9:1 MeCl:MeOH. The phosphorylated molecule appeared at or near the baseline. Molecule 18 (pyridine-dried three times) (0.26 g, 0.78 mmol, 1.6 eq (typically 1.2 - 1.3 eq were used)), TPSCl (0.71 g, 2.34 mmol, 3 eq) and tetrazole (Aldrich) (0.49 g, 7.02 mmol, 9 eq) were added. The condensation was complete in 1 hour as monitored on tlc plates developed in ether followed by 9:1 MeCl:MeOH where the blue tlc band of phosphorylated 2 was observed to move from the origin. The work-up and purification was carried out as described for 35.

The deprotection of 36 followed Scheme #2 in Figure 2.8. The first step involved treating 36 (30 mg, 0.035 mmol) with TBAF for 1 minute. Tlc plates developed in ether

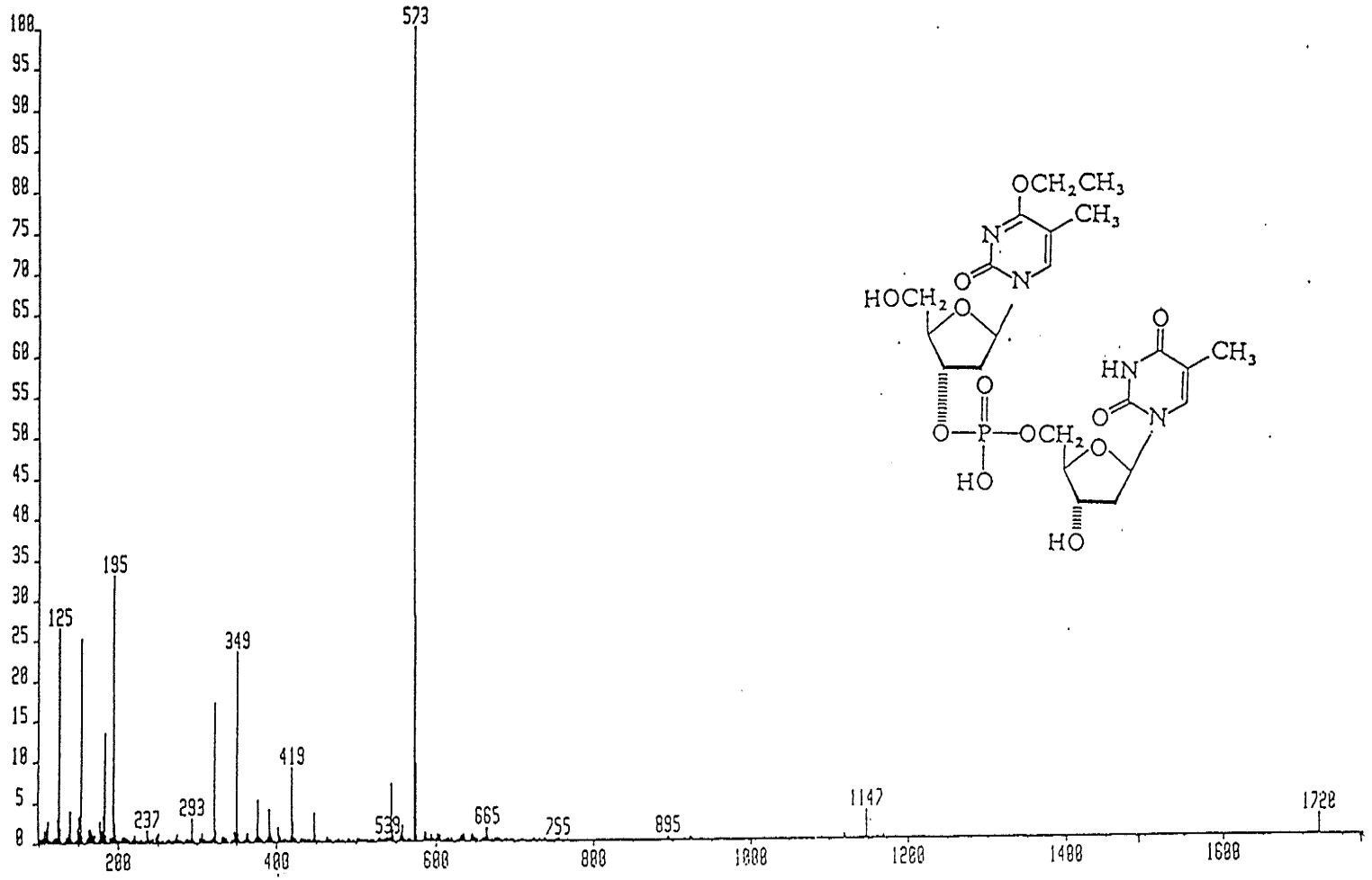

Figure 2.9: FAB-MS (-ve ion) spectrum of d(e⁴TpT) (Molecular weight = 574).

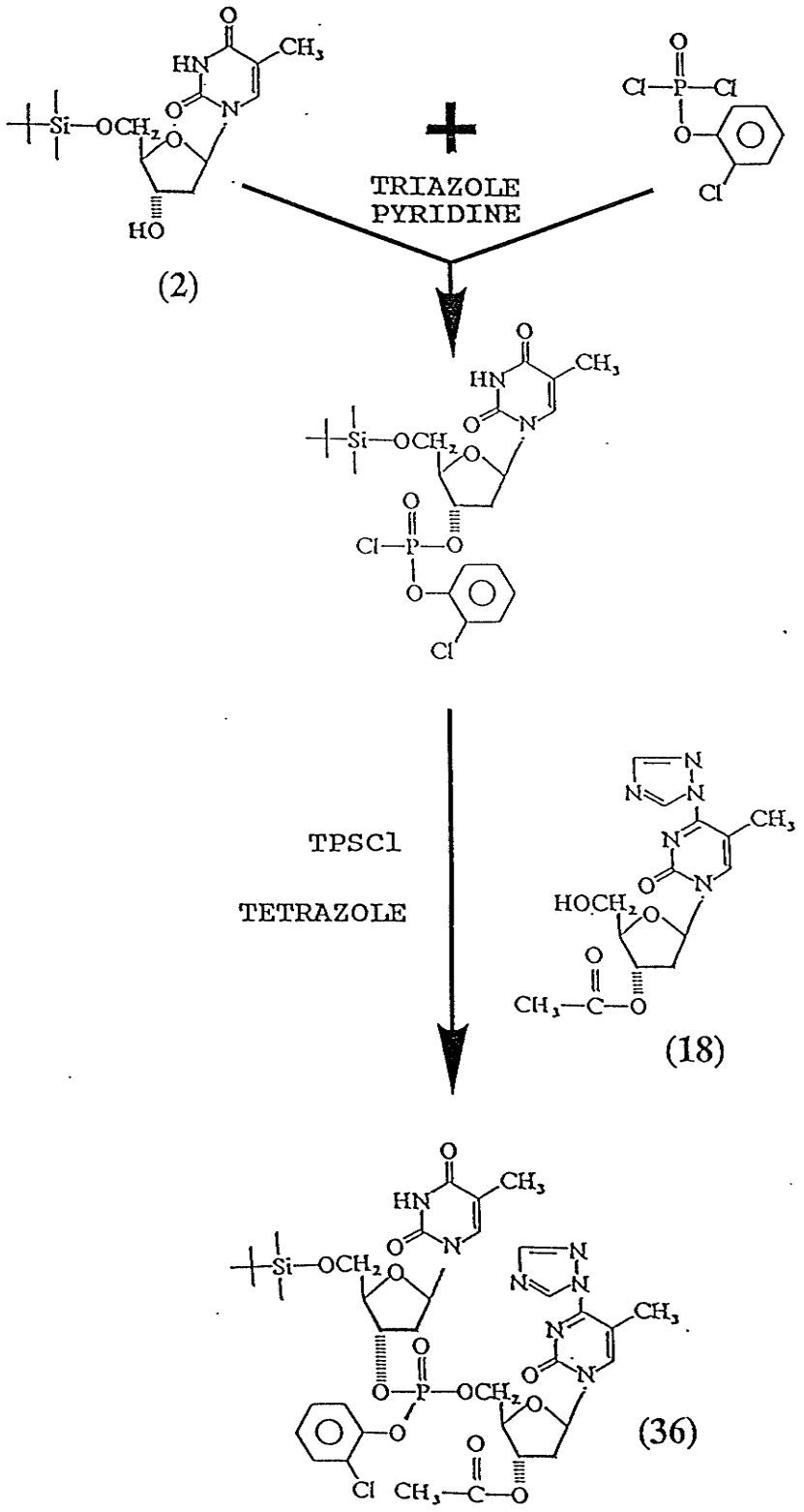

Figure 2.10: Strategy for the synthesis of fully protected d(Tpe⁴T) (36).

followed by 9:1 MeCl:MeOH revealed the movement of the blue fluorescent band of the dimer to the baseline; indicating that the phosphate protecting group had been removed (Ogilvie et al., *(1976)). Dowex-50 (Na^+ form) was added and stirred for 10 minutes. The solids were filtered out and the solvents removed by rotary evaporation. The material was treated for 1 hour with 0.7 mL of ethanolic NaOEt (0.3 M) followed by neutralization with glacial acetic acid. A pure product was obtained through descending paper chromatography followed by HPLC.*

UV: *λ_{max} = 272 nm; λ_{min} = 240 nm (H_20).*

FAB-MS *(-ve ion): MW = 574; 573(100, [M - H]$^-$); 1147(2.3, [2M - H]$^-$); 125(154, [thymine - H]$^-$); 153(14, [O4-ethylthymine - H]$^-$); 321(19, [3'dTMP - H]$^-$); 349(30, [5'e^4dTMP - H]$^-$).*

2.5.3 d(r^4TpT)*: Precursors 7 - 11 were coupled to 20 to create the fully protected d(r^4TpT) dimers with r equal to methyl (m), propyl (p), isopropyl (i), butyl (b), and isobutyl (ib). These dincleotides were all deprotected following Scheme #1 in Figure 2.8.*

Molecule 35, containing O4-isopropylthymine instead of O4-ethylthymine, was also deblocked to yield d(m^4TpT) and d(e^4TpT) by using NaOMe and NaOEt, respectively, instead of sodium isopropoxide (NaOIso) during deprotection. Lower yields were obtained when the reverse was attempted, for example, the conversion of the O4-methyl analogue of 35 to d(i^4TpT).

2.5.4 d(i^4TpT)*:*

UV: *λ_{max} = 272 nm, λ_{min} = 239 nm (H_2O).*

FAB-MS *(-ve ion): MW = 588; 1175(1.6, [2M - H]$^-$) 587(100, [M - H]$^-$); 545(6.0, [M - $CH(CH_3)_2$]$^-$); 363(23, [3'i^4TMP - H]$^-$); 321(23, [5'TMP - H]$^-$); 167(41, [O4-isopropylthymine - H]$^-$); 125(65, [thymine - H]$^-$).*

2.5.5 d(Tpi^{4}T)*: d(Tpi^{4}TpT) (133 A_{260} units) was partially degraded in a 1.5 mL micro-centrifuge tube (Fisher) by snake venom phosphodiesterase (Russel's Viper Venom,*

Calbiochem, 249 units) suspended in a 0.1 M Tris (Base) buffer (pH = 8.0). After 24 hours in a 32°C water bath the mixture was placed in boiling water for 2 minutes, centrifuged, and the DNA containing solvent pipetted out. HPLC revealed only two bands, one with a retention time identical to 5'dTMP and the other with a retention time similar to d(i⁴TpT). NMR, FAB-MS and UV data identified the latter band as d(Tpi⁴T).

UV: λ_{max} *= 270 nm,* λ_{min} *= 238 nm* (H_2O).

***FAB-MS** (-ve ion): MW = 588; 1175(4.0, [2M - H]⁻); 587(100, [M - H]⁻); 545(18, [M - CH(CH₃)₂]⁻); 363(21, [5'i⁴TMP - H]⁻); 321(19, [3'i⁴TMP - H]⁻); 167(7, [O4-isopropylthymine - H]⁻); 125(62, [thymine - H]⁻).*

2.5.6 d(TpT): NaOH (pH > 13) was used instead of NaOEt during the deprotection of 35 using Scheme #1 in Figure 2.8. The observed UV maximum of d(TpT) in H_2O *agrees with the value reported by Kan* et al. *(1973).*

UV: λ_{max} *= 267 nm;* λ_{min} *= 234 nm* (H_2O).

***FAB-MS** (-ve ion): MW = 546; 545(100, [M - H]⁻); 419(6.0, [M - thymine]⁻) 321(32, [3'dTMP - H]⁻ + [5'dTMP - H]⁻); 125(61, [thymine - H]⁻).*

2.5.7 d(i⁴TpG): Molecules 8 and 32 were coupled and then deprotected following Scheme #1 in Figure 2.8.

UV: λ_{max} *= 255, 273 nm;* λ_{min} *= 233 nm* (H_2O).

2.5.8 d(e⁴TpG): Molecules 6 and 32 were coupled and then deprotected following Scheme #1 in Figure 2.8.

UV: λ_{max} *= 255, 273 nm;* λ_{min} *= 233 nm* (H_2O).

***FAB-MS** (-ve ion): MW = 599; 690(1.3, [M + glycerol - H]⁻); 598(43, [M - H]⁻); 570(3.3, [M - ethyl]⁻); 349(49, [3'e⁴dTMP - H]⁻); 346(9.1, [5'dGMP - H]⁻); 153(83, [O4-ethylthymine - H]⁻); 150(38, [guanine - H]⁻); 125(33, [thymine - H]⁻).*

2.5.9 d(TpG): Fully protected d(e⁴TpG) was deprotected following Scheme #1 in Figure 2.8 using NaOH (pH > 13).

UV: λ_{max} = 255 nm; λ_{min} = 228 nm (H_2O).

FAB-MS *(-ve ion): MW = 571; 570(100, [M - H]⁻); 346(20, [5'dGMP - H]⁻); 321(42, [3'dTMP - H]⁻); 150(51, [guanine - H]⁻); 125(72, [thymine - H]⁻).*

2.5.10 d(e⁴TpA): Precursors ***15*** *and* ***25*** *were coupled. The resulting dimer (80 mg, 0.074 mmol) was deprotected following Scheme #3 in Figure 2.8 by first removing the DMT group with 1.0 M $ZnBr_2$ (2 mL, 2.0 mmol). The reaction was monitored on tlc plates developed first in ether and then in 9:1 MeCl:MeOH. The plates were then heated. The detritylated dimer had a lower R_f then the parent molecule and did not turn yellow after heating. The solvents were removed, the product was resuspended in MeCl, and the solution was washed with H_2O until the red color disappeared. The MeCl was removed by rotary evaporation and the material treated with oximate followed by NaOEt as described previously.*

UV: λ_{max} = 262 nm; λ_{min} = 235 nm (H_2O).

FAB-MS *(-ve ion): MW = 583; 674(5.6, [M + glycerol - H]⁻); 582(100, [M - H]⁻); 554(9.7, [M - ethyl]⁻); 349(39, [3'e⁴dTMP - H]⁻); 330(20, [5'dAMP - H]⁻); 153(58, [O4-ethylthymine - H]⁻); 134(39, [adenine - H]⁻).*

2.5.11 d(i⁴TpA): d(i⁴TpA) was synthesised as described for d(e⁴TpA) except ***16*** *was used instead of* ***15*** *in the coupling reaction and NaOIso was used instead of NaOEt during deprotection.*

UV: λ_{max} = 263 nm; λ_{min} = 236 nm (H_2O).

FAB-MS *(-ve ion): MW = 597; 688(3.8, [M + glycerol - H]⁻); 596(100, [M - H]⁻); 554(8.9, [M - isopropyl]⁻); 363(42, [3'i⁴dTMP - H]⁻); 330(24, [5'dAMP - H]⁻); 167(81, [O4-isopropylthymine - H]⁻); 134(54, [adenine - H]⁻).*

2.5.12 d(TpA): Fully protected d(i⁴TpA) was deprotected following Scheme #1 (Figure 2.9) using NaOH (pH > 13). The observed UV maximum in H_2O agrees with the value reported by Kan et al. *(1973).*

UV: λ_{max} = 260 nm; λ_{min} = 231 nm (H_2O).

***FAB-MS** (-ve ion): MW = 555; 646(6.8, [M + glycerol - H]⁻); 554(100, [M - H]⁻); 330(22, [5'dAMP - H]⁻); 321(22, [3'dTMP - H]⁻); 134(19, [adenine - H]⁻); 125(49, [thymine - H]⁻).*

***2.5.13 d(Ape⁴T)**: Molecules 27 and 18 were coupled and then deprotected following Scheme #2 in Figure 2.8. The N-benzoyl group was difficult to remove and therefore required overnight treatment with NaOEt.*

***UV**: λ_{max} = 262 nm; λ_{min} = 235 nm (H_2O).*

***FAB-MS** (-ve ion): MW = 583; 674(5.5, [M + glycerol - H]⁻); 582(100, [M - H]⁻); 554(12, [M - ethyl]⁻); 349(60, 5'e⁴dTMP - H]⁻); 330(14, [3'dAMP - H]⁻); 153(24, [O4-ethylthymine - H]⁻); 134(94, [adenine - H]⁻).*

***2.5.14 d(ApT)**: Fully protected d(Ape⁴T) was deprotected following Scheme #2 in Figure 2.8 using NaOH (pH > 13). The observed UV maximum in H_2O agrees with the value reported by Kan* et al. *(1973).*

***UV**: λ_{max} = 260 nm; λ_{min} = 231 nm (H_2O).*

***FAB-MS** (-ve ion): MW = 555; 646(12, [M + glycerol - H]⁻); 554(100, [M - H]⁻); 330[19, [3'dAMP - H]⁻); 321(69, [5'dTMP - H]⁻); 134(57, [adenine - H]⁻); 125(52, [thymine - H]⁻).*

***2.5.15 d(e⁴TpC)**: Precursors 6 and 34 were coupled and then deprotected following Scheme #1 in Figure 2.8. (d(e⁴TpC) was synthesised by Dr. T.M. Razi with the HPLC purification and NMR analysis conducted by GWB).*

***UV**: λ_{max} = 274 nm; λ_{min} = 246 nm (H_2O).*

***2.5.16 d(i⁴TpC)**: d(e⁴TpC) was treated with NaOIso* (ca. *0.3 M) overnight. HPLC revealed a new peak with a longer retention time than the starting material (Table 2.1).*

***UV**: λ_{max} = 274 nm; λ_{min} = 247 nm (H_2O).*

***2.5.17 d(m⁴TpC)**: d(e⁴TpC) was treated with NaOMe* (ca. *0.3 M) overnight. HPLC revealed a new peak with a shorter retention time than the starting material (Table 2.1).*

UV: λ_{max} = 274 nm; λ_{min} = 247 nm (H_2O).

2.5.18 d(Tpi⁴TpT): Molecule 37 (Figure 2.11) (2.9 g, 2.8 mmol) was synthesised from 8 and 20. It was then 1) detritylated with $ZnBr_2$, 2) worked up as described for d(e⁴TpA), 3) purified by DCFC using a gradient of MeOH in MeCl, 4) phosphorylated at the 5'-end (1.7 g, 2.3 mmol) and 5) coupled to 12 (1.7 g, 2.2 mmol) (Figure 2.12). The product, 38, was isolated by DCFC using a gradient of MeOH in MeCl, and deprotected following Scheme #3 in Figure 2.8.

UV: λ_{max} = 269 nm, λ_{min} = 237 nm (H_2O).

***FAB-MS** (-ve ion): MW = 892; 891(100, [M - H]⁻); 849(11, [M - $CH(CH_3)_2$]⁻); 667(36, [Tpi⁴Tp - H]⁻ + [pi⁴TpT - H]⁻); 587(4.6, [Tpi⁴T - H]⁻ + [i⁴TpT - H]⁻); 321(59, [3'dTMP - H]⁻ + [5'dTMP - H]⁻); 167(14, [O4-isopropylthymine - H]⁻); 125(92, [thymine - H]⁻).*

2.5.19 d(Tpe⁴TpT): Molecule 38 was deprotected following Scheme #3 in Figure 2.8 using NaOEt.

UV: λ_{max} = 269 nm; λ_{min} = 237 nm (H_2O).

***FAB-MS** (-ve ion): MW = 878; 877(55, [M - H]⁻); 850 (849?)(--, [M - CH_2CH_3]⁻); 653(20, [Tpe⁴Tp - H] + [pe⁴TpT - H]⁻); 321(44, [3'dTMP - H]⁻ + [5'dTMP - H]⁻); 573(3.0, [Tpe⁴T - H]⁻ + [e⁴TpT - H]⁻); 153(15, [O4-ethylthymine - H]⁻); 125(100, [thymine - H]⁻).*

2.5.20 d(Tpm⁴TpT): Molecule 38 was deprotected following Scheme #3 in Figure 2.8 using NaOMe.

UV: λ_{max} = 269 nm; λ_{min} = 236 nm (H_2O).

***FAB-MS** (-ve ion): MW = 864; 863(82, [M - H]⁻); 849(9.9, [M - CH_3]⁻); 639(31, [Tpm⁴Tp - H]⁻ + [m⁴TpTp - H]⁻); 559(4.4, [Tpm⁴T - H]⁻ + [m⁴TpT - H]⁻); 321(59, [3'dTMP - H]⁻ + [5'dTMP - H]⁻); 139(23, [O4-methylthymine - H]⁻); 125(100, [thymine - H]⁻).*

2.5.21 d(TpTpT): Molecule 38 was deprotected following Scheme #3 in Figure 2.8 using NaOH (pH > 13).

UV: λ_{max} = 266 nm, λ_{min} = 234 nm (H_2O).

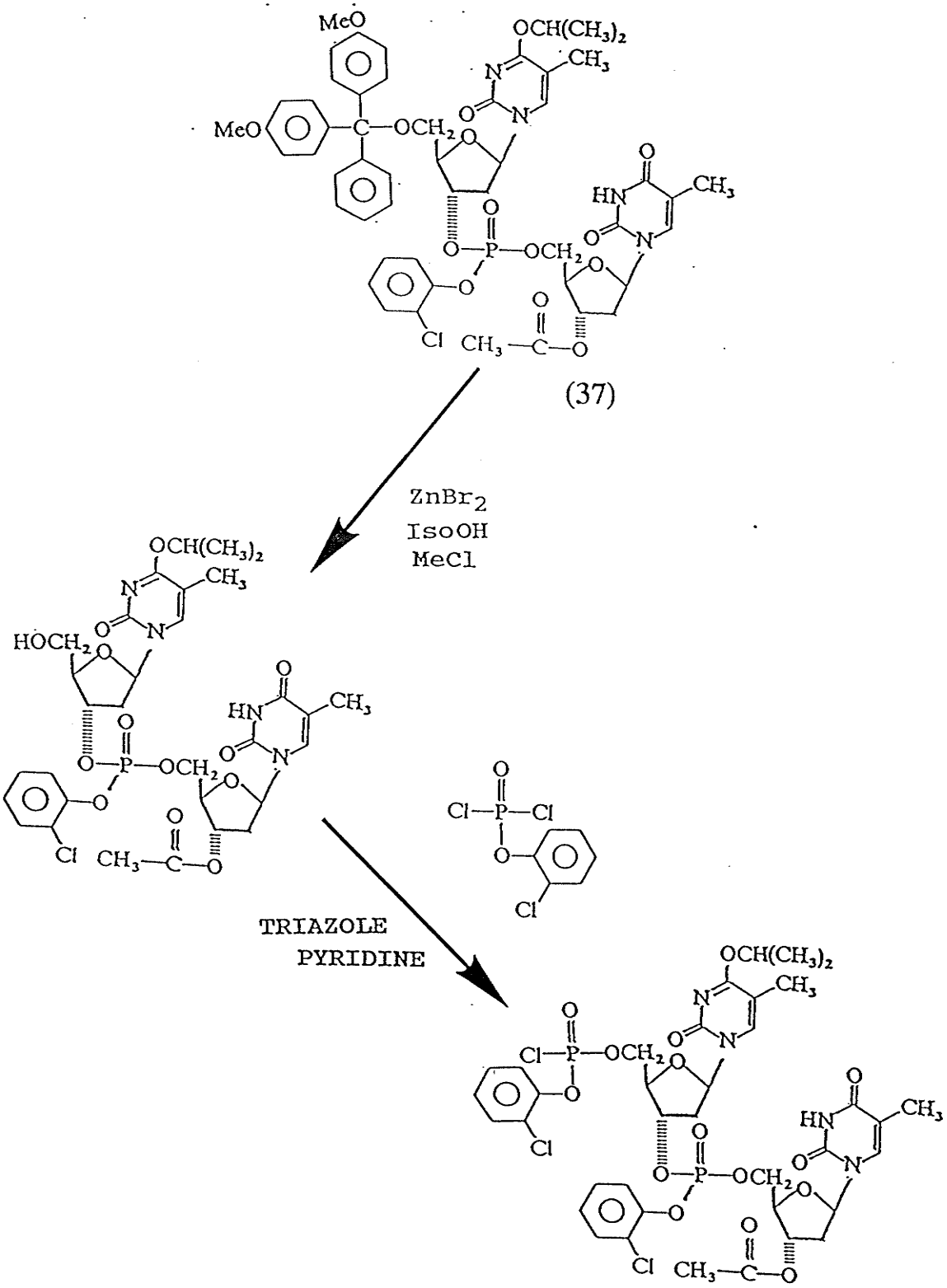

Figure 2.11: Strategy for the synthesis of fully protected d(Tpe⁴TpT) (38); Part 1.

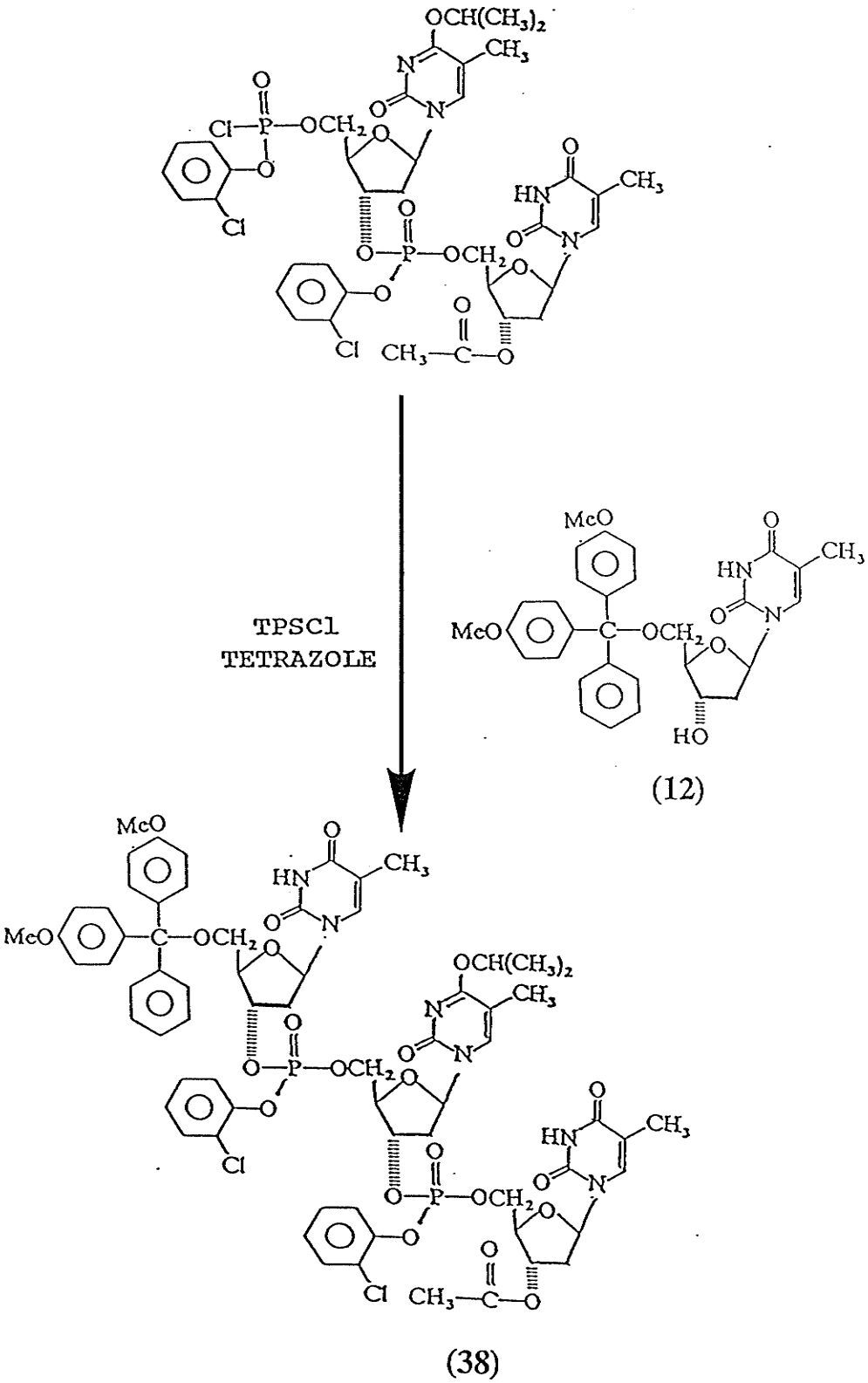

Figure 2.12: Strategy for the synthesis of fully protected d(Tpe^{4}TpT) (38); Part 2.

FAB-MS *(-ve ion): MW = 851; 872(29, [M + Na - H]⁻); 850(53, [M - H]⁻); 625(22, [pTpT - H]⁻ + [TpTp - H]⁻); 321(57, [5'dTMP - H]⁻ + [3'dTMP - H]⁻); 125(100, [thymine - H]⁻).*

2.5.22 d(Ape⁴TpA): Fully protected d(e⁴TpA) was (i) detritylated with $ZnBr_2$, (ii) purified by DCFC using a gradient of MeOH in MeCl (iii) phosphorylated at the 5'-end (0.42 g, 0.5 mmol), and (iv) coupled to 28 (0.41 g, 0.65 mmol). The product, fully protected d(Ape⁴TpA), was isolated by DCFC with a gradient of MeOH in MeCl and deblocked following Scheme #3 in Figure 2.8.

UV: *λ_{max} = 261 nm; λ_{min} = 243 nm (H_2O).*

FAB-MS *(-ve ion): MW = 896; 895(23, [M - H]⁻); 867(2.9, [M - CH_2CH_3]⁻); 662(18, ([Ape⁴Tp - H]⁻ + [pe⁴TpA]⁻); 330(50, [3'dAMP - H]⁻ + [5'dAMP - H]⁻); 153(29, (O4-ethylthymine - H]⁻); 134(100, [adenine - H]⁻).*

2.5.23 d(ApTpA): Fully protected d(Ape⁴TpA) was deprotected following scheme #3 in Figure 2.8 using NaOH (pH > 13).

UV: *λ_{max} = 259 nm; λ_{min} = 230 nm (H_2O).*

FAB-MS *(-ve ion): MW = 868; 867(54, [M - H]⁻); 634(43, [ApTp - H]⁻ + [pTpA]⁻); 330(79, [3'dAMP - H]⁻ + [5'dAMP - H]⁻); 134(100, [adenine - H]⁻); 125(71, [thymine - H]⁻).*

2.5.24 d(e⁴TpApe⁴TpA): Fully protected d(Ape⁴TpA) was (i) detritylated with $ZnBr_2$, (ii) purified by DCFC using a gradient of MeOH in MeCl, (iii) phosphorylated at the 5'-end (1.4 g, 0.8 mmol), and (iv) condensed with 15 (0.6 g, 1.0 mmol). The product, fully protected d(e⁴TpApe⁴TpA), was isolated by DCFC using a MeOH gradient in MeCl and deprotected following Scheme #3 in Figure 2.8.

UV: *λ_{max} = 262.5 nm; λ_{min} = 235 nm (H_2O).*

FAB-MS *(-ve ion): MW = 1228; 1319(1.3, [M + glycerol - H]⁻); 1227(14, [M - H]⁻); 994(5.9, [e⁴TpApe⁴Tp - H]⁻); 662(23, [e⁴TpAp - H]⁻ + [pe⁴TpA - H]⁻); 349(37, [3'de⁴TMP*

-H]⁻); 330(35, [5'dAMP - H]⁻); 153(100, [O4-ethylthymine - H]⁻); 134(65, [adenine - H]⁻).

2.5.25 d(e⁴TpApTpA): During the synthesis and deprotection of d(e⁴TpApe⁴TpA) some O4 dealkylation of thymine occurred at the third base from the 5'-end (or 15 contaiminated with a substantial amount of 12 was used in the synthesis). A quantity sufficient for NMR was obtained by HPLC (Table 2.1 and Figure 2.2).

UV: *λ_{max} = 261 nm; λ_{min} = 234 nm (H_2O).*

FAB-MS *(-ve ion): MW = 1200; 1199(1.3, [M - H]⁻); 662(17, [e⁴TpAp - H]⁻); 634(3.0, [pTpA - H]⁻); 349(8.9, [3'de⁴TMP - H]⁻); 330(41, [5'dAMP - H]⁻); 153(32, [O4-ethylthymine - H]⁻); 134(100, [adenine - H]⁻); 125(20, [thymine - H]⁻).*

2.5.26 d(TpApe⁴TpA): During the synthesis and deprotection of d(e⁴TpApe⁴TpA) some O4 dealkylation of thymine occurred at the 5'-base (or 15 contaiminated with a substantial amount of 12 was used in the synthesis). A quantity sufficient for NMR was obtained by HPLC (Table 2.1 and Figure 2.2).

UV: *λ_{max} = 261 nm; λ_{min} = 234 nm (H_2O).*

CHAPTER 3

NMR. ^{1}H and ^{13}C Spectral Assignments

3.1. INTRODUCTION:

The ^1H NMR spectra of DNA oligomers contain a set of resonances for each nucleotidyl unit. In turn, each nucleotidyl unit has two distinct groups of proton resonances: 1) the deoxyribose sugar which contains seven protons that form a scalar coupled group; and 2) the base. The phosphate group that connects nucleosides also insulates the spins of different sugar residues from homonuclear couplings. With the pyrimidine bases, the coupling between the H5 and H6 of cytosine and the Me5 and H6 of thymine can be used to identify these resonances. With the purine bases, the base protons cannot be distinquished by couplings as both guanine and adenine have an isolated H8, with adenine having an additional isolated H2. Hence, through a number of NMR experiments, briefly described below, it is possible to group the sugar resonances belonging to the same residue and to group the pyrimidine resonances belonging to the same base. Once these groupings are established, the sugar and base resonances can then be linked to the proper nucleotide.

One common technique used to identify coupled protons is the homonuclear double resonance (decoupling) experiment (Harris, 1983). The pulse sequence is illustrated in Figure 3.1A using homo-decoupling (HD). The proton to be decoupled is irradiated only during the dwell time, the period of digitization during which the receiver is off. The HD power is varied between 20-50 L (millwatt range) depending on the knowledge of the location of the resonance being decoupled and the chemical shifts of neighbouring resonances. The effect on the spectrum is the removal of the irradiated signal(s) and a simplification of the resonance pattern of nuclei to which the irradiated proton is coupled. The identification of coupled protons may be facilitated by subtracting the free induction decay (FID) of the fully coupled spectrum from the FID of the decoupled spectrum, a procedure called difference decoupling (Sanders and Mersh, 1982). Such experiments are widely used to identify the DNA ^1H resonances which are coupled (Cheng and Sarma,

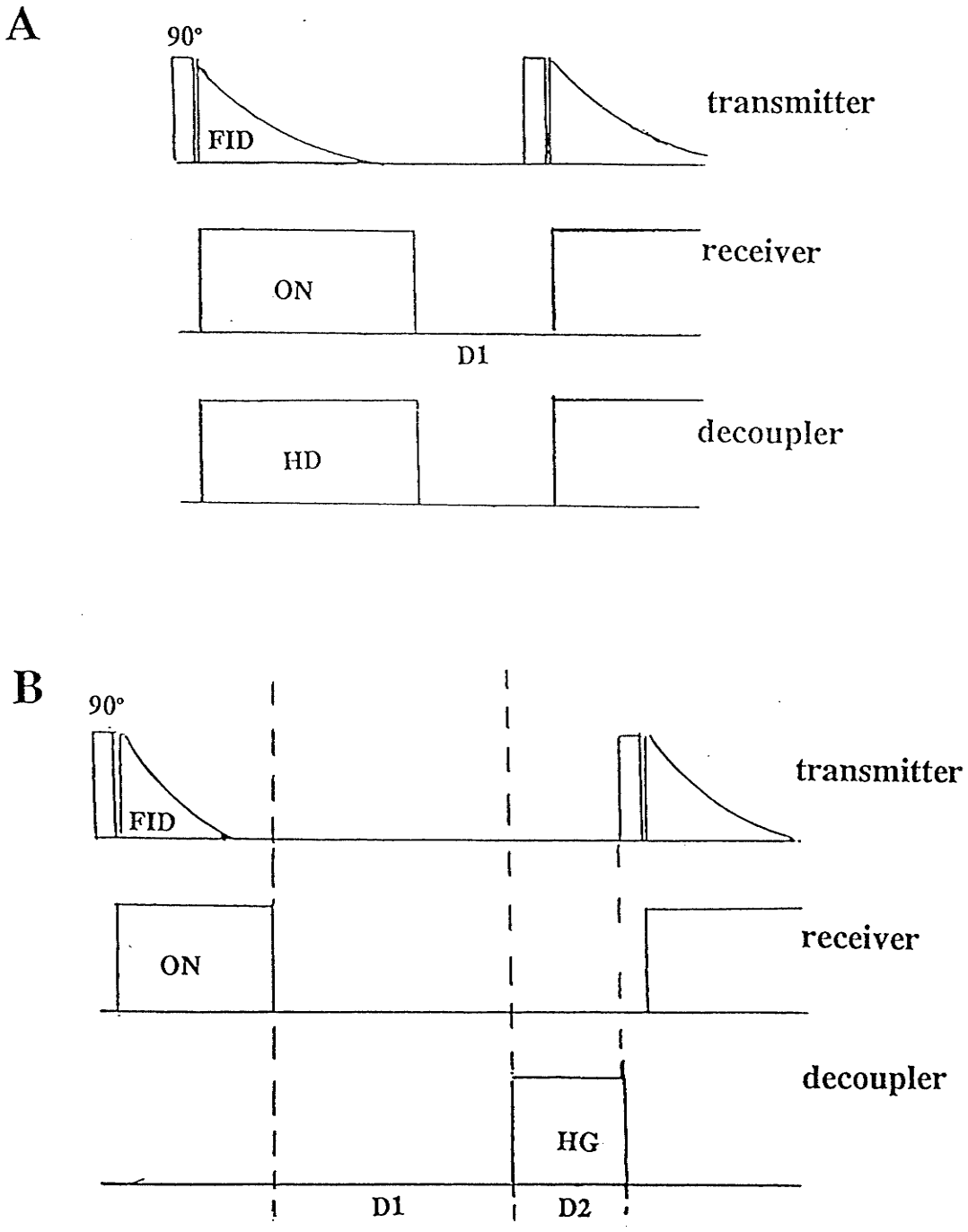

Figure 3.1: A) Pulse sequence for a homonuclear decoupling experiment. B) Pulse sequence for a nuclear Overhauser enhancement experiment (NOE).

1977; Lee and Tinoco, 1980; Cheng et al., *1982; Rinkel* et al., *1986); some examples are given in Figure 3.9 and 3.12.*

Another technique used to identify coupled spins is 2D correlated spectroscopy (COSY) (Aue et al., *1976). The general pulse sequence is 90° - t_1 - 45° where t_1 is incremented after every 1D experiment. The 45° pulse is called the mixing pulse which transfers magnetization between coupled spins. A series of 1-D FIDs are obtained and are Fourier transformed (F2, horizontal). After the F2 Fourier transformations the data is again Fourier transformed perpendicular to F2 (F1, vertical). The result is a spectrum as a function of two frequencies, F1 and F2, or chemical shift versus chemical shift. Magnetization transfers between spin states of the same nuclei result in peaks that fall on the diagonal (F1 = F2). Magnetization transfers between spin states of two different, but coupled, nuclei result in cross peaks at off-diagonal coordinates (δ_A, δ_B) and (δ_B, δ_A). Consequently the DNA sugar δs can be followed via ^1H-^1H couplings from H1' to H2' and H2", from H2'/H2" to H3', from H3' to H4', and from H4' to H5' and H5" (Feigon* et al., *1983; Kan* et al., *1987; Kalnik* et al., *1988a; Flynn* et al., *1988). Examples of COSY spectra are reproduced in Figures 3.2, 3.3, and 3.16 - 3.18.*

One problem with the COSY experiment is that the H3', H4', H5', and H5" deoxyribose sugar resonances fall within a narrow chemical shift range. Consequently, these latter cross peaks are near the diagonal and are poorly resolved, with assignments becoming more difficult as the oligomer length increases. In such situations the identification of coupled resonances may be assisted with relay coherence transfer spectroscopy (RELAY) (Bolton, 1982; Bolton and Bodenhausen, 1982; Eich et al., *1982).*

The RELAY experiment is essentially a double COSY with a refocussing pulse inserted in the middle:

$$90° - t_1 - 90° - \tau - 180° - \tau - 90°$$

COSY#1 REFOCUS COSY#2

For a three proton system, A, B, and C with A coupled to B, B coupled to C, but C not coupled to A, magnetization from A is transferred to B (COSY#1) and then through to C (COSY#2). Coherence is generated between two protons, A and C, not directly coupled to each other but coupled to a common proton B. The fixed delays, τ, depend on J (τ = 1/4J) and therefore an average value for DNA sugars is usually used ($J_{average}$ = 5.5 Hz). The RELAY technique has been used to analyze short DNA and RNA molecules (Hughes et al., *1985; Buchko, 1986). Because magnetization from H3' can be transferred through H4' to H5' and H5" and through H2' and H2" to H1', a "slice" of the RELAY 2D spectrum at a H3' resonance will contain the 1D spectrum of that H3' sugar (Figure 3.10). While the RELAY experiment is useful to identify coupled spins in small oligomers it becomes less efficient as the extent of resonance overlap increases with sequence length. One solution is longer, five and six bond, transfers of proton magnetization (total correlation spectroscopy (TOCSY) (Braunschweiler and Ernst, 1983; Flynn* et al., *1988)).*

After the sugar resonances are grouped to individual residues via decoupling, COSY and RELAY experiments, it is often necessary to assign these resonances to the proper nucleotidyl unit. One method of associating the sugar and base proton resonances with a nucleotide is the NOE experiment (Noggle and Schirmer, 1971) which can make through space nuclear connections. The NOE pulse sequence is illustrated in Figure 3.1B. The sequence is similar to a decoupling experiment except that the resonance of interest is irradiated (homo-gated decoupling (HG)) prior to the 90° pulse. The HG irradiation alters the spin state populations of this proton so that zero and double quantum transitions between nearby nuclei, less than 0.4 nm away, are favourable. Such transitions may enhance or decrease the resonance intensity of nuclei within the 0.4 nm parameter of the irradiated spin with the size and sign of the NOE depending on the magnetogyric ratios, the correlation time (τ_c), and the internucleotide distance (r). In stacked right-handed B DNA, H1' is approximately 0.35 nm away from the pyrimidine H6 or the purine H8 of its

attached base. The interproton distance is within the range where an NOE may be generated directly although cross relaxation through H2' and H2" is more likely (Feigon et al., *1983; Wemmer and Reid, 1985). Hence, NOEs may be used to link sugar resonances to a nucleotidyl unit as illustrated in Figures 3.11 and 3.19.*

Through the use of these decoupling, NOE, COSY, and RELAY experiments it was possible to assign most of the ^1H resonances of our oligomers. A description of the results of these assignment experiments follows, broken down into four parts: DIMERS, d(Tpr^{4}TpT), d(ApTpA)/d(Ape^{4}TpA), and TETRAMERS.

3.2 DIMERS:

3.2.1 General: Assignment of the dimer proton resonances was not difficult for a number of reasons.

First, in every oligomer, H5'/H5" and H3' may be recognized and assigned to the 5'- and 3'-sugar, respectively, by the absence of vicinal coupling to phosphorus. Starting from either of these assignments, the resonances belonging to the 5'- or 3'-residue may be identified by decoupling, COSY, and/or RELAY experiments. By elimination the remaining resonances belong to the other sugar.

Second, base proton assignments were usually definite since most of the dimers studied contained two different bases. Furthermore, alkylation at the O4 position of thymine alters its electronic configuration (Birnbaum et al., *1986; Brennan* et al., *1986) which results in a downfield shift of the H6 and Me5 resonances (Hruska and Blonski, 1982, Birnbaum* et al., *1988). Therefore, O4-alkylation of one of the thymine bases of* ***d(TpT)*** *creates a heterodimer and it is easy to differentiate between alkylated and non-alkylated thymine base protons. Further assistance is provided from the 0.1 to 0.2 Hz smaller* $^4J_{H6\text{-}Me5}$ *of the* r^4T *base in comparison to the T base (Birnbaum* et al., *1988). The base protons of the only homodimer,* ***d(TpT)****, were assigned following trends reported first by Wood* et al. *(1974) and later Rycyna and Alderfer (1985).*

Last, all the non-alkylated deoxyribose dimers have previously been studied with their proton δs and Js reported in the literature (Cheng and Sarma, 1977). Therefore it was possible to compare our proton assignments of the non-alkylated dimers to literature values.

In all our oligomers the H5' and H5" protons were assigned according to the literature (Remin and Shugar, 1972; Lee et al., *1976) with H5" upfield. The H2' and H2" protons were assigned on the basis of the expected near equality of* $^3J_{2'\text{-}3'}$ *with* $^3J_{3'\text{-}4'}$ *(Wood* et al., *1974). When these latter couplings were unavailable, then H2' and H2" assignments were based on* $^3J_{1'\text{-}2'}$ *being larger than* $^3J_{1'\text{-}2''}$ *(Davies and Danyluk, 1974).*

To illustrate these methods the approach used to assign the resonances of d(Ape⁴T) will be described in detail.

3.2.2 d(Ape⁴T): The assignment of the base protons of d(Ape⁴T) was not difficult because of characteristic features of the resonances of the two different bases. There were three sets of resonances in the aromatic region (> 7.0 ppm). Two of these downfield resonances were singlets and must therefore be the H2 and H8 protons of the Ap unit. The most downfield of these two resonance was assigned to H8 on the basis of similar assignments for d(ApT) and d(ApC) (Cheng and Sarma, 1977). The remaining aromatic signal was, by elimination, the H6 resonance of pe⁴T. This H6 is centered at 7.72 ppm (60°C) which is 0.21 ppm downfield of the corresponding resonance in d(ApT). Also note that $^4J_{H6\text{-}Me5}$ in d(Ape⁴T) is smaller (1.1 Hz) than that for the corresponding resonance in d(ApT) (1.3 Hz). The latter two observations are consistent with the effect of O4-ethylation on dT (Birnbaum et al., *1988). The pe⁴T Me5 was then identified by a COSY cross peak from H6. This Me5 is a large doublet (1.74 ppm, 60°C), slightly downfield of the analogous resonance in d(ApT) (1.71 ppm, 60°) and with a slightly smaller $^4J_{H6\text{-}Me5}$ than in d(ApT). The latter two observations are again consistent with the effect of O4-ethylation on dT (Birnbaum* et al., *1988).*

The sugar protons of d(Ape⁴T) were assigned with the help of a COSY experiment. Starting from the isolated H5' and H5" protons of the 5'-terminal sugar it was possible to "walk through" the Ap sugar resonances as indicated in Figure 3.2: H5'/H5" left to H4', H4' left to H3', H3' right to H2'/H2", and H2'/H2" left to H1'. Beginning with any of the remaining sugar protons, for example the other H1', the resonances of the pe⁴T sugar were similarly assigned (Figure 3.3).

The only resonances left to identify were the methyl and methylene protons of the O4-ethyl group which were exposed by a COSY cross peak.

After the assignments were made coupling constants and chemical shifts were estimated

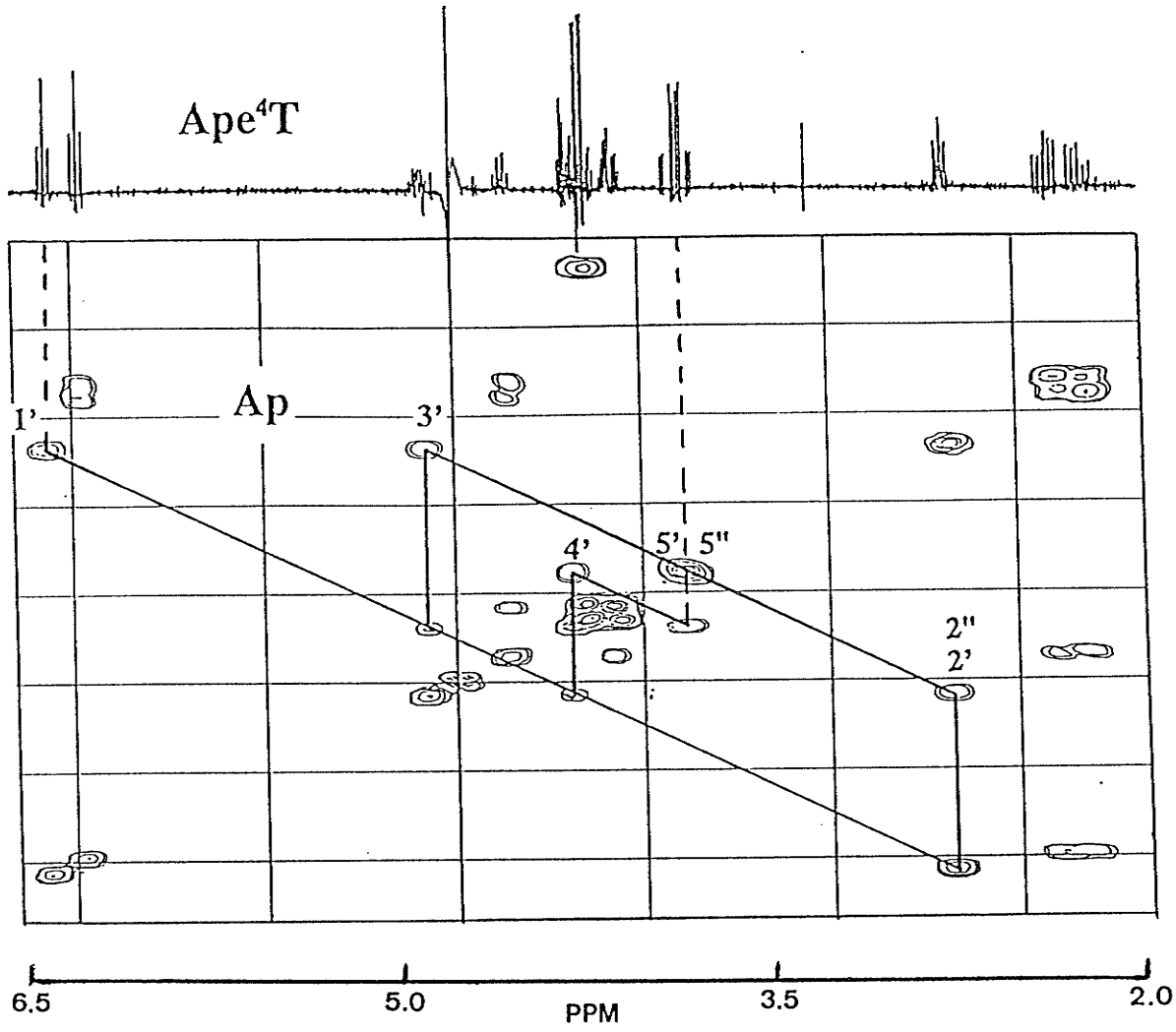

Figure 3.2: 300 MHz COSY-45 2D NMR of d(Ape⁴T) highlighting the Ap sugar. Spectra obtained at 27°C in D_2O. The data were processed with a sine-bell squared function in both domains followed by symmetrization to produce a final 256 x 256 W matrix.

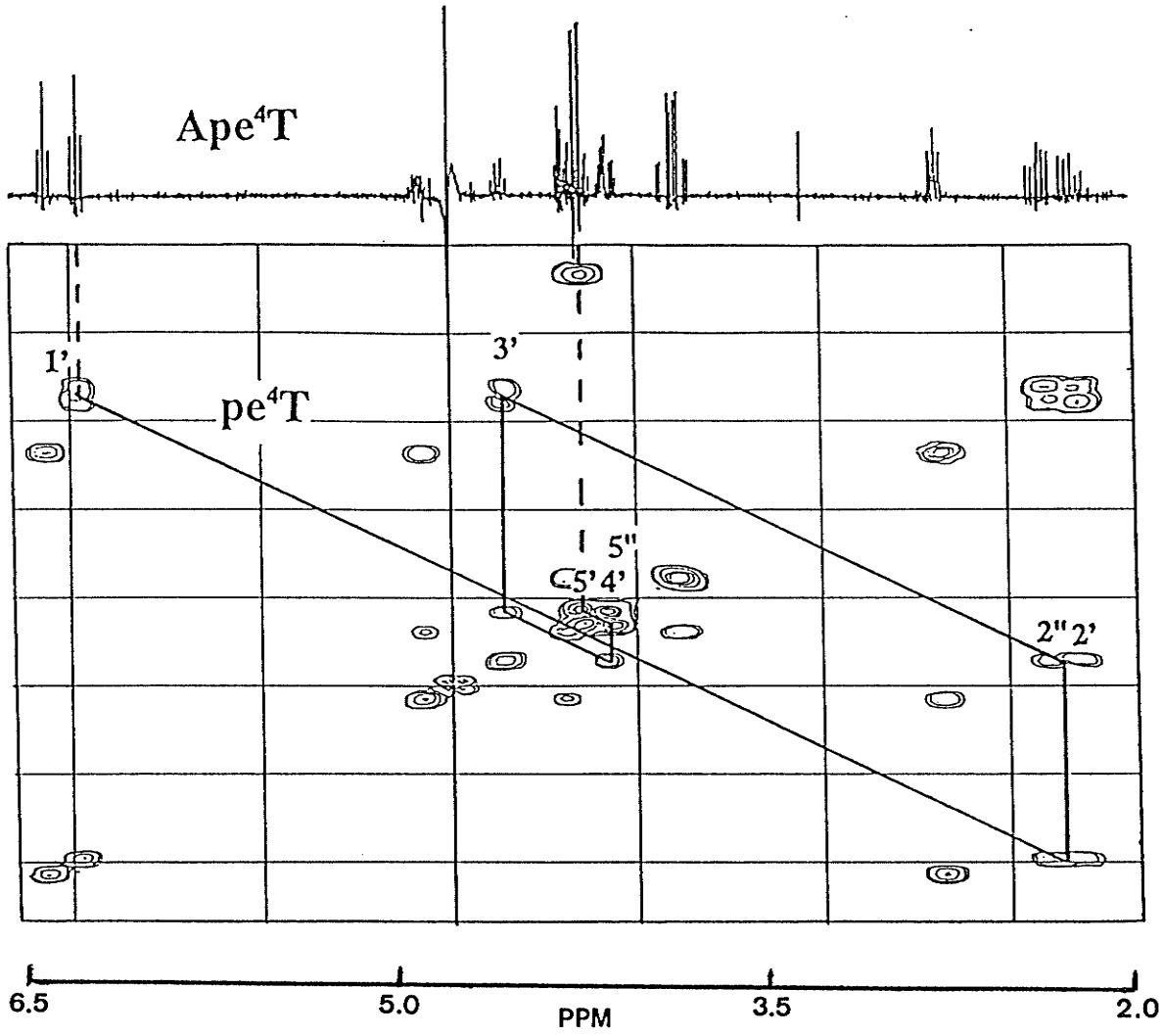

<u>Figure 3.3</u>: 300 MHz COSY-45 2D NMR of d(Ape⁴T) highlighting the pe⁴T sugar. Spectra obtained at 27°C in D_2O. The data were processed with a sine-bell squared function in both domains followed by symmetrization to produce a final 256 x 256 W matrix.

from the resonance patterns. These values were then refined by computer simulations of the spectrum using NUMARIT (Quirt and Martin, 1971). Simulation of the spectrum is evidence for correct assignments. Such simulations for the individual sugars of ***d(Ape^{4}T)*** *are compared to the actual spectrum of* ***d(Ape^{4}T)*** *in Figure 3.4.*

The other dinucleotide proton resonances were assigned in a similar manner. The only additional NMR technique used was difference decoupling which involved irradiating H3' to find H4' in instances when H4' formed an ABC system with H5'/H5". The δs and Js for all the dimers, as refined by NUMARIT, are presented in Tables 3.2 to 3.15.

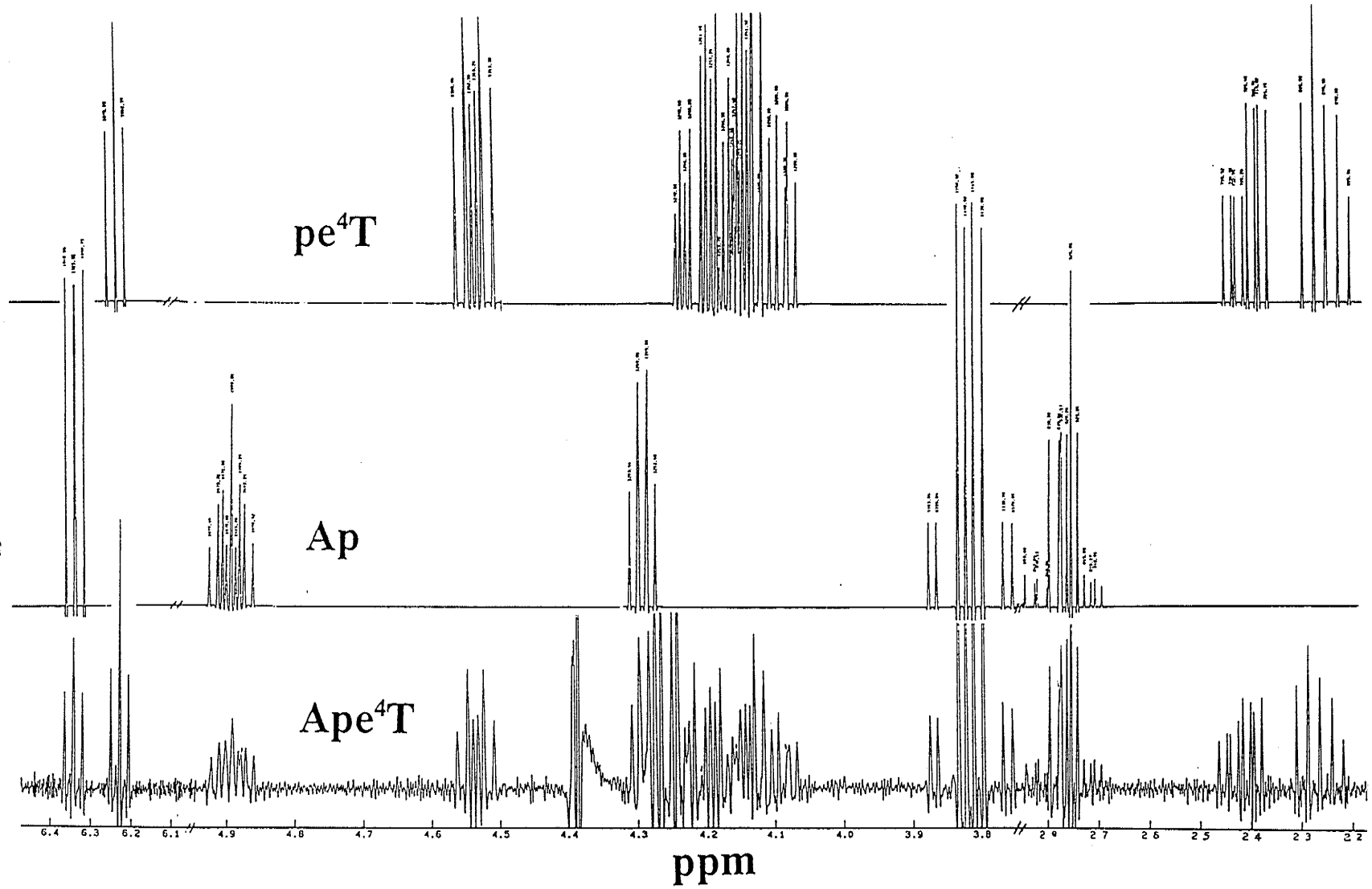

<u>Figure 3.4</u>: NUMARIT simulations (top two spectra) of the 300 MHz ^1H NMR spectrum of the sugar protons of d(Ape⁴T) (60°C).

3.3 d(Tpr^{4}TpT):

Normal ***d(TpTpT)*** *has been analyzed by Cheng* et al. *(1978) and Rycyna* et al. *(1988). Attempts to computer simulate our spectra under our slightly different conditions of ionic strength and temperature were not fully successful. As a result the δs and Js presented in Table 3.16 for* ***d(TpTpT)*** *are from Rycyna* et al. *(1988). However, the variable temperature data for* ***d(TpTpT)****, used in some variable temperature plots in Chapter 5, were obtained at the University of Manitoba.*

Three O4-alkylated trimers were synthesised: ***d(Tpm^{4}TpT)****,* ***d(Tpe^{4}TpT)****, and* ***d(Tpi^{4}TpT)****. The ^{1}H NMR spectra of these trimers were similar at all temperatures and therefore, once the resonances of one molecule were assigned,* ***d(Tpe^{4}TpT)****, it was possible to assign the resonances of the other two.*

At the trinucleotide level the overlap of resonances, particularly among H4', H5' and H5", was severe enough to warrant the use of a RELAY experiment. The Tp and pT sugar resonances were assigned first by recognizing the absence of vicinal phosphorus coupling to H5'/H5' and H3', respectively, and "walking through" the sugar rings (Figure 3.5 and 3.7). By elimination the remaining sugar proton resonances were due to the pe^{4}Tp unit (Figure 3.6). Note that four bond transfers of magnetization through an intermediate was occasionally weak but nonetheless present in all instances permissable. In addition to the four bond transfers, some single or back transfers were also present (COSY peaks) as illustrated in the expansion reproduced in Figure 3.8. For the Tp unit highlighted, the weakest cross peak is between H3' and H4', a COSY transfer. Such weak magnetization transfers are acceptable because the cycling sequence is set up to maximize RELAY and not COSY signals (Hughes et al., *1985). However, the presence of both RELAY and COSY cross peaks allows one to "look down" an H3' resonance and assign all the sugar protons. For example, "looking down" the Tp H3', one sees H2', H2", H5", H5', H4' then H1' (top to bottom). It is therefore possible to take a "slice" of the 2D RELAY spectrum and produce*

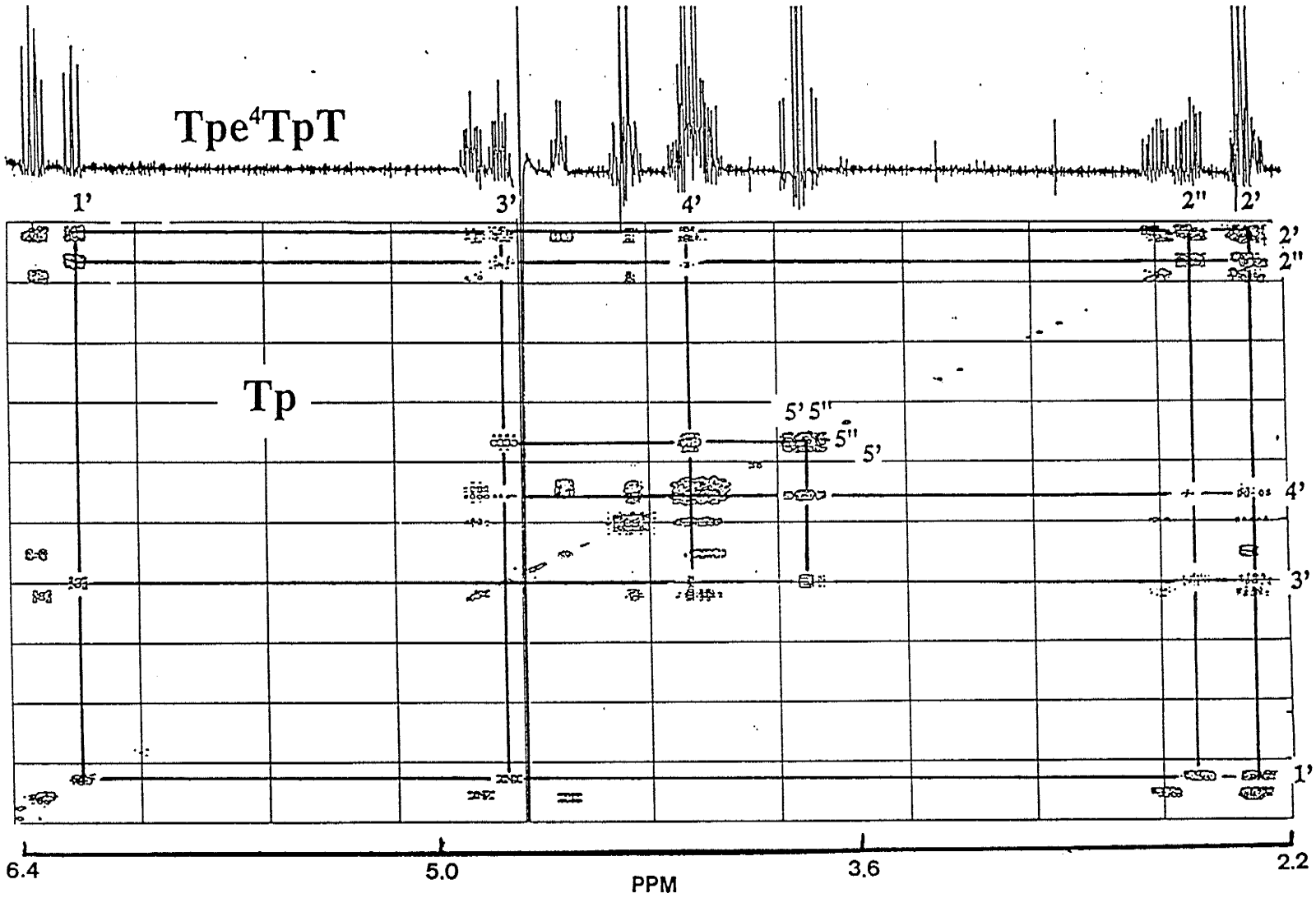

Figure 3.5: 300 MHz RELAY 2D NMR of d(Tpe⁴TpT) highlighting the Tp sugar. Spectra obtained at 32°C in NMR buffer. The data were processed with a sine-bell function in both domains followed by symmetrization to produce a final 1 x 1 K matrix.

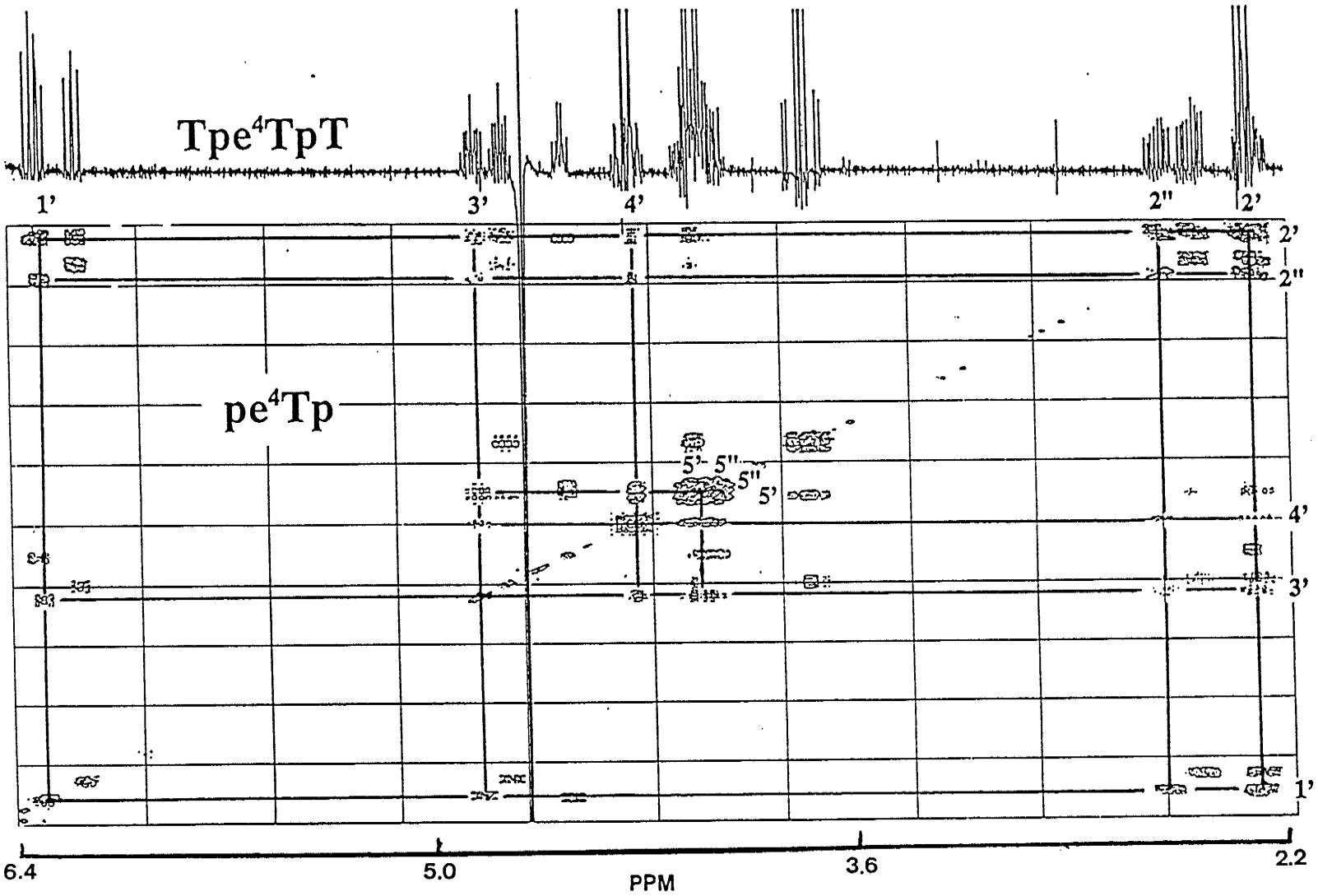

Figure 3.6: 300 MHz RELAY 2D NMR of d(Tpe⁴TpT) highlighting the pe⁴Tp sugar. Spectra obtained at 32°C in NMR buffer. The data were processed with a sine-bell function in both domains followed by symmetrization to produce a final 1 x 1 K matrix.

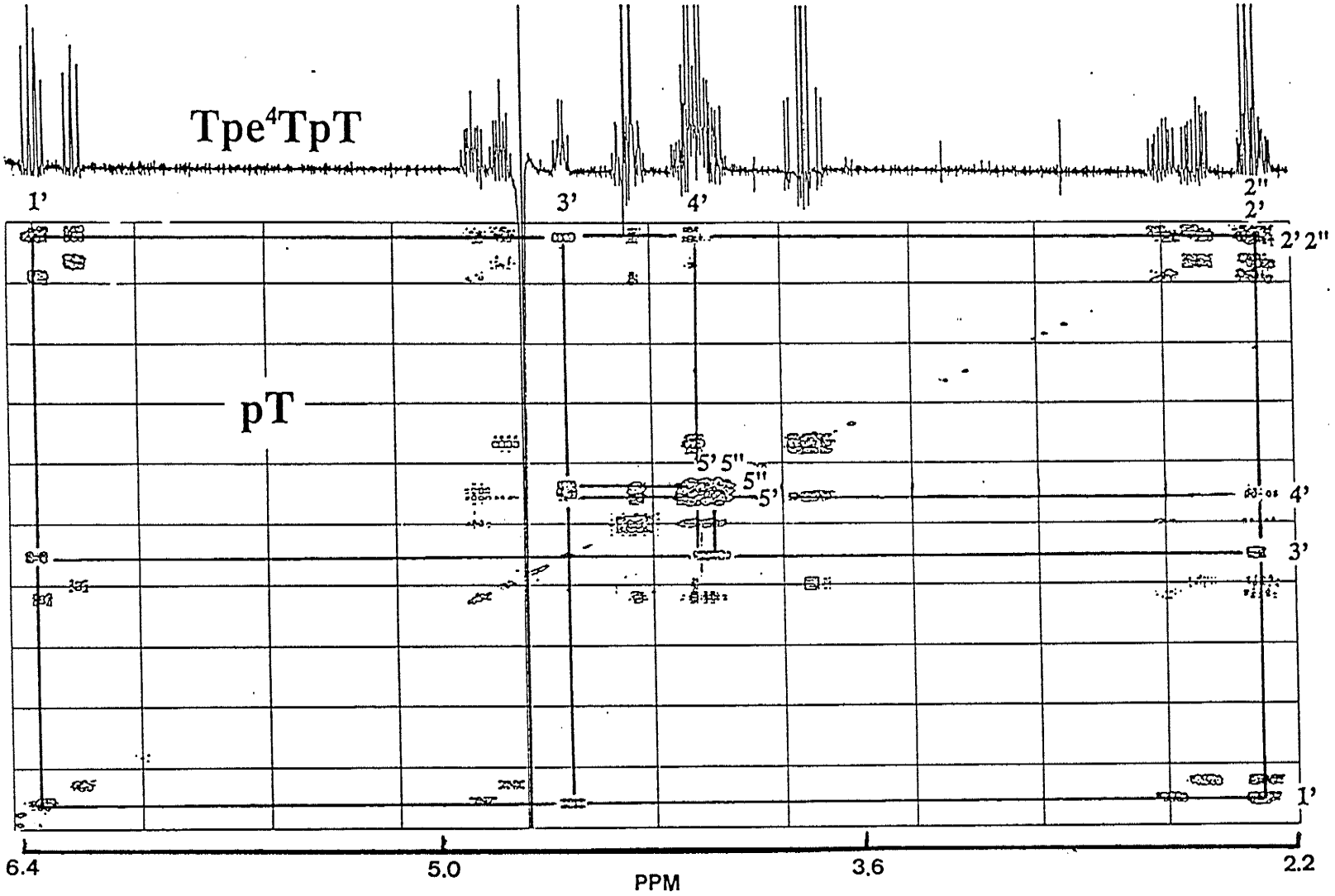

Figure 3.7: 300 MHz RELAY 2D NMR of d(Tpe⁴TpT) highlighting the pT sugar. Spectra obtained at 32°C in NMR buffer. The data were processed with a sine-bell function in both domains followed by symmetrization to produce a final 1 x 1 K matrix.

a 1D spectrum of all the protons of that H3' sugar, as illustrated in Figure 3.10 for the 5.0 - 3.6 ppm region of all three sugars of ***d(Tpe⁴TpT)****. Note that the resolution of this RELAY experiment was 1.0 Hz/point which explains the broadness of the lines and illustrating the necessity of conducting some 1D difference decoupling experiments when resonances were too close to each other. For example, difference decoupling experiments were necessary to assign the H4' protons of Tp and pT by individually decoupling both H3' protons. The latter experiment revealed the Tp H4' to be downfield of the pT H4' (Figure 3.9).*

Difference decoupling was also used to assign the Tp and pe⁴Tp H2' resonances because they were almost coincident. By decoupling H1' at various temperatures and closely examining the 500 MHz spectra (second order effects of the geminal H2' and H2" resonances) it was possible to assign the downfield set of signals to pe⁴Tp at low temperature; above 60°C they crossed over.

Due to resonance overlap it was also difficult to assign the H5' and H5" protons to the pe⁴Tp and pT sugars. Expansion of the RELAY plot (Figure 3.8) enabled the assignment, in the overlap region, of the pT H5" to the more upfield signals and the pe⁴Tp H5' to the more downfield signals. From here it was possible to assign the resonances of the accompanying H5' and H5" protons.

After assigning the sugar protons only the base protons remained. The pe⁴Tp H6 resonance was assigned first by its downfield position relative to the H6 resonances of the non-alkylated bases in the trimer. The pe⁴Tp Me5 was then identified by a COSY cross peak from the downfield pe⁴Tp H6. These latter assignments were confirmed by the observation that their $^3J_{H6\text{-}Me5}$ were also smaller than for the other non-alkylated H6 and Me5 protons in the trimer, as observed in the monomers (Birnbaum et al., *1988). A difference NOE experiment, which involved irradiating the upfield Tp H1', produced an NOE of the most upfield H6 (Figure 3.11). The Tp Me5 was assigned to the middle of the three Me5 resonances by decoupling the NOE assigned Tp H6 (Figure 3.12, top). By the process of*

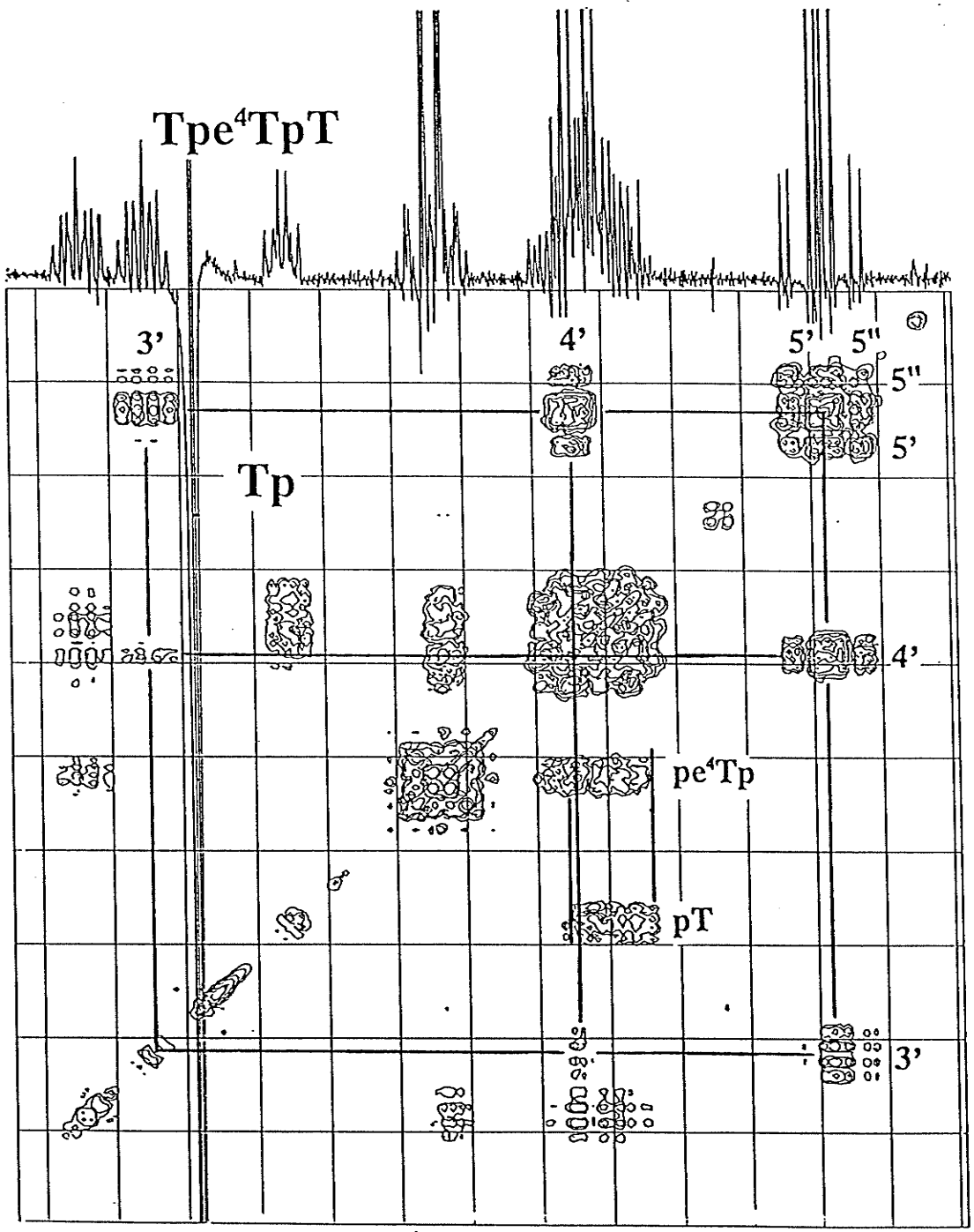

Figure 3.8: 300 MHz RELAY 2D NMR expansion (3.6 - 5.0 ppm) of d(Tpe⁴TpT). Spectra obtained at 32°C in NMR buffer. Data processed with a sine-bell function in both domains followed by symmetrization to produce a final 1 x 1 K matrix.

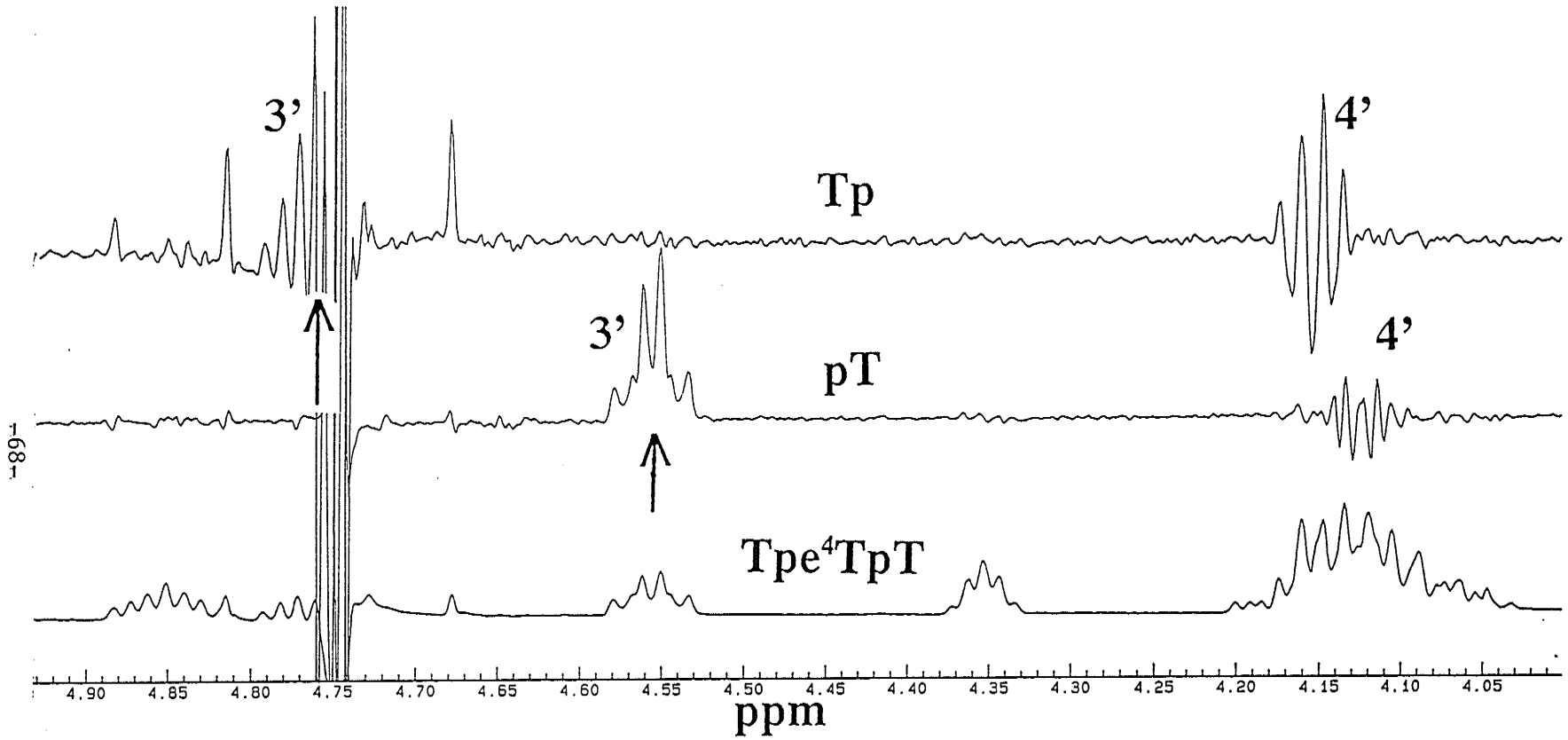

Figure 3.9: 300 MHz difference decoupling experiments (27°C) used to assign the H4' resonances of the pT and Tp sugars of d(Tpe⁴TpT) by irradiation of the respective 3' proton (solid arrows).

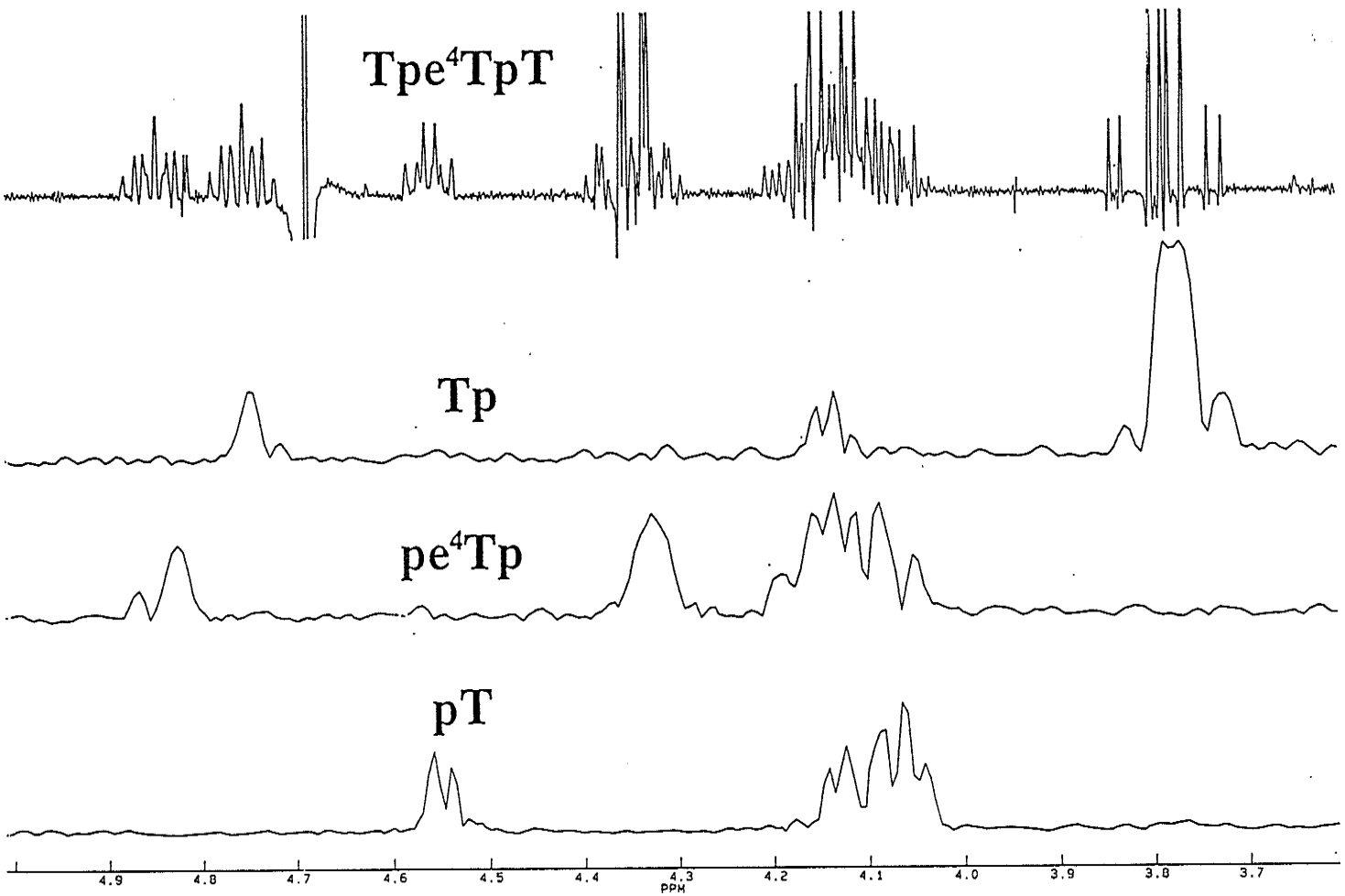

Figure 3.10: 1D "slices" through the H3' resonances of the 2D RELAY NMR of d(Tpe⁴TpT) (32°C).

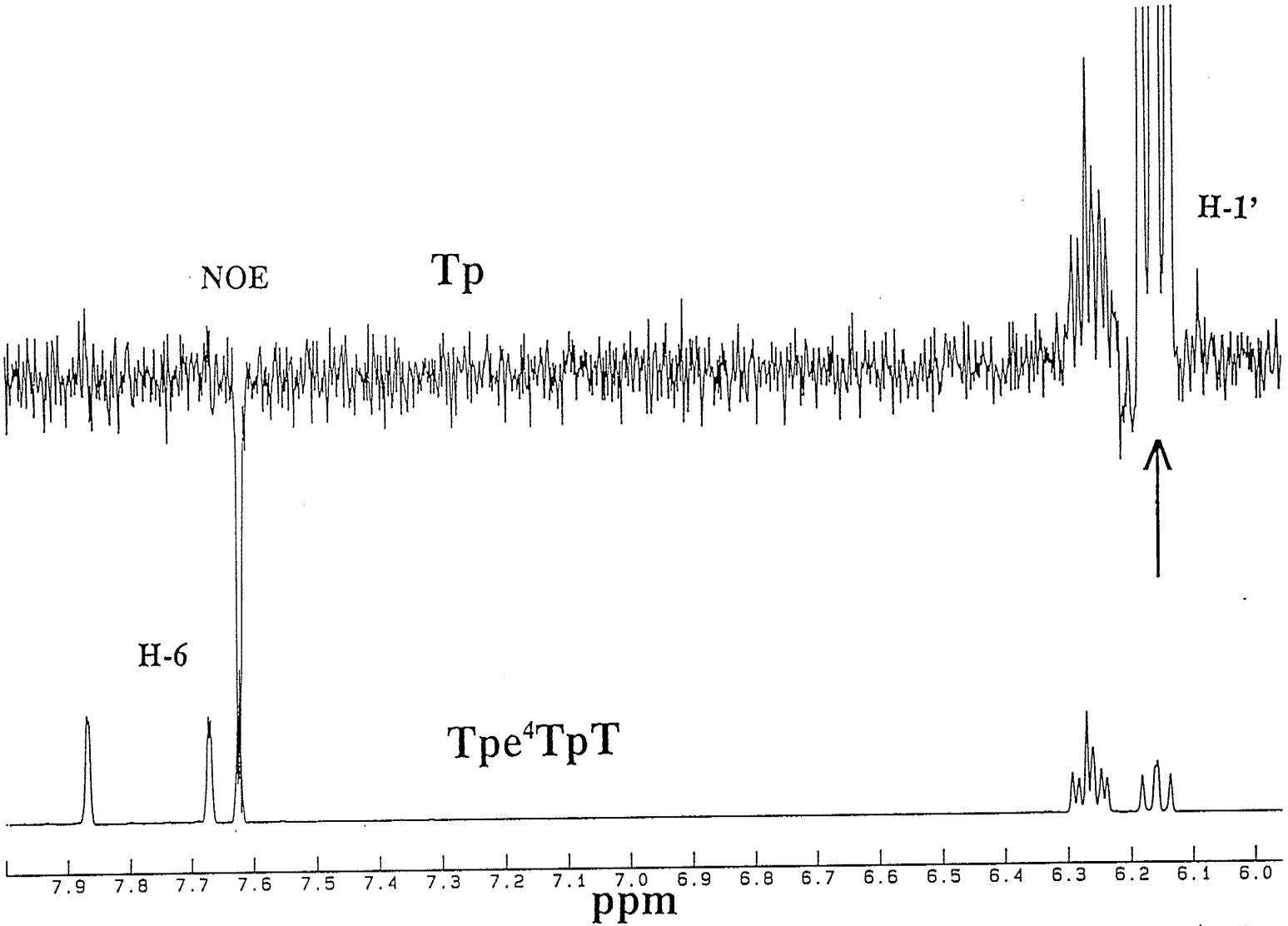

Figure 3.11: Result of the 300 MHz difference NOE experiment used to assign the Tp H6 resonance of d(Tpe⁴TpT) by irradiation of the respective H1'. Parameters: D1 = 4.0 sec, D2 = 5.0 sec, SI = 32K, NS = 208, DP = 45L. Resolution enhancement (GM): LB = 0.0, GB = 0.1 (top spectrum).

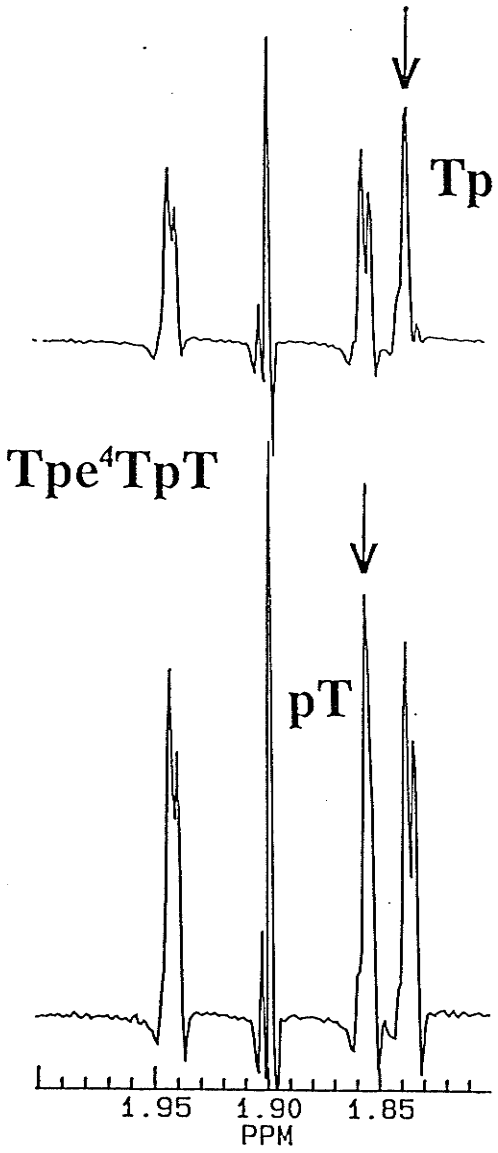

Figure 3.12: Results of the 300 MHz decoupling experiments (27°C) used to assign the Me5 protons of d(Tpe⁴TpT) by irradiation of the respective H6 proton. The decoupling effect is highlighted by the solid arrow. Peak at 1.90 ppm = NH_4OAc.

elimination the remaining H6 and Me5 protons belonged to the pT unit, whose position on the same base was confirmed by decoupling the H6 (Figure 3.12, bottom).

After assigning the resonances of ***d(Tpe^{4}TpT)****, the resonance assignment of the other two isomers,* ***d(Tpm^{4}TpT)*** *and* ***d(Tpi^{4}TpT)****, was not difficult because the only difference between these molecules was the alkyl group, which did not produce drastic changes in the spectra as indicated by the similarities in the computer simulated* δ *and J data presented in Tables 3.17 to 3.19 at 20 and 70°C. Difference decoupling experiments were only necessary to identify the position of the Tp and pT H4' in* ***d(Tpm^{4}TpT)*** *and* ***d(Tpi^{4}TpT)*** *via irradiation of the appropriate H3'. Assignment of the* ***d(TpTpT)*** *resonances for variable temperature studies were based on the d(Tpr^{4}TpT) assignments, together with a COSY experiment on* ***d(TpTpT)*** *and the* ***d(TpTpT)*** *data published by Rycyna* et al. *(1988).*

3.4 d(ApTpA)/d(Ape⁴TpA):

The d(ApTpA) ^1H resonances were assigned first from COSY and RELAY data. To illustrate the proton assignments for d(ApTpA), the RELAY spectra are reproduced in Figures 3.13 to 3.15 highlighting each nucleotidyl sugar. The Ap and pA sugar resonances were assigned by recognizing the absence of vicinal phosphorus coupling to H5'/H5' and H3', respectively, and "walking through" the sugar rings (Figure 3.13 and 3.15). By elimination the remaining sugar proton resonances were due to the pTp unit (Figure 3.14). In these RELAY spectra some four bond coherence transfers were too weak to be detected. For instance, the H2" to H4' cross peaks in pTp and pA are absent while others are barely detectable. However, coherence transfer from H3' to H5'/H5" is present for all three sugars and this is the most useful four bond magnetization transfer. This four bond information, with assistance from the COSY data, made assignment of all the sugar resonances possible.

The base protons were assigned next. There was only one pair of resonances in the appropriate locations with a characteristic coupling of 1.3 Hz (60°C) and a COSY cross peak; the pTp H6 (7.39 ppm) and Me5 (1.72 ppm). To assign the H8 and H2 resonances of the Ap and pA units it was necessary to follow trends in dimers and similar tetramers and to conduct an NOE experiment. Generally, the adenine H8 is downfield of the adenine H2 in deoxyribose dimers (Kan et al., *(1973), Cheng and Sarma, 1977), which leads to the assignment of the two most upfield signals at 8.14 and 8.13 ppm (60°C) to H2. Unambiguous assignment of H2 to Ap or pA was not possible, but, the most upfield H2 was assigned to the Ap unit based on trends in d(ApT), d(TpA) (Cheng and Sarma, 1977), d((TpApTpA), and d(ApTpApT) (Mellema* et al., *1984). However, distinguishing between the H2 resonances of Ap and pA is not critical since they rarely differ by more than 0.009 ppm over the temperature range studied (10 - 60°C).*

The H8 resonances were assigned on the basis of an observable NOE between the Ap H1' to the second most downfield resonance at 8.19 ppm (27°C). The most downfield

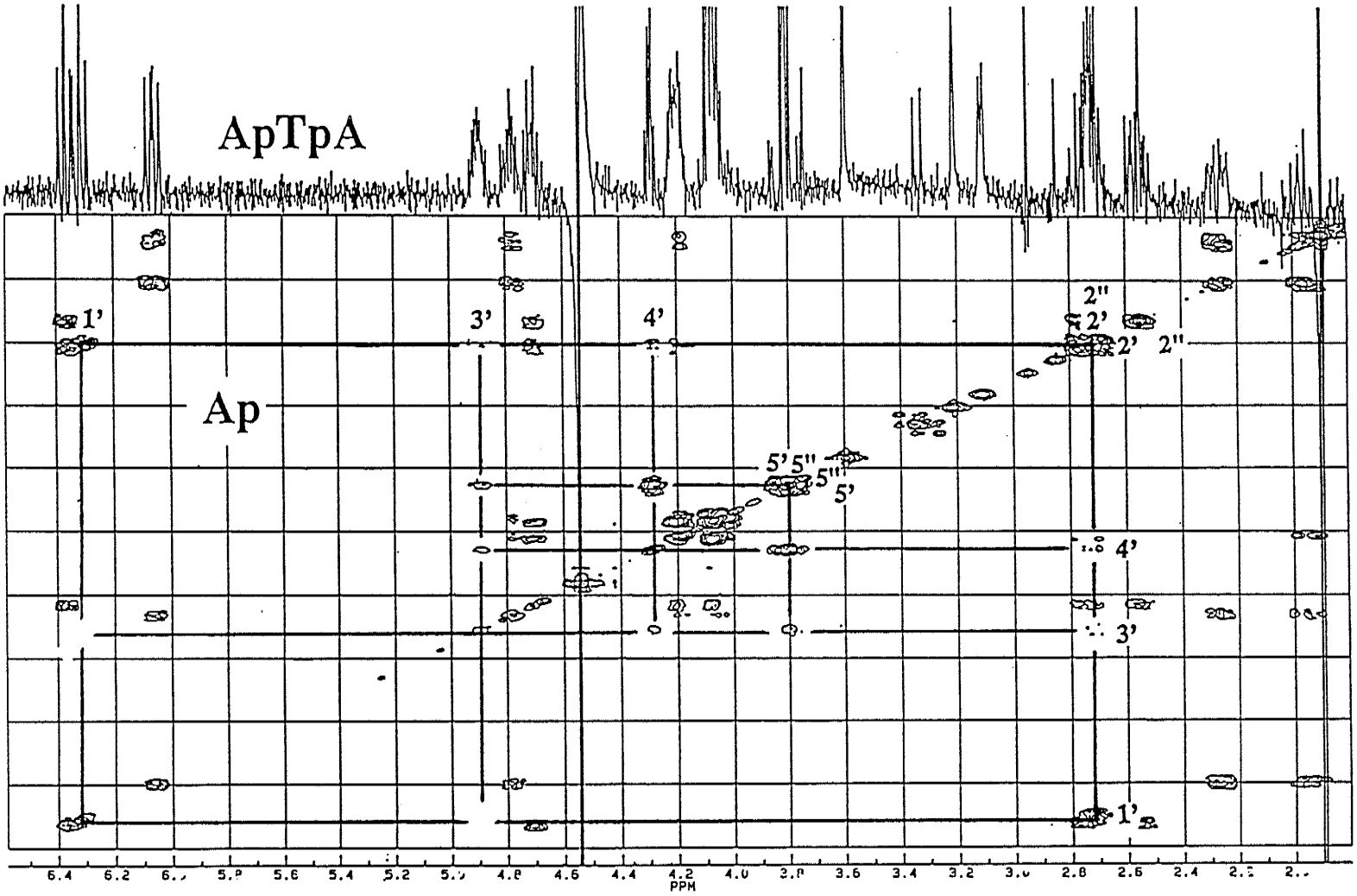

Figure 3.13: 300 MHz RELAY 2D NMR of d(ApTpA) highlighting the Ap sugar. Spectra obtained at 45°C in NMR buffer. The data were processed with a sine-bell function in both domains followed by symmetrization to produce a final 512 x 512 W matrix.

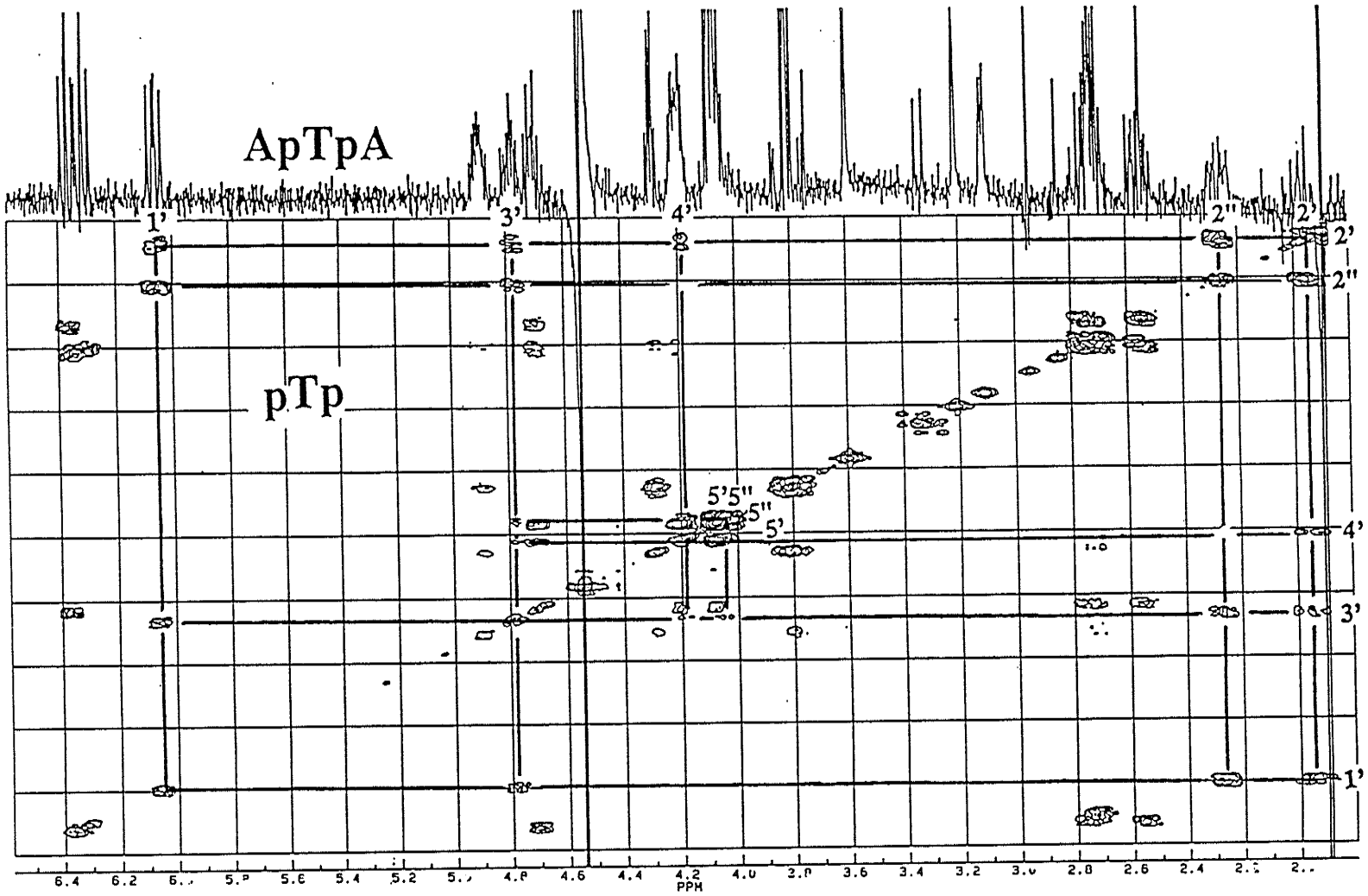

Figure 3.14: 300 MHz RELAY 2D NMR of d(ApTpA) highlighting the pTp sugar. Spectra obtained at 45°C in NMR buffer. The data were processed with a sine-bell function in both domains followed by symmetrization to produce a final 512 x 512 W matrix.

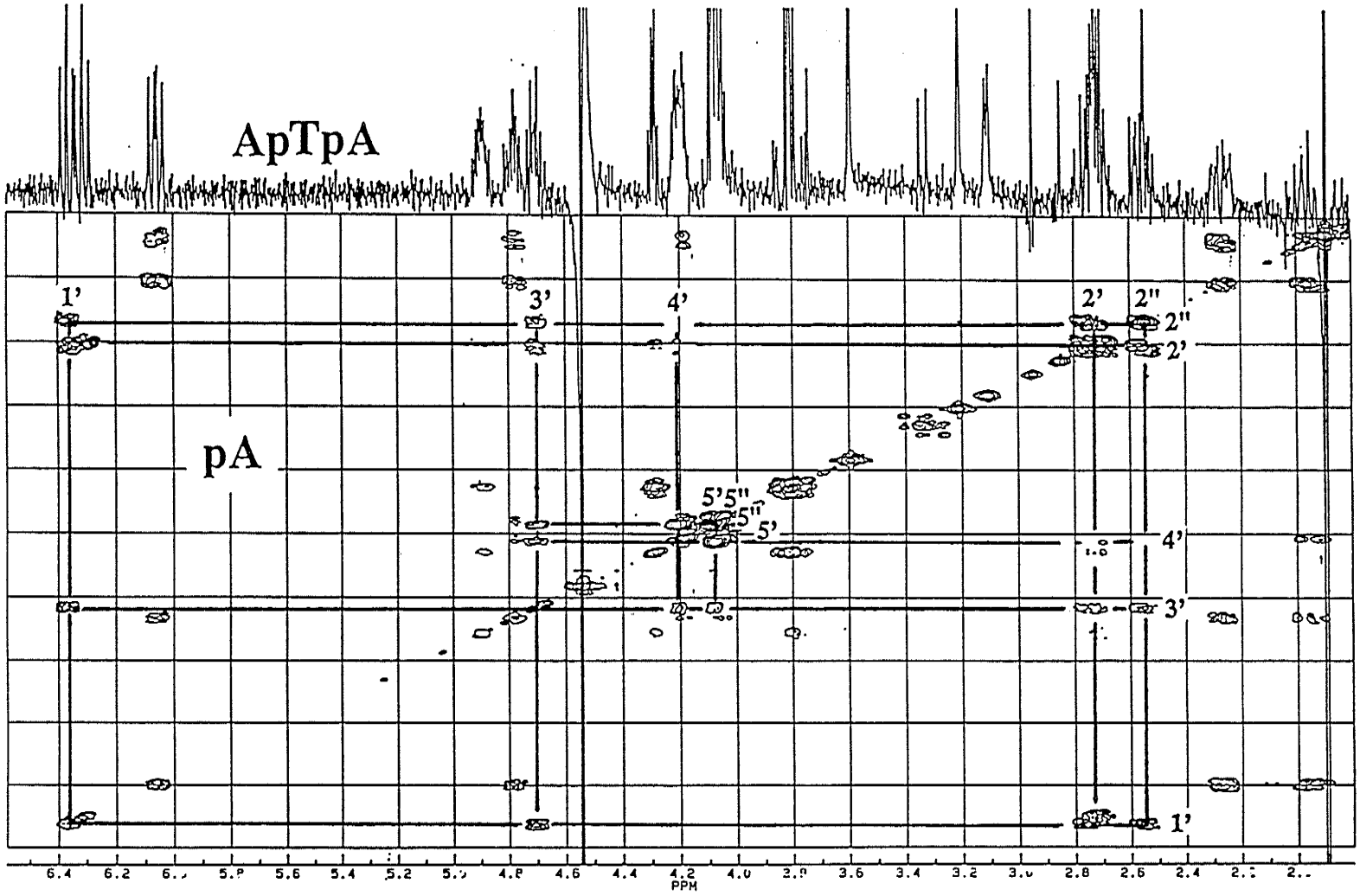

Figure 3.15: 300 MHz RELAY 2D NMR of d(ApTpA) highlighting the Ap sugar. Spectra obtained at 45°C in NMR buffer. The data were processed with a sine-bell function in both domains followed by symmetrization to produce a final 512 x 512 W matrix.

resonance, at 8.31 ppm (27°), therefore belonged to pA. These H8 assignments are consistent with variable temperature chemical shift trends for d(TpApTpA) and d(ApTpApT) tetramers (Mellema et al., *1984) which show that the pA H8 is relatively unaffected by temperature while the Ap H8 moves downfield as the temperature is lowered.*

In this manner enough of the resonances were assigned to obtain computer simulated δ *and J values for most of the* ***d(ApTpA)*** *protons at 10 and 60°C. The exceptions were the pA H5'/H5" protons at 10°C, where the overlap of other resonances prevented the acquisition of their* δ*s and their Js to phosphorus. The data for* ***d(ApTpA)*** *is presented in Table 3.20.*

After assigning the ***d(ApTpA)*** *resonances, a COSY experiment was sufficient for sugar proton assignments in* ***d(Ape^{4}TpA)*** *(Figures 3.16 to 3.18). The base protons were assigned by following trends in the dimers,* ***d(Ape^{4}T)*** *and* ***d(e^{4}TpA)****, and by an NOE between the Ap H1' and the second most downfield H8 resonance (Figure 3.19). The overlap of most of the H5', H5" and H4' resonances prevented acquisition of all the* δ*s and Js for pe^{4}Tp and pA at 10°C and for pA at 60°C. The available computer simulated data for* ***d(Ape^{4}TpA)*** *is tabulated in Table 3.21.*

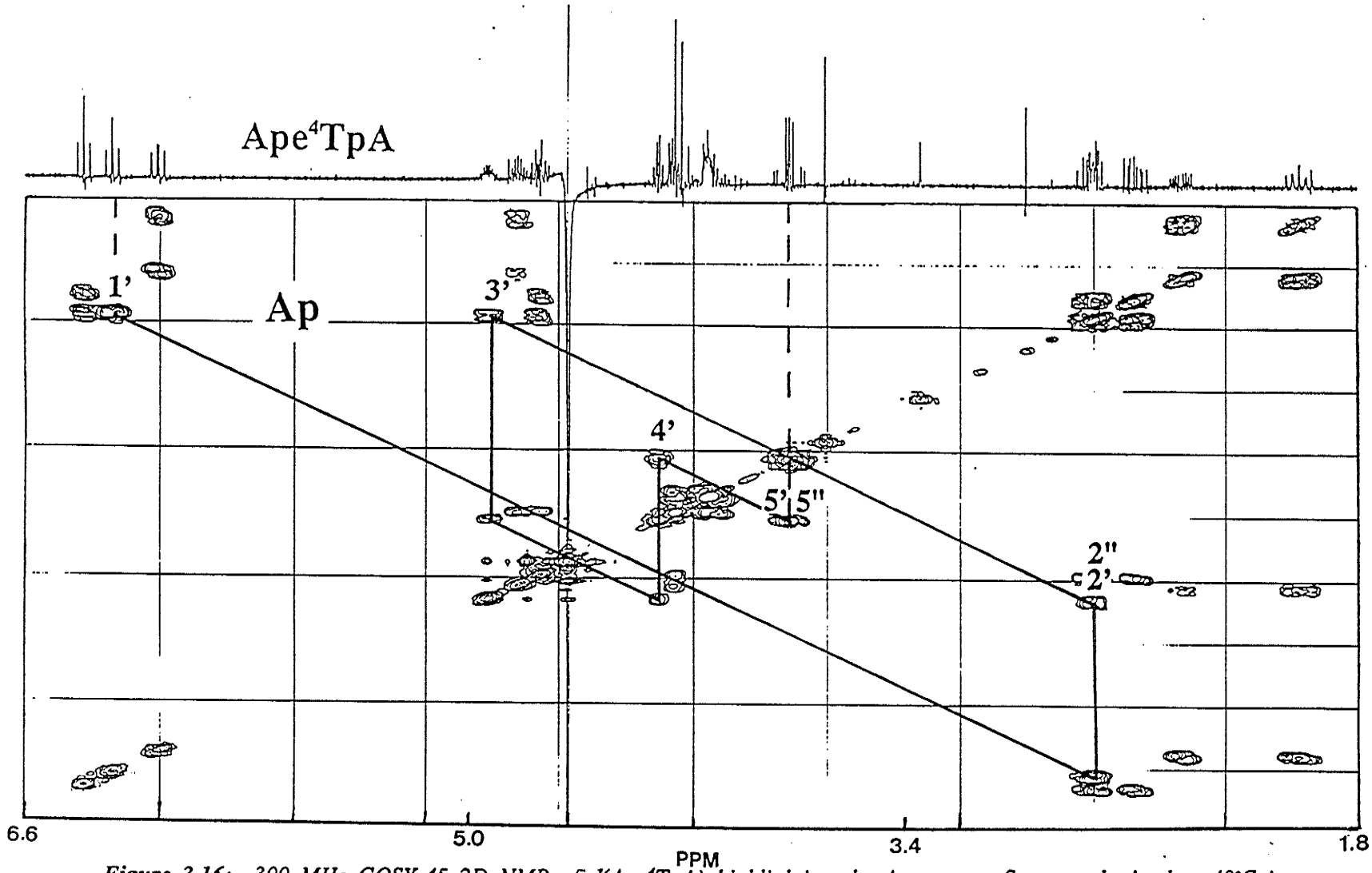

Figure 3.16: 300 MHz COSY-45 2D NMR of d(Ape⁴TpA) highlighting the Ap sugar. Spectra obtained at 40°C in NMR buffer. The data were processed with a sine-bell function in both domains followed by symmetrization to produce a final 512 x 512 W matrix.

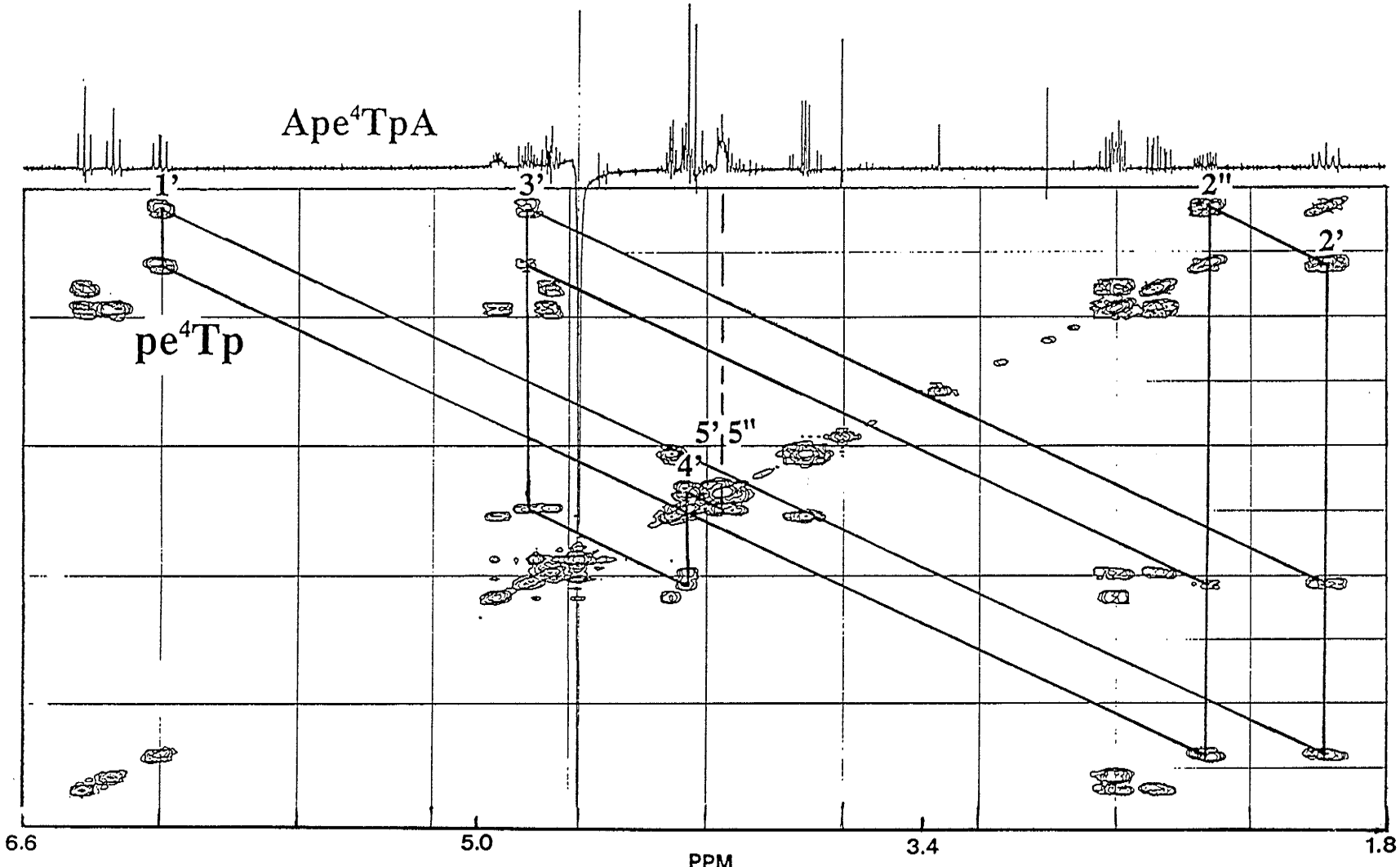

Figure 3.17: 300 MHz COSY-45 2D NMR of d(Ape⁴TpA) highlighting the pe⁴Tp sugar. Spectra obtained at 40°C in NMR buffer. The data were processed with a sine-bell function in both domains followed by symmetrization to produce a final 512 x 512 W matrix.

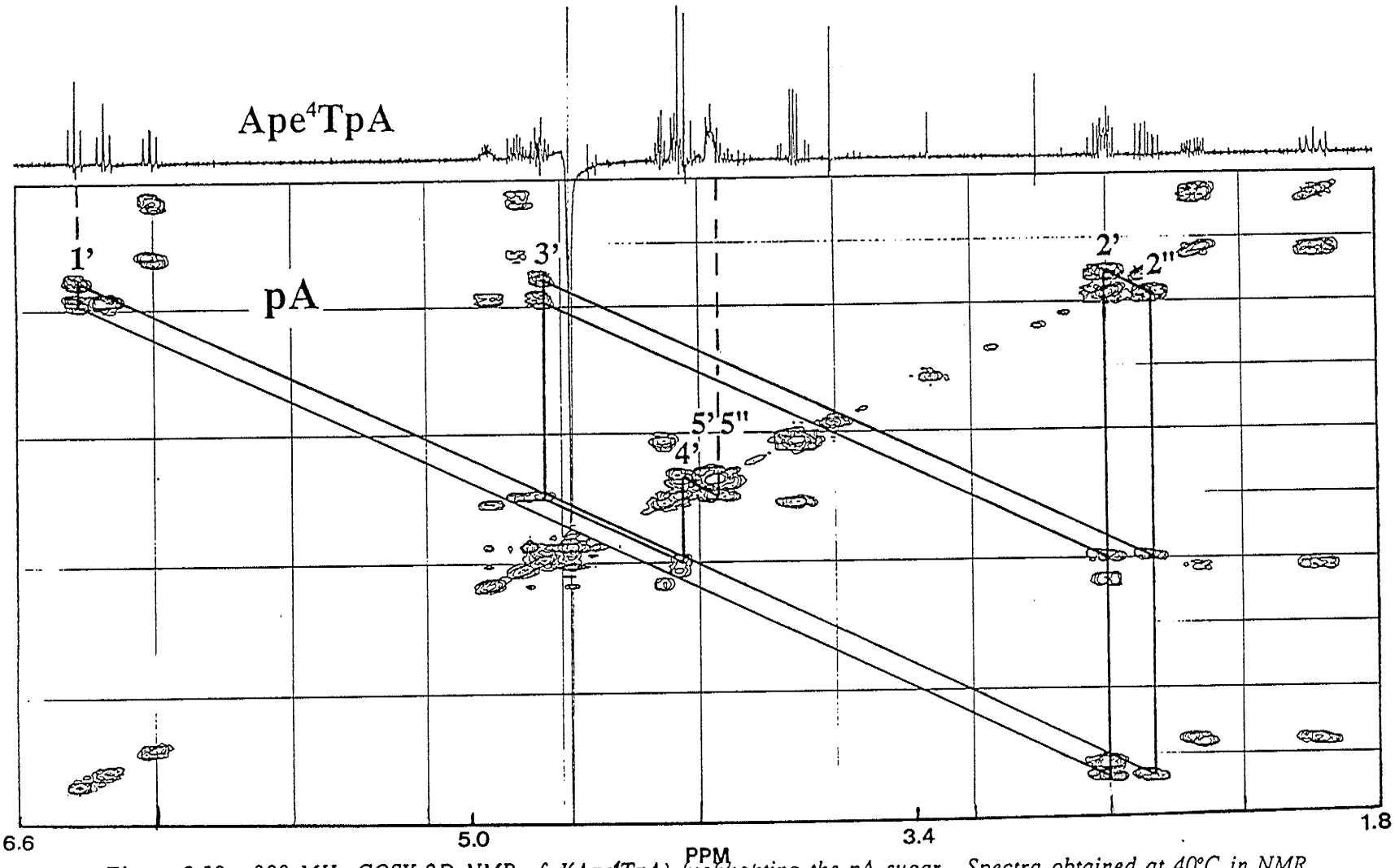

Figure 3.18: 300 MHz COSY 2D NMR of d(Ape⁴TpA) highlighting the pA sugar. Spectra obtained at 40°C in NMR buffer. The data were processed with a sine-bell function in both domains followed by symmetrization to produce a final 512 x 512 W matrix.

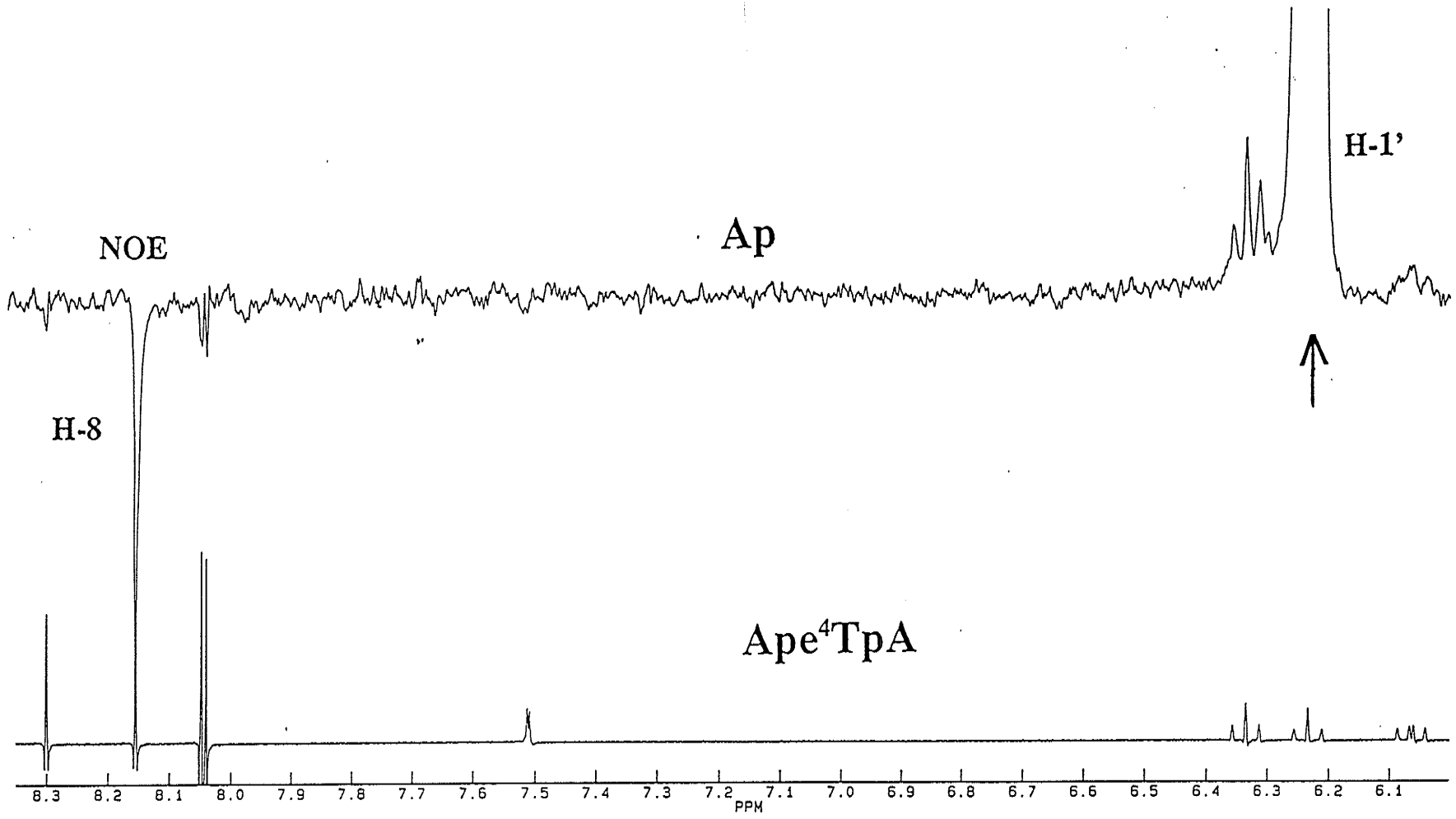

***Figure 3.19**: Result of the 300 MHz difference NOE experiment used to assign the H8 resonance of Ap via the irradiation of H1' (solid arrow). Parameters: D1 = 4.0 sec, D2 = 5.0 sec.*

3.5 TETRAMERS:

The RELAY spectra used to assign the sugar protons of ***d(e⁴TpApe⁴TpA)*** *are reproduced in Figures 3.20 to 3.23 with the magnetization transfer pathways highlighted for each sugar. Coherence transfer from H1' to H3' was observed but some cross peaks are absent for H2' and/or H2" to H4'. However, the H4', H5', H5" overlap was too extensive to obtain much coupling information. The 5'-terminal sugar was recognized by the absence of vicinal phosphorus coupling to the H5'/H5" protons. The pe⁴Tp sugar was then identified on the basis of similar H2'/H2" resonance patterns in comparison to the e⁴Tp unit of* ***d(e⁴TpApe⁴TpA)*** *and the pe⁴Tp unit of* ***d(Ape⁴TpA)****. Furthermore, the pe⁴Tp H1'* δ *was positioned upfield, near the e⁴Tp H1'* δ*, as expected from the strong ring current influences of adenosine 3' to these pyrimidines in a right-handed stack (see Chapter 5). Upon assigning the thymidine sugars, the dA sugars were distinguished by the absence of phosphorus coupling to the 3'-terminal H3'.*

In the two mono-alkylated tetramers, ***d(e⁴TpApTpA)*** *and* ***d(TpApe⁴TpA)****, the only sugar protons studied were the H1's. These H1'* δ*s were assigned by comparing the spectra of* ***d(e⁴TpApT)*** *and* ***d(TpApe⁴TpA)*** *to* ***d(e⁴TpApe⁴TpA)*** *at various temperatures. For the dA nucleotides there were only minor differences attributable to the substitution of a neighbouring e⁴T base for a T base. For instance, the* ***d(TpApe⁴TpA)*** *and* ***d(e⁴TpApe⁴TpA)*** *H1'* δ*s assigned to pA are identical at 10°C (6.317 ppm) while the pAp H1'* δ*s differ slightly (6.180 and 6.187 ppm, respectively). Similar arguments were used to assign the downfield H1' resonance in* ***d(e⁴TpApTpA)*** *to pA.*

In contrast, the pyrimidine H1's were too close together in both mono-alkylated tetramers to allow assignment using similar arguments. Instead the H1' with a smaller coupling constant sum ($^3J_{1'-2'} + {}^3J_{1'-2''} = \Sigma 1'$*) was assigned to the O4-alkylated nucleotide, a feature noted in the monomers (Birnbaum* et al.*, 1988), dimers and trimers (Chapter 5). For example, in* ***d(TpApe⁴TpA)****, one* Σ*1' is 1.4 Hz smaller at 10°C and was therefore assigned*

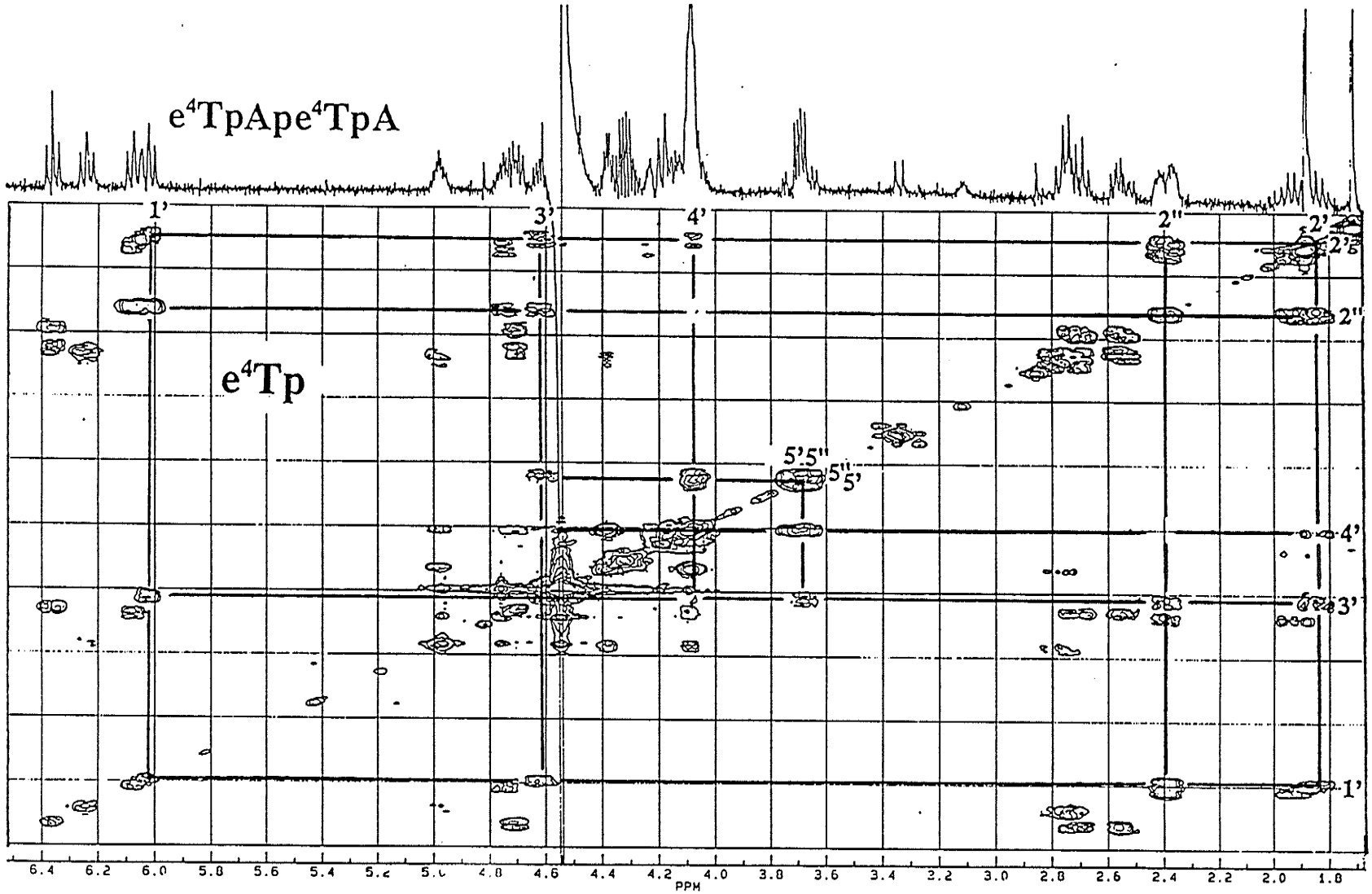

Figure 3.20: 300 MHz RELAY 2D NMR of d(e⁴TpAp⁴TpA) highlighting the e⁴Tp sugar. Spectra obtained at 45°C in NMR buffer. The data were processed with a sine-bell function in both domains followed by symmetrization to produce a final 512 x 512 W matrix.

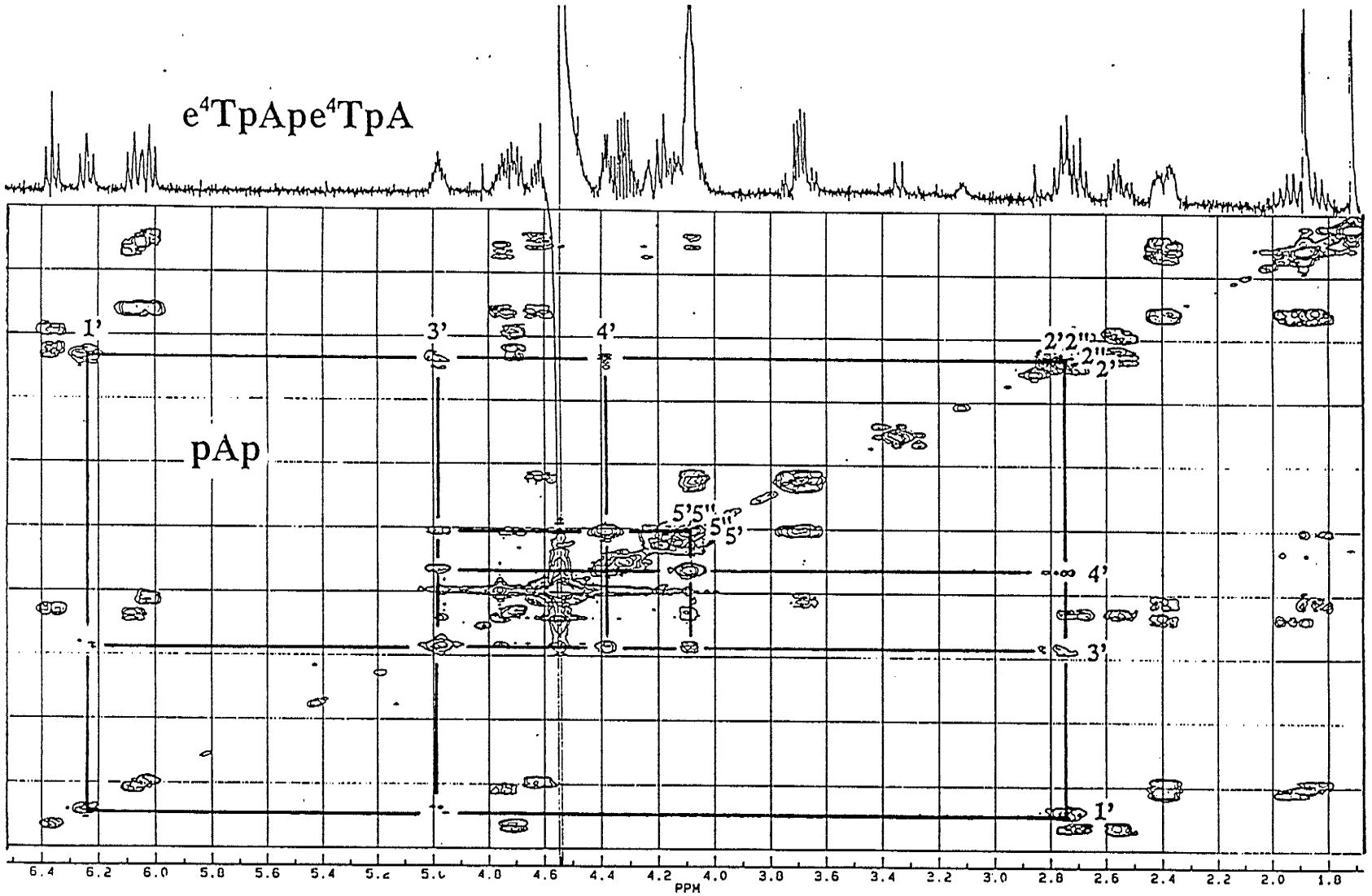

Figure 3.21: 300 MHz RELAY 2D NMR of d(e⁴TpAp⁴TpA) highlighting the pAp sugar. Spectra obtained at 45°C in NMR buffer. The data were processed with a sine-bell function in both domains followed by symmetrization to produce a final 512 x 512 W matrix.

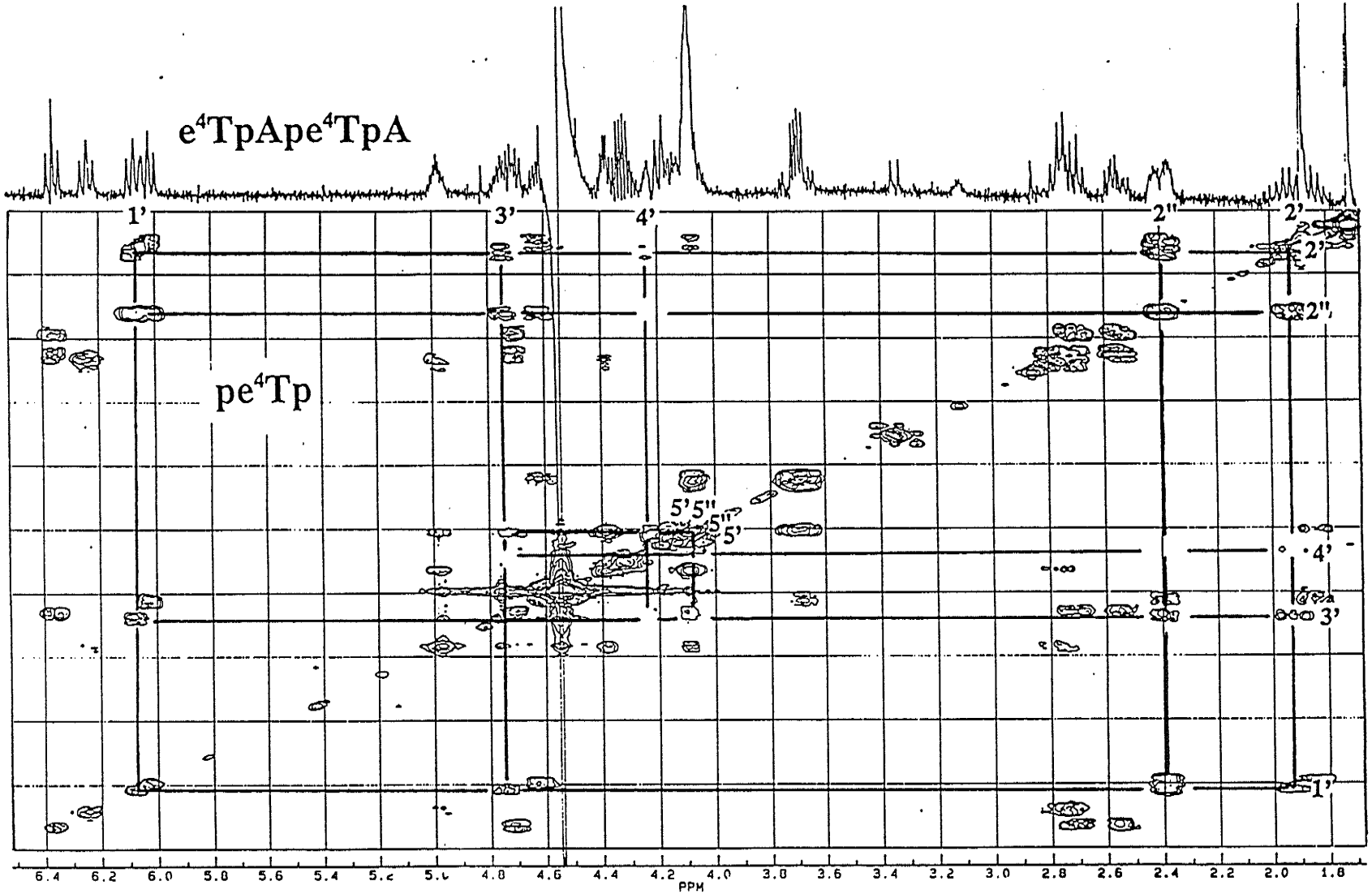

Figure 3.22: 300 MHz RELAY 2D NMR of d(e⁴TpAp⁴TpA) highlighting the pe⁴Tp sugar. Spectra obtained at 45°C in NMR buffer. The data were processed with a sine-bell function in both domains followed by symmetrization to produce a final 512 x 512 W matrix.

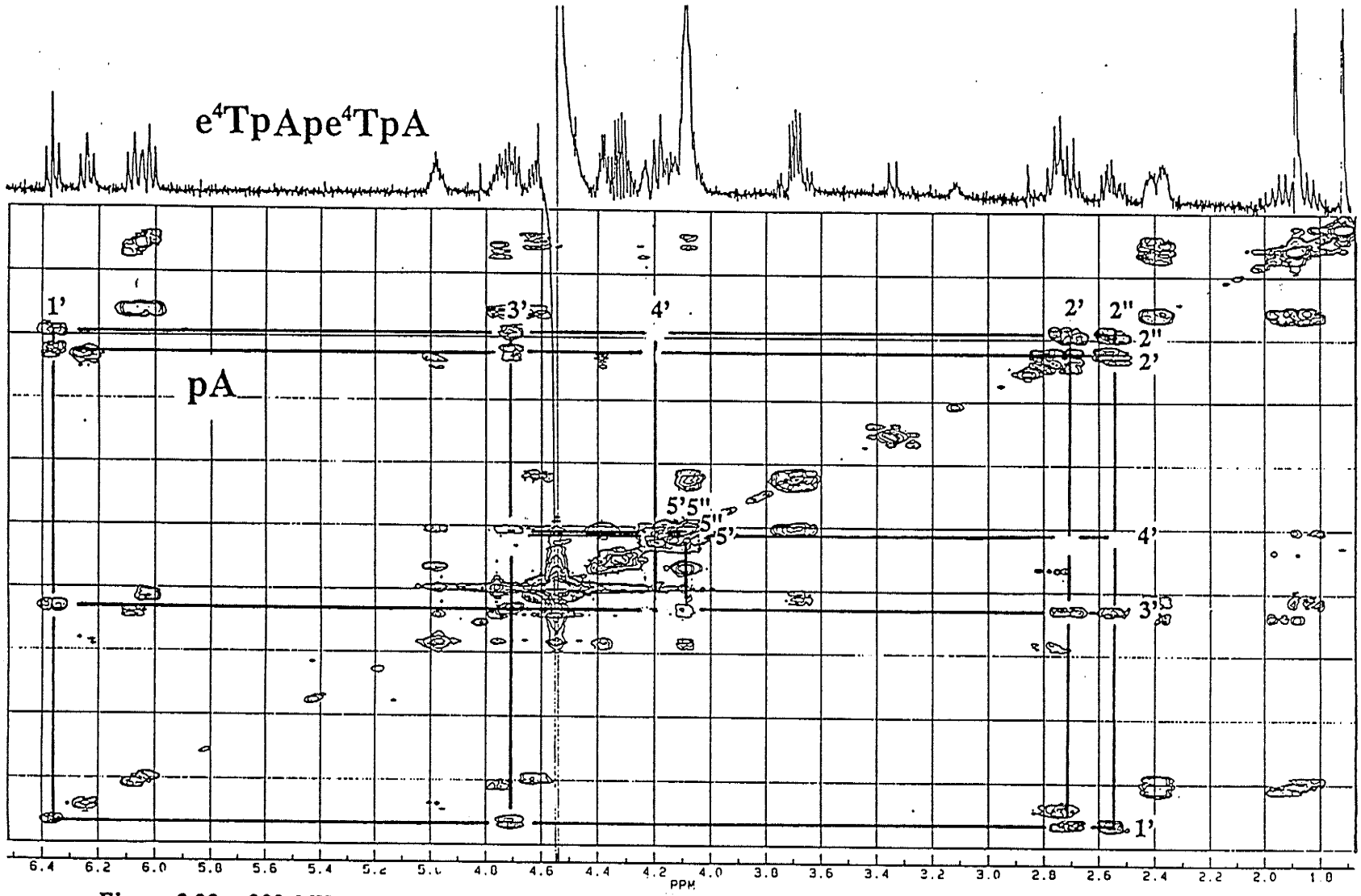

***Figure 3.23**: 300 MHz RELAY 2D NMR of d(e⁴TpAp⁴TpA) highlighting the pA sugar. Spectra obtained at 45°C in NMR buffer. The data were processed with a sine-bell function in both domains followed by symmetrization to produce a final 512 x 512 W matrix.*

to the Tp unit. In ***d(e⁴TpApTpA)*** *the e⁴Tp and pTp H1' resonances overlapped and were broad at low temperature therefore similar arguments could only be used at high temperature to distinguish between the two protons (a 0.8 Hz Σ1' difference at 70°C).*

The e⁴T H6 of ***d(TpApe⁴TpA)*** *and* ***d(e⁴TpApTpA)*** *was identified on the basis of its downfield shift, in comparison to the T H6, due to O4-ethylation (Birnbaum* et al., *1988). These e⁴T H6s also had a characteristically 0.1 Hz smaller $^4J_{H6\text{-}Me5}$ in comparison to T. The H6 resonances of* ***d(e⁴TpApe⁴TpA)*** *were then assigned by comparing their δs with those for the singularly O4-ethylated tetramers as displayed in Figure 3.24 (27°C).*

After assigning the H6s, the Me5s of ***d(e⁴TpApe⁴TpA)*** *were identified by cross peaks in the RELAY experiment. In the other two tetramers the Me5 belonging to the O4-alkylated base was assigned to the resonance with the smaller $^4J_{H6\text{-}Me5}$.*

The assignment of the adenine protons in the tetramers was more difficult. As with ***d(Ape⁴T)***, ***d(ApT)***, ***d(TpA)***, ***d(e⁴TpA)***, ***d(Ape⁴TpA)*** *and* ***d(ApTpA)***, *the downfield signals were assigned to H8, the upfield ones to H2. In* ***d(Ape⁴TpA)*** *the most upfield H8 resonance was assigned with an NOE from the Ap H1' and it was observed that this H8 moved more with temperature in comparison to the pA H8. In normal d(TpApTpA) Mellema* et al. *(1984) also reported little temperature dependence of the pA H8 resonance. On the basis of these observations, the tetramer H8 that varied least with temperature was assigned to the pA unit.*

Arguments similar to those used for the assignment of the H2 resonances of ***d(ApTpA)*** *and* ***d(Ape⁴TpA)*** *lead to the assignment of the downfield resonance in the three tetramers to pA. Furthermore, two pyrimidine bases surrounding an adenine (pAp) should produce a greater upfield shift of H2 in comparison to one neighbouring pyrimidine base next to an adenine (pA).*

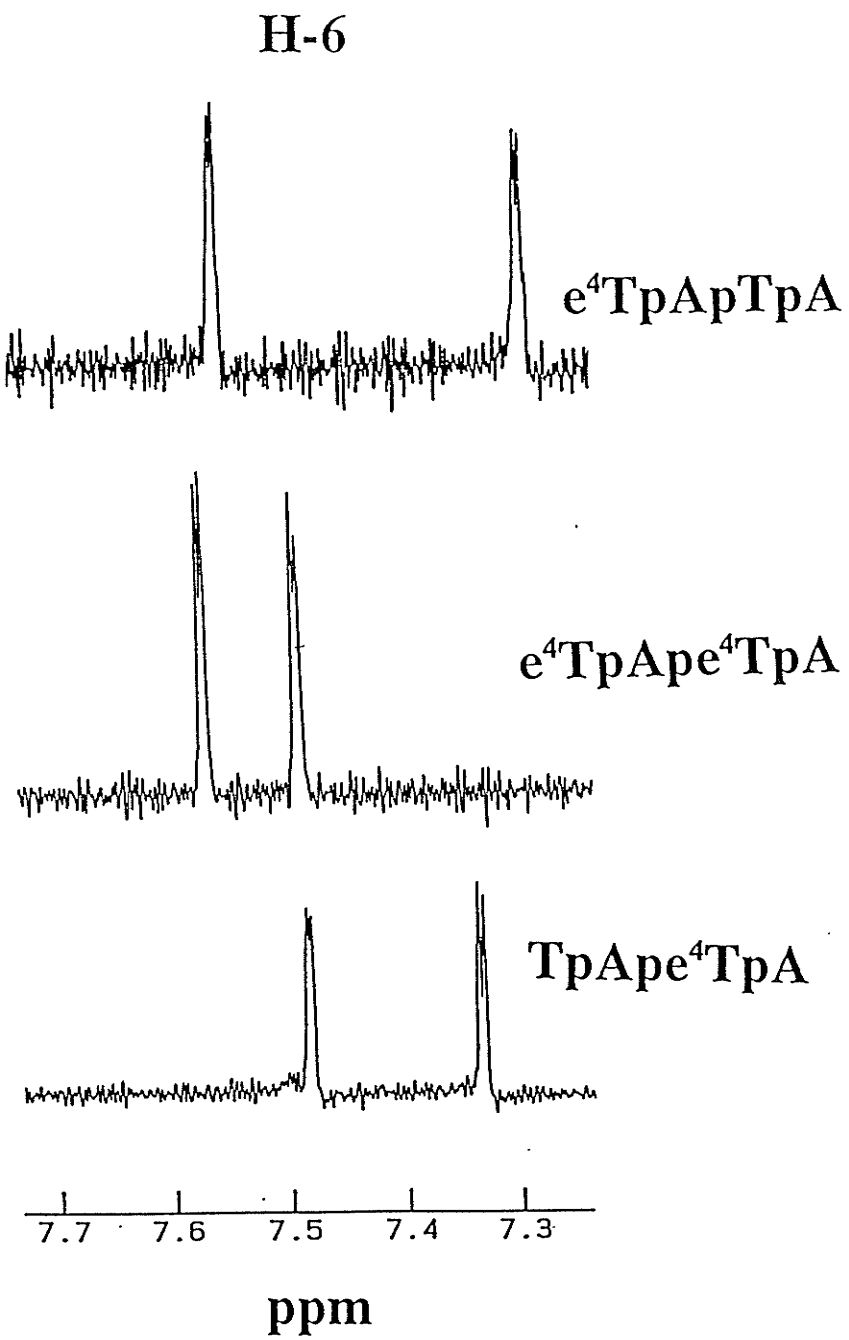

Figure 3.24: 300 MHz NMR spectra of the upfield region containing the H6 protons of d(e⁴TpApTpA), d(e⁴TpApe⁴TpA) and d(TpApe⁴TpA) (27°C).

3.6 CARBON-13:

Proton decoupled natural abundance ^{13}C (75.5 MHz) NMR spectra were obtained for ***dT, i^{4}dT, d(i^{4}TpT), d(Tp^{4}T), d(TpT), d(TpTpT), and d(Tpi^{4}TpT)*** *at 27°C (Buchko* et al., *1989b) using the POWGATE.AU pulse program described in the Appendix. Except for* ***d(Tpi^{4}TpT)****, the oligomer concentrations were less than 9 mM and therefore ^{13}C spectral acquisition required overnight data collection. In the absence of an access to more spectrometer time, higher spectrometer fields, or more oligomer, the ^{13}C studies were limited to these latter molecules.*

The base carbons of the O4-isopropylated molecules were assigned by the downfield shift of their C2, C4 and C6, and the upfield shift of their C5, as observed in the ***r^{4}dT*** *monomers relative to* ***dT*** *(Birnbaum* et al., *1988). The sugar carbons were assigned on the basis of: i) trends in the ^{13}C-^{31}P coupling constants for nucleotides and DNA oligonucleotides (Rycyna and Alderfer, 1985; Rycyna* et al., *1988) and ii) selective ^1H continuous wave decoupling experiments to assign the Me5, C1', and C3' resonances of* ***d(Tpi^{4}TpT)****. The δs and Js for these molecules are presented in Tables 3.24 and 3.25.*

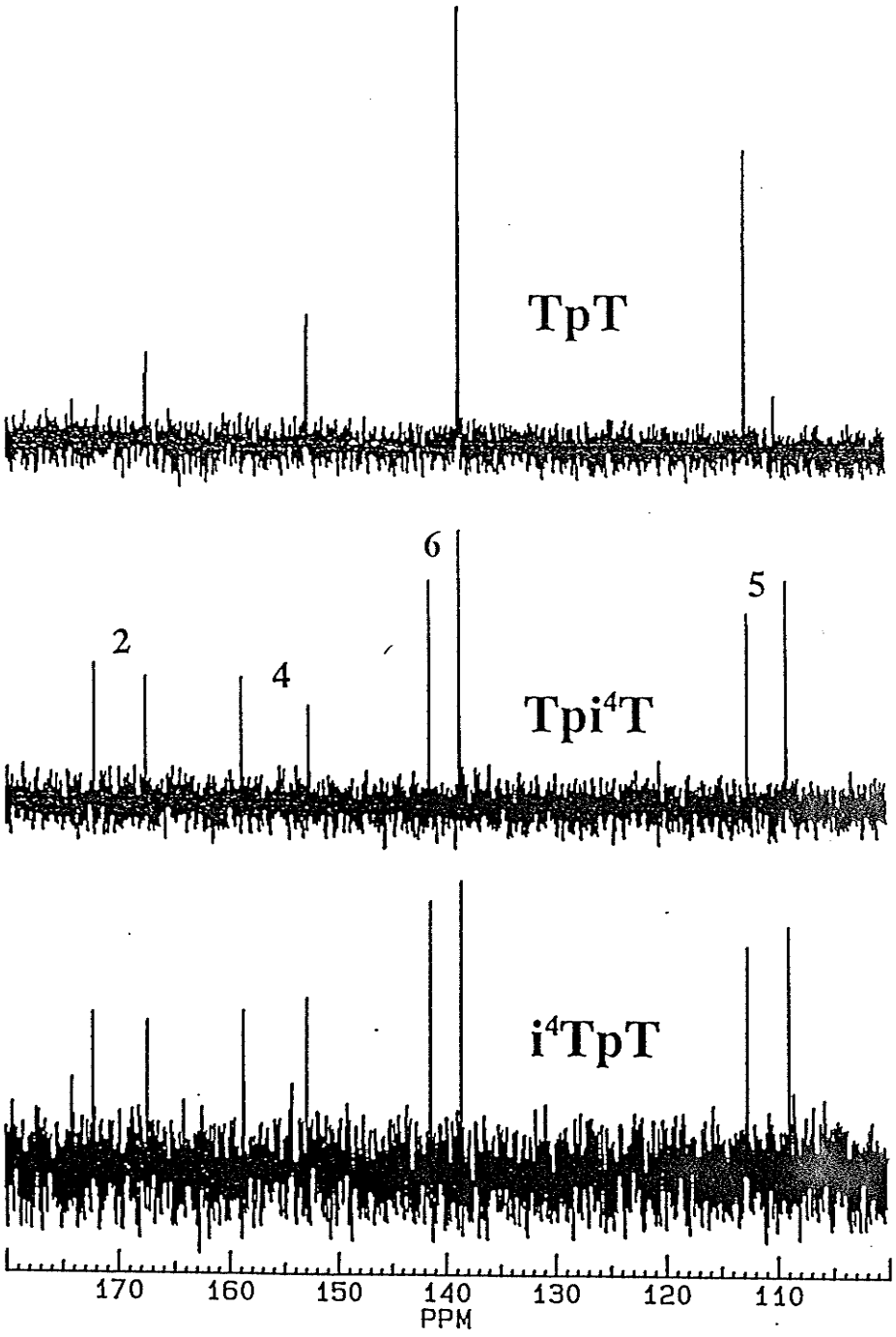

Figure 3.25: 75.5 MHz ^{13}C proton decoupled spectra of the endocyclic base carbons of d(TpT), d(Tpi^{4}T), and d(i^{4}TpT) (27°C).

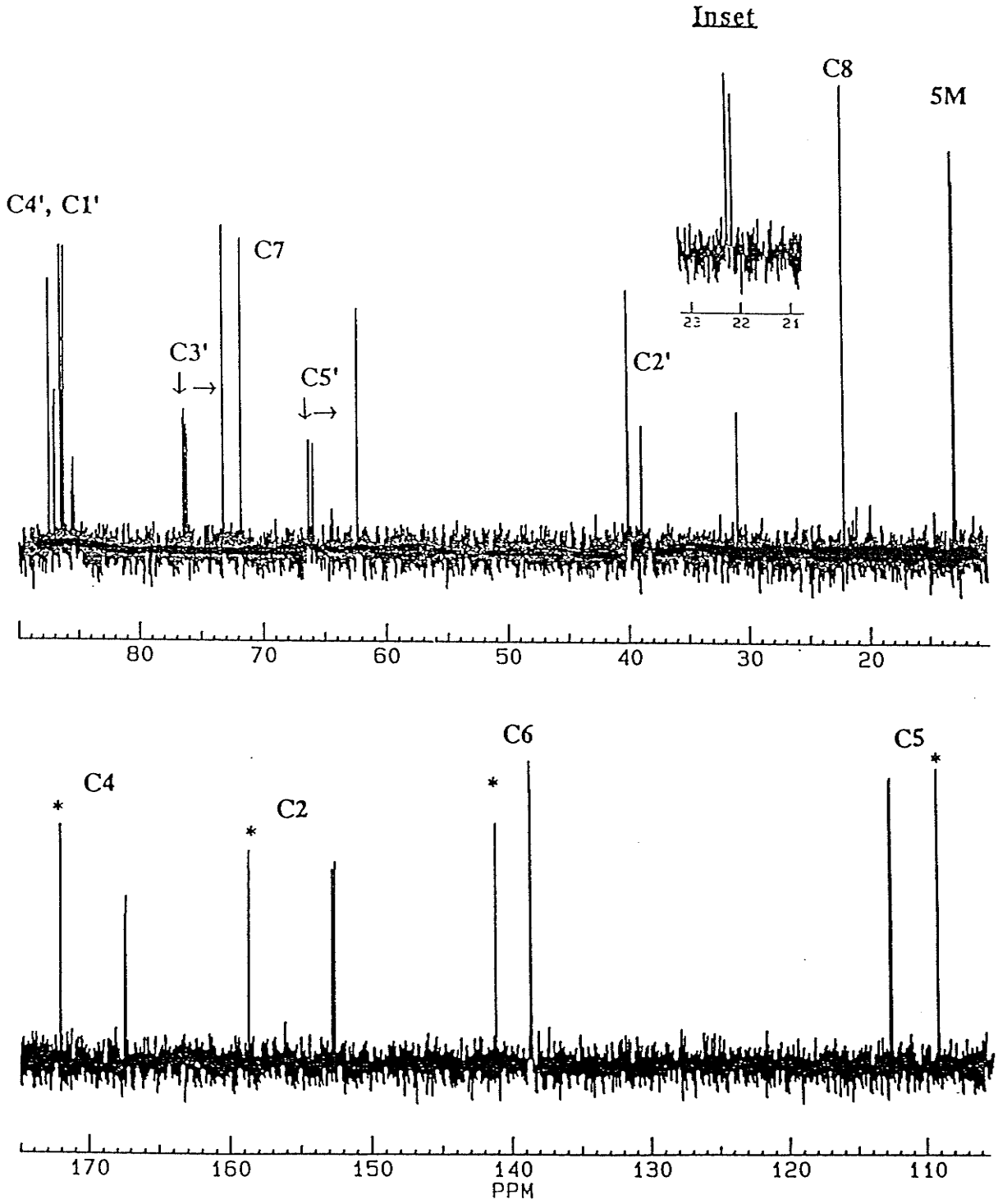

Figure 3.26: 75.5 MHz ^{13}C proton decoupled spectrum of d(Tpi^{4}TpT) (27°C). The signal at 31 ppm is due to tert-*butanol. C7 = α-carbon of the O4-isopropyl group, C8 = methyl carbons of the O4-isopropyl group, * = e^{4}T base carbons. INSET: Methyl carbons of the O4-isopropyl group of d(i^{4}TpT) (27°C).*

Table 3.1. ^{1}H chemical shifts (ppm) and coupling constants (Hz) of m^4dT, e^4dT, and i^4dT[a]

	m^4dT	e^4dT	i^4dT		m^4dT	e^4dT	i^4dT
δ				J			
1'	6.28	6.28	6.29	1'2'	6.5	6.6	6.6
2'	2.32	2.32	2.32	1'2"	6.5	6.5	6.5
2"	2.49	2.49	2.48	2'2"	-14.1	-14.2	-14.1
3'	4.46	4.46	4.46	2'3'	6.6	6.7	6.7
4'	4.09	4.09	4.08	2"3'	4.3	4.3	4.3
5'	3.88	3.87	3.87	3'4'	4.3	4.0	4.1
5"	3.79	3.79	3.78	4'5'	3.5	3.8	3.5
6	7.90	7.89	7.87	4'5"	5.1	5.1	5.2
Me5	1.99	1.99	1.97	5'5"	-12.6	-11.7	-11.7
8[b]	3.97	4.41	5.32	56	1.1	1.1	1.1
9[b]	----	1.39	1.36	89	----	7.1	6.2

[a]Data acquired at 300.1 MHz and 27°C for e^4dT and i^4dT, 270 MHz and 25°C for m^4dT. Data from Birnbaum *et al.* (1988).

[b]8 and 9 refer to the protons of the α and β carbons, respectively, of the O4-alkyl group.

Table 3.2. ^{1}H chemical shifts (ppm) of d(e^{4}TpT) and d(Tpe^{4}T)[a]

	d(e^{4}TpT)				d(Tpe^{4}T)			
	e^{4}Tp		pT		Tp		pe^{4}T	
δ	20°C	70°C	20°C	70°C	20°C	70°C	20°C	70°C
1'	6.104	6.189	6.270	6.259	6.127	6.157	6.293	6.285
2'	2.409	2.329	2.336[b]	2.339	2.346	2.318	2.323	2.304
2''	2.631	2.627	2.335[b]	2.362	2.519	2.513	2.443	2.466
3'	4.688	4.744	4.552	4.533	4.733	4.755	4.569	4.538
4'	4.191	4.200	4.098	4.118	4.144	4.140	4.150	4.154
5'	3.887	3.858	4.148	4.120	3.811	3.806	4.174	4.148
5''	3.806	3.784	4.063	4.064	3.760	3.748	4.079	4.077
6	7.927	7.822	7.667	7.622	7.662	7.580	7.902	7.861
Me5	1.939	1.951	1.800	1.852	1.861	1.869	1.948	1.965
-CH_2(A)	4.342	4.403	----	----	----	----	4.314	4.367
-CH_2(B)	4.370	4.403	----	----	----	----	4.347	4.386
-CH_3	1.375	1.368	---	---	----	---	1.351	1.349

[a]Data acquired at 300.1 MHz, 0.1 M NaCl, Conc: d(e^{4}TpT) (7.0 mM), d(Tpe^{4}T) (1.7 mM).
[b]Estimated since δ2'~δ2''.

Table 3.3. Coupling constants (Hz) of d(e^{4}TpT) and d(Tpe^{4}T)[a]

	d(e^{4}TpT)				d(Tpe^{4}T)			
	e^{4}Tp		pT		Tp		pe^{4}T	
J	20°C	70°C	20°C	70°C	20°C	70°C	20°C	70°C
1'2'	5.9	6.5	6.5 ┐	6.9	6.9	6.7	6.5	6.6
1'2''	5.9	6.4	6.5 ┘	6.7	6.2	6.6	6.5	6.6
2'2''	-13.9	-14.2	-14.0[b]	-14.2	-14.1	-14.2	-14.1	-14.1
2'3'	6.1	6.7	5.9 ┐	6.7	6.6	6.6	6.7	6.7
2''3'	6.1	4.3	5.9 ┘	4.2	3.9	3.8	4.8	4.3
3'4'	5.3	4.2	4.5	3.7	3.8	3.7	4.5	4.4
4'5'	2.9	3.4	2.5	2.9	3.3	3.5	2.5	2.8
4'5''	4.1	4.8	3.0	4.2	4.5	5.0	3.3	4.5
5'5''	-12.8	-12.6	-11.5	-11.7	-12.7	-12.6	-11.7	-11.9
56	1.2	1.2	1.3	1.3	1.3	1.3	1.1	1.2
78[c]	7.1	7.1	---	---	---	---	7.1	7.1
AB[d]	-10.6	---	---	---	---	---	-10.6	---
3'P[e]	6.4	6.7	---	---	6.6	6.5	---	---
5'P	---	---	3.9	4.7	---	---	4.5	4.8
5''P	---	---	3.6	5.0	---	---	4.1	4.5

[a]Data acquired at 300.1 MHz, 0.1 M NaCl, Conc: d(e^{4}TpT) (7.0 mM), d(Tpe^{4}T) (1.7 mM).

[b]When $\delta(2') \sim \delta(2'')$, $^2J_{2'-2''}$ is arbitrary and only the sum of the connected couplings (]) is significant.

[c]J_{7-8} is between the methylene and methyl protons of the O4-ethyl group

[d]J_{A-B} is the geminal coupling constant of the methylene protons of the O4-ethyl group.

[e]A $^4J_{4'-P}$ of 2.0 to 2.5 Hz was observed in some of the spectra.

Table 3.4. ^{1}H Chemical shifts (ppm) of d(TpT), d(i^{4}TpT), and d(Tpi^{4}T)[a]

	d(TpT)				d(i^{4}TpT)				d(Tpi^{4}T)			
	Tp		pT		i^{4}Tp		pT		Tp		pi^{4}T	
σ	20°C	70°C	20°C	70°C	20°C	70°C	20°C	70°C	20°C	70°C	20°C	70°C
1'	6.189	6.198	6.301	6.273	6.135	6.201	6.278	6.261	6.157	6.168	6.286	6.281
2'	2.333	2.344	2.368	2.369[b]	2.371	2.317	2.341[b]	2.342	2.332	2.315	2.318	2.301
2"	2.544	2.541	2.346	2.362[b]	2.627	2.624	2.344[b]	2.364	2.504	2.505	2.450	2.468
3'	4.752	4.773	4.578	4.543	4.716	4.754	4.555	4.534	4.742	4.757	4.561	4.534
4'	4.167	4.162	4.108	4.115	4.200	4.201	4.109	4.123	4.152	4.141	4.159	4.162
5'	3.811	3.818	4.136	4.116	3.871	3.851	4.145	4.119	3.792	3.795	4.170	4.144
5"	3.764	3.760	4.063	4.063	3.798	3.780	4.064	4.065	3.748	3.740	4.078	4.076
6	7.650	7.584	7.671	7.629	7.889	7.800	7.670	7.624	7.639	7.573	7.886	7.848
Me5	1.859	1.874	1.870	1.890	1.925	1.934	1.814	1.858	1.857	1.866	1.944	1.952
-CH_3(A)	----	----	----	----	1.324	1.339	----	----	----	----	1.309	1.320
-CH_3(B)	----	----	----	----	1.365	1.350	----	----	----	----	1.331	1.328
-CH	----	----	----	----	5.243	5.292	----	----	----	----	5.232	5.269

[a]Data acquired at 300.1 MHz, 0.1 M NaCl, Conc: **d(TpT)** (1.8 mM), **d(i^{4}TpT)** (4.8 mM), **d(Tpi^{4}T)** (8.3 mM).
[b]Estimated since δ2' ~ δ2".

Table 3.5. Coupling constants (Hz) of d(TpT), d(i^{4}TpT), and d(Tpi^{4}T)[a]

	d(TpT)				d(i^{4}TpT)				d(Tpi^{4}T)			
	Tp		pT		i^{4}Tp		pT		Tp		pi^{4}T	
J	20°C	70°C	20°C	70°C	20°C	70°C	20°C	70°C	20°C	70°C	20°C	70°C
1'2'	7.4	7.0	6.8	6.8	6.2	6.5	6.6	6.7	7.4	7.4	6.5	6.6
1'2"	6.2	6.4	6.8	6.8	6.3	6.4	6.6	6.9	6.1	6.3	6.5	6.6
2'2"	-14.1	-14.1	-14.3	-14.2[b]	-14.0	-14.2	-14.1[b]	-14.1	-14.0	-14.1	-14.0	-14.1
2'3'	6.4	6.8	6.7	5.5	6.4	6.7	5.7	6.2	6.4	6.7	6.6	6.7
2"3'	3.5	3.4	4.2	5.5	5.0	4.1	5.7	4.6	3.4	3.4	4.5	4.3
3'4'	3.5	3.5	3.9	4.1	4.6	4.2	4.1	3.7	3.3	3.4	4.4	4.3
4'5'	3.4	3.5	2.3	2.6	3.1	3.5	2.5	2.8	3.4	3.6	2.6	2.7
4'5"	4.6	4.9	3.3	4.5	4.3	4.9	3.0	4.3	4.5	4.8	3.6	4.5
5'5"	-12.6	-12.4	-11.5	-11.8	-12.8	-12.5	-11.4	-11.8	-12.5	-12.4	-11.9	-11.9
56	1.3	1.3	1.3	1.3	1.2	1.1	1.3	1.3	1.3	1.3	1.2	1.2
78[c]	---	---	---	---	6.2	6.2	---	---	---	---	6.2	6.2
3'P	6.5	6.7	---	---	6.5	6.8	---	---	6.5	6.7	---	---
5'P	---	---	4.4	4.5	---	---	4.1	4.8	---	---	4.5	4.8
5"P[d]	---	---	4.2	5.1	---	---	3.8	5.0	---	---	4.2	4.9

[a]Data acquired at 300 .1MHz, 0.1 M NaCl, Conc: **d(TpT)** (1.8 mM), **d(i^{4}TpT)** (4.8 mM), **d(Tpi^{4}T)** (8.3 mM). Data for **d(TpT)** from Rycyna and Alderfer, (1985).

[b]When δ2' ~ δ2", $^2J_{2'-2"}$ is arbitrary and only the sum of the connected couplings (]) is significant.

[c]J_{7-8} is between the methine and methyl protons of the O4-isopropyl group.

[d]A $^4J_{P-H4'}$ of 2.0 to 2.5 Hz was observed in some of the spectra.

Table 3.6. ^{1}H Chemical shifts (ppm) of d(p^{4}TpT), d(b^{4}TpT), and d(ib^{4}TpT)[a]

	d(p^{4}TpT)				d(b^{4}TpT)				d(ib^{4}TpT)			
	p^{4}Tp		pT		b^{4}Tp		pT		ib^{4}Tp		pT	
σ	20°C	70°C	20°C	70°C	20°C	70°C	20°C	70°C	20°C	70°C	20°C	70°C
1'	6.110	6.192	6.269	6.258	6.114	6.190	6.268	6.256	6.120	6.194	6.269	6.257
2'	2.397	2.326	2.337[b]	2.337	2.400	2.326	2.336[b]	2.339	2.396	2.325	2.339[b]	2.348[b]
2"	2.630	2.628	2.337[b]	2.364	2.629	2.625	2.337[b]	2.360	2.630	2.626	2.339[b]	2.348[b]
3'	4.696	4.748	4.551	4.533	4.694	4.743	4.550	4.531	4.701	4.747	c	c
4'	4.193	4.202	4.102	4.117	4.193	4.200	4.099	4.115	4.195	4.200	c	c
5'	3.884	3.857	4.147	4.120	3.881	3.855	4.145	4.117	3.882	3.856	c	c
5"	3.805	3.785	4.064	4.065	3.803	3.781	4.061	4.063	3.804	3.783	c	c
6	7.921	7.823	7.666	7.623	7.914	7.818	7.661	7.619	7.920	7.824	7.663	7.621
Me5	1.945	1.958	1.803	1.854	1.942	1.953	1.804	1.851	1.963	1.972	1.805	1.853
-CH_2(A)	4.241	4.308	----	----	4.290	4.352	----	----	4.066	4.133	----	----
-CH_2(B)	4.279	4.308	----	----	4.342	4.369	----	----	4.122	4.153	----	----
-CH_2-(8)[d]	1.784	1.775	----	----	1.758	1.751	----	----	2.089	2.089	----	----
-CH_2-(9)	----	----	----	----	1.448	1.441	----	----	----	----	----	----
-CH_3	0.984	0.975	----	----	0.933	0.931	----	----	0.989	0.981	----	----

[a]Data acquired at 300.1 MHz, 0.1 M NaCl, Conc: **d(p^{4}TpT)** (13.9 mM), **d(b^{4}TpT)** (2.4 mM), **d(ib^{4}TpT)** (3.2 mM).

[b]Estimated since δ2' ~ δ2".

[c]Due to extensive overlap, primarily due to the methylene resonances of the O4-isobutyl group, these values are not available.

[d]Resonances of the β carbon protons of the O4-alkyl group of **d(p^{4}TpT)** and **d(b^{4}TpT)** or the methine proton of the O4-isopropyl group of **d(ib^{4}TpT)**.

Table 3.7. Coupling constants (Hz) of d(p^{4}TpT), d(b^{4}TpT), and d(ib^{4}TpT)[a]

	d(p^{4}TpT)				d(b^{4}TpT)				d(ib^{4}TpT)			
	p^{4}Tp		pT		b^{4}Tp		pT		ib^{4}Tp		pT	
J	20°C	70°C	20°C	70°C	20°C	70°C	20°C	70°C	20°C	70°C	20°C	70°C
1'2'	5.7	6.5	6.6	6.6	5.8	6.5	6.6	6.7	6.2	6.5	6.6	6.8
1'2"	6.4	6.4	6.6	6.9	6.2	6.4	6.6	6.8	6.2	6.4	6.6	6.8
2'2"	-14.0	-14.2	-14.1[b]	-14.1	-13.9	-14.2	-14.1[b]	-14.3	-14.0	-14.2	-14.1[b]	c
2'3'	6.6	6.7	5.9	6.3	6.5	6.8	5.9	6.8	5.8	6.6	c	c
2"3'	5.4	4.2	5.9	4.3	5.6	4.3	5.9	4.0	5.4	4.2	c	c
3'4'	4.9	4.1	4.3	3.7	4.6	4.2	4.5	3.8	4.3	4.3	c	c
4'5'	3.0	3.5	2.6	2.9	3.0	3.5	2.4	3.0	3.2	3.5	c	c
4'5"	4.2	4.8	3.1	4.4	4.3	4.9	2.7	4.2	4.4	4.8	c	c
5'5"	-12.8	-12.5	-11.5	-11.7	-12.8	-12.6	-11.2	-11.8	-12.8	-12.5	c	c
56	1.2	1.1	1.3	1.2	1.2	1.2	1.3	1.3	1.2	1.1	1.3	1.3
A8[d]	6.7	6.5	----	----	6.6	6.4	----	----	6.7	6.8	----	----
B8[d]	6.6	6.5	----	----	6.4	6.5	----	----	6.6	6.5	----	----
AB[e]	-10.5	----	-----	----	-10.6	-10.4	----	----	-10.4	-10.4	----	----
89	7.4	7.4	----	----	7.5	7.4	----	----	6.7[f]	6.7[f]	----	----
9(10)	----	----	----	----	7.5	7.4	----	----	----	----	----	----
3'P	6.6	6.7	----	----	6.9	6.9	----	---	7.1	6.6	----	----
4'P	----	----	2.5	2.3	----	----	2.1	2.1	----	----	c	c
5'P	----	----	3.9	5.3	----	----	3.9	4.5	----	----	c	c
5"P	----	----	3.6	4.8	----	----	3.9	4.9	----	----	c	c

[a]Data acquired at 300.1 MHz, 0.1 M NaCl, Conc: d(p^{4}TpT) (13.9 mM), d(b^{4}TpT) (2.4 mM), d(ib^{4}TpT) (3.2 mM).

[b]When δ2' ~ δ2", $^2J_{2'-2"}$ is arbitrary and only the sum of the connected couplings (]) is significant.

[c]Due to extensive overlap, primarily because of the methylene resonances of the O4-isobutyl group, these values are not available.

[d]J_{A-8} and J_{B-8} are between the magnetically non-equivalent α-methylene protons and the proton(s) of the β-carbon of the O4-alkyl group.

[e]J_{A-B} is the geminal coupling constant of the α-methylene protons of the O4-alkyl group.

[f]Coupling constant between the -CH(8) and the methyl protons of the O4-isobutyl group.

Table 3.8. ^{1}H Chemical shifts (ppm) of d(m^{4}TpC), d(e^{4}TpC), and d(i^{4}TpC)[a]

	d(m^{4}TpC)				d(e^{4}TpC)				d(i^{4}TpC)			
	m^{4}Tp		pC		e^{4}Tp		pC		i^{4}Tp		pC	
σ	10°C	60°C	10°C	60°C	20°C	70°C	20°C	70°C	10°C	60°C	10°C	60°C
1'	6.146	6.207	6.234	6.254	6.172	6.215	6.242	6.256	6.183	6.219	6.244	6.258
2'	2.435	2.372	2.271	2.260	2.395	2.338	2.271	2.258	2.378	2.331	2.284	2.264
2"	2.609	2.613	2.395	2.418	2.605	2.611	2.403	2.422	2.599	2.604	2.400	2.420
3'	4.670	4.726	4.525	4.505	4.693	4.739	4.521	4.502	4.702	4.738	4.530	4.507
4'	4.198	4.203	4.107	4.136	4.200	4.202	4.127	4.137	4.204	4.201	4.131	4.141
5'	3.870	3.852	4.151	4.123	3.861	3.849	4.144	4.119	3.850	3.843	4.143	4.120
5"	3.794	3.778	4.059	4.060	3.788	3.777	4.059	4.055	3.783	3.773	4.059	4.055
6	7.906	c	7.859	7.841	7.873	7.807	7.852	7.841	7.855	7.794	7.859	7.845
H5 or Me5	1.943	1.954	5.939	6.011	1.949	1.956	5.966	6.022	1.931	1.937	5.971	6.024
-CH$_2$(A)[d]	----	----	----	----	4.354	4.405	----	----	1.327	1.339	----	----
-CH$_2$(B)[d]	----	----	----	----	4.369	4.405	----	----	1.352	1.346	----	----
-CH	----	----	----	----	----	----	----	----	5.247	5.288	----	----
-CH$_3$	6.234	6.254	----	----	1.369	1.365	----	----	----	----	----	----

[a]Data acquired at 300.1 MHz, 0.1 M NaCl, Conc: **d(m^{4}TpC)** (4.0 mM), **d(e^{4}TpC)** (1.8 mM), **d(i^{4}TpC)** (1.6 mM).

[b]Estimated since δ2' ~ δ2".

[c]Due to extensive overlap this value is not accurately obtainable.

[d]For **d(i^{4}TpC)** these δs are the magnetically non-equivalent methyl resonances of the O4-isopropyl group.

Table 3.9. Coupling constants (Hz) of d(m^{4}TpC), d(e^{4}TpC), and d(i^{4}TpC)[a]

	d(m^{4}TpC)				d(e^{4}TpC)				d(i^{4}TpC)			
	m^{4}Tp		pC		e^{4}Tp		pC		i^{4}Tp		pC	
I	10°C	60°C	10°C	60°C	20°C	70°C	20°C	70°C	10°C	60°C	10°C	60°C
1'2'	6.0	6.6	6.3	6.6	6.4	6.8	6.4	6.6	6.4	6.7	6.4	6.6
1'2"	6.1	6.5	6.4	6.5	6.3	6.4	6.5	6.5	6.2	6.3	6.5	6.5
2'2"	-14.0	-14.2	-13.9	-14.1	-14.1	-14.2	-14.0	-14.1	-14.3	-14.1	-14.0	-14.1
2'3'	6.7	6.8	6.6	6.7	6.3	7.0	6.7	6.7	6.6	6.7	6.6	6.7
2"3'	5.0	4.2	4.9	4.2	4.4	4.0	4.6	4.3	4.4	3.7	4.5	4.3
3'4'	3.9	4.0	5.1	4.6	4.3	3.9	4.6	4.0	3.8	3.6	4.2	4.3
4'5'	3.5	3.6	2.7	2.8	3.2	3.6	2.7	3.1	3.4	3.4	2.7	3.0
4'5"	4.4	4.9	3.1	4.3	4.4	4.9	3.4	4.4	4.5	4.9	3.6	4.0
5'5"	-12.8	-12.5	-11.6	-11.6	-12.8	-12.5	-11.5	-12.0	-12.7	-12.5	-12.0	-11.6
56[c]	1.2	1.1	7.6	7.5	1.1	1.1	7.6	7.5	1.2	1.2	7.6	7.5
78[d]	---	---	---	---	---	---	7.1	7.1	6.2	6.2	---	---
AB[e]	---	---	---	---	-10.6	---	---	---	---	---	---	---
3'P	7.0	6.8	---	---	6.9	6.9	---	---	6.7	6.7	---	---
4'P	---	---	2.6	2.1	---	---	2.3	1.9	---	---	2.4	2.2
5'P	---	---	4.5	4.9	---	---	4.4	4.9	---	---	4.4	4.9
5"P	---	---	3.7	4.7	---	---	4.3	5.1	---	---	4.6	5.1

[a]Data acquired at 300.1 MHz, 0.1 M NaCl, Conc: d(m^{4}TpC) (1.6 mM), d(e^{4}TpC) (1.8 mM), d(i^{4}TpC) (1.0 mM).

[b]When $\delta 2' \sim \delta 2''$, $^2J_{2'-2''}$ is arbitrary and only the sum of the connected couplings (J) is significant.

[c]J_{5-6} is either between the Me5 and H6 of thymine or H5 and H6 of cytosine.

[d]J_{7-8} is either between the methine and methyl protons of the O4-isopropyl group, or methylene and methyl protons of the O4-ethyl group.

[e]J_{A-B} is the geminal coupling constant of the methylene protons of the O4-ethyl group.

Table 3.10. ^{1}H Chemical shifts (ppm) of d(TpG), d(e^{4}TpG), and d(i^{4}TpG)[a]

	d(TpG)				d(e^{4}TpG)				d(i^{4}TpG)			
	Tp		pG		e^{4}Tp		pG		i^{4}Tp		pG	
α	10°C	70°C	10°C	70°C	10°C	70°C	10°C	70°C	10°C	70°C	10°C	70°C
1'	6.058	6.100	6.184	6.243	6.069	6.127	6.183	6.231	6.094	6.149	6.212	6.246
2'	1.640	1.981	2.816	2.789	1.760	1.988	2.762	2.760	1.724	2.018	2.813	2.780
2"	2.229	2.365	2.500	2.518	2.399	2.482	2.479	2.506	2.379	2.488	2.491	2.513
3'	4.614	4.662	4.761	4.704	4.601	4.648	4.736	4.693	4.600	4.658	4.751	4.692
4'	4.045	4.069[c]	4.173	4.180	4.084	4.106	4.169	4.179	4.076[c]	4.108	4.185[c]	4.186
5'	3.641	3.703	4.048[c]	4.062[c]	3.691	3.730	4.089[c]	4.088	3.659	3.726	4.080[c]	4.084
5"	3.641	3.657	4.048[c]	4.062[c]	3.666	3.674	4.069[c]	4.064	3.643	3.668	4.080[c]	4.062
6 or 8	7.410	7.446	8.043	7.994	7.646	7.670	8.011	7.982	7.628	7.666	8.015	7.982
Me5	1.838	1.860	----	----	1.919	1.934	----	----	1.920	1.924	----	----
-CH$_2$(A)[d]	----	----	----	----	4.301	4.374	----	----	1.323	1.338	----	----
-CH$_2$(B)[d]	----	----	----	----	4.352	4.402	----	----	1.375	1.353	----	----
-CH(7)	----	----	----	----	----	----	----	----	5.233	5.285	----	----
-CH$_3$(8)	----	----	----	----	1.376	1.369	----	----	----	----	----	----

[a]Data for **d(e^{4}TpG)** and **d(i^{4}TpG)** acquired at 300.1 MHz, **d(TpG)** at 500.1 MHz, all in 0.1 M NaCl, Conc: **d(TpG)** (14.0 mM), **d(e^{4}TpG)** (8.0 mM), **d(i^{4}TpG)** (4.9 mM).

[b]Estimated since δ2' ~ δ2".

[c]Due to extensive overlap these δs are only 1st order estimates.

[d]For **d(i^{4}TpG)** these δs are the magnetically non-equivalent methyl resonances of the O4-isopropyl group.

Table 3.11. Coupling constants (Hz) of d(TpG), d(e^{4}TpG), and d(i^{4}TpG)[a]

	d(TpG)				d(e^{4}TpG)				d(i^{4}TpG)			
	Tp		pG		e^{4}Tp		pG		i^{4}Tp		pG	
J	10°C	70°C	10°C	70°C	10°C	70°C	10°C	70°C	10°C	70°C	10°C	70°C
1'2'	8.9	8.0	6.9	6.7	7.8	7.5	6.5	6.8	8.0	7.4	6.7	6.7
1'2"	5.6	6.1	6.6	6.7	5.9	6.1	6.6	6.7	5.8	6.1	6.7	6.7
2'2"	-14.0	-14.3	-13.9	-14.1	-14.1	-14.1	-13.8	-14.0	-14.1	-14.2	-14.0	-14.0
2'3'	5.9	6.4	6.6	6.6	6.1	6.6	6.6	6.6	6.3	6.7	6.6	6.7
2"3'	2.1	2.9	4.2	4.2	3.1	3.3	4.3	4.3	2.7	3.5	4.3	4.3
3'4'	2.1	2.9	3.7	3.9	3.1	3.4	4.2	4.2	3.0	3.4	4.0	4.0
4'5'	4.2[c]	3.7	2.8	3.8	3.2	3.5	3.1	3.0	3.5[c]	3.5	3.4[c]	3.1
4'5"	4.2[c]	5.0	2.8	3.8	4.7	5.0	3.1	4.3	4.4[c]	5.1	3.4[c]	4.7
5'5"	-12.8[c]	-12.4	-11.8[c]	-11.8[c]	-12.8	-12.5	-11.5	-11.5	-12.1[c]	-12.5	-11.4[c]	-11.4
56	1.3	1.3	----	----	1.1	1.2	----	----	1.1	1.1	----	----
78[d]	----	----	----	----	7.1	7.1	----	----	6.2	6.2	---	---
AB[e]	----	----	----	----	-10.6	-10.7	----	-----	----	----	----	----
3'P	6.0	6.8	----	----	6.1	6.6	----	---	6.4	6.7	----	---
4'P	----	----	2.8	1.9	----	----	2.0	1.7	----	----	3.0[c]	1.6
5'P	----	----	3.6[c]	3.4[c]	----	----	c	4.8	---	---	c	5.1
5"P	----	----	3.6[c]	3.4[c]	----	----	c	4.4	---	---	c	4.9

[a]Data for d(TpG) and d(i^{4}TpG) acquired at 300.1 MHz, d(e^{4}TpG) at 500.1 MHz, all in 0.1 M NaCl, Conc: d(TpG) (14.0 mM), d(e^{4}TpG) (8.0 mM), d(i^{4}TpG) (4.9 mM).

[b]When $\delta 2' \sim \delta 2''$, $^2J_{2'-2''}$ is arbitrary and only the sum of the connected couplings (J) is significant.

[c]Due to extensive overlap these values are 1st order estimates, except for d(TpG), where the values are from Cheng and Sarma, (1977).

[d]J_{7-8} is between the methine and methyl protons of the O4-isopropyl group, or the methylene and methyl protons of the O4-ethyl group.

[e]J_{A-B} is the geminal coupling constant of the methylene protons of the O4-ethyl group.

Table 3.12. ^{1}H Chemical shifts (ppm) of d(TpA), d(e^{4}TpA), and d(i^{4}TpA)[a]

	d(TpA)				d(e^{4}TpA)				d(i^{4}TpA)			
	Tp		pA		e^{4}Tp		pA		i^{4}Tp		pA	
σ	10°C	70°C	10°C	70°C	10°C	70°C	10°C	70°C	10°C	70°C	10°C	70°C
1'	5.935	6.030	6.382	6.439	5.937	6.053	6.351	6.425	5.973	6.067	6.402	6.439
2'	1.511	1.858	2.883	2.849	1.545	1.866	2.820	2.809	1.470	1.844	2.865	2.826
2"	2.126	2.276	2.582	2.605	2.261	2.404	2.572	2.599	2.232	2.389	2.583	2.603
3'	4.568	4.619	4.798	4.738	4.542	4.608	4.768	4.724	4.541	4.605	4.790	4.727
4'	4.002	4.022	4.217	4.222	4.052	4.073	4.215	4.223	4.057[c]	4.067	4.227	4.225
5'	3.640	3.684	4.048[b]	4.063[b]	3.689	3.721	4.060[b]	4.087	3.667	3.708	4.052[b]	4.026[b]
5"	3.618	3.631	4.048[b]	4.063[b]	3.642	3.654	4.060[b]	4.066	3.599	3.641	4.052[b]	4.026[b]
6 or 8	7.313	7.372	8.392	8.358	7.541	7.600	8.364	8.349	7.521	7.585	8.396	8.356
Me5 or 2	1.834	1.853	8.100	8.207	1.892	1.916	8.307	8.175	1.912	1.911	8.075	8.183
-CH$_2$(A)[c]	----	----	----	----	4.281	4.365	----	----	1.332	1.339	----	----
-CH$_2$(B)[c]	----	----	----	----	4.304	4.380	----	----	1.403	1.364	----	----
-CH(7)	----	----	----	----	----	----	----	----	5.219	5.272	----	----
-CH$_3$(8)	----	----	----	----	1.384	1.372	----	----	----	----	----	----

[a]Data acquired at 300.1 MHz, 0.1 M NaCl, Conc: **d(TpA)** (6.1 mM), **d(e^{4}TpA)** (12.8 mM), **d(i^{4}TpA)** (1.8 mM).

[b]Estimated since δ5' ~ δ5".

[c]For **d(i^{4}TpA)** these δs are the magnetically non-equivalent methyl resonances of the O4-isopropyl group.

Table 3.13. Coupling constants (Hz) of d(TpA), d(e^{4}TpA), and d(i^{4}TpA)[a]

	d(TpA)				d(e^{4}TpA)				d(i^{4}TpA)			
	Tp		pA		e^{4}Tp		pA		i^{4}Tp		pA	
J	10°C	70°C	10°C	70°C	10°C	70°C	10°C	70°C	10°C	70°C	10°C	70°C
1'2'	8.5	7.8	6.8	6.6	7.8	7.4	6.6	6.6	8.1	7.7	6.6	6.5
1'2"	5.8	6.2	6.6	6.7	5.9	6.1	6.6	6.6	5.9	6.0	6.6	6.6
2'2"	-14.2	-14.2	-13.9	-14.0	-14.1	-14.2	-13.9	-14.0	-14.1	-14.2	-14.0	-14.0
2'3'	6.0	6.6	6.6	6.6	6.2	6.7	6.5	6.6	5.9	6.6	6.5	6.5
2"3'	2.2	3.0	4.2	4.3	3.0	3.4	4.4	4.4	2.4	3.2	4.4	4.5
3'4'	2.4	3.1	4.0	4.0	3.1	3.4	4.1	4.2	2.7	3.4	4.1	4.2
4'5'	3.7	3.6	2.6	3.5	3.2	3.6	2.6	2.8	3.2	3.5	2.8	3.5
4'5"	4.1	5.0	2.6	3.5	4.5	4.9	2.6	4.0	4.6	5.0	2.8	3.5
5'5"	-12.5	-12.4	-11.8[b]	-11.8[b]	-12.6	-12.5	-11.8[b]	-11.5	-12.5	-12.5	-12.2[b]	-11.4[b]
56	1.3	1.3	----	----	1.2	1.2	----	----	1.2	1.2	----	----
78[d]	----	----	----	----	7.1	7.1	----	----	6.2	6.2	---	---
AB[e]	----	----	----	----	-10.6	-10.6	----	-----	----	----	----	----
3'P	6.0	6.6	----	----	6.3	6.7	----	---	6.3	6.7	----	---
4'P	----	----	2.6	2.1	----	----	2.0	1.7	----	----	c	1.8
5'P	----	----	3.1	4.1	----	----	4.8	4.8	---	---	c	c
5"P	----	----	3.1	4.1	----	----	4.7	4.4	---	---	c	c

[a]Data acquired at 300.1 MHz, 0.1 M NaCl, Conc: d(TpA) (6.1 mM), d(e^{4}TpA) (12.8 mM), d(i^{4}TpA) (1.8 mM).

[b]When $\delta 5' \sim \delta 5''$, $^2J_{5'-5''}$ is arbitrary and only the sum of the connected couplings (J) is significant.

[c]Due to extensive overlap these values are only 1st order estimates or were not obtained.

[d]J_{7-8} is between the methine and methyl protons of the O4-isopropyl group, or the methylene and methyl protons of the O4-ethyl group.

[e]J_{A-B} is the geminal coupling constant of the methylene protons of the O4-ethyl group.

Table 3.14 ^{1}H Chemical shifts (ppm) of d(Ape^{4}T) and d(ApT)[a]

	d(Ape^{4}T)				d(ApT)			
	Ap		pe^{4}T		Ap		pT	
J	10°C	60°C	10°C	60°C	10°C	60°C	10°C	60°C
1'	6.301	6.342	6.153	6.228	6.347	6.391	6.144	6.202
2'	2.824[b]	2.789	2.242	2.268	2.810	2.817	2.260[b]	2.305[b]
2"	2.828[b]	2.746	2.358	2.418	2.832	2.782	2.260[b]	2.313[b]
3'	4.837	4.891	4.527	4.536	4.840	4.896	4.552	4.544
4'	4.292	4.291	4.106	4.150	4.310	4.309	4.062	4.103
5'	3.889	3.841	4.253	4.207	3.889	3.856	4.219	4.178
5"	3.831	3.790	4.099	4.105	3.831	3.802	4.087	4.092
6 or (2)	8.053	8.159	7.656	7.718	8.106	8.194	7.445	7.505
M5 or (8)	8.267	8.243	1.614	1.745	8.284	8.266	1.594	1.713
-CH_2(A)	----	----	4.214	4.247	----	----	----	----
-CH_2(B)	----	----	4.214	4.272	----	----	----	----
-CH_3	----	----	1.321	1.299	----	----	----	----

[a]Data for d(ApT) acquired at 500.1 MHz, d(Ape^{4}T) at 300.1 MHz, both in 0.1 M NaCl, Conc: d(Ape^{4}T) (2.6 mM), d(ApT) (7.2 mM).

[b]Estimated since $\delta(2') \sim \delta(2'')$.

Table 3.15. Coupling constants (Hz) of d(Ape^{4}T) and d(ApT)[a]

	d(Ape^{4}T)				d(ApT)			
	Ap		pe^{4}T		Ap		pT	
J	10°C	60°C	10°C	60°C	10°C	60°C	10°C	60°C
1'2'	6.4	7.4	5.7	6.6	6.7	7.4	6.7	6.9
1'2''	6.4	6.0	6.7	6.6	6.1	6.0	6.7	6.9
2'2''	-14.0[b]	-14.0	-14.0	-14.0	-13.8	-14.0	-14.2[b]	-14.1[b]
2'3'	5.4	6.2	7.3	6.9	5.9	6.1	5.9	5.5
2''3'	5.4	3.4	5.6	4.7	4.5	3.4	5.9	5.5
3'4'	3.8	3.6	5.4	4.6	3.5	3.4	4.9	4.9
4'5'	2.8	3.4	2.4	2.6	2.8	3.2	2.0	2.9
4'5''	3.7	4.1	3.1	3.9	3.7	4.3	2.9	3.8
5'5''	-12.9	-12.7	-11.7	-11.8	-12.9	-12.7	-11.5	-11.6
56	---	---	1.2	1.1	---	---	1.3	1.3
78[c]	---	---	7.1	7.1	---	---	---	---
AB[d]	---	---	---	-10.6	---	---	---	---
3'P	5.8	5.8	---	---	5.2	6.1	---	---
4'P	---	---	2.8	2.2	---	---	2.6	2.2
5'P	---	---	3.6	4.3	---	---	3.9	4.4
5''P	---	---	3.1	4.4	---	---	2.8	4.3

[a]Data for d(ApT) acquired at 500.1 MHz, d(Ape^{4}T) at 300.1 MHz, both in 0.1 M NaCl, Conc: d(Ape^{4}T) (2.6 mM), d(ApT) (7.2 mM).

[b]When $\delta(2') \sim \delta(2'')$, $^2J_{2'-2''}$ is arbitrary and only the sum of the connected couplings (]) is significant.

[c]J_{7-8} is between the methylene and methyl protons of the O4-ethyl group.

[d]J_{A-B} is the geminal coupling constant of the methylene protons of the O4-ethyl group.

Table 3.16. ^{1}H chemical shifts (ppm) and coupling constants (Hz) of d(TpTpT)[a]

	Tp	pTp	pT		Tp	pTp	pT
δ				J			
1'	6.214	6.295	6.305	1'2'	7.7	8.1	6.9 ┐
2'	2.336	2.370	2.370[b]	1'2"	6.1	6.1	6.9 ┘
2"	2.550	2.550	2.370[b]	2'2"	-14.1	-14.2	-14.1[b]
3'	4.792	4.891	4.590	2'3'	6.4	6.4	5.3 ┐
4'	4.192	4.332	4.114	2"3'	3.2	3.1	5.4 ┘
5'	3.830	4.144	4.159	3'4'	3.4	3.0	3.7
5"	3.788	4.010	4.010	4'5'	3.4	2.6	2.7
6	7.686	7.650	7.695	4'5"	4.6	3.1	3.6
Me5	1.897	1.885	1.907	5'5"	-12.6	-11.7	-11.7
				3'P'	6.5	6.3	----
				4'P	----	2.6	2.5
				5'P	----	4.5	4.5
				5"P	----	4.4	4.7
				56	1.2	1.2	1.2

[a]Data acquired at 500.1 MHz, 0.5 mM EDTA, 5 mM Na_2PO_4, at 30°C, with the δs relative to TSP. Data from Rycyna *et al.* (1988).

[b]Estimated since δ2'~δ2", therefore $^2J_{2'-2"}$ is arbitrary and only the sum of the connected couplings (J) is significant.

Table 3.17. ^{1}H chemical shifts (ppm) and coupling constants (Hz) of d(Tpm^{4}TpT)[a]

	Tp		pm^{4}Tp		pT	
δ	10°C	70°C	10°C	70°C	10°C	70°C
1'	6.117	6.154	6.220	6.271	6.271	6.257
2'	2.340	2.313	2.354	2.315	2.330[b]	2.332
2"	2.518	2.506	2.614	2.634	2.329[b]	2.357
3'	4.739	4.762	4.829	4.845	4.563	4.542
4'	4.153	4.143	4.328	4.342	4.104	4.124
5'	3.815	3.806	4.178	4.153	4.150	4.126
5"	3.773	3.753	4.093	4.085	4.065	4.073
6	7.679	7.584	7.913	7.863	7.664	7.635
Me5	1.847	1.861	1.931	1.958	1.820	1.863
-CH_3	----	----	3.922	3.945	----	----

	Tp		pm^{4}Tp		pT	
J	10°C	70°C	10°C	70°C	10°C	70°C
1'2'	6.6	7.3	6.5	7.4	6.8]	6.8
1'2"	6.2	6.3	6.3	6.2	6.8]	6.6
2'2"	-14.0	-14.2	-14.0	-14.1	-14.1[b]	-14.2
2'3'	6.4	6.7	6.4	6.6	5.5]	6.7
2"3'	3.9	3.6	4.3	3.5	5.5]	4.1
3'4'	3.9	3.6	4.2	3.4	4.1	4.1
4'5'	3.4	3.5	2.6	2.7	2.5	2.9
4'5"	4.2	4.8	2.8	3.8	3.2	4.2
5'5"	-12.7	-12.5	-11.5	-11.7	-11.7	-11.8
3'P'	6.4	6.7	6.3	6.6	----	----
4'P	----	----	2.7	2.3	2.3	1.9
5'P	----	----	4.6	5.0	3.9	4.8
5"P	----	----	3.1	4.4	4.0	4.9
56	1.3	1.3	1.2	1.2	1.3	1.3

[a]Data acquired at 500.1 MHz, 0.1 M NaCl, Conc: 16.3 mM.

[b]Estimated since δ2'~δ2", therefore $^{2}J_{2'-2"}$ is arbitrary and only the sum of the connected couplings (]) is significant.

Table 3.18. ^{1}H chemical shifts (ppm) and coupling constants (Hz) of d(Tpe^{4}TpT)[a]

	Tp		pe^{4}Tp		pT			Tp		pe^{4}Tp		pT	
δ	10°C	70°C	10°C	70°C	10°C	70°C	J	10°C	70°C	10°C	70°C	10°C	70°C
1'	6.109	6.150	6.222	6.271	6.270	6.257	1'2'	6.6	7.4	6.6	7.2	6.8	7.0
2'	2.339	2.307	2.351	2.313	2.330[b]	2.331	1'2"	6.3	6.3	6.4	6.4	6.8	6.7
2"	2.517	2.502	2.609	2.629	2.330[b]	2.357	2'2"	-14.0	-14.1	-14.2	-14.1	-14.1[b]	-14.0
3'	4.738	4.760	4.834	4.847	4.561	4.541	2'3'	6.4	6.6	6.5	6.8	5.5	6.6
4'	4.151	4.141	4.351[c]	4.261[c]	4.106	4.125	2"3'	3.9	3.5	4.3	3.4	5.5	3.7
5'	3.810	3.801	4.176	4.151	4.149	4.125	3'4'	3.8	3.5	4.2	3.4	4.0	4.1
5"	3.769	3.749	4.094	4.084	4.064	4.072	4'5'	3.3	3.5	2.2	2.8	2.5	2.9
6	7.675	7.582	7.897	7.852	7.663	7.636	4'5"	4.3	4.7	3.1	3.6	3.1	4.4
Me5	1.849	1.863	1.932	1.958	1.820	1.861	5'5"	-12.7	-12.5	-11.5	-11.8	-11.4	-11.7
-CH_2(A)	----	----	4.304	4.366	----	----	3'P'	6.4	6.7	6.3	6.6	----	----
-CH_2(B)	----	----	4.327	4.380	----	----	4'P	----	----	2.7	2.3	2.5	2.9
-CH_3	----	----	1.371	1.355	----	----	5'P	----	----	4.4	4.9	3.9	4.8
							5"P	----	----	3.2	4.6	4.0	4.8
							56	1.3	1.3	1.2	1.2	1.3	1.3
							78[d]	----	----	6.2	6.2	----	----
							AB[e]	----	----	-10.6	-10.7	----	----

[a]Data acquired at 500.1 MHz, 0.1 M NaCl, Conc: 10.8 mM.

[b]Estimated since δ2'~δ2", therefore $^{2}J_{2'-2"}$ is arbitrary and only the sum of the connected couplings (]) is significant.

[c]Due to extensive overlap of the methylene resonances of the O4-ethyl group these δs are 1st order estimations from decoupling experiments.

[d]J_{7-8} is between the methylene and methyl protons of the O4-ethyl group.

[e]J_{A-B} is the geminal coupling constant of the methylene protons of the O4-ethyl group.

Table 3.19. ^{1}H chemical shifts (ppm) and coupling constants (Hz) of d(Tpi^{4}TpT)[a]

	Tp		pi^{4}Tp		pT	
δ	10°C	70°C	10°C	70°C	10°C	70°C
1'	6.153	6.163	6.244	6.277	6.273	6.257
2'	2.313	2.301	2.328	2.307	2.337[b]	2.333
2"	2.492	2.490	2.611	2.630	2.333[b]	2.356
3'	4.753	4.761	4.845	4.848	4.559	4.540
4'	4.159	4.140	4.352	4.345	4.117	4.126
5'	3.786	3.789	4.168	4.147	4.144	4.122
5"	3.753	3.739	4.088	4.081	4.066	4.072
6	7.646	7.574	7.877	7.841	7.679	7.639
Me5	1.849	1.861	1.936	1.946	1.837	1.863
-CH(7)	----	----	5.219	5.264	----	----
-CH_3(8)	----	----	1.330	1.328	----	----

	Tp		pi^{4}Tp		pT	
J	10°C	70°C	10°C	70°C	10°C	70°C
1'2'	7.7	7.5	6.6	7.3	6.8	7.0
1'2"	6.0	6.2	6.3	6.2	6.8	6.6
2'2"	-14.1	-14.2	-14.2	-14.1	-14.1[b]	-14.1
2'3'	6.4	6.6	6.4	6.5	5.4	6.7
2"3'	3.2	3.4	3.7	3.4	5.4	3.6
3'4'	3.2	3.4	3.3	3.3	3.9	4.2
4'5'	3.4	3.5	2.8	2.8	2.7	2.9
4'5"	4.4	4.9	3.2	4.0	3.1	4.0
5'5"	-12.6	-12.5	-11.7	-11.8	-11.2	-11.6
3'P'	6.4	6.7	6.5	6.6	----	----
4'P	----	----	3.1	2.2	2.7	2.5
5'P	----	----	4.7	4.9	3.9	4.7
5"P	----	----	3.4	4.3	4.3	5.4
56	1.3	1.3	1.2	1.2	1.3	1.3
78[c]	----	----	6.2	6.2	----	----

[a]Data acquired at 500.1 MHz, 0.1 M NaCl, Conc: 2.5 mM.

[b]Estimated since δ2'~δ2", therefore $^{2}J_{2'-2"}$ is arbitrary and only the sum of the connected couplings (J) is significant.

[c]J_{7-8} is between the methine and methyl protons of the O4-isopropyl group.

Table 3.20. ^{1}H chemical shifts (ppm) and coupling constants (Hz) of d(ApTpA)[a]

	Ap		pTp		pA	
δ	10°C	60°C	10°C	60°C	10°C	60°C
1'	6.273	6.326	5.999	6.076	6.335	6.377
2'	2.723[b]	2.753	1.819	1.995	2.748	2.746
2"	2.723[b]	2.704	2.182	2.294	2.541	2.560
3'	4.888	4.898	4.780	4.779	4.730	4.700
4'	4.303	4.285	4.168	4.193	4.211	4.213
5'	3.846	3.824	4.089	4.076	c	4.086
5"	3.809	3.779	4.045	4.035	c	4.075
6	----	----	7.297	7.386	----	----
Me5	----	----	1.619	1.723	----	----
2	8.037	8.135	----	----	8.046	8.140
8	8.166	8.205	----	----	8.308	8.313

	Ap		pTp		pA	
J	10°C	60°C	10°C	60°C	10°C	60°C
1'2'	6.7	7.7	8.6	8.3	6.6	6.6
1'2"	6.7	6.0	6.0	6.1	6.5	6.6
2'2"	-14.0[b]	-14.0	-13.9	-14.2	-13.9	-14.0
2'3'	4.3	6.1	6.2	6.5	6.3	6.5
2"3'	4.3	3.0	3.0	2.6	3.9	4.1
3'4'	2.7	3.1	3.2	2.7	3.4	3.9
4'5'	3.0	3.1	2.0	2.6	3.1[c]	2.7
4'5"	3.4	4.2	3.0	3.9	3.1[c]	4.1
5'5"	-12.9	-12.7	-11.5	-11.8	c	-12.0[c]
3'P	6.1	6.0	6.4	6.6	----	----
4'P	----	----	3.3	4.2	2.5	1.9
5'P	----	----	4.2	4.2	c	4.3[c]
5"P	----	----	2.8	3.9	c	5.3[c]
56	----	----	1.2	1.3	----	----

[a]Data acquired at 500.1 MHz, 0.1 M NaCl, Conc: 3.1 mM.

[b]Estimated since δ2'~δ2", therefore $^{2}J_{2'-2"}$ is arbitrary and only the sum of the connected couplings (]) is significant.

[c]Due to extensive overlap these values are unavailable or are only 1st order approximations.

Table 3.21. ^{1}H chemical shifts (ppm) and coupling constants (Hz) of d(Ape^{4}TpA)[a]

	Ap		pe^{4}Tp		pA	
δ	10°C	60°C	10°C	60°C	10°C	60°C
1'	6.215	6.273	6.026	6.120	6.312	6.372
2'	2.716[b]	2.719	1.847	1.998	2.699	2.720
2"	2.711[b]	2.682	2.304	2.418	2.529	2.559
3'	4.875	4.893	4.774	4.783	4.715	4.697
4'	4.286	4.272	4.283[c]	c	c	c
5'	3.844	3.814	c	4.114[c]	c	c
5"	3.808	3.773	c	4.058[c]	c	c
6	----	----	7.483	7.576	----	----
Me5	----	----	1.629	1.741	----	----
2	7.997	8.110	----	----	8.008	8.116
8	8.141	8.180	----	----	8.296	8.312
-CH_2(A)	----	----	4.159	4.227	----	----
-CH_2(B)	----	----	4.138	4.242	----	----
-CH_3	----	----	1.338	1.314	----	----

	Ap		pe^{4}Tp		pA	
J	10°C	60°C	10°C	60°C	10°C	60°C
1'2'	6.7	7.8	7.9	7.8	6.6	6.6
1'2"	6.7	6.0	6.0	6.1	6.5	6.6
2'2"	-14.1[b]	-14.0	-14.0	-14.2	-13.8	-14.0
2'3'	4.6	5.9	6.5	6.5	6.4	6.5
2"3'	4.6	3.0	3.1	3.2	4.2	4.2
3'4'	3.0	3.1	3.3	3.3	4.1	4.1
4'5'	2.8	3.1	c	2.5[c]	c	c
4'5"	3.5	4.2	c	3.9[c]	c	c
5'5"	-12.8	-12.7	c	-11..8[c]	c	c
3'P	5.5	6.1	6.5	6.6	----	----
5'P	----	----	c	4.6[c]	c	c
5"P	----	----	c	3.9[c]	c	c
56	----	-----	1.1	1.2	----	----
78[d]	----	----	7.1	7.1	----	----
AB[e]	----	----	-10.7	-10.7	----	----

[a]Data acquired at 500.1 MHz, 0.1 M NaCl, Conc: 6.5 mM.

[b]Estimated since δ2'~δ2", therefore $^2J_{2'-2"}$ is arbitrary and only the sum of the connected couplings (J) is significant.

[c]Due to extensive overlap these values are unavailable or are only 1st order approximations.

[d]J_{7-8} is between the methylene and methyl protons of the O4-ethyl group.

[e]J_{A-B} is the geminal coupling constant of the methylene protons of the O4-ethyl group.

Table 3.22. ^{1}H chemical shifts (ppm) of d(e^{4}TpApe^{4}TpA)[a]

	e^{4}Tp		pAp		pe^{4}Tp		pA	
δ	30°C	70°C	30°C	70°C	30°C	70°C	55°C	70°C
1'	5.988	6.054	6.209	6.274	6.030	6.116	6.365	6.378
2'	1.790	1.914	2.775	2.767	1.857	1.991	2.708	2.715
2''	2.351	2.437	2.732	2.720	2.363	2.414	2.549	2.555
3'	4.609	4.632	4.976	4.977	b	4.759	4.696	4.689
4'	b	b	4.381	b	b	b	b	b
5'	3.713	3.719	b	b	b	b	b	b
5''	3.670	3.662	b	b	b	b	b	b
6(2)	7.572	7.598	7.996	8.074	7.493	7.590	8.060	8.131
Me5(8)	1.871	1.889	8.321	8.302	1.682	1.747	8.308	8.312
-CH_2(A)	4.262	4.340	----	----	4.148	4.216	----	----
-CH_2(B)	4.305	4.360	----	----	4.160	4.237	----	----
-CH_3	1.357	1.357	----	----	1.318	1.298	----	----

[a]Data acquired at 500.1 MHz, 0.1 M NaCl, Conc: (3.7 mM).

[b]Due to extensive overlap these values are unavailable.

Table 3.23. Coupling constants (Hz) of d(e^{4}TpApe^{4}TpA)[a]

	e^{4}Tp		pAp		pe^{4}Tp		pA	
J	30°C	70°C	30°C	70°C	30°C	70°C	55°C	70°C
1'2'	7.7	7.3	8.0	6.9	7.6	7.7	6.6	6.5
1'2''	6.0	6.1	5.7	6.7	6.0	6.0	6.6	6.6
2'2''	-14.1	-14.0	-14.7	-14.2	-14.1	-14.2	-13.9	-14.0
2'3'	6.5	6.7	5.9	6.7	6.5	6.6	6.5	6.5
2''3'	3.3	3.3	2.8	4.2	3.1	3.3	4.1	4.1
3'4'	3.3	3.4	2.8	3.7	c	3.3	4.0	4.0
4'5'	3.5[b]	3.5[b]	2.5	2.9	c	c	c	c
4'5''	4.6[b]	4.8[b]	3.0	4.2	c	c	c	c
5'5''	-12.6[b]	-12.6[b]	-11.5	-11.7	c	c	c	c
56	1.2	1.1	---	---	1.1	1.2	---	---
78[c]	7.1	7.1	---	---	7.1	7.1	---	---
AB[d]	-10.6	-10.6	---	---	-10.6	-10.6	---	---
3'P	6.5	6.6	5.5	5.9	---	6.7	---	---
5'P	---	---	2.8	2.7[e]	c	c	c	c
5''P	---	---	2.8	2.7[e]	c	c	c	c

[a]Data acquired at 500.1 MHz, 0.1 M NaCl, Conc: (3.7 mM).

[b]Due to extensive overlap these values are unavailable or are only 1st order estimates.

[c]$J_{7\text{-}8}$ is between the methylene and methyl protons of the O4-ethyl group

[d]$J_{A\text{-}B}$ is the geminal coupling constant of the methylene protons of the O4-ethyl group.

[e]Obtained at 55°C.

Table 3.24. ^{13}C chemical shifts (ppm) and coupling constants (Hz) of d(i^{4}TpT), d(Tpi^{4}T), d(TpT) and i^{4}dT at 27°C[a]

		d(i^{4}TpT)		d(Tpi^{4}T)		d(TpT)[b]	
δ	i^{4}dT	i^{4}Tp	pT	Tp	pi^{4}T	Tp	pT
C2	5.94	5.75	0.10	-0.23	6.16	152.84	152.67
C4	4.43	4.56	-0.11	-0.05	4.69	167.55	167.38
C5	-3.57	-3.78	-0.16	-0.16	-3.64	112.69	112.72
C6	2.63	2.54	-0.09	-0.02	2.83	138.64	138.51
Me5	-0.18	-0.18	-0.01	-0.01	-0.13	12.89	12.86
C1'	1.35	1.26	0.05	0.09	1.38	86.39	86.01
C2'	1.02	0.93	0.16	0.04	0.96	38.81	39.89
C3'	-0.14	-0.92	-0.19	0.06	-0.28	76.18	71.54
C4'	0.30	0.02	-0.01	0.05	0.27	86.86	86.19
C5'	-0.10	-0.43	-0.11	0.00	-0.22	62.17	66.01
-CH(7)	73.10	73.17	---	---	73.18	---	---
-CH_3(A)[c]	22.15	22.137	---	---	22.107	---	---
	---	22.179	---	---	22.160	---	---
-CH_3(B)[c]	22.15	22.244	---	---	22.199	---	---
	---	22.208	---	---	22.203	---	---
^{3}J(C2'P)	---	2.7	---	3.1	---	2.7	---
^{2}J(C3'P)	---	5.7	---	5.3	---	5.4	---
^{3}J(C4'P)	---	7.3	9.0	7.1	8.7	7.4	9.1
^{2}J(C5'P)	---	---	5.5	---	5.7	---	5.2

[a]Data acquired at 75.5 MHz, 0.1 M NaCl, Conc: d(i^{4}TpT) (4.8 mM), d(Tpi^{4}T) (8.3 mM), d(TpT) (1.8 mM). δ in ppm were measured relative to TMS using internal dioxane (dioxane = 67.86 ppm). δC2 through δC5' for d(i^{4}TpT) and d(Tpi^{4}T) are given relative to the corresponding δ in d(TpT), with positive numbers indicating a deshielding relative to d(TpT). The values for i^{4}dT are similarly presented relative to the dT

[b]The base carbon assignments for d(TpT) may be interchanged.

[c]The first entry is at 27°C, the second at 70°C.

Table 3.25. ^{13}C chemical shifts (ppm) and coupling constants (Hz) of d(Tpi^{4}TpT) and d(TpTpT) at 27°C[a]

	d(Tpi^{4}TpT)			d(TpTpT)[b]		
δ	Tp	pi^{4}Tp	pT	Tp	pTp	pT
C2	-0.06	5.95	-0.10	152.80	152.69	152.62
C4	-.014	4.74	-0.12	167.53	167.30	167.43
C5	-0.21	-3.67	-0.25	112.71	112.74	112.87
C6	-0.06	2.67	-0.01	138.64	138.42	136.52
Me5	-0.07	-0.13	0.06	12.94	12.87	12.87
C1'	0.07	1.37	0.06	86.38	86.05	86.12
C2'	-0.03	1.12	0.06	38.92	38.81	40.00
C3'	-0.21	-0.27	0.01	76.64	76.39	71.72
C4'	0.05	0.08	-0.07	86.93	85.36	86.41
C5'	-0.01	-0.39	-0.13	62.26	66.24	66.10
-CH(7)	---	73.22	---	---	---	---
-CH_3(A)	---	22.15	---	---	---	---
-CH_3(B)	---	22.17	---	---	---	---
^{3}J(C2'P)	2.5	3.0	---	3.1	3.0	---
^{2}J(C3'P)	5.5	5.6	---	5.0	5.3	---
^{3}J(C4'P3)	7.0	7.0	---	7.4	8.2	---
^{3}J(C4'P5')	---	8.6	8.8	---	8.2	9.0
^{2}J(C5'P)	---	5.6	5.4	---	5.8	5.6

[a]Data acquired at 75.5 MHz, 0.1 M NaCl, Conc: d(Tpi^{4}TpT) (50.0 mM), d(TpTpT) (3.0 mM). δs in ppm were measured relative to TMS using internal dioxane (dioxane = 67.86 ppm). δC2 through δC5' for d(Tpi^{4}TpT) are given relative to the corresponding δ in d(TpTpT), with positive numbers indicating a deshielding relative to d(TpTpT).

[b]The base carbon assignments for d(TpTpT) may be interchanged. The coupling constants for d(TpTpT) are taken from Rycyna *et al.* (1988).

CHAPTER 4

CIRCULAR DICHROISM

A CD spectrum represents the difference in absorption of left and right circularly polarized light. Nucleic acid bases display no CD spectrum because they contain a plane of symmetry and therefore are not optically active. The introduction of a sugar to the base removes the symmetry in the molecule and results in measurable optical activity (Cantor et al., *1970). In oligomers, base-base interactions produce significant changes in the magnitude and shape of the CD spectra relative to the sum of the constituent mononucleosides. These changes in the CD spectra are both sequence and temperature dependent. Consequently, CD spectra can provide information regarding the DNA conformation (Bush and Brahms, 1973; Tinoco* et al., *1980).*

Variable temperature CD spectra for our oligomers were obtained as described in Chapter 2 at concentrations less than 3.6 x 10^{-4} M, where intermolecular association is minimal (Jaskunas, et al., *1968). The absence of any intermolecular association at such low concentrations is supported by the lack of changes in the CD spectra of the monomers,* ***dT*** *and* ***e^4dT****, between 10 and 80°C. Recall that the* ε *values for some of the oligomers were estimated, as described in Chapter 2, because of the lack of time to experimentally obtain these values. The accuracy of these* ε *estimates are unknown and consequently, so is the accuracy of the CD solution concentrations of some of the oligomers. Unfortunately, the concentration is important in determining the magnitude of the [Θ]. Therefore, when comparing the shape of the CD spectra of these molecules, the best indicators of spectral differences are the position of the maximum and minimum of the long and short* λ *bands and the [Θ] ratios (/[Θ] maximum/[Θ] minimum/). The effect of temperature on the CD spectra can also be examined, with an increase in the magnitude of [Θ] with decreasing temperature associated with an increase in the population of stacked states (Brahms* et al., *1967). However, if the CD spectrum of the fully stacked state is unknown, it is impossible to correlate temperature dependent [Θ] magnitude changes with a specific amount of base-stacking. At 10°C none of the populations of our oligomers are 100% stacked.*

While the CD spectra of dT and e^4dT show no temperature dependence, these spectra differ in a number of ways (Figure 4.1) which may be useful to identify r^4dT monomers. First, the position of the maximum of the long λ positive CD band is red shifted 4 nm in e^4dT (280 nm) relative to dT (Table 4.1). Second, the cross over point (zero [Θ]) for e^4dT is blue shifted relative to dT (258 nm). Last, the short λ negative CD band observed in dT (minimum at 240 nm) is absent in e^4dT.

Figures 4.2 and 4.3 contain various comparisons of the CD spectra of d(e^4TpT), d(i^4TpT), d(Tpe^4T), d(Tpi^4T), and d(TpT). Our CD spectra for d(TpT) is similar to that obtained by Cantor et al. *(1970) in terms of maxima and minima band positions and [Θ] ratios (Table 4.1). Notable features of the CD spectra of these five oligomers are: 1) all the spectra possess a positive band at long λ with the position of the maximum not varying much between molecules, at 280 + 3 nm (Table 4.1); 2) the negative band at short λ for d(TpT) (minimum at 253 nm) is lost, or greatly reduced, in the d(r^4TpT) and d(Tpr^4T) spectra (Figure 4.2A). This is reflected in the [Θ] ratios which are greater than 7.7 for these O4-alkylated dimers while the [Θ] ratio for d(TpT) is 1.3; 3) the CD spectra of d(i^4TpT) and d(e^4TpT) (Figures 4.2C) and d(Tpe^4T) and d(Tpi^4T) (Figure 4.2D) are similar at 10°C, especially with regards to the magnitude of the positive long λ band, implying that the size of the alkyl group is not affecting the conformation of these dimers; 4) the magnitudes of the positive and negative bands increases with decreasing temperature in all five molecules, although the degree of change is smaller for d(Tpr^4T) (Figures 4.3A and B) than for d(r^4TpT) (Figures 4.3C and D). Note that while these observations suggest that the bases are stacking as the temperature is lowered, it does not mean that d(r^4TpT) is stacking to a greater degree than d(Tpr^4T) because CD spectra of these molecules in a 100% stacked state are not available.*

Figures 4.4 and 4.5 contain comparisons of the CD spectra of d(e^4TpA), d(Ape^4T), d(TpA) and d(ApT). Our CD spectra for d(TpA) and d(ApT) agree with the spectra obtained

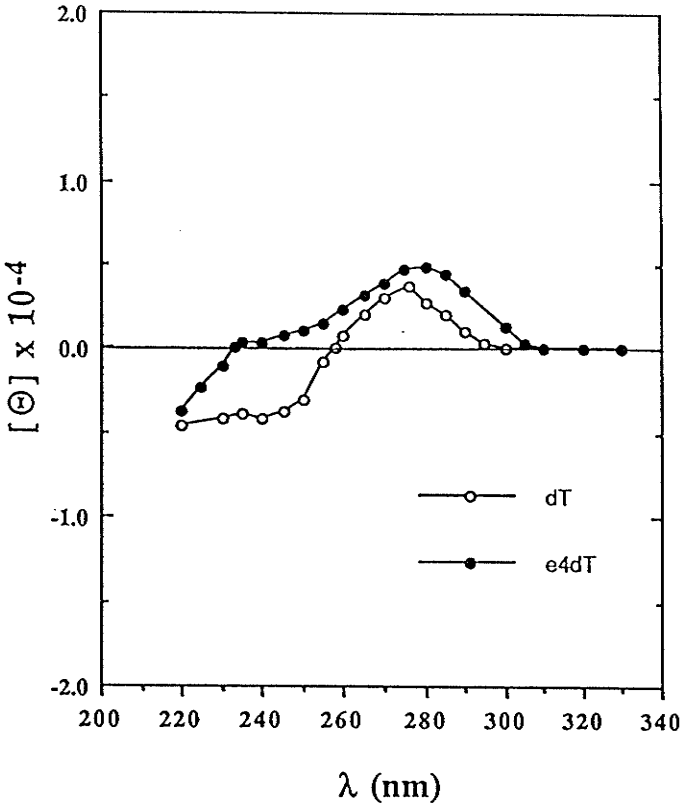

Figure 4.1: CD comparisons. dT and e⁴dT at 23°C.

Table 4.1. Low temperature CD data for the spectra in Figures 4.1 - 4.10[a].

	Maximum		Cross Over	Minimum	
MOLECULE	λ(nm)	[Θ] x 10^{-4}	λ(nm)	λ(nm)	[Θ] x 10^{-4}
dT	276	0.38	258	240	-0.42
dT (literature)	274	0.38	----	240	-0.38
e^4dT	280	0.49	233	----	------
d(TpT)	279	0.87	265	253	-0.68
d(TpT) (literature)	279	0.72	----	250	-0.62
d(e^4TpT)	283	1.62	258	235	-0.21
d(i^4TpT)	283	1.74	257	----	------
d(Tpe^4T)	280	0.49	257	250	-0.08
d(Tpi^4T)	278	0.85	244	246	-0.01
d(TpG)	285	0.41	276	259	-1.26
d(TpGp) (literature)	285	0.35	----	260	-0.73
d(e^4TpG)	279	1.16	259	247	-0.53
d(TpA)	273	1.07	263	252	-1.45
d(TpAp) (literature)	270	0.85	----	250	-1.07
d(e^4TpA)	281	0.80	264	257	-0.21
d(ApT)	273	1.36	264	253	-1.30
d(ApT) (literature)	273	1.62	----	252	-1.43
d(Ape^4T)	282	0.61	270	258	-0.73
d(TpC) (literature)	279	0.85	----	239	-0.32
d(e^4TpC)	282	0.71	223	----	------
d(TpTpT)	277	1.10	264	254	-0.87
d(pTpTpT) (literature)	278	0.99	----	249	-0.77
d(Tpe^4TpT)	280	0.93	256	245	-0.25
d(Tpi^4TpT)	279	0.68	252	240	-0.13
d(ApTpA)	271	1.01	261	250	-1.54
d(Ape^4TpA)	283	0.53	269	257	-0.43

[a]Data recorded in NMR buffer (0.1 M NaCl, 0.01 M sodium phosphate, 0.001M EDTA). [Θ] are in units of deg M^{-1} cm^{-1}. Literature values are from Cantor *et al.* (1970).

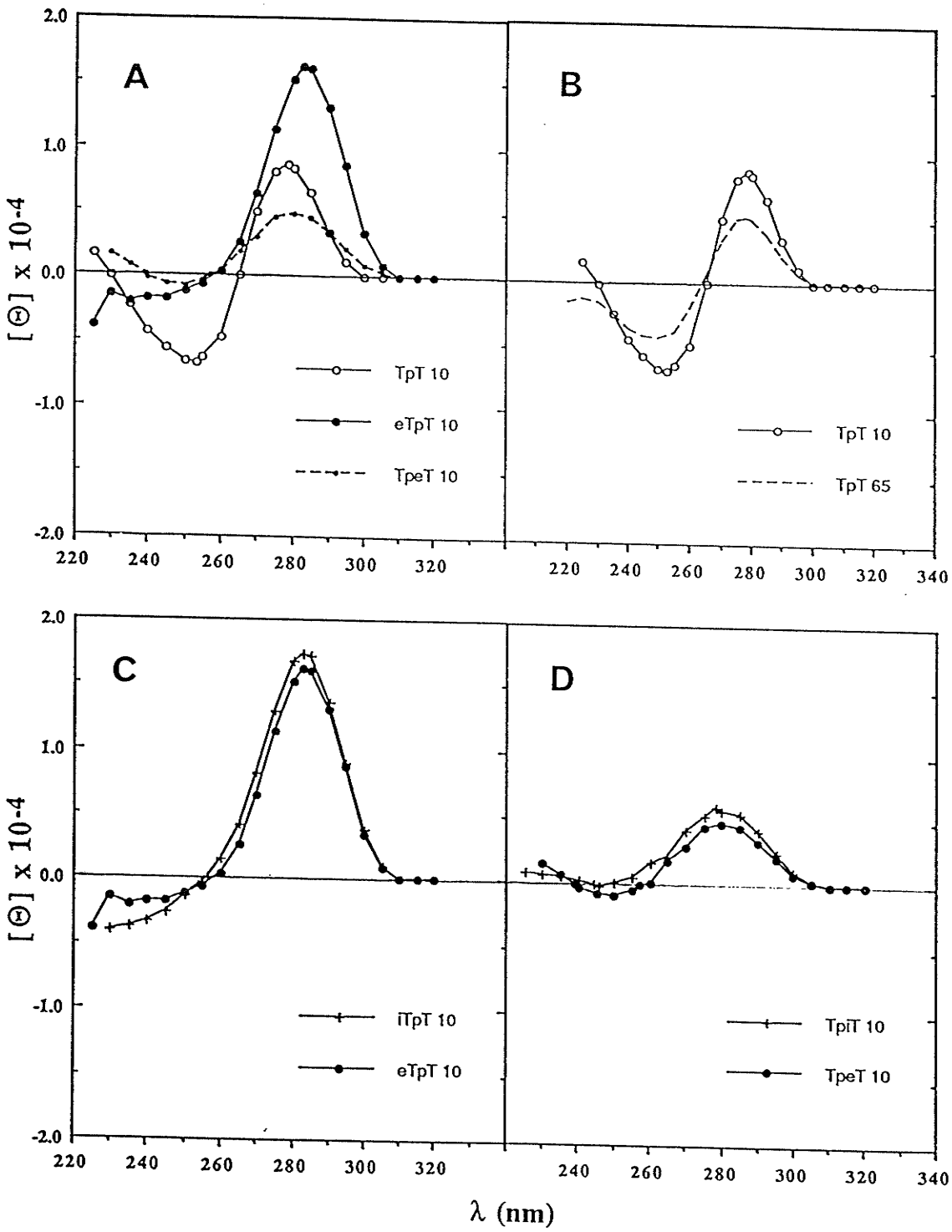

Figure 4.2: CD comparisons. A) d(TpT), d(e⁴TpT), and d(Tpe⁴T) at 10°C. B) d(TpT) at 10 and 65°C. C) d(i⁴TpT) and d(e⁴TpT) at 10°C. D) d(Tpi⁴T) and d(Tpe⁴T) at 10°C.

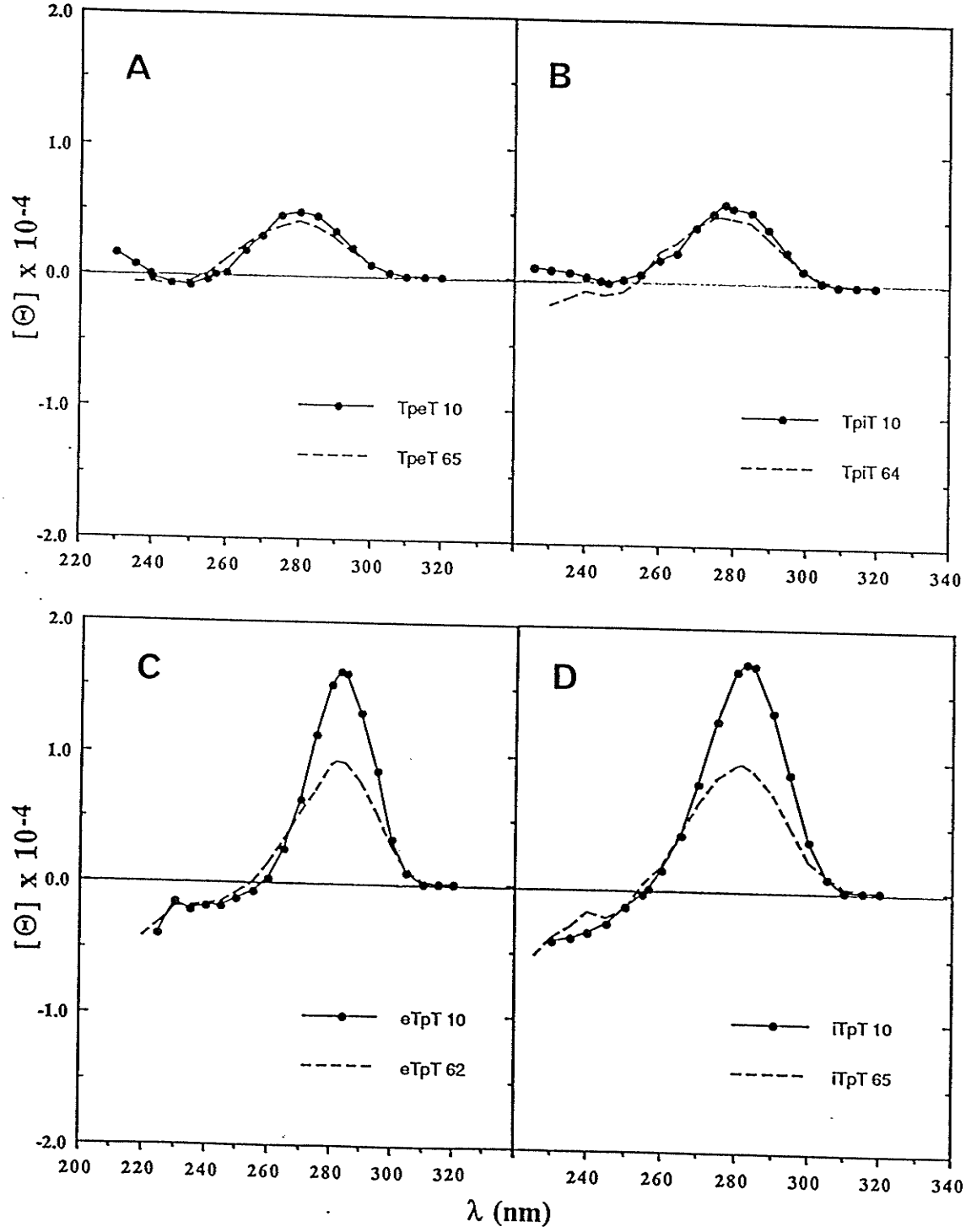

Figure 4.3: CD comparisons. A) d(Tpe^{4}T) at 10 and 65°C. B) d(Tpi^{4}T) at 10 and 64°C. C) d(e^{4}TpT) at 10 and 62°C. D) d(i^{4}TpT) at 10 and 65°C.

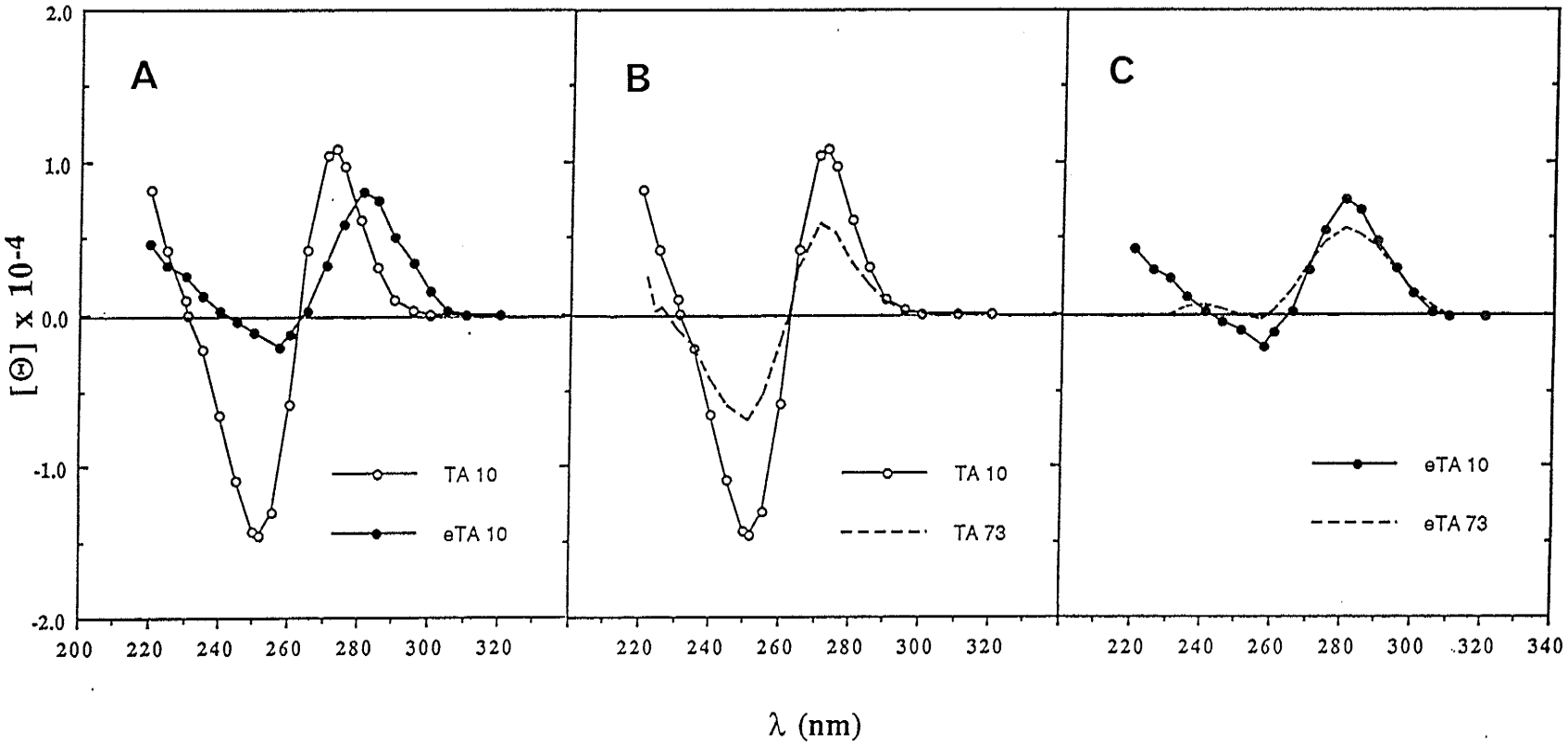

Figure 4.4: *CD comparisons. A) d(TpA) and d(e⁴TpA) at 10°C. B) d(TpA) at 10 and 73°C. C) d(e⁴TpA) at 10 and 73°C.*

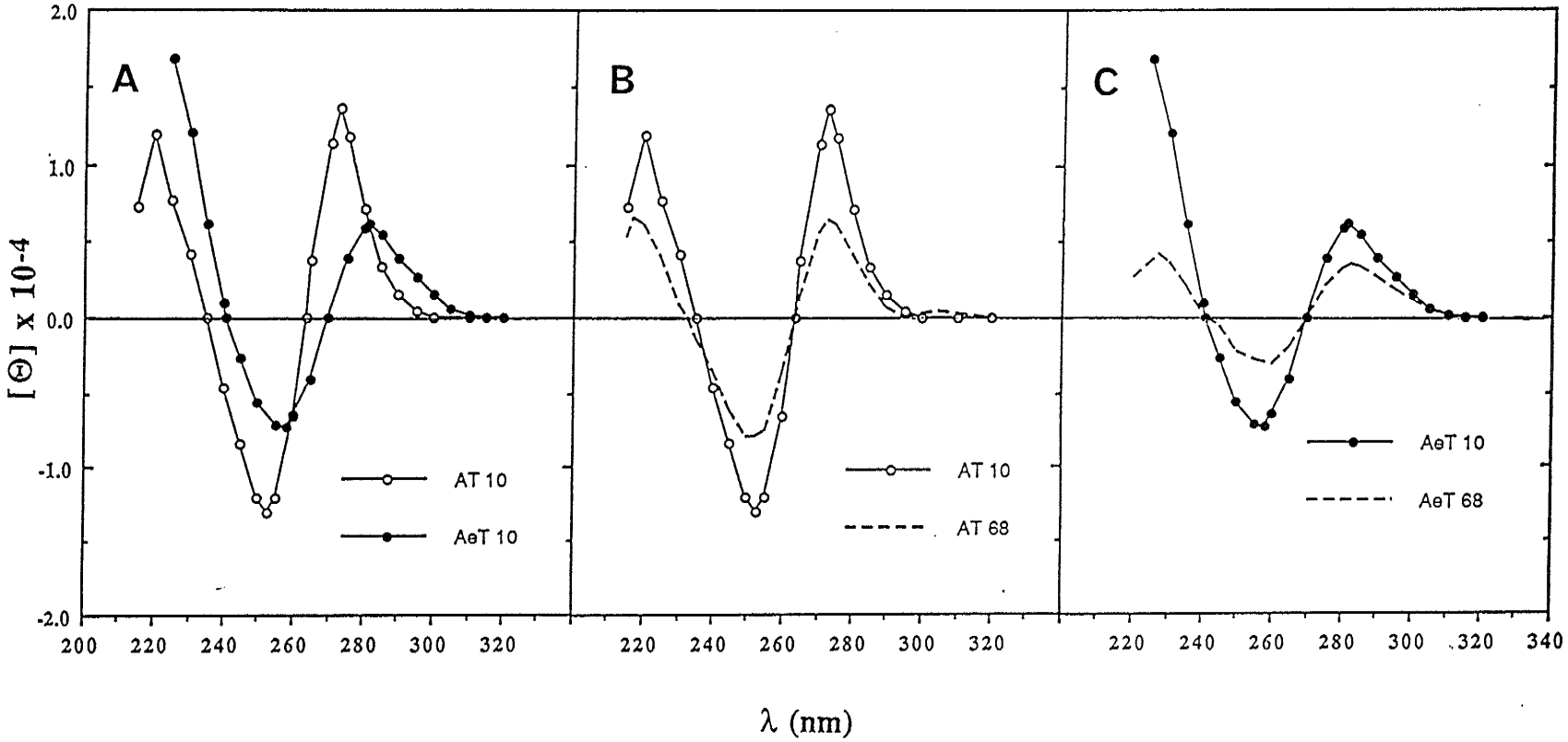

Figure 4.5: *CD comparisons. A) d(Ape⁴T) and d(TpA) at 10°C. B) d(ApT) at 10 and 68°C. C) d(Ape⁴T) at 10 and 68°C.*

by Cantor et al. *(1970) for* ***d(ApT)*** *and d(TpAp) in terms of maxima and minima band positions and [Θ] ratios. Notable features of these CD spectra are: 1) the position of the maximum of the long λ band of* ***d(e⁴TpA)*** *and* ***d(Ape⁴T)*** *are red shifted 8 - 9 nm in comparison to* ***d(TpA)*** *and* ***d(ApT)****; 2) the magnitude of the short λ band of d(e⁴TpA) is reduced relative to that for* ***d(TpA)*** *(Figure 4.4A). This is reflected in an increase in the [Θ] ratio for* ***d(e⁴TpA)*** *(3.8) relative to* ***d(TpA)*** *(0.7). The magnitude of the short λ band for* ***d(Ape⁴T)*** *is also reduced relative to that for* ***d(ApT)*** *(Figure 4.5A). However, the [Θ] ratio for* ***d(Ape⁴T)*** *(0.8) decreases relative to* ***d(ApT)*** *(1.1). The latter pair of oligomers is the only example where the [Θ] ratio decreases upon the O4-alkylation of a T and implies that the magnitude of the long λ band is reduced to a greater extent than that of the short λ band; 3) the magnitudes of the positive and negative bands both increase in all four dimers as the temperature is lowered. The temperature dependence of the CD spectra of* ***d(Ape⁴T)*** *(Figure 4.5C) is greater than that of* ***d(e⁴TpA)*** *(Figure 4.4C), in contrast to the order in* ***d(Tpe⁴T)*** *(Figure 4.3A) and* ***d(e⁴TpT)*** *(Figure 4.3C). On the other hand, the temperature dependence of the CD spectra of* ***d(TpA)*** *and* ***d(ApT)*** *are similar (Figure 4.4B and 4.5B).*

Figure 4.6 contains comparisons of the CD spectra of ***d(TpG)*** *and* ***d(e⁴TpG)****. Our CD spectra for* ***d(TpG)*** *agree with the spectra obtained by Cantor* et al. *(1970) for d(TpGp) with the maximum of the long λ band at identical positions in both molecules and the position of the minimum of the short λ band differing by 1 nm. However, the [Θ] ratios differ, 0.3 for* ***d(TpG)*** *and 0.5 for d(TpGp), but this may be due to the 3'-phosphorylation of* ***d(TpG)****. Notable features of these spectra are: 1) the position of the maximum of the positive band at long λ for* ***d(e⁴TpG)*** *is blue shifted 6 nm relative to* ***d(TpG)****; 2) the position of the minimum of the negative band at short λ for* ***d(e⁴TpG)*** *(247 nm) is reduced in intensity and is blue shifted 13 nm relative to* ***d(TpG)****. The reduction in the magnitude of the negative band is reflected in an increase in the [Θ] ratio for* ***d(e⁴TpG)*** *(2.1) relative*

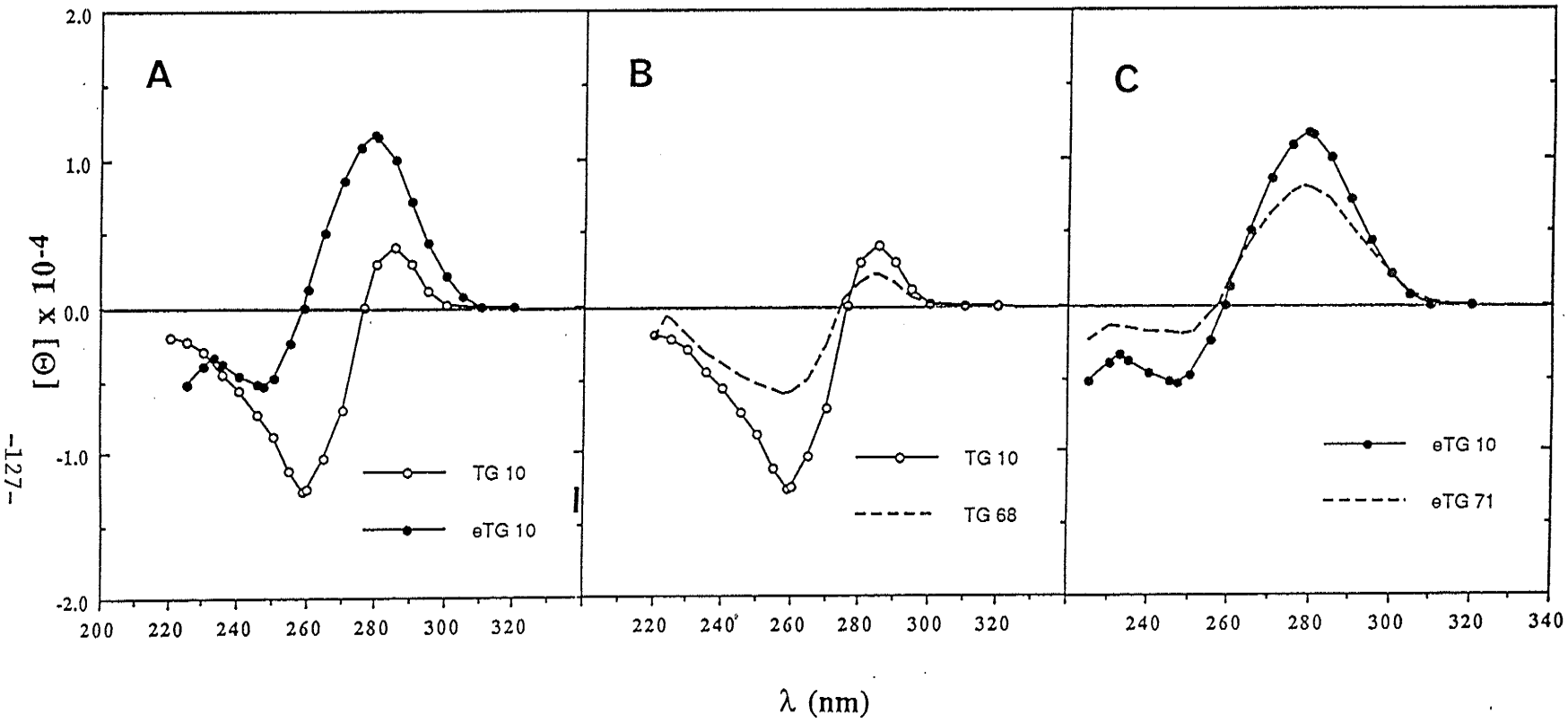

Figure 4.6: *CD comparisons. A) d(TpG) and d(e⁴TpG) at 10°C. B) d(TpG) at 10 and 68°C. C) d(e⁴TpG) at 10 and 71°C.*

to d(TpG) (0.3); 3) the magnitudes of the positive and negative bands increase in both dimers as the temperature is lowered. The CD spectra for d(TpG) (Figure 4.6B) show a larger temperature dependence than those for d(e⁴TpG) (Figure 4.6C).

The CD spectra for d(e⁴TpC) at 10 and 69°C are similar (Figure 4.9C). There is a positive band at long λ (maximum at 282 nm) which is red shifted 3 nm relative to the value obtained by Cantor et al. *(1970) for d(TpC). Cantor* et al. *(1970) also observed a negative band at short λ (minimum at 239 nm), a feature that is absent in d(e⁴TpC). The magnitude of the long λ band increases as the temperature is lowered.*

Figures 4.7 to 4.10 contain various comparisons of the CD spectra of the trimers, d(Tpe⁴TpT), d(Tpi⁴TpT), d(TpTpT), d(Ape⁴TpA), and d(ApTpA). The CD spectrum for d(pTpTpT) has been obtained by Cantor et al. *(1970) and the maximum and minimum band positions, at 278 and 249 nm, respectively, are similar to the values we obtained for d(TpTpT) without a 5'-phosphate. Notable features of these trimer spectra are: 1) they all contain a positive band at long λ that is red shifted: 1 - 2 nm for d(Tpr⁴TpT) relative to d(TpTpT), and 12 nm for d(Ape⁴TpA) relative to d(ApTpA); 2) the negative band at short λ for d(TpTpT) is reduced in magnitude and is blue shifted relative to d(Tpr⁴TpT). The reduction in the negative band's magnitude is reflected in larger [Θ] ratios for the d(Tpr⁴TpT) trimers relative to d(TpTpT). In d(Ape⁴TpA) the magnitude of the negative band is reduced and is red shifted 7 nm relative to d(ApTpA). The reduction in the negative band magnitude is also reflected in a larger [Θ] ratio for d(Ape⁴TpA) (1.2) relative to d(ApTpA) (0.7); 3) the magnitudes of the positive and negative bands increase in all the trimers as the temperature is lowered. The temperature dependence of the CD spectra for d(TpTpT) (Figure 4.8D), d(Tpe⁴TpT) (Figure 4.8A), and d(Tpi⁴TpT) (Figure 4.8B) are similar, with a small decrease in the order listed. On the other hand, the CD spectra for d(ApTpA) (Figure 4.10B) have a larger temperature dependence than those for d(Ape⁴TpA) (Figure 4.10C); 4) the CD spectra of d(Tpe⁴TpT) and d(Tpi⁴TpT) (Figure 4.8C) are not as similar as those of*

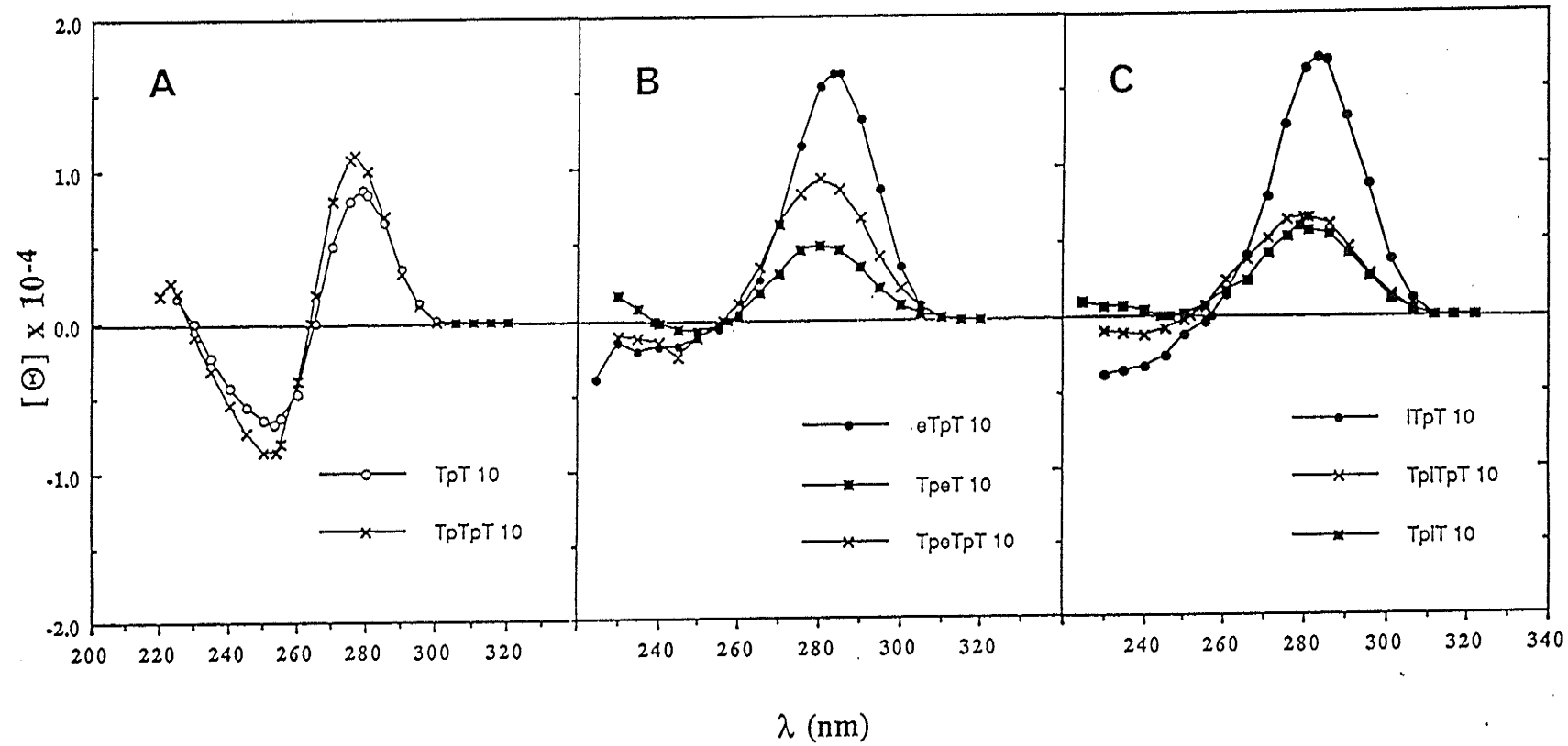

Figure 4.7: CD comparisons. A) d(TpT) and d(TpTpT) at 10°C. B) d(e⁴TpT), d(Tpe⁴T), and d(Tpe⁴TpT) at 10°C. C) d(i⁴TpT), d(Tpi⁴T), and d(Tpi⁴TpT) at 10°C.

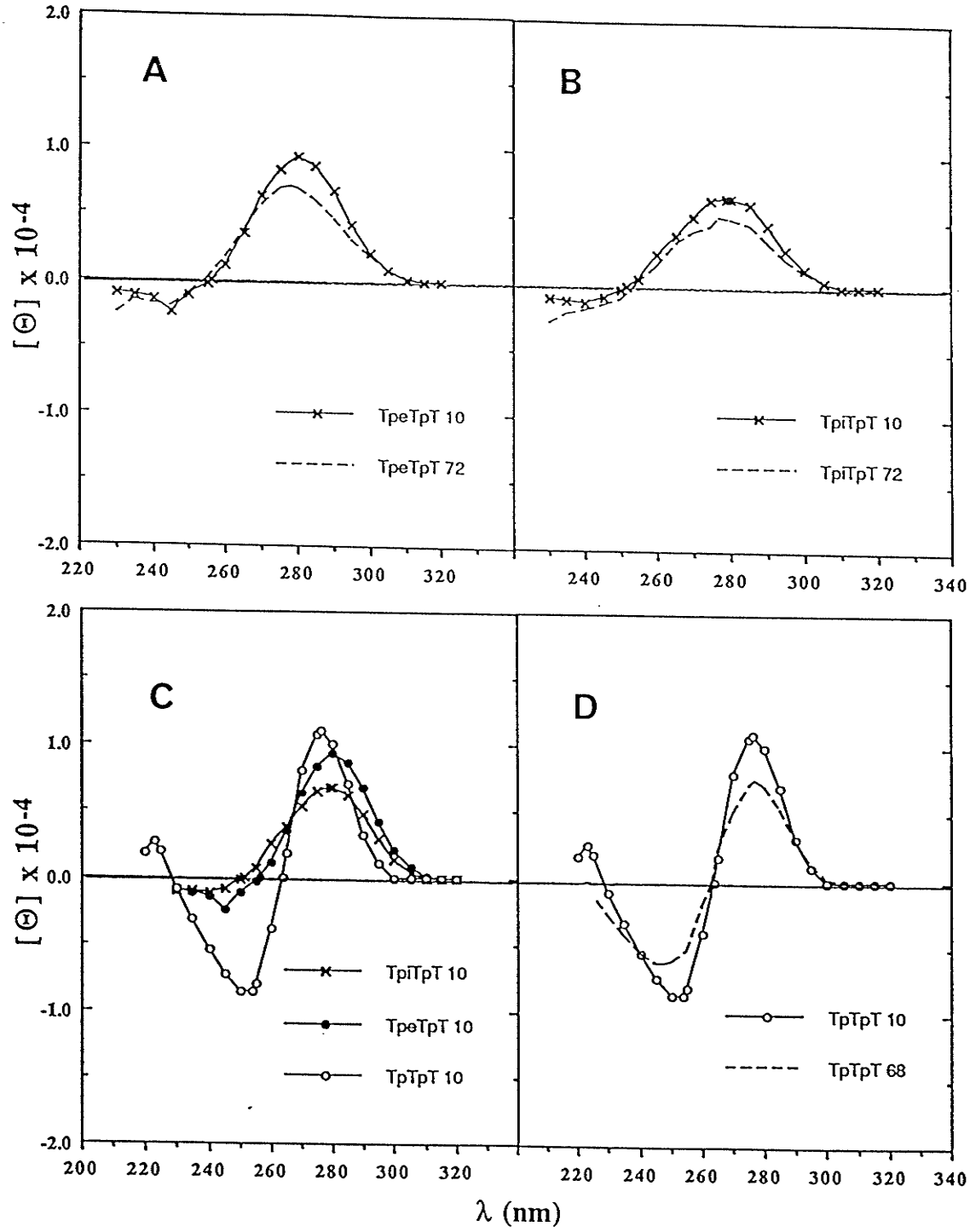

Figure 4.8: CD comparisons. A) d(Tpe⁴TpT) at 10 and 72°C. B) d(Tpi⁴TpT) at 10 and 72°C. C) d(Tpi⁴TpT), d(Tpe⁴TpT), and d(TpTpT) at 10°C. D) d(TpTpT) at 10 and 68°C.

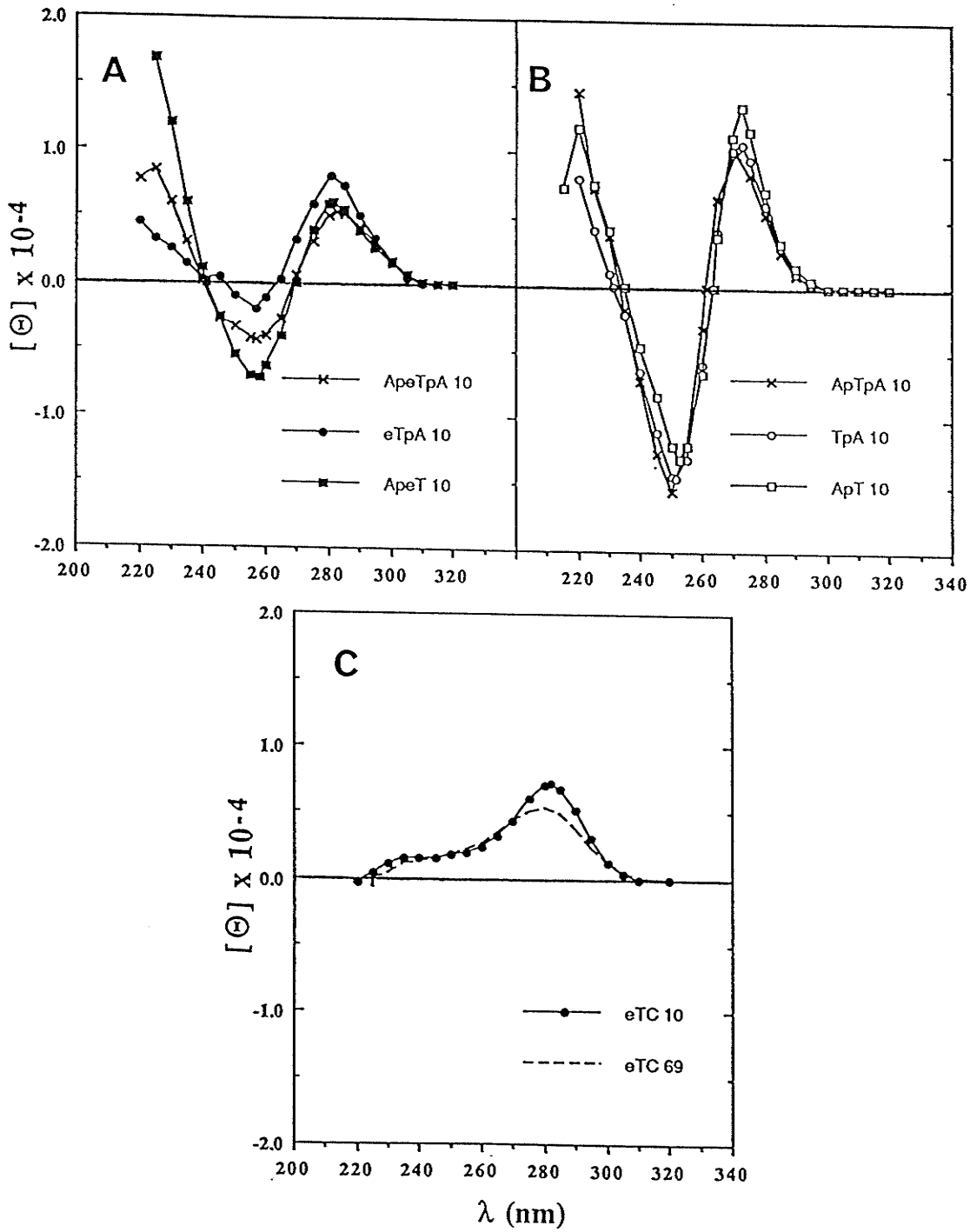

Figure 4.9: CD Comparisons. A) d(Ape⁴TpA), d(e⁴TpA), and d(Ape⁴T) at 10°C. B) d(ApTpA), d(TpA), and d(ApT) at 10°C. C) d(e⁴TpC) at 10 and 69°C.

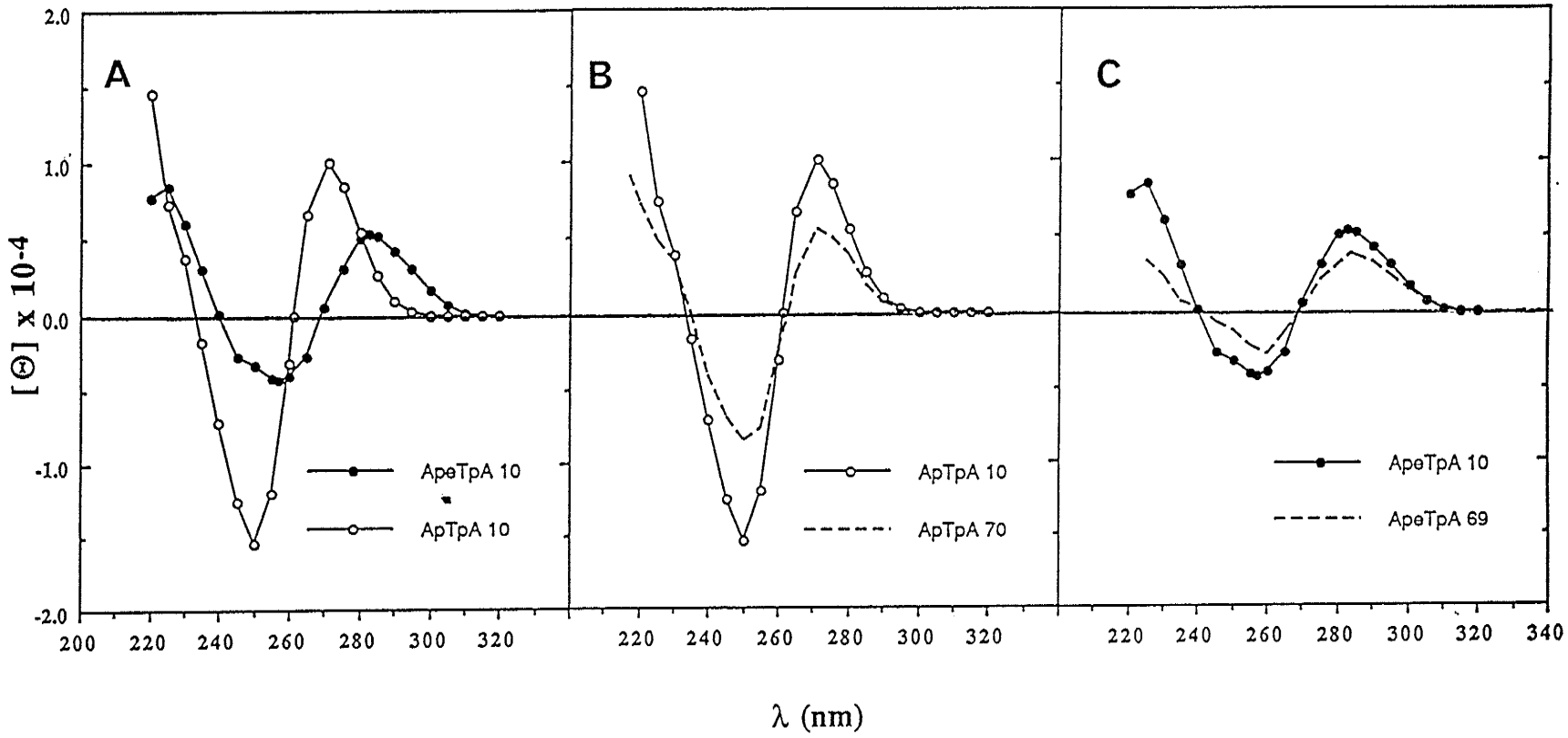

Figure 4.10: CD comparisons. A) d(Ape⁴TpA) and d(ApTpA) at 10°C. B) d(ApTpA) at 10 and 70°C. C) d(Ape⁴TpA) at 10 and 69°C.

d(r⁴TpT) (Figure 4.2C) and d(Tpr⁴T) (Figure 4.2D), especially with respect to the magnitude of the positive band. The difference could be a reflection of slightly different conformations of the two trimers manifested by different O4-alkyl groups; 5) the CD spectra of d(TpTpT) and d(TpT) (Figure 4.7A) are similar in shape and, consequently, [Θ] ratios, as are the CD spectra of d(ApTpA), d(TpA), and d(ApT) (Figure 4.9B), suggesting the global structure of both sets of molecules are comparable. Alternatively, the shape and, more importantly, the [Θ] ratios, of the CD spectra of d(Tpe⁴TpT), d(e⁴TpT), and d(Tpe⁴T) (Figure 4.7B), d(Tpi⁴TpT), d(i⁴TpT), and d(Tpi⁴T) (Figure 4.7C), and d(Ape⁴TpA), d(e⁴TpA), and d(Ape⁴T) (Figure 4.9A) differ to a greater extent, suggesting that the global structure of these sets of molecules are not as comparable.

In summary, the major points to be made about the oligomer CD data are: 1) a positive CD band at long λ is present in all the molecules. Such a band has been observed for other DNA oligomers which have been studied by different methods, such as NMR, Raman spectroscopy, and fibre X-ray diffractometry. The latter methods show that these DNA oligomers, with a positive long λ CD band, are forming right-handed stacks (Tunis-Schneider and Maestre, 1970; Ivanov et al., *1973; Johnson* et al., *1981; Nishimura* et al., *1986; Fairall* et al., *1989) On the other hand, left-handed Z-DNA is characterized by a negative long λ band (Pohl and Jovin, 1972; Behe and Felsenfeld, 1981). Hence, the CD spectra of our oligomers, with and without an O4-alkylthymine, suggest that these molecules also are adopting right-handed stacks in solution; 2) the negative short λ CD band for the non-alkylated oligomers is absent or reduced in analogous oligomers with an O4-alkylthymine. This observation is correlated with an increase in the [Θ] ratios for the O4-alkylated oligomers relative to the non-alkylated molecules, except for d(Ape⁴T) relative to d(ApT). In comparing A-DNA to B-DNA, a smaller negative band at short λ has been associated with the former helix (Tunis-Schneider, 1970; Ivanov* et al., *1973; Fairall* et al., *1989), reflecting different base stacking geometries in both types of DNA. Note that A-DNA is characterized*

by sugars in the 3'-endo *conformation as opposed to B-DNA, whose sugars are predominately in the 2'*-endo *conformation (Chapter 5). The different sugar conformations in the two forms of DNA alter the geometry of the helix and consequently, alter the base-stacking geometries (Saenger, 1984). Perhaps the reduction in the negative band at short* λ *is a reflection of more A-DNA character in the O4-alkylated oligmers in comparison to the analogous non-alkylated oligomers, especially in terms of increases in the 3'*-endo *sugar populations which are observed in the NMR data (Chapter 5); 3) an increase in* $[\Theta]$ *with decreasing temperature is usually associated with an increase in base-stacked states (Brahms* et al., *1967; Bush and Brahms, 1973). All of the oligomers containing an O4-alkylthymidine had CD spectra whose magnitude increased with decreasing temperature, suggesting that the amount of base-stacking was increasing in these molecules as temperature was being lowered; 4) the CD spectra for the O4-alkylated and non-alkylated oligomers differ and some of the different features noted may be used to identify DNA containing* r^4dT. *Unfortunately, there appears to be no apparent correlation between the position of the O4-alkylthymidine in the oligomer and the* λ *shifts of the positive and negative bands.*

CHAPTER 5

DISCUSSION

5.1 INTRODUCTION:

From the J and δ values of the ^{1}H and ^{13}C NMR resonances tabulated in Tables 3.1 - 3.25 it is possible to obtain conformational information on the solution structure of DNA. This is possible because the vicinal coupling constant (^{3}J) depends on the torsion angle (Θ) about the bond to which the coupled spins are attached (Davies, 1978; van de Ven and Hilbers, 1988) and the δ depends on the magnetic environment of the nucleus (Giessner-Prettre and Pullman, 1988). There are a number of ways to use the J and δ data to obtain conformational information and the methods chosen are described below.

5.1.1 NOMENCLATURE:

Before the data may be discussed it is necessary to define all the conventions and definitions pertaining to the conformational analysis of nucleic acids. IUPAC guidelines (IUPAC-IUB, 1970) will be adhered to in the text that follows. The torsion angles, Θ, along the backbone are designated α, β, γ, δ, ε, and ζ starting with the P-O5' bond (Figure 5.1A). The sugar endocyclic torsion angles are designated υ_0 to υ_4 commencing with the O4'-C1' bond and moving clockwise. The sign of Θ follows the Klyne-Prelog convention (1960) with the eclipsed form equal to zero and positive values obtained by moving the rear bond clockwise with respect to the front bond. Shorthand designations for the staggered conformations are g^+ (Θ ~ 60°), t (Θ ~ 180°) and g^- (Θ ~ 300°) (Figure 5.1B). The glycosyl C1'-N bond is called χ. When the six member ring of purines or the O2 of pyrimidines is over the sugar, then χ is said to be in the syn *position; a 180° rotation brings the base into the* anti *position.*

5.1.2 FURANOSE CONFORMATION:

The sugar torsion angles, υ_0 to υ_4, are not free to assume any value between 0 and 360° because the ring is closed. These five mutually related angles can therefore be described by a two parameter equation via pseudorotational analysis. The two parameters are called P, the phase angle, and τ_m, the amplitude of pucker. An analysis of the X-ray

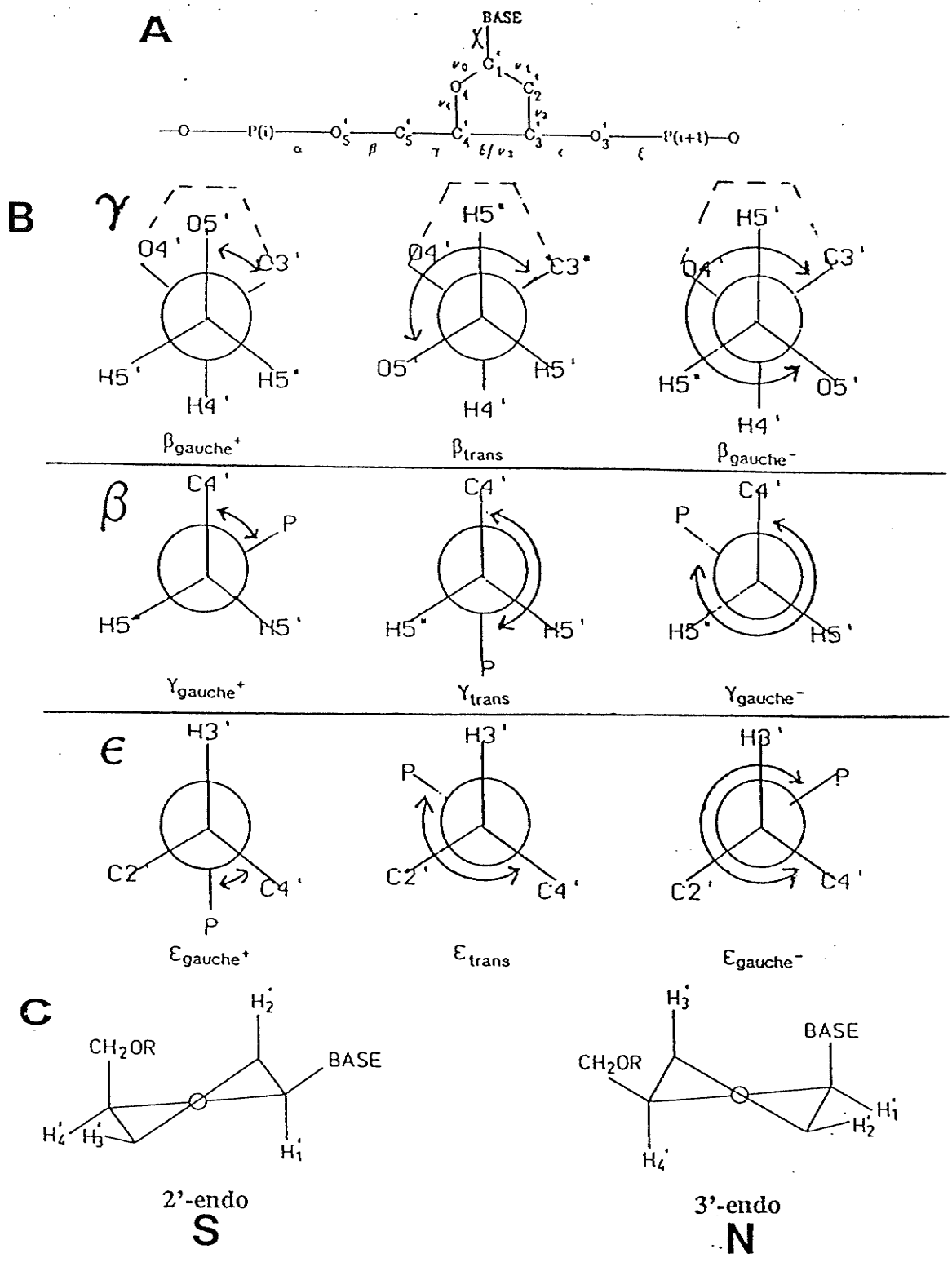

Figure 5.1: Conventions and definitions pertaining to the conformational analysis of nucleic acids. A) Definition of bonds; the phosphodiester backbone (α to ζ), the sugar ring (υ_0 to υ_4), and χ. B) Newman projections about β, γ, and ε. C) The two idealized sugar conformers, 2'-endo (S) and 3'-endo (N). A reproduced from van de Ven and Hilbers (1988), B from Buchko (1986), and C from Altona (1982). ...137.

*data of many nucleosides and nucleotides shows that two ranges of the "conformational wheel" are predominantly occupied (Altona and Sundaralingam, 1972). These ranges are called the 2'-*endo *(S) and 3'-*endo *(N) conformations; an example of each is given in Figure 5.1C.*

Values for P and τ_m *can be obtained in solution from the five sugar coupling constants,* $^3J_{1'-2'}$ *to* $^3J_{3'-4'}$*, by computer programs such as PSEUROT (Altona, 1982). The Ps and* τ_m*s calculated via PSEUROT have been related to the sums of various vicinal proton coupling constants (Rinkel and Altona, 1987). For instance, the fraction of sugars in the S conformation (fS) may be estimated from the sum of* $^3J_{1'-2'}$ *and* $^3J_{1'-2'}$ *(*$\Sigma 1'$*) using the following equation:*

$$fS = (\Sigma 1' - 9.8)/5.9 \qquad (I)$$

Experimentally, it is often easier to use $\Sigma 1'$ *since it is simply the separation between the outer peaks of the H1' multiplet. Furthermore, it is often difficult to accurately obtain the five coupling constants needed to obtain P and* τ_m *values. For these two reasons equation I was used to estimate the sugar conformation of our oligomers.*

Perturbations in the sugar conformation based on the $\Sigma 1'$ *data were checked by other methods. For example, Hruska (1973) observed a correlation between* $^3J_{3'-4'}$*,* $^3J_{1'-2'}$*, and the sugar pucker in monomers. Perturbations that increase the population of the N sugar conformation manifest an increase in* $^3J_{3'-4'}$ *and a decrease in* $^3J_{1'-2'}$*. On the other hand, the inverse effect is observed with perturbations that increase the population of the S sugar conformation,* $^3J_{3'-4'}$ *decreases and* $^3J_{1'-2'}$ *increases. This* $^3J_{3'-4'}$ *and* $^3J_{1'-2'}$ *correlation with the sugar pucker extends into oligonucleotides, as illustrated in Figure 5.2 (van de Ven and Hilbers, 1988), where the three drawn lines represent "allowed" combinations of* $^3J_{3'-4'}$ *and* $^3J_{1'-2'}$ *as the pseudorotation cycle is traversed for various* τ_m *values. Note that the experimental points scatter in between pure S and N puckers, as expected if individual J values represent a weighted average of two J values. Consequently, we used changes in*

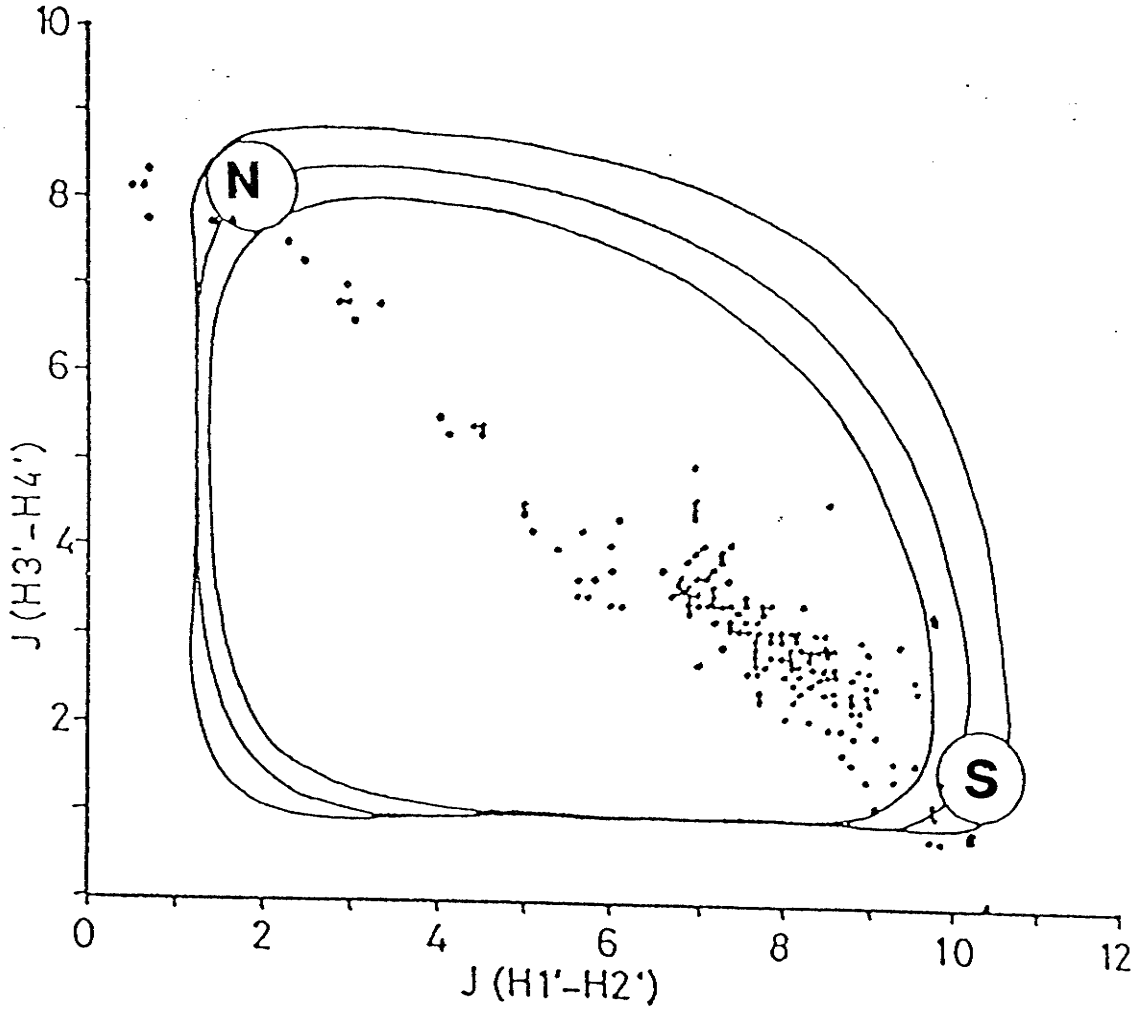

<u>Figure 5.2</u>: Plot of the J(H1'-H2') and J(H3'-H4') coupling constants for a variety of single-stranded, double-stranded, circular, platinated, and base-deleted oligonucleotides at various temperatures. Pure N- and S-type conformers are indicated as encircled regions. The solid lines represent "allowed" combinations of the two coupling constants as the pseudorotation cycle is traversed with pucker amplitudes of 30, 35, and 45° starting with the inner curve. Reproduced from van de Ven and Hilbers (1988).

$\Sigma 1'$ to monitor temperature dependent perturbations in the proportion of S conformations. Trends in $^3J_{3'-4'}$ and $^3J_{1'-2'}$ were then noted to verify $\Sigma 1'$ observations.

5.1.3 THE SUGAR-PHOSPHATE BACKBONE:

There are six torsion angles along the sugar-phosphate backbone (Figure 5.1A). The conformation about the C4'-C3' bond, δ, is intimately related to the sugar pucker. No ^1H-^1H, ^1H-^{13}C, or ^{13}C-^{13}C vicinal couplings exists about α and ζ so as to obtain any information regarding their orientation. This leaves three sugar-phosphate backbone bonds for which conformational information may be obtained from the NMR data in Tables 3.1 - 3.25.

5.1.3.1 The C4'-C5' (γ) Bond: *X-ray crystallographic studies of nucleosides and nucleotides show that three staggered conformations about γ exist, two gauche (γ^+ and γ^-) and one trans (γ') (Sundaralingam, 1973) (Figure 5.1B). In solution, the proportion (f) of these three states can be estimated from $^3J_{4'-5'}$ and $^3J_{4'-5''}$ using the following equations:*

$$f\gamma^- = 0.1228(^3J_{4'-5'}) - 0.0027(^3J_{4'-5''}) - 0.2952 \quad (II)$$

$$f\gamma' = -0.0334(^3J_{4'-5'}) + 0.1094(^3J_{4'-5''}) - 0.062 \quad (III)$$

$$f\gamma^+ = -0.0894(^3J_{4'-5'}) - 0.1068(^3J_{4'-5''}) + 1.3533 \quad (IV)$$ *(Rinkel and Altona, 1984).*

5.1.3.2 The C5'-O5' (β) Bond: *In crystals, without exception, all 5'-phosphorylated nucleotides are in the trans (β') conformation (Altona, 1982). In solution, the proportion of β' can be estimated from the sum (Σ) of the vicinal proton-phosphorus couplings, $^3J_{5'-P}$ and $^3J_{5''-P}$ using the following equation:*

$$f\beta' = (23.9 - \Sigma)/18.9 \quad (V)$$ *(Altona, 1982).*

5.1.3.3 The C3'-O3' (ε) Bond: *X-ray crystallographic studies of 3'-nucleotides suggest that the ε^+ conformation is "forbidden" (Sundaralingam, 1969), presumably due to steric repulsion of the phosphate group and the sugar moiety (Yokoyama* et al., *1981). Solution studies are hampered by the presence of only one vicinal proton coupling constant between H3' and P3. Because the orientation of the phosphorus is approximately symmetrical with respect to H3' in the ε^- and ε' conformations, $^3J_{3'-P}$ provides little information about these*

populations. However, if ^{13}C spectra are acquired, the ε rotamer populations can be better estimated from $^{3}J_{C4'-P3}$ and $^{3}J_{C2'-P3}$ using the following equations:

$$f\varepsilon^{t} = {}^{3}J_{C4'-P3}/9.2 \qquad (VI)$$

$$f\varepsilon^{-} = ({}^{3}J_{C2'-P3} - 1.0)/9.2 \qquad (VII)$$

(Alderfer and Ts'O, 1977).

5.1.4 THE C1'-N (χ) BOND:

X-ray crystallographic studies of nucleotides and nucleosides generally locate pyrimidines in the anti *orientation and purines in either the* anti *or* syn *form (Davies, 1978). No ^{1}H homonuclear vicinal coupling constants exist so as to provide information about χ in solution. However, it is possible to acquire information from ^{1}H-^{13}C coupling constants if enough sample is present to acquire the ^{13}C spectrum (which is usually not the case). Therefore, it is only possible to make inferences about the orientation of the base from chemical shift trends (Kan* et al., *1973) or NOEs (van de Ven and Hilbers, 1988).*

5.1.5 VARIABLE TEMPERATURE PROFILES:

In solution a two state mechanism, involving stacked and unstacked states, is generally sufficient to explain the behaviour of single stranded DNA helices (Powell et al., *1973; Olsthoorn* et al., *1980; Reich and Tinoco, 1980). Decreasing the temperature increases the fraction of molecules in the base-stacked state. Such transitions into a stacked state, while accompanied with torsion angle changes that can be observed with Js, are also often accompanied with changes in the magnetic environment of the nuclei. These magnetic environment changes are reflected in changes in the δs. Hence, by plotting δ versus temperature base-stacking information is obtained. Such plots for the base and some sugar protons have been obtained for most of my oligomers.*

5.1.5.1 Sugar Variable Temperature Profiles: *The δs of the sugar protons depend on: 1) the χ conformation; 2) the orientation of neighbouring bases; 3) the conformation of the sugar; 4) the position of the endocyclic sugar oxygen; and 5) the position of the phosphate group. These five influences may shield or deshield the sugar protons and hence,*

it is often difficult to interpret their profiles. However, when large temperature dependent changes in any of these resonances are observed, it is at least possible to say that the conformation is changing and perhaps assume that a particular shielding or deshielding influence is responsible. The largest temperature dependent changes in sugar δs were observed for H1', H2', and H2" and hence, these are the only sugar protons whose resonances were plotted as a function of temperature.

***5.1.5.2 Base Variable Temperature Profiles**: The H8 of purines and the H6 of pyrimidines are near the deoxyribose ring oxygen and the phosphate group when stacked in a right handed helix with the bases in the* anti *conformation. As a result any ring current shielding of these protons due to base-stacking may be countered with deshielding due to diamagnetic anisotropic effects of the ring oxygen and the phosphate group which make interpretations of the H8 and H6 profiles difficult. On the other hand, in a similar right-handed/*χ-anti *orientation, the dT Me5, dC H5, and dA H2 chemical shifts are primarily influenced by the ring currents of stacked bases, and hence, these protons are the best monitors of base-base interactions (Lee and Tinoco, 1980). With r⁴T the O4-alkyl group protons are even further removed from the sugar-phosphate backbone relative to Me5 and therefore, these δs should be influenced predominately by interactions with other bases as well. Since the O4-alkyl protons are in a different location than the Me5 they also monitor a slightly different "space".*

***5.1.6 DISCUSSION STRATEGY**: Because of the large number of oligomers, the discussion is broken up into five parts: d(r⁴TpT), d(NpX), d(XpN), TRIMERS, and TETRAMERS. Each part is further subdivided into sections: the sugar conformation, the sugar-phosphate backbone, the base protons, and summary.*

5.2 *d(r⁴TpT):*

5.2.1 *THE O4-ALKYL GROUP:*

A set of ***d(r⁴TpT)*** *dimers was synthesised with r equal to methyl (m), ethyl (e), propyl (p), butyl (b), isobutyl (ib) and isopropyl (i) to study the effect of O4-alkyl group size on the conformation of these molecules. Since the O4-alkyl group is the feature unique to all these dimers, and all the new oligomers, it is this moiety which will be discussed first.*

5.2.1.1 d(m⁴TpT): The O4-methyl protons of ***d(m⁴TpT)*** *appear as a singlet in the NMR spectrum, as in* ***m⁴dT****. The O4-methyl* $\Delta\delta^{\circ}$ *(high temperature* δ *- low temperature* δ *from the data in Tables 3.1 - 3.25) is small, < 0.03 ppm, and is similar to the O4-methyl* $\Delta\delta^{\circ}$ *of* ***m⁴dT*** *(Figure 5.8). Consequently, the pT base is not significantly influencing the O4-methyl profile of* ***d(m⁴TpT)****.*

5.2.1.2 d(e⁴TpT): Due to the presence of the chiral centres in the sugar, the α*-methylene protons of the O4-ethyl group of* ***d(e⁴TpT)*** *are diastereotopic and can be labelled pro-R (*H_R*) and pro-S (*H_S*) (Figure 5.3). At the nucleoside level, the O4-ethyl group of* ***e⁴dT*** *displays an* A_2X_3 *pattern in the* ^1H *NMR spectrum (methylene quartet, methyl triplet), which indicates that the sugar is too distant to induce any observable differential shielding of* H_R *and* H_S*. However, in* ***d(e⁴TpT)*** *these protons are not equally shielded, as is evident in the temperature dependent* ABX_3 *pattern of the O4-ethyl group (Figure 5.3). At 70°C a quartet pattern is observed for the* α*-methylene protons of the O4-ethyl group of* ***d(e⁴TpT)****. Lowering the temperature to 60°C produces an* ABX_3 *pattern for these* α*-methylene protons, and at 10°C a* $\Delta\delta$ *(downfield* $\delta(B)$ *- upfield* $\delta(A)$*) of 9.4 Hz is observed between these protons.*

Since a $\Delta\delta$ *is not observed for the* α*-methylene protons of* ***e⁴dT****, its presence in* ***d(e⁴TpT)*** *would seem to be a manifestation of intramolecular base-stacking. This effect may be explained in terms of a right handed base-stack with the bases in the* anti *position and the N3-C4-O4-*C_α *torsion angle near zero* (syn-*periplanar) as in crystalline* ***e⁴dT*** *(Birnbaum* et al., *1986). There are three low-energy rotational isomers of the O4-ethyl group about the*

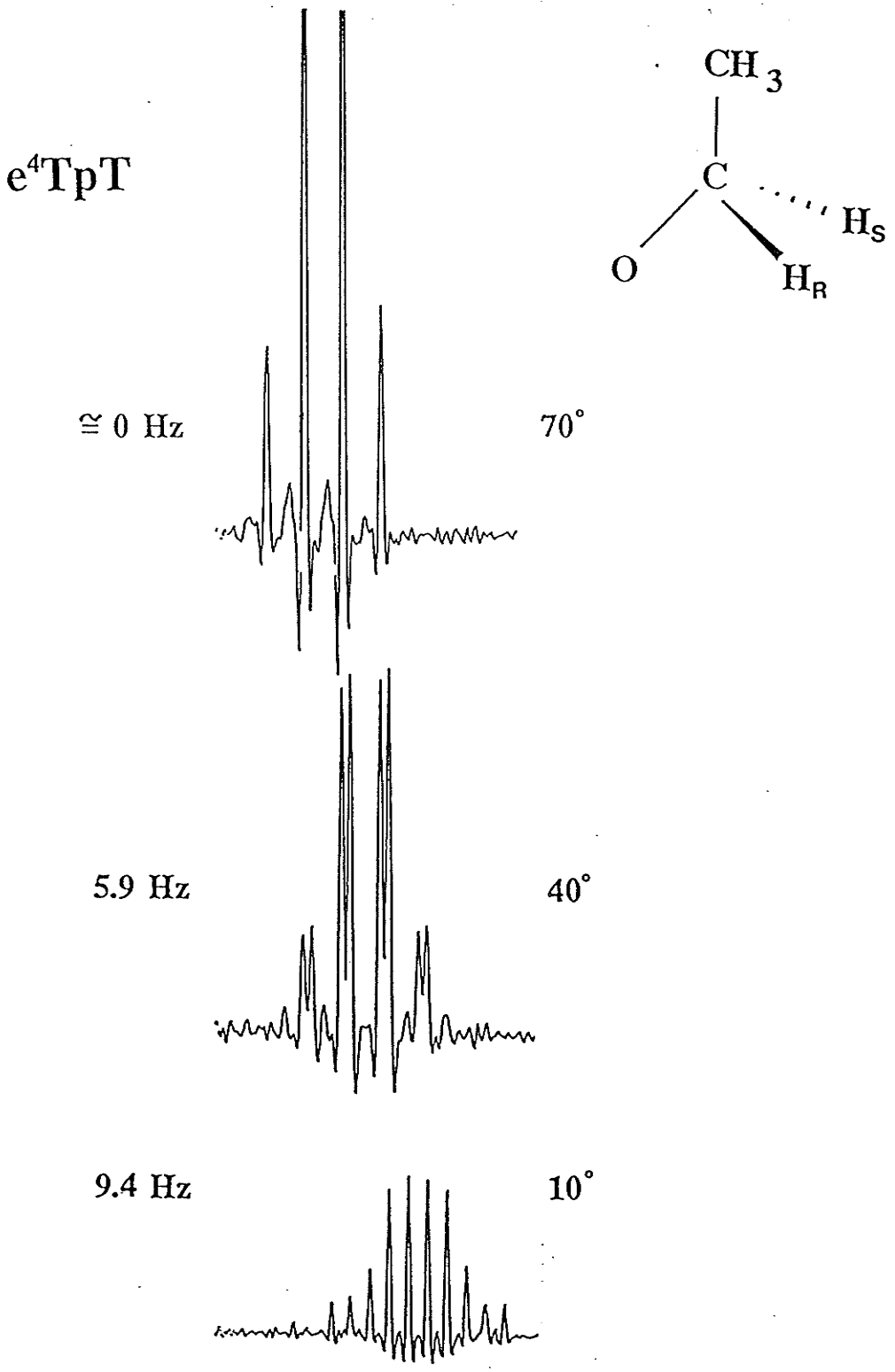

Figure 5.3: Temperature effect on the 300 MHz ^1H NMR band of the H_R and H_S α-methylene resonances of the O4-ethyl function of d(e⁴TpT). The value in Hz is the difference in the chemical shifts of these resonances (Δδ) at the temperature indicated.

O4-C_α bond, as illustrated in Figures 5.4A to C. Conformer A, with the α-methylene protons straddling the base, is the conformation in the ***e⁴dT*** *crystal (Birnbaum* et al., *1986) and probably is the preferred conformation in solution because conformers B and C place the methyl group too near the ring N3 where unfavourable van der Waals interactions might occur. If conformer A is the dominant state in solution, then as base-stacking occurs H_R will be subjected to a greater shielding effect from the neighbouring base than H_S. If this is true, then the upfield proton (A) plotted in Figure 5.8 can be assigned to the pro-R proton. Further evidence for the preference of conformation A in the base-stacked state is the variable temperature profiles of the methyl protons of the O4-ethyl group which show a weak temperature dependence that is similar to the monomer (Figure 5.20). The latter observation suggests that the neighbouring base has little effect on the methyl of the O4-ethyl group as stacking occurs because it is projected away from the stack.*

<u>5.2.1.3 d(p⁴TpT), d(b⁴TpT), and d(ib⁴TpT)</u>: The α-methylene protons of the O4-alkyl groups of these dimers display NMR spectra similar to ***d(e⁴TpT)****. In* ***d(p⁴TpT)*** *and* ***d(b⁴TpT)*** *both α-methylene protons display an ABX_2 pattern with a Δδ of 13.2 and 18.1 Hz, respectively, at 10°C (Figures 5.5 and 5.6). In* ***d(ib⁴TpT)*** *the α-methylene resonances of the O4-isobutyl group display an ABX pattern with a 20.0 Hz Δδ at 10°C (Figure 5.7). In all three dimers, Δδ decreases as the temperature is raised. Presumably, Δδ and its temperature dependence for the α-methylene resonances of the O4-propyl, -butyl, and -isobutyl group of these* ***d(r⁴TpT)*** *dimers are due to the same reason given for the O4-ethyl group of* ***d(e⁴TpT)*** *- base-stacking.*

Figure 5.8 is a variable temperature plot containing the α-methylene resonances for the O4-ethyl, -propyl, -butyl, and -isobutyl group of ***d(r⁴TpT)****. Note that the Δδ of the α-methylene protons of different O4-alkyl groups are rarely the same at identical temperatures. Additional data presented in Figure 5.11 and in Tables 3.2, 3.4, and 3.6 concerning the Me5 protons of the pT base suggest that the amount of base-stacking in all the* ***d(r⁴TpT)*** *dimers are similar. Hence, the different α-methylene Δδs must be due to something else other than*

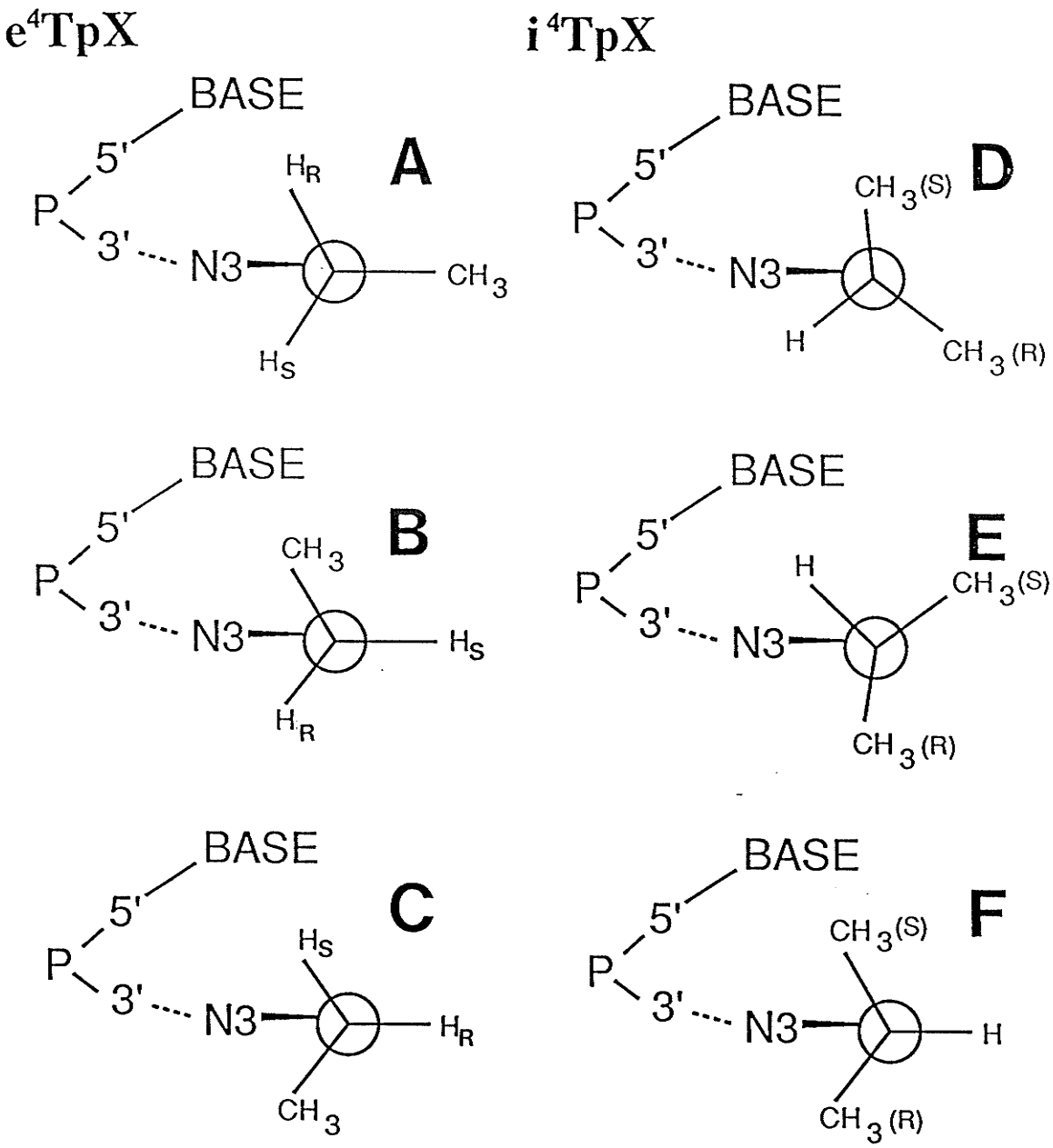

Figure 5.4: Conformational states about the O4-C_α bond with the O4-alkyl group in the syn-periplanar position. N3 is projected towards the viewer, such that the flanking groups of the O4-alkyl function are actually close to being above or below it. A) Orientation present in the e^4dT crystal with both α-methylene protons of the O4- ethyl straddling the base. B and C) Two other eclipsed conformations which are probably less favourable than A due to the bulky methyl group of the O4-ethyl function crowding the base. D and E) The two most likely conformations of the O4-isopropyl group based upon the crystal structure of i^2dT with the pro-S methyl in D, and the pro-R methyl in E, oriented almost 90° relative to the plane of the base. F) Third possible eclipsed conformation which is probably least favourable because both bulky methyl groups crowd the base.

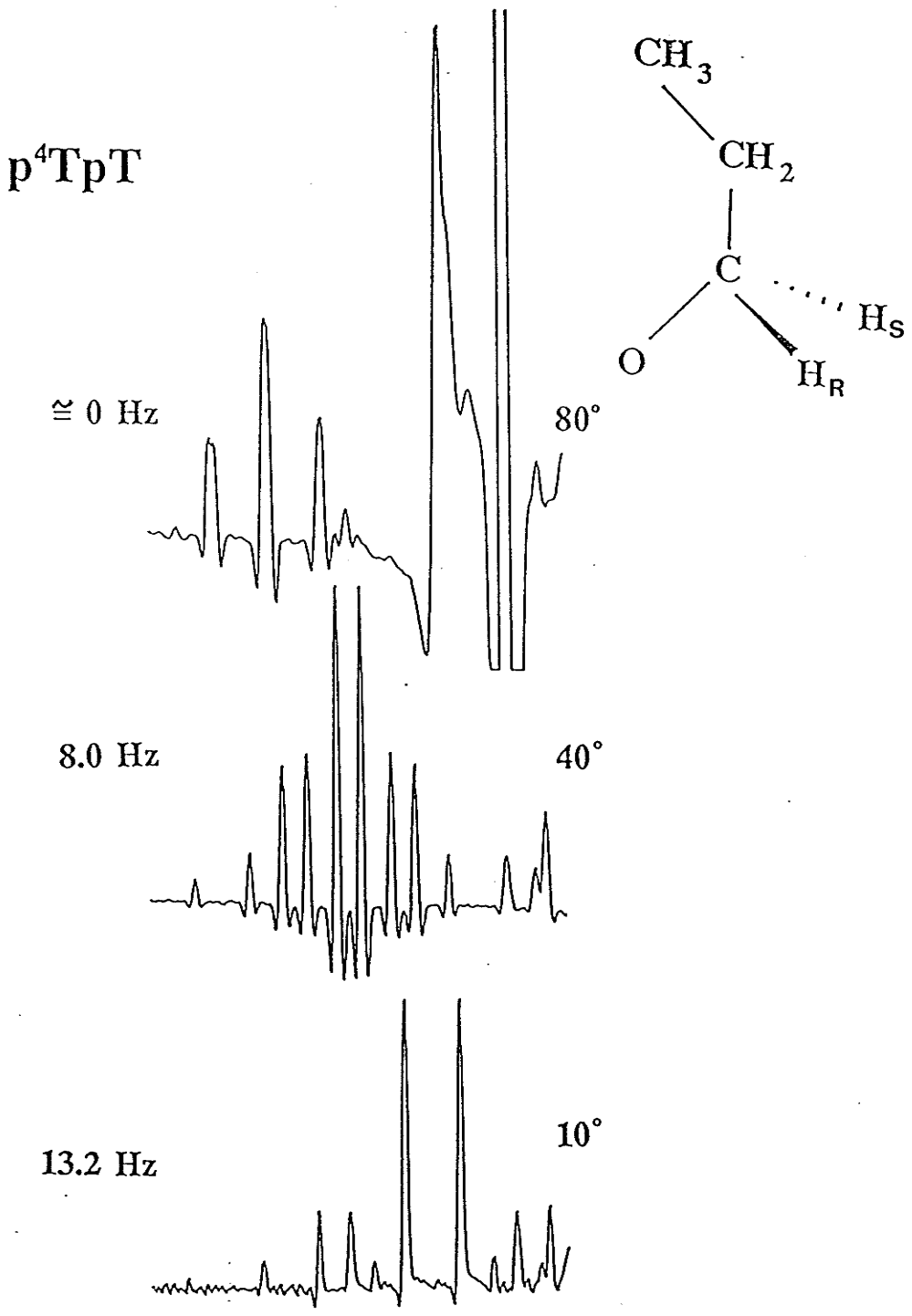

Figure 5.5: Temperature effect on the 300 MHz ^1H NMR band of the H_R and H_S α-methylene resonances of the O4-propyl function of d(p⁴TpT). The value in Hz is the difference in the chemical shifts of these resonances (Δδ) at the temperature indicated.

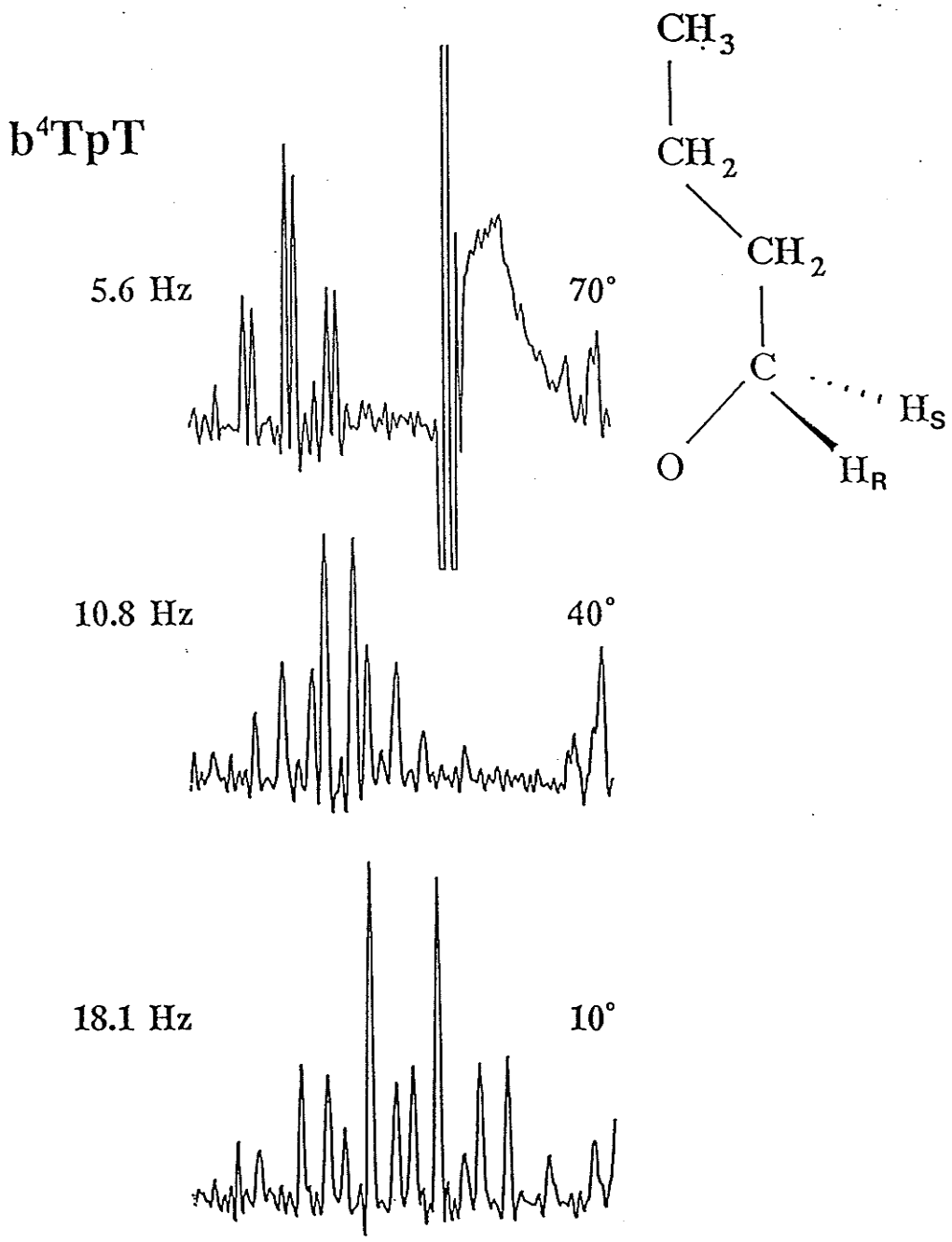

Figure 5.6: Temperature effect on the 300 MHz ^1H NMR band of the H_R and H_S α-methylene resonances of the O4-butyl function of d(b⁴TpT). The value in Hz is the difference in the chemical shifts of these resonances (Δδ) at the temperature indicated.

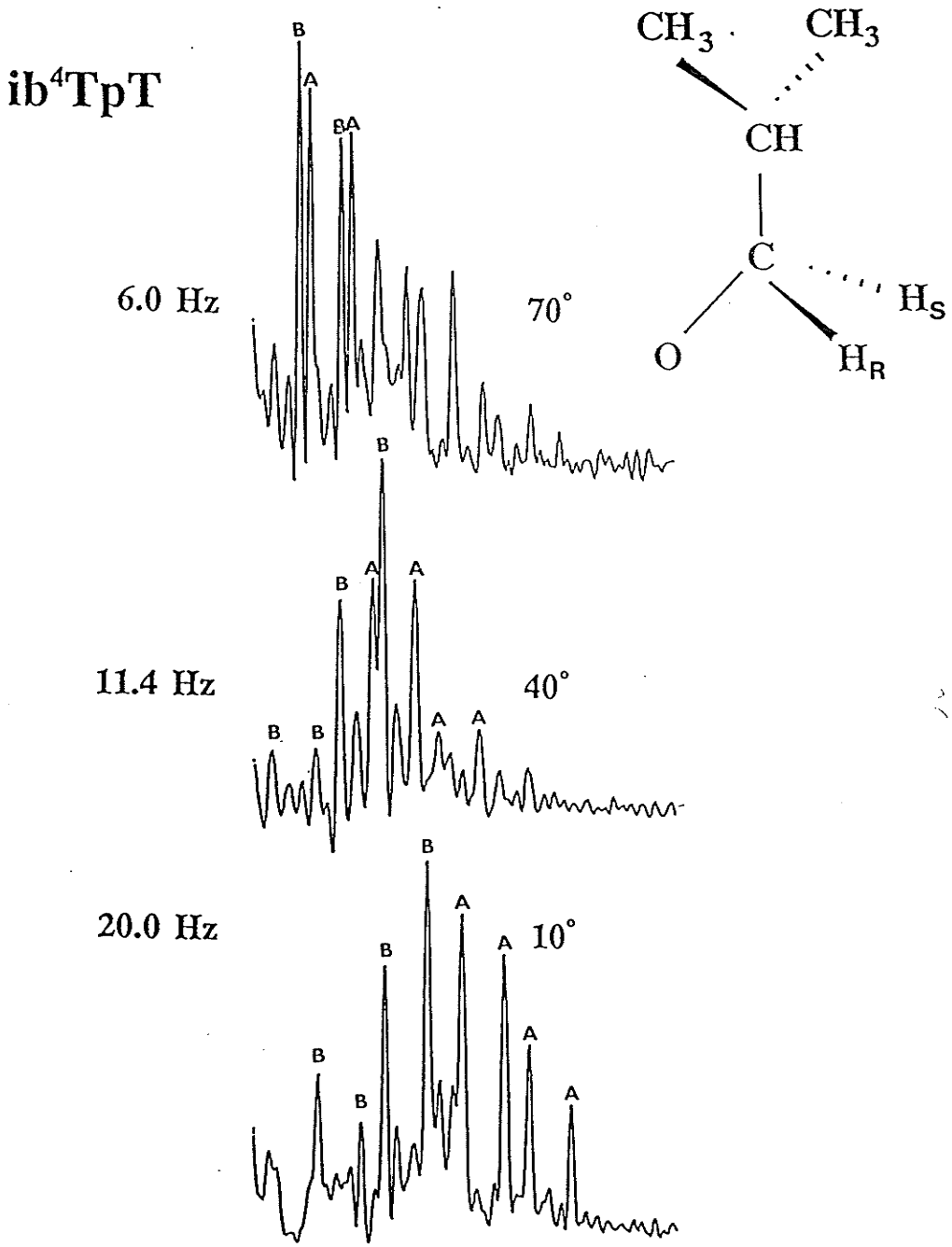

Figure 5.7: Temperature effect on the 300 MHz ^1H NMR band of the H_R and H_S α-methylene resonances of the O4-isobutyl function of d(ib⁴TpT). The value in Hz is the difference in the chemical shifts of these resonances (Δδ) at the temperature indicated.

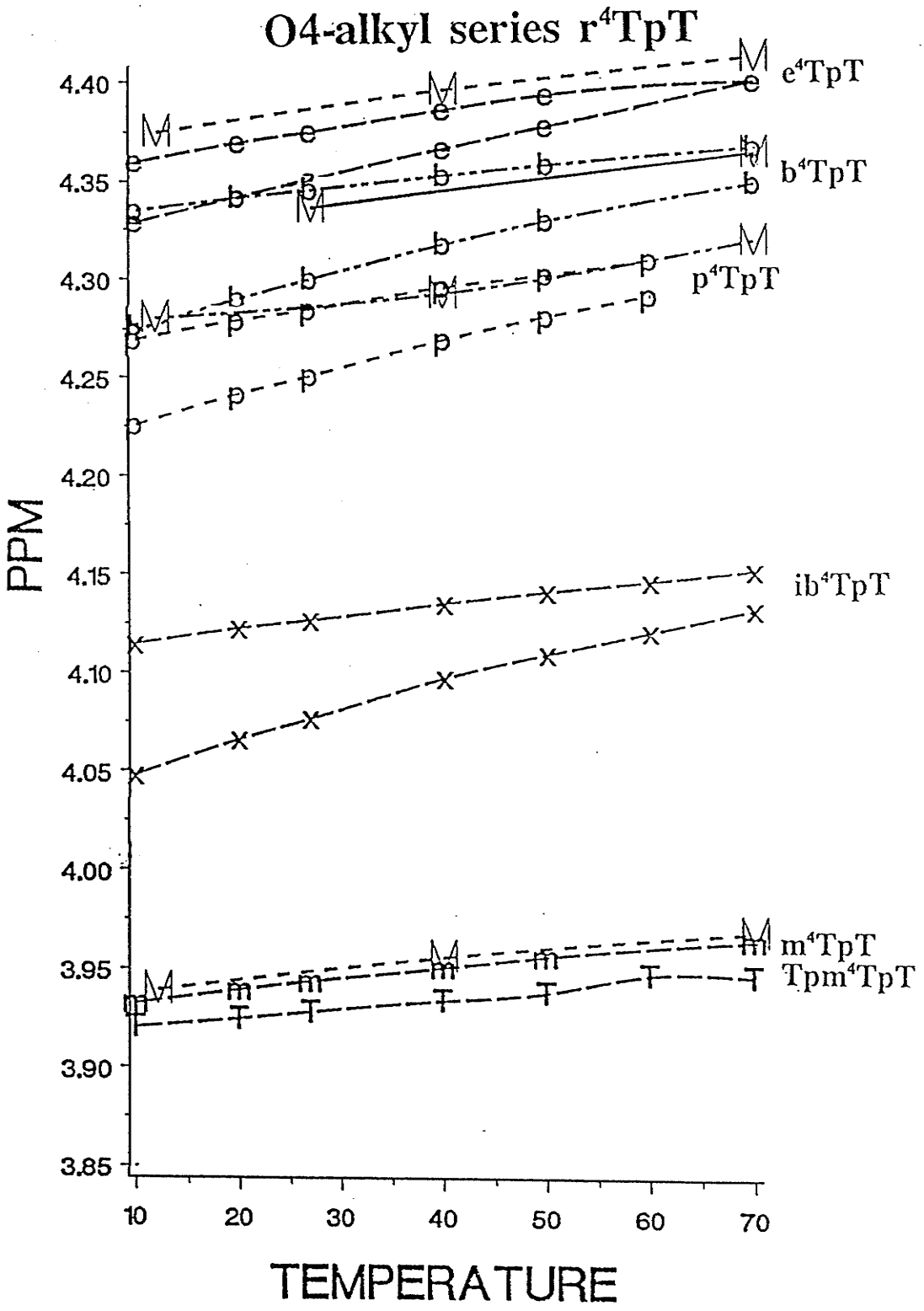

Figure 5.8: Variable temperature plot of the O4-methyl protons of m⁴dT (M), d(m⁴TpT) (m), and d(Tpm⁴TpT) (T), and the O4-α-methylene protons of e⁴dT (M), d(e⁴TpT) (e), b⁴dT (M), d(b⁴TpT) (b), p⁴dT (M), d(p⁴TpT) (p), and d(ib⁴TpT) (x).

different amounts of base-stacking. If the α-methylene profiles of each O-alkyl group is overlaid at positions where the Δδs are equal, for example ***d(e⁴TpT)*** *at 10°C and d(p⁴TpT) around 30°C, the plots are observed to overlap. Furthermore, at identical temperature, Δδ is bigger for the larger O4-alkyl group: isobutyl > butyl > propyl > ethyl. Because the Me5 pT data suggest that the degree of base-stacking is similar in the* ***d(r⁴TpT)*** *dimers, the α-methylene Δδ differences at identical temperatures is likely due to an increase in the population of conformer A (Figure 5.4). One possible explanation for an increase in the population of conformation A may be larger van der Waals clashes between N3 and the bigger O4-alkyl group in states B and C which make these latter conformations less favourable.*

*Note that except for the α-methylene protons of these O4-alkyl groups, the remaining resonances of the O4-alkyl groups behave like the monomers, even though some of these protons are also diastereotopic (Tables 3.2, 3.4, and 3.6). These observation support conformation A as the dominant rotamer in a right-handed/*χ-anti *stack because in this orientation the rest of the O4-alkyl group is projected outwards from the stacked bases, like the methyl of the O4-ethyl group of* ***d(e⁴TpT)****, where they are not likely to feel ring current effects.*

5.2.1.4 d(i⁴TpT)*: Due to the presence of chiral centres in the sugar, the methyl groups of the O4-isopropyl function of* ***d(i⁴TpT)*** *are also diastereotopic and can be labelled pro-R and pro-S (Figure 5.4). On the nucleoside level,* ***i⁴dT****, these O4-isopropyl methyl groups appear as a doublet in the ¹H NMR spectrum, and thus we can conclude that the sugar is too distant from the O4-isopropyl group to cause differential shielding, in line with the observation that such shielding falls off rapidly with the distance between chiral and prochiral centres (Jennings, 1975). On the other hand, in* ***d(i⁴TpT)****, the methyl resonances of the O4-isopropyl group appear as two doublets separated by 15.1 Hz at 12°C (Figure 5.9) (Buchko* et al., *1989b). Furthermore, the Δδ of these methyl groups decreases as the temperature is raised.*

Since a Δδ is not observed for the methyl resonances of the O4-isopropyl function of ***i⁴dT****, its presence in* ***d(i⁴TpT)*** *suggests that it is a manifestation of base-stacking, as proposed for the α-methylene resonances of* ***d(e⁴TpT)****. However, the explanation for the Δδ observation in the O4-isopropyl NMR spectrum of* ***d(i⁴TpT)*** *is more complicated than for the α-methylene Δδ of the O4-ethyl resonances of* ***d(e⁴TpT)****. Figure 5.10 contain variable temperature profiles of the methyl resonances of the O4-isopropyl group of* ***d(i⁴TpT)****. Note that one O4-isopropyl methyl resonance moves slightly upfield as the temperature is lowered (A), similar to the* ***i⁴dT*** *monomer, while the other methyl resonance (B) moves downfield. Based on the crystal structure of O2-isopropylthymidine (Birnbaum* et al., *1988) two different O4-isopropyl orientations about the base should dominate in solution. One state has the pro-S methyl flanking the base towards its 3'-hydroxyl group (Figure 5.4D), and the other has the pro-R methyl flanking the base towards its 5'-hydroxyl group (Figure 5.4E). A third conformation, with both O4-isopropyl methyls straddling the base, is unlikely, because it is more unfavourable for two methyl groups to be in this position than one. In fact, to partially remove the methyl-N3 contact in conformations 5.4D and 5.4E, the methine proton is brought in 30° towards the base in the* ***i²dT*** *crystal relative to either of the α-methylene protons in the* ***e⁴dT*** *crystal, placing the methyl group nearest the base almost 90° above (Figure 5.4D) or below (Figure 5.4E) it.*

Unfortunately, it is not possible to deduce from chemical shifts trends alone which O4-isopropyl conformation, D or E (Figure 5.4), is preferred in solution. The uncertainty is due to not knowing which orientation is responsible for the deshielding and shielding influences on the methyl groups. For example, in conformer D the pro-S methyl may be in a deshielding zone of the plane of the adjacent base while in conformer E this pro-S methyl may be in a deshielding zone of its own base. The methine proton, unfortunately, does not offer any assistance. The methine resonance moves upfield with decreasing temperature (Figure 5.25) but it is not possible to directly compare this movement to the α-methylene

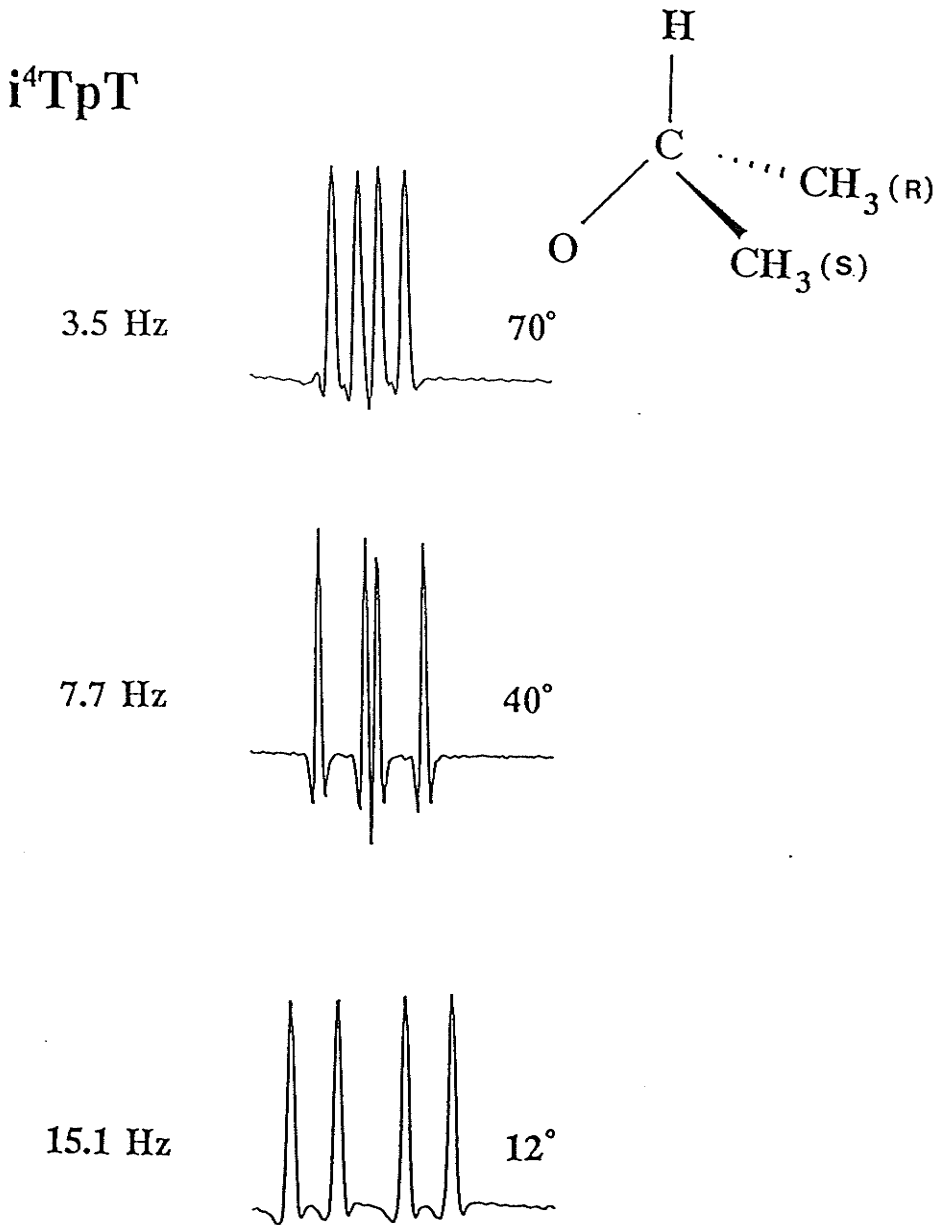

Figure 5.9: Temperature effect on the 300 MHz ^1H NMR band of the CH_3 (pro-S) and CH_3 (pro-R) methyl resonances of the O4-isopropyl function of d(i⁴TpT). The value in Hz is the difference in the chemical shifts of these resonances ($\Delta\delta$) at the temperature indicated.

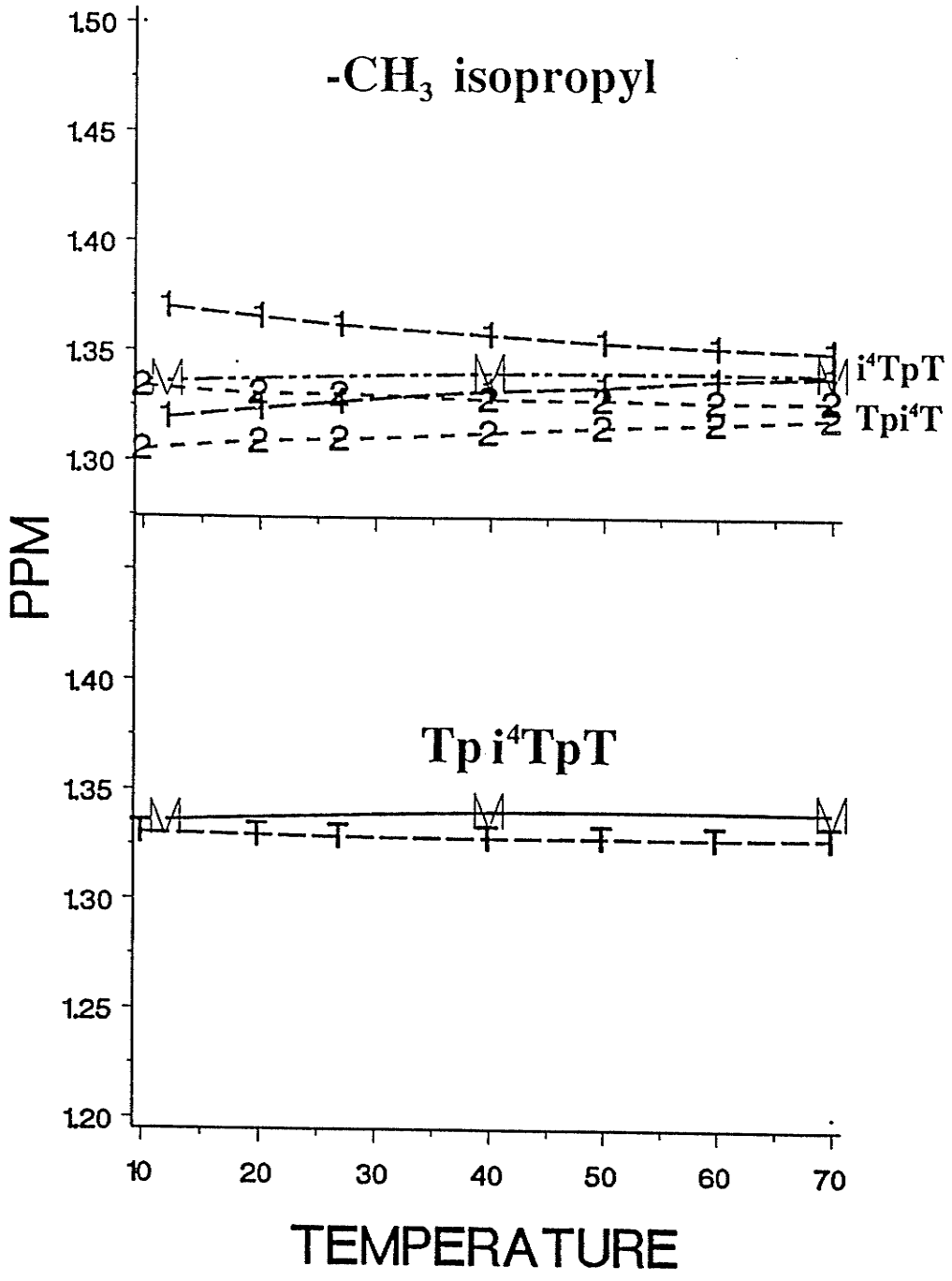

Figure 5.10: Temperature (C°) profiles of the chemical shifts (δ) of the methyl protons of the O4-isopropyl groups of i⁴dT (M), d(i⁴TpT) (1), d(Tpi⁴T) (2), and d(Tpi⁴TpT) (T).

resonances because the i^2dT and e^4dT crystal structures suggest the O4-isopropyl methine proton is closer to N3 then the O4-ethyl α-methylene protons and it is not known what effect this has on the respective chemical shifts. Therefore, in the absence of NOEs, which were attempted (without detection), it is not possible to rule out conformer D or E in Figure 5.4 as being the less favourable orientation of the O4-isopropyl group in a base-stacked state.

*5.2.1.5 Summary: Except for **d(m^4TpT)**, a temperature dependent Δδ was observed for the α-methylene resonances of the O4-alkyl group of all the **d(r^4TpT)** dimers and for the methyl resonances of the O4-isopropyl function of **d(i^4TpT)**. These Δδs may be explained in terms of a differential shielding of these protons due to base-stacking. Such a phenomenon is an additional method of monitoring structural changes in oligonucleotides containing an O-alkylated thymidine (Buchko* et al., *1987) and may be especially useful in larger double helical structures. However, in longer oligomers the α-methylene resonances of O-alkyl groups might be lost amidst the H4', H5', and H5" multiplets. Consequently, the best O-alkyl resonances to use for the study of conformational changes in larger oligomers may be those of the methyl protons of the O4-isopropyl group because: 1) they are found in an upfield region with few interfering resonances; and 2) their larger intensities make them stand out in the spectrum.*

5.2.3 THE BASE δs:

*5.2.3.1 The Me5 Profiles: Figure 5.11 is a variable temperature plot comparing the effect of m^4Tp, e^4Tp, i^4Tp, and Tp on the Me5 resonances of the pT unit. All the r^4Tp moieties shift the pT Me5 profile upfield relative to that with Tp. Two possible explanations for this shift are: 1) the larger ring current effects of a thymine locked in its enol tautomeric form (Geissner-Prettre and Pullmam, 1988); and 2) more base-stacking in the O-alkylated dimers. The Me5 Δδ° is 0.02 ppm for the pT unit of **d(TpT)** and between 0.04 and 0.05 ppm for the pT unit of all the **d(r^4TpT)** dimers, a small difference that may be due to the two reasons given directly above and different base-base overlap in **d(r^4TpT)** relative to d(TpT).*

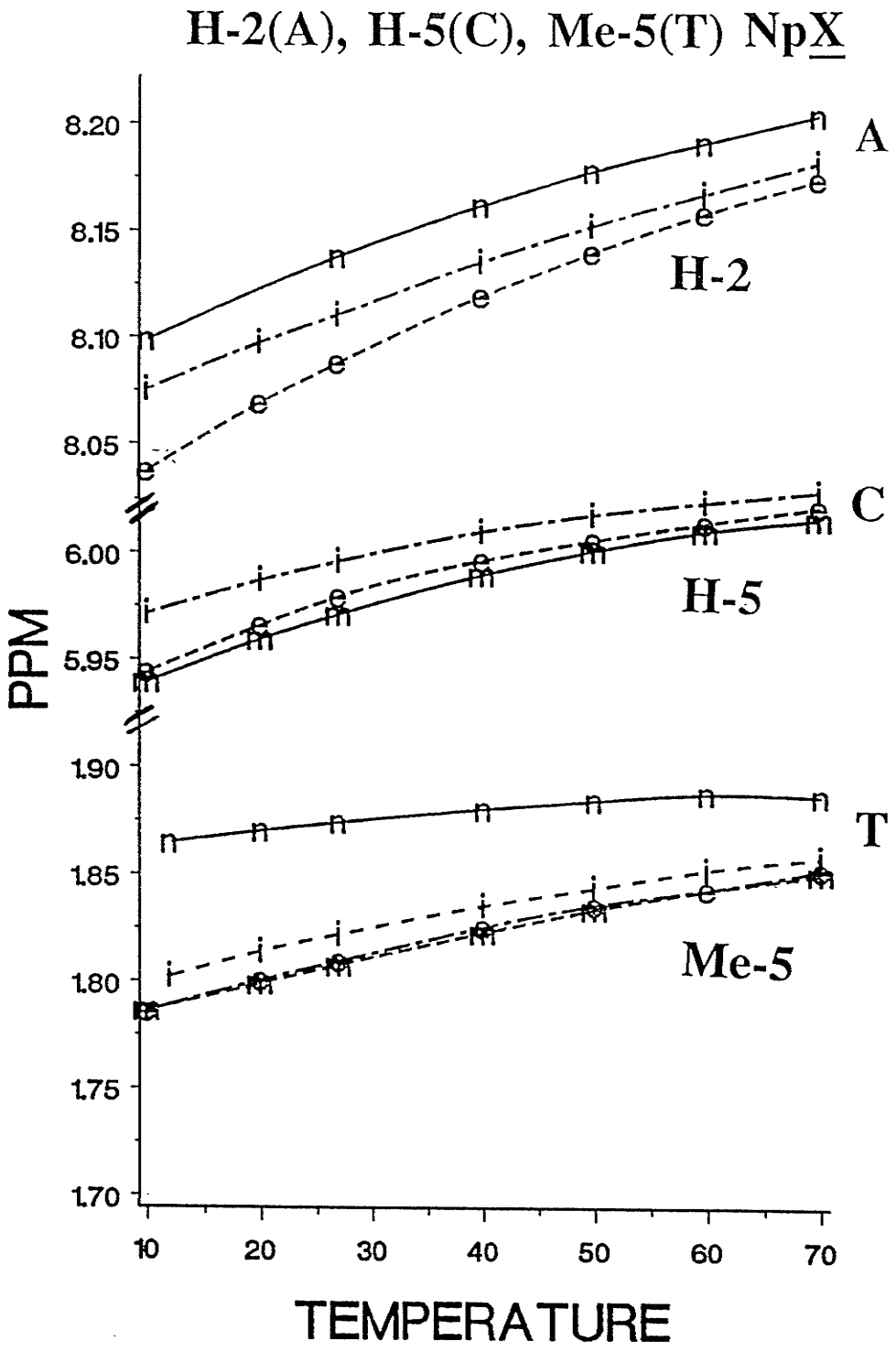

Figure 5.11: Temperature (C°) profiles of the chemical shifts (δ) of the adenine (A) H2, cytosine (C) H5, and thymine (T) Me5 base protons of the pX unit of d(NpX) with N equal to T (n), m^4T (m), e^4T (e), and i^4T (i).

Figure 5.12 is a variable temperature plot containing the m⁴Tp, e⁴Tp, i⁴Tp, and Tp Me5 profiles of d(NpT). (NOTE: N indicates a T or r⁴T base, X indicates an A, G, C, or T base). The Np Me5 Δδ°s are small (< 0.02 ppm) for the four molecules plotted in Figure 5.12 plus those for the p⁴Tp, b⁴Tp, and ib⁴Tp units of d(NpT) listed in Table 3.6. Note that the r⁴Tp profiles are very similar to those of the monomers which suggest little, if any, ring current influences from the pT base. The O4-methyl profile of d(m⁴TpT) also suggests the pT base does not influence the δs of the Np base because its profile is almost identical to that of the monomer m⁴dT (Figure 5.8, Section 5.2.2.1).

<u>5.2.3.2 The H6 Profiles</u>: The pT H6 variable temperature profiles of four d(NpT) dimers are presented in Figure 5.13 where they are all observed to overlap and to move downfield with decreasing temperature to the same extent as the monomer, dT (Buchko et al., *1989a). On the other hand, the H6 Δδ° of the Np units of d(NpT) are all between -0.07 to -0.11 ppm and these profiles are upfield of that for the Tp H6 of d(TpT). The latter observation is likely a result of the different electronic conjugation of e⁴T relative to T (Birnbaum* et al., *1988). The downfield shift of all the H6 resonances with decreasing temperature, in both the Np and pT units, indicate that factors other than the ring current effects of the neighbouring base must be dominant. Comparable temperature effects have been noted earlier in pyrimidine dimers but were not easily explained (Wood* et al., *1974; Lee* et al., *1976). The temperature dependence of the H6 resonances of the monomers indicate that simple solvent effects are relatively important. Indeed, evidence has been presented that such effects can mask the upfield effects of ring currents even for stacked purine bases (Hruska* et al., *1968). Hence, these H6 profiles cannot be interpreted with any degree of certainty and at best we can just make note of the observations.*

<u>5.2.3.3 Summary</u>: There are differences between the base proton variable temperature profiles of d(TpT) and the d(r⁴TpT) dimers. However, many of the differences that do exist may be explained by: 1) the different electronic conjugation of e⁴T relative to T; 2) the

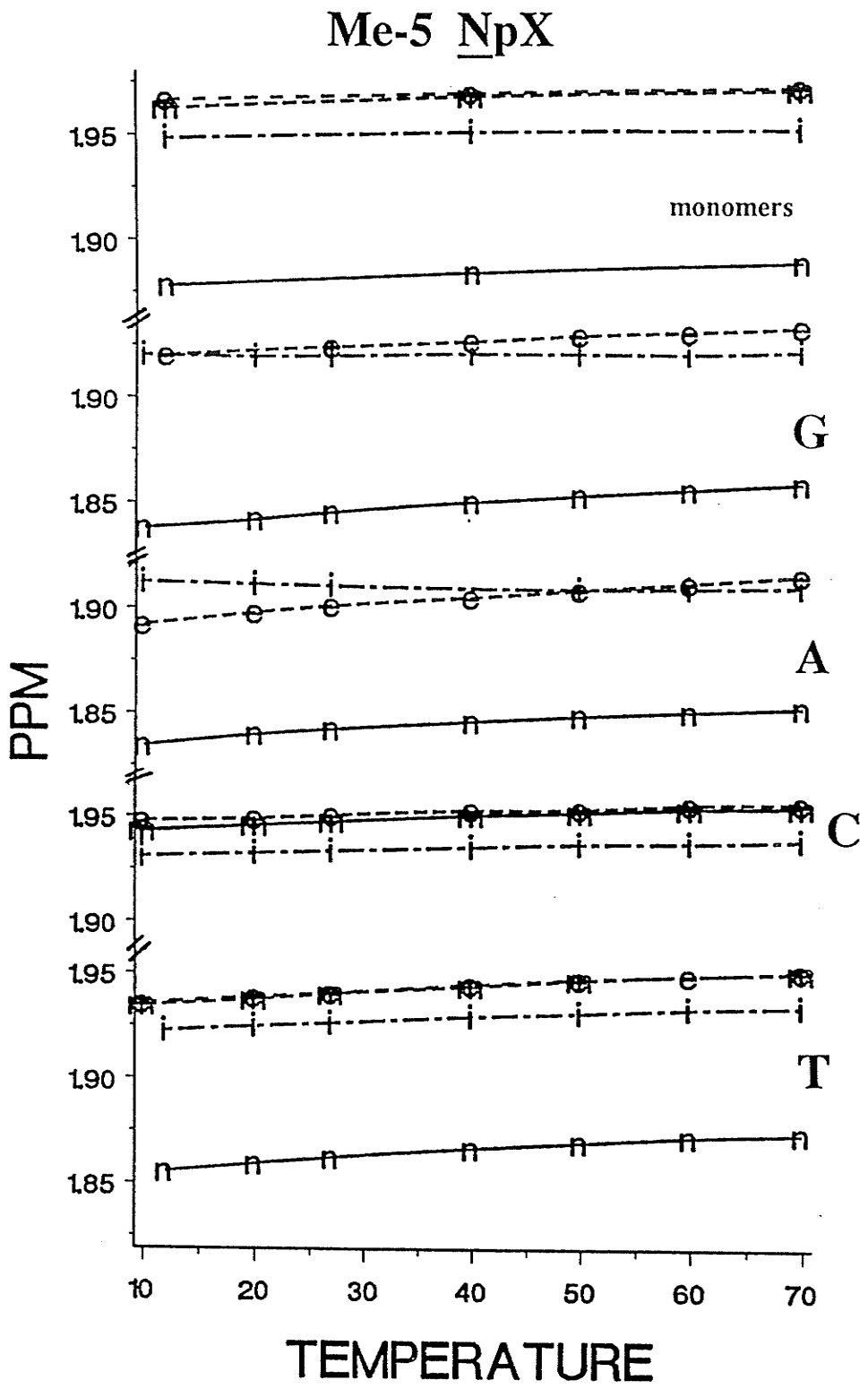

Figure 5.12: Temperature (C°) profiles of the chemical shifts (δ) of the T (n), m⁴T (m), e⁴T (e) and i⁴T (i) Me5 base protons of the Np unit of d(NpX) with X equal to guanine (G), adenine (A), cytosine (C), and thymine (T). Also included at the top of the plot are the Me5 profiles for the monomers dT (n), m⁴dT (m), e⁴dT (e) and i⁴dT (i).

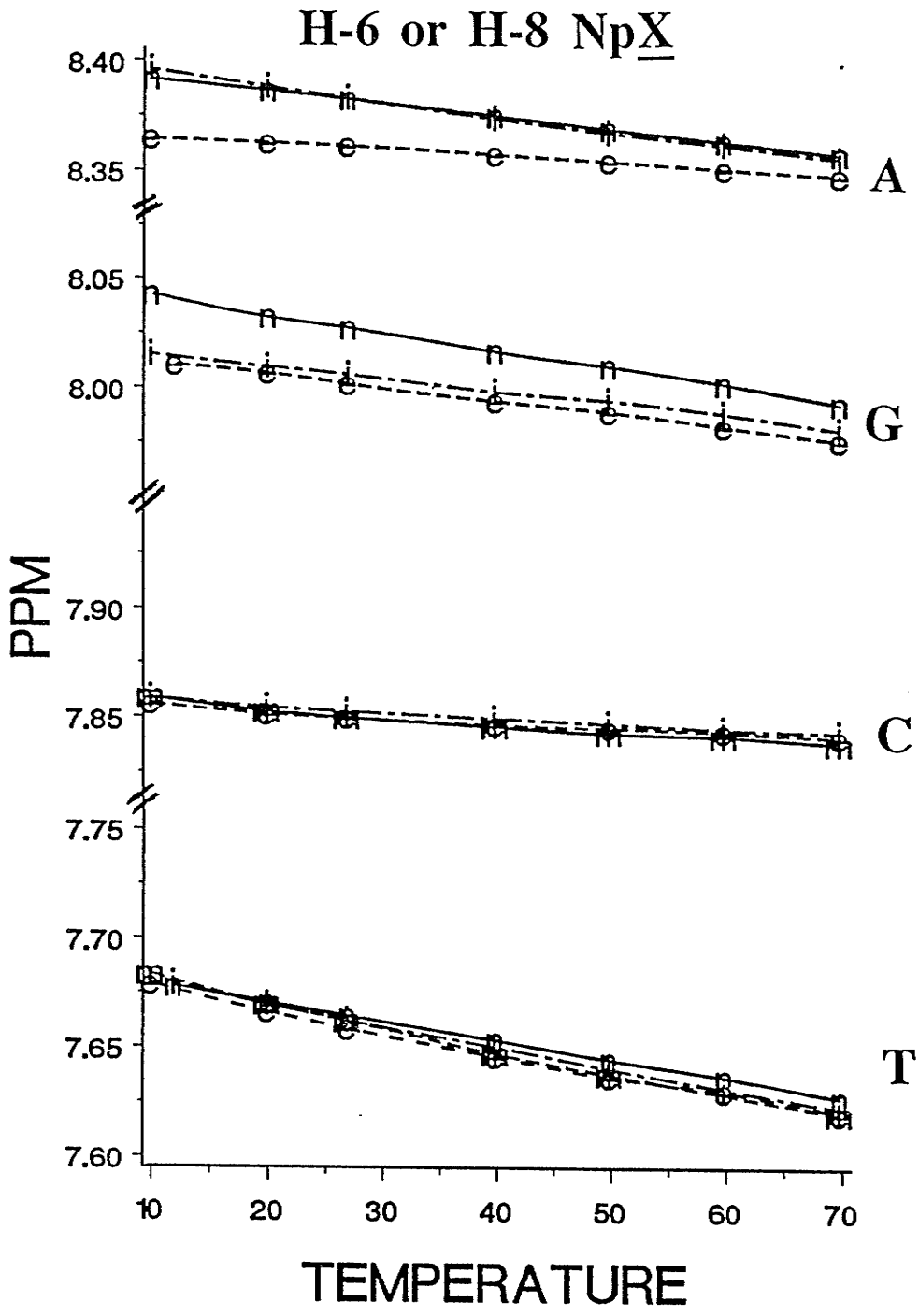

Figure 5.13: Temperature (C°) profiles of the chemical shifts (δ) of the adenine (A) and guanine (G) H-8 and the cytosine (C) and thymine (T) H6 base protons of the pX unit of d(NpX) with N equal to T (n), m⁴T (m), e⁴T (e), and i⁴T (i).

larger ring current effects of r[A]T relative to T; 3) an increase in base-stacking in the O-alkylated molecules; or to 4) different base-base overlap geometries in the d(r[A]TpT) dimers relative to d(TpT). Because pyrimidines themselves are weakly involved in base-stacking (Topal and Warshaw, 1976, Giessner-Prettre and Pullman, 1988) it is likely that the first two explanations given above account for most of the differences. However, it can be concluded that the d(r[A]TpT) dimers and d(TpT) are similar in terms of the formation of right-handed/χ anti *stacks.*

5.2.4 THE SUGAR CONFORMATIONS:

While it appears as if the gross base-base geometries of the d(r[A]TpT) and d(TpT) dimers are similar, an analysis of the d(NpT) sugar coupling constants reveal a difference in the conformation of the r[A]Tp sugar with a smaller, parallel, change in the pT fragment.

5.2.4.1 The Np Sugars: *The sugar pucker of the Tp unit of d(TpT) does not vary much with temperature as is evident by the Σ1' temperature profile of this unit in Figure 5.17. In contrast, the S conformation of the r[A]Tp sugars of the d(NpT) dimers is approximately 10% smaller at 70°C (Table 5.1). As the temperature is lowered to 20°C the S conformation of the r[A]Tp sugars decreases up to 20% (Table 5.1) and at 10°C there is approximately a 30% difference in the conformations of the Tp and e[A]Tp sugars (Figure 5.17). This shift towards N pucker is e[A]Tp is unusual since S is favoured in small 2'-deoxyribonucleotides in aqueous solution (Cheng* et al., *1978; Rinkel and Altona, 1987).*

The shift towards larger N populations of the r[A]Tp sugar with decreasing temperature is supported by trends in $^3J_{1'-2'}$ and $^3J_{3'-4'}$. As mentioned, these couplings are related to the sugar conformation and move in opposite directions depending on the S/N population shift of the sugar pucker. With the Tp unit of d(TpT), $^3J_{1'-2'}$ increases 0.4 Hz in going from 70 to 20°C while $^3J_{3'-4'}$ remains constant at 3.5 Hz (Table 3.5), in line with the absence of major changes in its Σ1' temperature profile (Figure 5.17). However, using the e[A]Tp unit of d(e[A]TpT) as an example, $^3J_{1'-2'}$ decreases 0.6 Hz and $^3J_{3'-4'}$ increases 1.1 Hz over the same

temperature range (Table 3.3), consistent with the reduction observed in the S conformation (Figure 5.17). These trends in the $^3J_{1'-2'}$ *and* $^3J_{3'-4'}$ *of* e^4*Tp are also observed in the other* r^4*Tp units of the* ***d(r^{4}TpT)*** *dimers.*

The 3'-endo *shift of the* r^4*Tp sugar of the* ***d(r^{4}TpT)*** *dimers may rationalize differences between the H2' and H2" Δδ°s of the* r^4*Tp and Tp sugars. In the* ***d(r^{4}TpT)*** *dimers, the* r^4*Tp H2' Δδ°s are between -0.05 - -0.08 ppm and their H2" Δδ°s are less than 0.01 ppm while in* ***d(TpT)****, the Tp H2' and H2" Δδ°s are both < 0.02 ppm (Tables 3.2, 3.4, and 3.6). The largest difference between the H2' and H2" Δδ°s of the Tp and* r^4*Tp units of the d(NpT) dimers is for H2' which suggests an altered environment of this proton as temperature is lowered. It is difficult to interpret sugar δs (Section 5.1.5.1). However, space-filling molecular models suggest that the 3'*-endo *conformation would place the* r^4*Tp H2' nearer the pT O4' and O5' where it could lead to deshielding. Whatever the reason for the H2' and H2" Δδ°s, note that the small Δδ°s of the Tp H2' and H2" of* ***d(TpT)*** *is consistent with the lack of major changes it its S sugar population while the larger H2' Δδ°s of the* r^4*Tp units of the* ***d(r^{4}TpT)*** *dimers correlate with the larger conformational changes observed in these sugars.*

Differences between the H1' Δδ°s of the r^4*Tp (0.07 - 0.09 ppm) (Tables 3.2, 3.4, and 3.6) and Tp (0.01 ppm) (Table 3.4) units of* ***d(NpT)*** *are perhaps related to the 3'*-endo *shifts observed in the* r^4*Tp sugars with decreasing temperature.*

5.2.3.2 The pT Sugars*: The pT sugar conformation in* ***d(TpT)*** *does not change with temperature, remaining at approximately 64% S, while the S conformation of the pT sugar of the* ***d(r^{4}TpT)*** *dimers, which are identical to that of* ***d(TpT)*** *at 70°C, decrease by 5 - 10% over the same temperature range (Table 5.1). Due to the overlap of the pT H2' and H2" resonances at either 70 or 20°C it is not possible to use* $^3J_{1'2'}$ *to corroborate these sugar pucker changes observed from Σ1's. However, the pT* $^3J_{3'-4'}$ *of* ***d(TpT)*** *is observed to decrease slightly from 70 to 20°C (0.2 Hz) (Table 3.4) while the pT* $^3J_{3'-4'}$ *increases by at least 0.6 Hz*

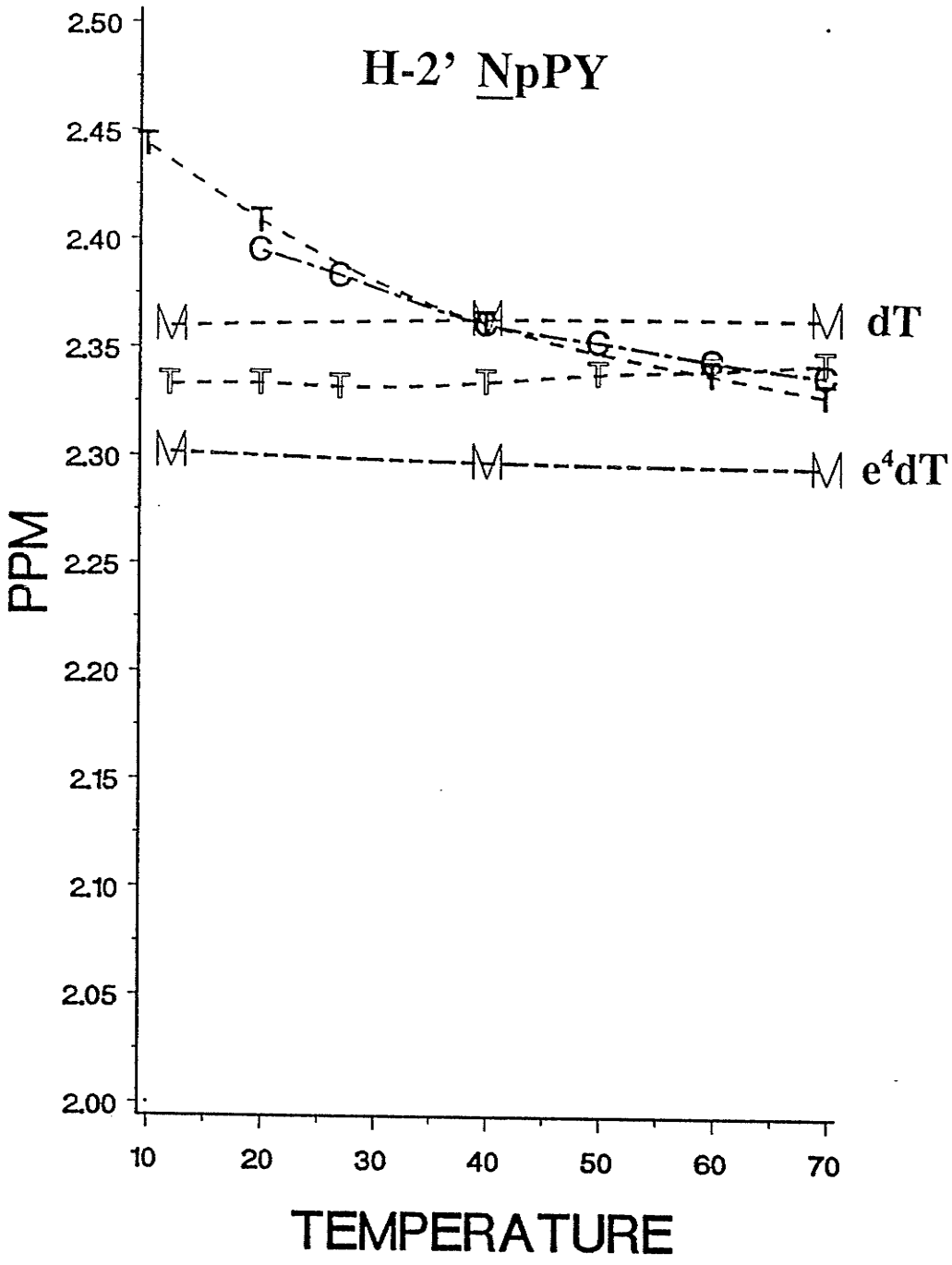

Figure 5.14: Temperature (C°) profiles of the chemical shifts (δ) of the H2' sugar protons of the Np unit of d(NpPY) with PY equal to cytosine (C) and thymine (T). Bold letters: N = e^4T, hollow letters: N = T. Also included are the H2' profiles for the monomers (M) dT and e^4dT.

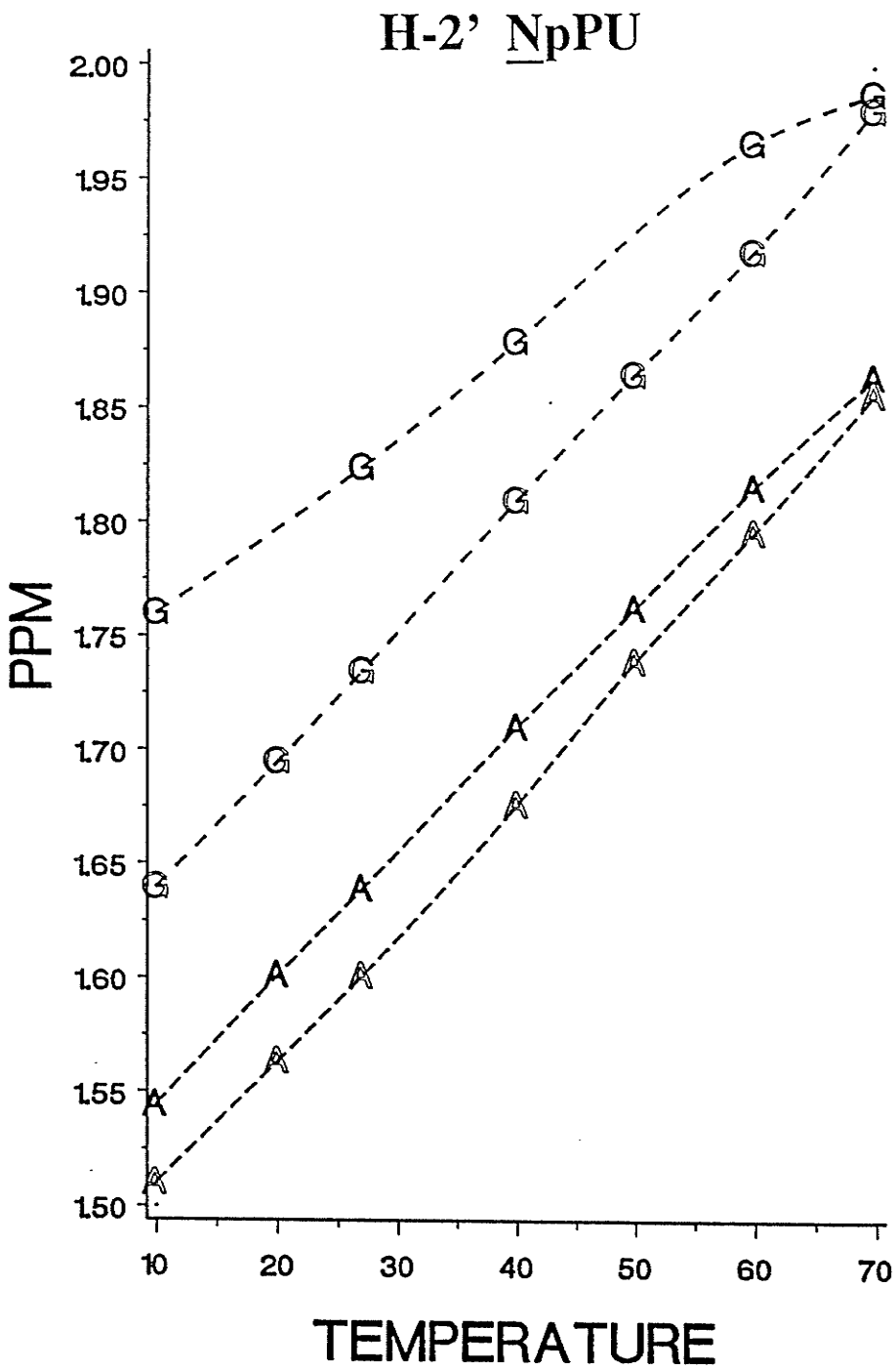

Figure 5.15: Temperature (C°) profiles of the chemical shifts (δ) of the H2' sugar protons of the Np unit of d(NpPU) with PU equal to guanine (G) and adenine (A). Bold letters: N = e⁴T, hollow letters: N = T.

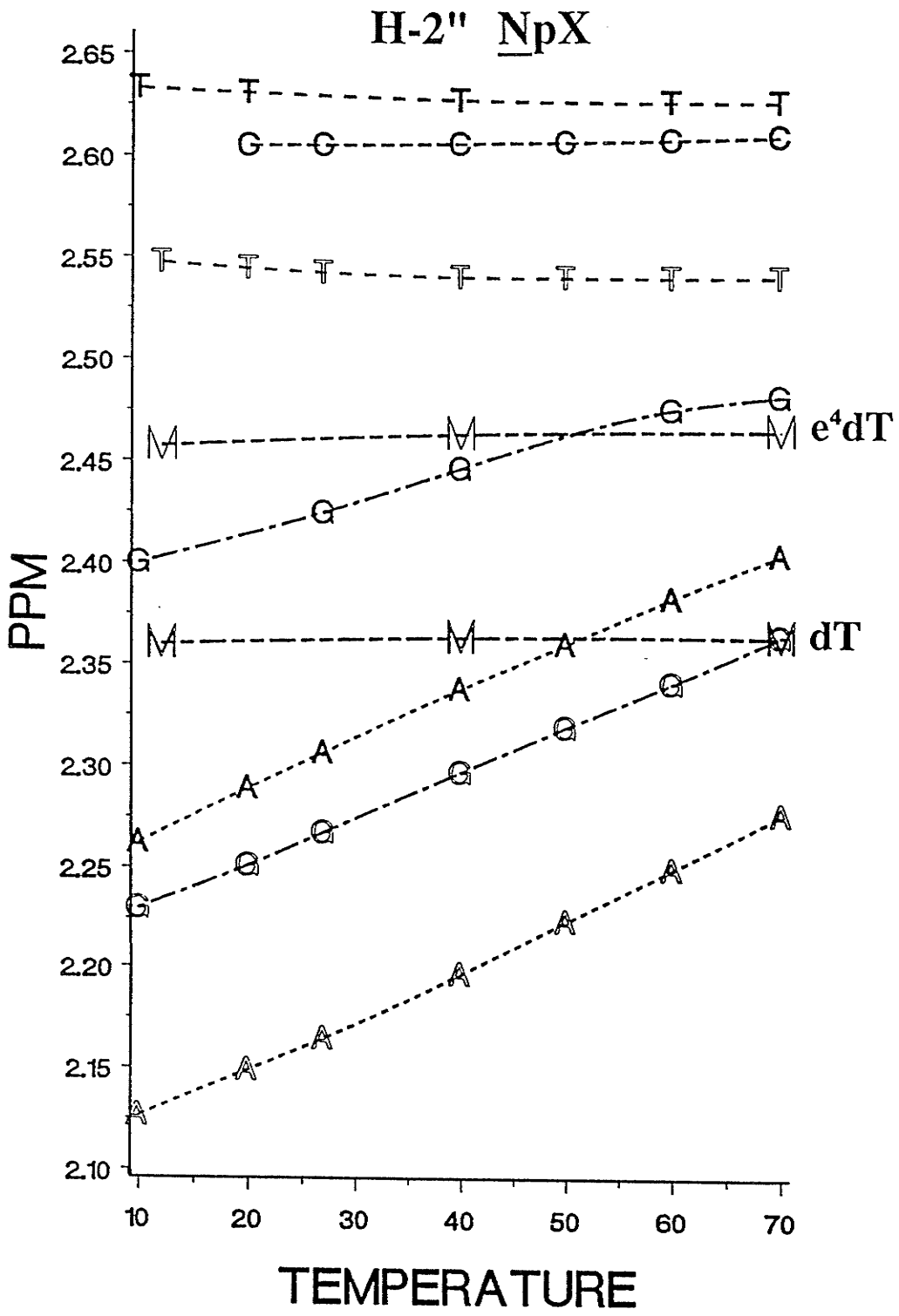

Figure 5.16: Temperature (C°) profiles of the chemical shifts (δ) of the H2" sugar protons of the Np unit of d(NpPU) with PU equal to adenine (A), guanine (G), cytosine (C), and thymine (T). Bold letters: N = e⁴T, hollow letters: N = T. Also included are the H2" profiles for the monomers (M) dT and e⁴dT.

in all the d(r^{A}TpT) dimers (Tables 3.2, 3.4, and 3.6), in line with the sugar pucker changes suggested by the Σ1' profiles. In the same Tables it may be noted that the pT H1', H2', and H2" Δδ°s for the d(NpT) dimers are small, < 0.03 ppm upfield or downfield. Hence, any differences between dimers with N equal to r^{A}T relative to dimers with N equal to T are slight and therefore, do not offer any clear insights into changes of the pT sugar conformation with temperature.

5.2.5 THE SUGAR-PHOSPHATE BACKBONE:

Inspection of the d(NpT) γ populations (Table 5.1) reveal γ $^+$ to be the most highly populated state, followed by γ ^{t} with a residual proportion of γ $^-$. The population of γ $^+$ increases at the expense of the other states upon lowering the temperature, as expected in small DNA oligomers with an increase in base-stacking (Altona, 1982). The pT units contain the largest percentage of γ $^+$ states (> 80% at 20°C) while the Tp and r^{A}Tp fragments are between 56 and 66%. The smaller γ $^+$ populations observed at the 5'-terminus of these dimers is a feature common to DNA oligomers and is associated with more freedom of movement at this end of the molecule (Mellema et al., *1984). There is a small difference in the increases of γ $^+$ with the lowering of temperature between the Tp and r^{A}Tp units of the d(NpT) dimers. That is, the γ $^+$ state of the Tp unit of d(TpT) increases 4% upon lowering the temperature while the γ $^+$ state of the r^{A}Tp units of the d(r^{A}TpT) dimers increases between 7 and 12%. While the population of the γ $^+$ rotamer increases with an increase in the base stacked population, Hruska (1973) also observed a correlation between γ $^+$ and the 3'-*endo *conformation in a wide variety of monomers. That is, the 3'-*endo *conformation appeared to favour the γ $^+$ rotamer and hence, in these dimers, the larger increases in the γ $^+$ state for the r^{A}Tp units relative to the Tp unit of the d(NpT) dimers may be a reflection of the increase in the N conformation.*

The β^t populations of the d(NpT) increase between 5 and 14% upon lowering the temperature which also suggests some base-stacking is occurring (Altona, 1982). Note that

Table 5.1. Furanose conformations and exocyclic bonds rotamer distributions for d(r^4TpT)[a]

Molecule	%S	%γ^-	%γ^t	%γ^+	%β^t	%ε^t/%ε^-
Tp	64(61)	11(12)	33(36)	56(52)	-------	80/18
pT	64(64)	-2(1)	22(34)	80(64)	81(76)	-------
e^4Tp	34(53)	5(11)	29(35)	66(54)	-------	-------
pT	54(64)	0(5)	18(30)	81(65)	87(75)	-------
p^4Tp	39(53)	6(13)	30(35)	64(53)	-------	-------
pT	58(63)	2(5)	19(32)	79(62)	87(73)	-------
b^4Tp	37(53)	6(12)	31(36)	63(52)	-------	-------
pT	58(63)	-1(6)	15(30)	85(64)	85(77)	-------
ib^4Tp	44(53)	10(12)	31(35)	60(53)	-------	-------
pT	58(64)	-------	-------	-------	-------	-------
i^4Tp	46(53)	7(12)	30(36)	62(52)	-------	79/18
pT	58(64)	0(4)	18(31)	81(64)	85(75)	-------

[a]%S calculated according to equation I, %γ according to equations II, III, and IV, %β according to equation V, and %ε according to equations VI and VII. Coupling constast used in these equations were taken from Tables 3.3, 3.5, 3.7, and 3.24. The first number is at 20°C, the number in brackets is at 70°C.

at low temperature the β' populations are similar for the d(NpT) dimers, between 81 - 87%, implying that O4-aklyation is not altering the β rotamer populations.

Carbon spectra were acquired at 27°C for d(i⁴TpT) and d(TpT) and hence, it is possible to acquire information on ε for these dimers. Using equation VI and VII ε' for the i⁴Tp unit of d(i⁴TpT) is calculated to be 79% and ε⁻ is calculated to be 18%, while the ε' and ε⁻ populations of the Tp unit of d(TpT) are determined to be 80% and 18%, respectively. The similar ε values for the i⁴Tp and Tp units of d(NpT) suggests no major alteration in the C3'-O3' torsion angle due to the presence of the O4-isopropyl group. Since the CD and NMR data previously discussed appear to indicate that the d(r⁴TpT) molecules behave similarly in solution, the ε observations for d(i⁴TpT) may extend to the other O4-alkylated dimers.

5.2.6 SUMMARY:

*The major effect of O4-alkylation on the conformation of the d(r⁴TpT) dimers, in comparison to d(TpT), is a shift towards the 3'-*endo *sugar pucker in the r⁴Tp fragment. A similar, but smaller, 3'-*endo *shift is also observed in the pT unit upon lowering the temperature. The NMR data, like the CD data, suggest that some base-stacking is occurring as temperature is lowered. However, because of the different chemical shift anisotropy effects of r⁴T relative to T and the possibility of slightly different base-base geometries between the bases of the d(r⁴TpT) and d(TpT) dimers, it is not possible to deduce whether O-alkylation results in more or less base-stacking over the same temperature range. One explanation for the change in the sugar conformation of the r⁴Tp unit towards more 3'-*endo *upon lowering the temperature is that it may be necessary to allow for the most favourable base-stacking interactions to occur with a pT unit. Note that the γ and β populations do not vary much due to O4-alkylation, and the ε populations are identical, which suggest little change in the phosphodiester backbone due to the presence of r⁴Tp in the place of Tp in the d(NpT) dimers. The size of the O4-alkyl group produce little change in the proton variable temperature*

profiles, Δδ°s, and conformer populations of the ***d(r^{A}TpT)*** *dimers. Therefore, in these molecules at least, one can conclude that the size of the O4-alkyl group has little effect on the molecular conformation. Perhaps the most noteworthy feature of the O-alkylated molecules is the magnetic non-equivalence of the α-methylene resonances of the O4-ethyl, -propyl, -butyl, and -isobutyl function of the* ***d(r^{A}TpT)*** *dimers and the methyl resonances of the O4-isopropyl function of* ***d(i^{x}TpT)*** *which appear to be useful probes of conformational changes in these molecules with temperature (Buchko* et al., *1987).*

5.3 d(NpX):

A set of dimers with r equal to isopropyl and ethyl, and with X equal to T, G, C, or A was synthesised to study the 5'-nucleotidyl base effect on r^4T. The only exception was d(TpC) where the Js and δs were obtained from Cheng and Sarma (1977).

5.3.1 THE SUGAR CONFORMATIONS:

5.3.1.1 The Np Sugars: *The increase in the 3'-*endo *conformation of the r^4Tp sugars with decreasing temperature in the **d(r^4TpT)** dimers is also observed in the **d(r^4TpX)** molecules. However, the extent of the r^4Tp 3'-*endo *shift depends on the pX unit (Buchko* et al., *1989c) as is evident in Figure 5.17 where the Σ1's for the Np fragments of the d(NpX) dimers are plotted as a function of temperature. At all temperatures, for identical pX fragments, Σ1' is smaller for a e^4Tp sugar than for a Tp sugar, and consequently, the 2'-*endo *population of the e^4Tp sugars are smaller than those of the Tp sugars. Note that the Σ1' profiles of the i^4Tp unit of the **d(i^4TpX)** dimers follow a similar, attenuated, pattern (Figure 5.18) relative to the Σ1' profiles of the e^4Tp unit of the **d(e^4TpX)** dimers. To facilitate the discussion it will be useful to break it into two parts: purines (PU) and pyrimidines (PY).*

5.3.1.1.A The Np Sugars of the d(NpPY) Dimers: *The **d(e^4TpT)** dimer has already been discussed and it can be seen in Figures 5.17 and 5.18 that there is a similar, smaller, increase in the 3'-*endo *conformation of the r^4Tp sugar with decreasing temperature in the **d(r^4TpC)** dimers. This 3'-*endo *shift is supported by trends in the $^3J_{1'-2'}$ and $^3J_{3'-4'}$ of the Np unit of the **d(NpC)** dimers. For the Tp sugar of d(TpC), a 10% increase in the S conformation is reported by Cheng and Sarma (1977) with a 1.7 Hz increase in $^3J_{1'-2'}$ and 0.6 Hz decrease in $^3J_{3'-4'}$ as the temperature is lowered (80 to 20°C). On the other hand, for the r^4Tp unit of the **d(NpC)** dimers, $^3J_{1'-2'}$ decreases as much as 0.6 Hz and $^3J_{3'-4'}$ increases as much as 0.4 Hz over a smaller temperature range (Table 3.9). The relative behaviour of $^3J_{1'-2'}$ and $^3J_{3'-4'}$ with decreasing temperature is in opposite directions depending on wether N is e^4T or T and this is in line with the opposite behaviour of the conformations of the e^4Tp*

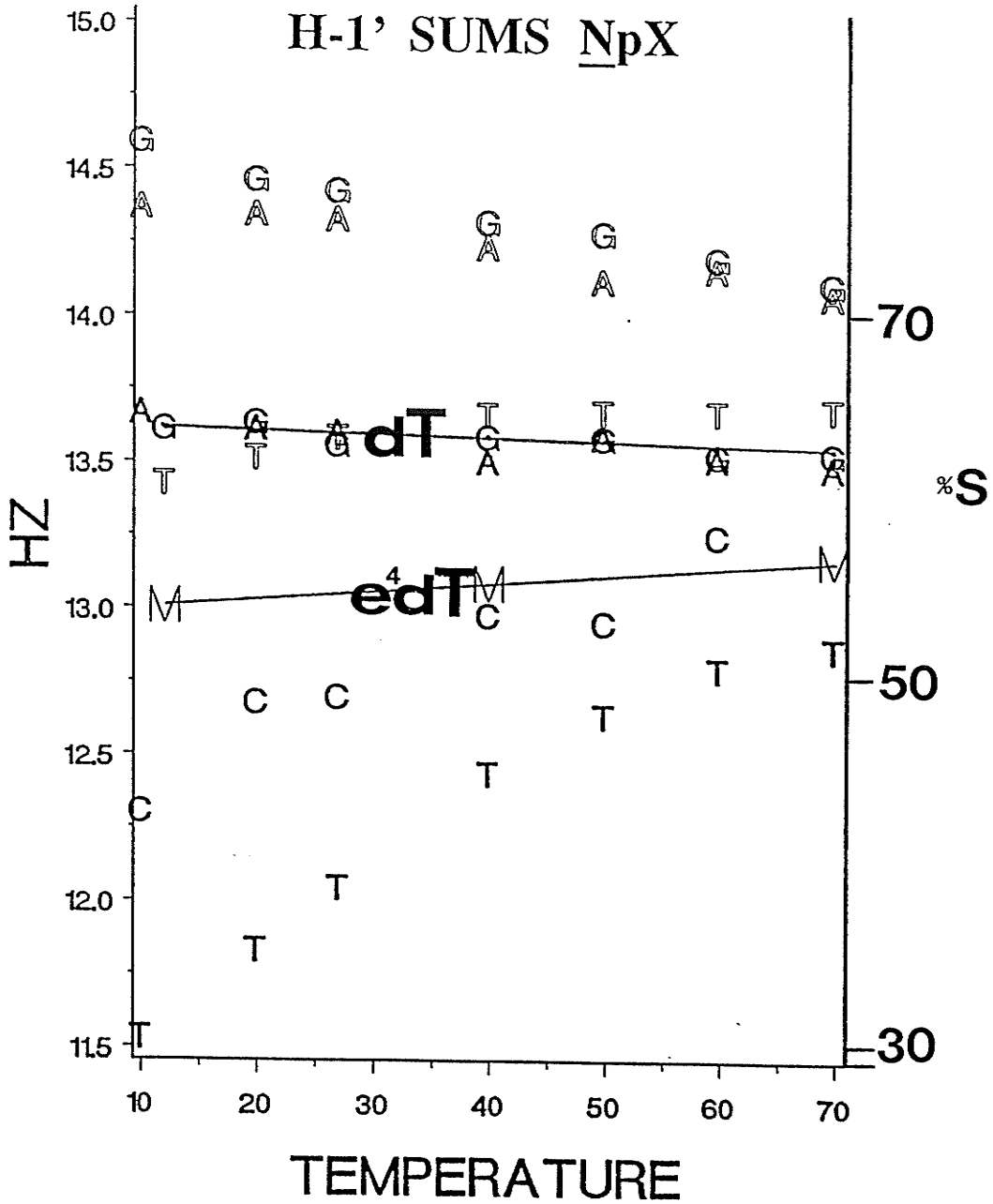

Figure 5.17: Temperature (C°) profiles of ΣI' in Hz for the Np unit of the d(NpX) dimers with X equal to adenine (A), guanine (G), cytosine (C), and thymine (T). Bold letters: N = e^4T, hollow letters: N = T. Also included are the ΣI' profiles for the monomers (M) dT and e^4dT. The vertical axis at the right provides the %S (2'-endo) conformation of the sugar ring calculated according to equation I.

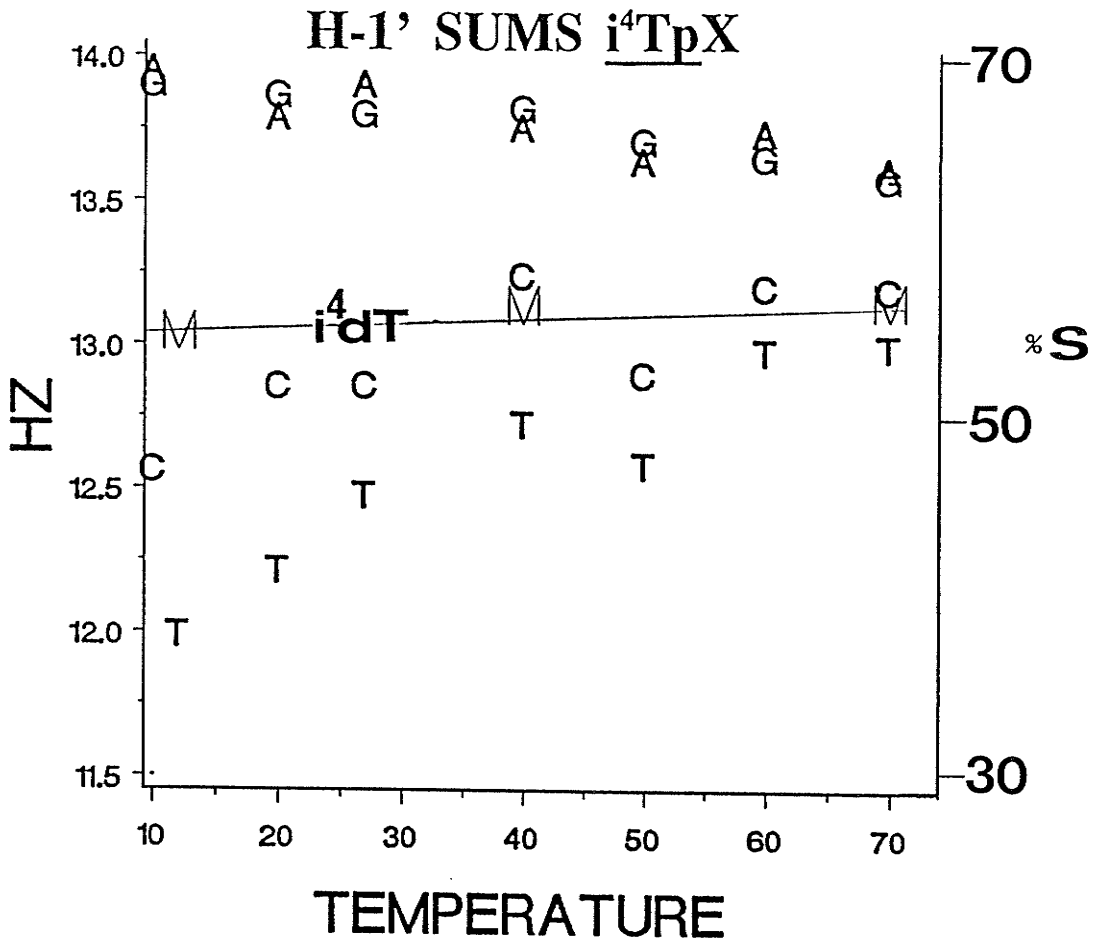

Figure 5.18: Temperature (C°) profiles of Σ1' in Hz for the i⁴Tp unit of the d(i⁴TpX) dimers with X equal to adenine (A), guanine (G), cytosine (C), and thymine (T). Also included are the Σ1' profiles for the monomer (M) i⁴dT. The vertical axis at the right provides the %S (2'-endo) conformation of the sugar ring calculated according to equation I.

and Tp sugars of the d(NpC) dimers with decreasing temperature.

The 3'-endo *shifts of the r⁴Tp sugars of the d(r⁴TpC) dimers may rationalize the temperature dependence of the r⁴Tp H2' and H2". In d(TpC), the Tp H2' and H2" both move 0.03 ppm upfield with decreasing temperature (Cheng and Sarma, 1977) while in the d(r⁴TpC) dimers the r⁴Tp H2' moves downfield between 0.05 - 0.06 ppm and the H2" moves upfield less than 0.01 ppm (Table 3.8). The largest difference between Δδ°s is for H2'. The reason for the differences in the H2' Δδ°s of the r⁴Tp and Tp units are not clear because of the many influences on sugar δs (Section 5.1.5.1). However, similar differences observed between the r⁴Tp and Tp units of the d(r⁴TpT) dimers were interpreted in terms of an increase in the 3'*-endo *conformation of the r⁴Tp sugars with decreasing temperature that placed the r⁴Tp H2' nearer the pT O4' and O5' (Section 5.2.4.1). Perhaps the same thing is happening in the d(r⁴TpC) dimers.*

The difference in the r⁴Tp and Tp H1' Δδ°s of the d(NpC) dimers may be related to the different preferred conformation of the r⁴Tp and Tp sugars. The H1' Δδ° for the Tp unit of d(TpC) is zero (Cheng and Sarma, 1977) but between 0.06 and 0.04 ppm for the r⁴Tp units of the d(r⁴TpC) dimers.

5.3.1.1.B The Np Sugars of the d(NpPU) Dimers: *The 3'*-endo *population shift of the r⁴Tp sugar relative to that of Tp, when X is a pyrimidine, is accompanied by a decrease in the S conformation of the r⁴Tp sugar with decreasing temperature. On the other hand, when X is a purine, the S conformation of the r⁴Tp sugar is still reduced relative to that of Tp. However, with decreasing temperature, the S population increases for both the r⁴Tp and Tp sugars, with a smaller increase in the O-alkylated nucleotide (Figures 5.17 and 5.18). The smaller increases in the 2'*-endo *conformation, with decreasing temperature, of the r⁴Tp sugars relative to the Tp sugars when X is a purine are supported by $^3J_{1'-2'}$ and $^3J_{3'-4'}$ trends (Tables 3.11 and 3.13). For example, the Tp $^3J_{1'-2'}$ increases 0.9 Hz in d(TpG) and only 0.3 to 0.6 Hz for the r⁴Tp unit of the d(r⁴TpG) dimers. Meanwhile, the Tp $^3J_{3'-4'}$ decreases 0.8*

Hz in d(TpG) and only 0.3 to 0.4 Hz in the r⁴Tp unit of the d(r⁴TpG) dimers. A similar trend in $^3J_{1'-2'}$ and $^3J_{3'-4'}$ is noted for the d(NpA) molecules.

*The Np H2' and H2" profiles of the d(NpG) dimers (Figures 5.15 and 5.16) may be related to the increase in the 2'-*endo *conformation with decreasing temperature that is attenuated in the r⁴Tp sugars relative to the Tp sugar. The Np H2' Δδ°s are between 0.23 and 0.34 ppm and the H2" Δδ°s are between 0.08 and 0.14 ppm with the values for d(TpG) at the high end of both ranges (Table 3.10). The large upfield movement observed in both the H2' and H2" resonances of the Np sugar of the d(NpG) dimers suggest large ring current influences from the pX unit and this is usually associated with an increase in base-stacking. Perhaps the larger H2' and H2" Δδ°s of the Tp unit relative to the r⁴Tp units of the d(NpG) dimers are related to the larger temperature dependent increase in the S conformation of the Tp sugar of d(TpG) relative to those of the r⁴Tp sugars of the d(r⁴TpG) dimers.*

An analysis of the Np H2' and H2" profiles of d(NpA) find these Δδ°s in narrower ranges than those for the d(NpG) dimers. The Np H2' Δδ°s for the d(NpA) dimers are between 0.32 and 0.37 ppm and those for H2" are between 0.14 and 0.16 ppm (Table 3.12) with the Δδ°s for the Tp unit of d(TpA) in the middle of these ranges. While the largest H2' and H2" Δδ°s are not observed for the Tp sugar, as with the d(NpG) dimers, these Δδ°s are all large and therefore, strongly suggest that the bases are stacking as temperature is lowered.

*The r⁴Tp and Tp H1' Δδ°s of the d(NpPU) dimers do not vary much, moving upfield between 0.04 to 0.06 ppm with pG and 0.09 to 0.12 ppm with pA. The larger H1' Δδ°s with pA are presumably due to the larger ring current effects of A relative to G. Considering that the 2'-*endo *population of the Np sugar is increasing with decreasing temperature in the d(NpPU) dimers, similar H1' Δδ°s for the alkylated and non-alkylated Np units might be expected. In contrast the Np H1' Δδ°s for the alkylated and non-alkylated Np units of the d(NpPY) dimers differ by a larger degree, in line with the larger sugar*

pucker differences between Tp and r^{A}Tp units.

*5.3.1.3 The pT Sugars: In the d(r^{A}TpT) dimers it was observed that the pT sugar shifted slightly towards 3'-*endo *with decreasing temperature. A similar shift in the pC unit of d(r^{A}TpC) is very weak if it exists at all. However, one dimer, d(m^{A}TpC), does show a 7% increase in the N conformation with decreasing temperature (Table 5.2).*

*In the d(NpPU) dimers the 2'-*endo *population of the pPU sugar is smaller than that of the Np sugar. For the d(NpX) dimers, the pX sugar conformation varies less than 2% with decreasing temperature, except for d(e^{A}TpG), which shows a 7% increase in the N conformation with decreasing temperature (Table 5.2).*

5.3.2 THE SUGAR-PHOSPHATE BACKBONE:

5.3.2.1 d(TpPY): The γ *and* β *rotamer populations suggest that the conformation of the sugar-phosphate backbone of the d(r^{A}TpC) dimers is similar to that of d(TpC) (Table 5.2). The* γ^+ *state is always the most heavily populated at all temperatures followed by* γ'*, which is typical of small DNA oligomers (Altona, 1982). The* γ^+ *population at low temperature for the r^{A}Tp fragment (57 - 60%) of the d(NpC) dimers are larger relative to the Tp fragment (52%) of d(TpC) as was noticed in the r^{A}Tp and Tp units of the d(NpT) dimers. This difference could be due to the same reason given for the d(NpT) dimers: an increase in the 3'-*endo *conformation with decreasing temperature that favours an increase in* γ^+ *(Hruska, 1973). With regards to the pC fragment, no differences in the* γ *populations due to O4-alkylation are evident, with* γ^+ *between 73 - 78% at low temperature in all the d(NpC) dimers. Note that* γ^+ *is more populated in the pC unit than in the Np unit as is typical of small DNA oligomers (Mellema* et al., *1984).*

The β' *populations of the d(NpC) dimers are similar to those for the d(NpT) dimers and at low temperature are all between 79 - 87%.*

Except for the Tp γ^+ *of d(TpC), the* γ^+ *and* β' *populations of all the units of the d(NpC) dimers increase with decreasing temperature which suggests that a larger population*

Table 5.2. Furanose conformations and exocyclic bonds rotamer distributions for d(r^{4}TpX)[a]

Molecule	%S	%γ^-	%γ^t	%γ^+	%β^t	%ε^t/%ε^-
Tp	64(61)	11(12)	33(36)	56(52)	------	80/18
pT	64(64)	-2(1)	22(34)	80(64)	81(76)	------
e^{4}Tp	34(53)	5(11)	29(35)	66(54)	------	------
pT	54(64)	0(5)	18(30)	81(65)	87(75)	------
i^{4}Tp	46(53)	7(12)	30(36)	62(52)	------	79/18
pT	58(64)	0(4)	18(31)	81(64)	85(75)	------
Tp	69(59)	10(10)	37(37)	52(52)	------	------
pC	59(61)	-1(6)	25(27)	75(66)	79(72)	------
m^{4}Tp	39(56)	12(13)	30(35)	57(51)	------	------
pC	49(56)	3(4)	19(31)	78(64)	83(76)	------
e^{4}Tp	49(58)	9(13)	31(35)	60(51)	------	------
pC	53(56)	3(7)	22(32)	75(61)	80(74)	------
i^{4}Tp	47(54)	11(11)	32(36)	57(53)	------	------
pC	53(56)	3(6)	24(28)	73(66)	79(74)	------
Tp	76(71)	15(13)	26(36)	58(50)	------	------
pA	61(59)	2(13)	14(20)	84(67)	94(83)	------
e^{4}Tp	66(63)	9(13)	32(35)	59(51)	------	------
pA	58(58)	2(4)	14(28)	84(68)	76(78)	------
i^{4}Tp	72(66)	9(12)	33(37)	58(51)	------	------
pA	58(56)	2(13)	18(20)	80(67)	------	------
Tp	80(73)	21(14)	26(36)	53(49)	------	------
pG	63(61)	4(16)	15(23)	80(61)	88(90)	------
e^{4}Tp	66(64)	9(12)	35(37)	56(51)	------	------
pG	56(63)	8(6)	17(31)	75(63)	---(78)	------
i^{4}Tp	68(63)	12(12)	30(38)	57(50)	------	------
pG	61(61)	11(7)	20(35)	69(57)	---(74)	------

[a]%S calculated according to equation I, %γ according to equations II, III, and IV, %β according to equation V, and %ε according to equations VI and VII. Coupling constants used in these equations were taken from Tables 3.3, 3.5, 3.9, 3.10, 3.13, and 3.24. The first number is at 20°C, the number in brackets is at 70°C, except for d(m^{4}TpC), d(i^{4}TpC), and d(NpA) where the first number is at 10°C and d(m^{4}TpC) and d(i^{4}TpC) where the number in brackets is at 60°C. Populations for d(TpC) calculated with the Js from Cheng and Sarma (1977) at 20 and 80°C

of ordered structures (base-stacked) exist at low temperature (Altona, 1982). Furthermore, there appears to be no major differences in the γ and β populations of these dimers at high and low temperature which suggest no major distortions in the sugar-phosphate backbone of the d(r⁴TpC) dimers relative to d(TpC).

5.3.2.2 d(TpPU): The γ and β populations of the d(r⁴TpPU) dimers also do not vary much from their non-alkylated analogues (Table 5.2). At low temperature the γ⁺ populations of the Np fragments are between 53 - 59% The pPU units have a higher population of γ⁺ states than the Np fragments, due to more conformational freedom at the 5'-end (Mellema et al., *1984), with a narrower range for pA (80 - 84%) than for pG (69 - 80%).*

Of the six d(NpPU) dimers studied, phosphorus coupling to the C5' protons are only available for three of these dimers at low temperature. Hence, it is not possible to make any conclusions as to the effects of O4-alkylation on the β' populations of these d(NpPU) dimers.

In summary, from γ⁺ data, there appears to be no major distortions in the sugar-phosphate backbone of the d(r⁴TpPU) dimers relative to the corresponding d(TpPU) dimers.

5.3.3 THE BASE AND H1' δs:

5.3.3.1 The Np Me5 Profiles: The base protons associated with all the d(NpX) dimers are the Me5s of the Np fragments, plotted as a function of temperature in Figure 5.12. In all instances the r⁴Tp Me5 profiles are downfield of the analogous Tp Me5 profiles, following the pattern in the r⁴dT and dT nucleosides. Furthermore, the Np Me5 Δδ°s of the d(NpX) dimers are all < 0.03 ppm which suggest that the ring currents of the base of the pX unit, regardless of whether it is a pyrimidine or purine, is not significantly influencing the Np δs.

5.3.3.2 The A(H2), C(H5) and T(Me5) Profiles: The temperature profiles of the A(H2), C(H5) and T(Me5) base resonances of the pX moiety of the d(NpX) dimers (Figure 5.11) show that a r⁴T moves these profiles upfield relative to a T, due to the greater ring current effects associated with r⁴T or perhaps more base-stacking associated with r⁴T. The pC H5

*$\Delta\delta^{o}$ of the **d(r^{4}TpC)** dimers (0.05 - 0.07 ppm) is greater than that of the pC unit of d(TpC) (0.02 ppm (Cheng and Sarma, 1977)), following the trend observed in the pT units of the **d(NpT)** dimers (r^{4}Tp: 0.04 - 0.05 ppm, Tp: 0.02 ppm). However, for **d(NpA)**, the pA H2 $\Delta\delta^{o}$ with Tp and i^{4}Tp are identical, 0.11 ppm, while that with e^{4}Tp is 0.14 ppm, suggesting that base-stacking is occurring in all three dimers but perhaps the base-base overlap is a little different between the O4-ethylated and O4-isopropylated molecules. The larger $\Delta\delta^{o}$ values for the A(H2), C(H5) and T(Me5) resonances of the base of the pX units relative to the $\Delta\delta^{o}$s of the Me5s of the Np units are in line with a right handed stack with the bases in the* anti *conformation because in this orientation the Np Me5 is <u>not</u> over the base of the pX unit while the A(H2), C(H5) and T(Me5) protons of pX are over the base of the Np unit where they can feel its ring current influences.*

<u>5.3.3.3 The O4-Ethyl Group</u>: *Additional support for a right handed/*χ-anti *stack is in the profiles of the O4-alkyl resonances which serve as a supplementary monitor of base-base interactions (Buchko* et al., *1987). Figure 5.19 is a variable temperature plot of the* α*-methylene resonances of the O4-ethyl group of the **d(e^{4}TpX)** dimers. These resonances move upfield and their separation increase as the temperature is lowered. The* α*-methylene* $\Delta\delta$ *depends on the pX unit, with the largest difference at 10°C for pG, followed by pT, pA, then pC. This* $\Delta\delta$ *progression does not coincide with the size of the pX ring current influences, A > G > C > T (Giessner-Prettre and Pullman, 1988), probably because* $\Delta\delta$ *also depends on the amount of base-stacking and the orientation of the stacked bases. Note that the position of the more upfield* α*-methylene profile of each **d(e^{4}TpX)** dimer does more closely agree with the ring current influences of the X base, as illustrated on the bottom of Figure 5.19, with A > G > T > C. In an attempt to explain these trends in the* α*-methylene resonances of the O4-ethyl group of the **d(e^{4}TpX)** dimers it will be convenient to separate these molecules into two groups, with X equal to purines and pyrimidines, since PY-PU and PY-PY stacking interactions differ (Haasnoot and Altona, 1979; Saenger, 1984).*

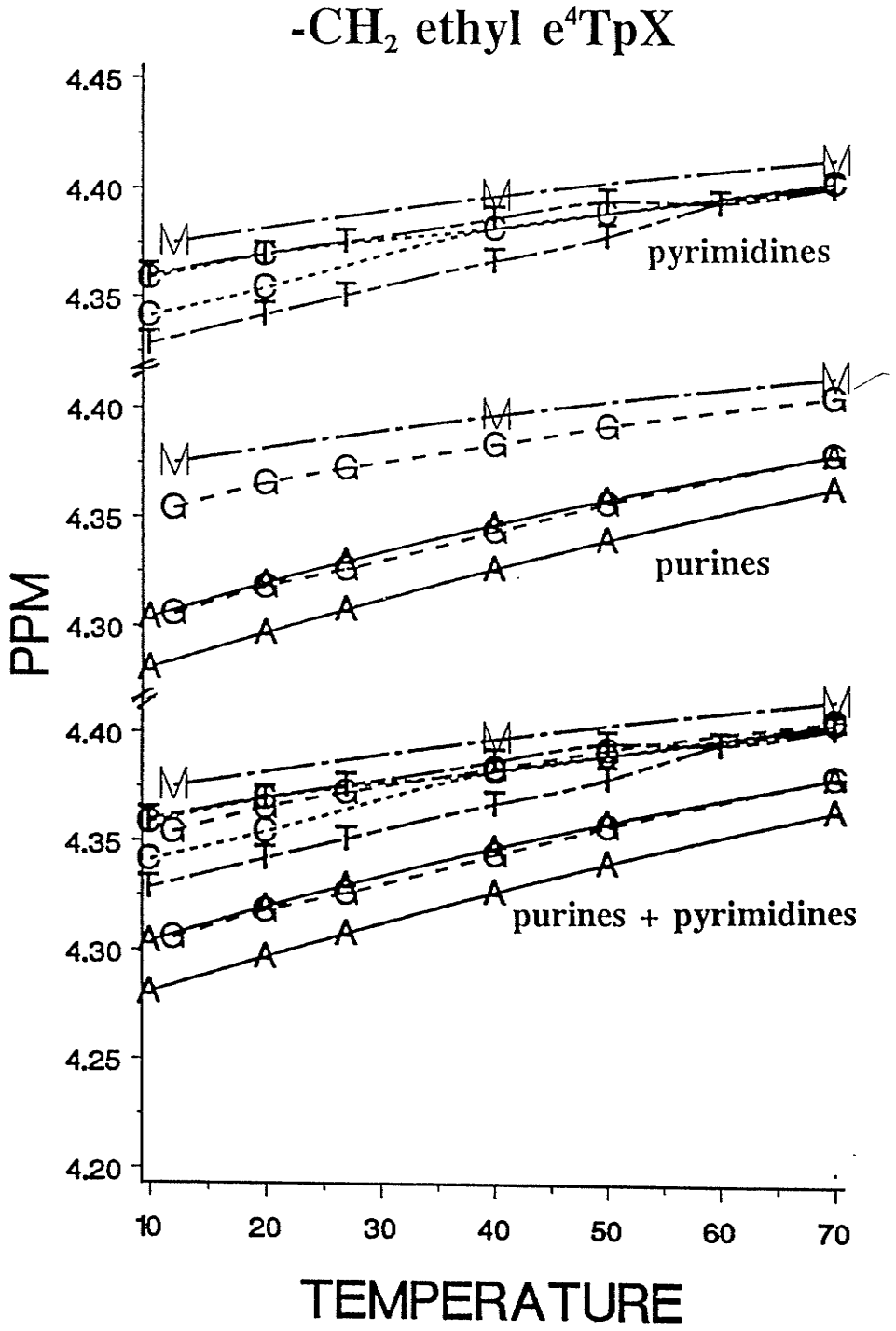

Figure 5.19: Temperature (C°) profiles of the chemical shifts (δ) of the O4-ethyl α-methylene protons of d(e⁴TpX) with X equal to adenine (A), guanine (G), cytosine (C), and thymine (T). Also included are the α-methylene proton profiles of the O4-ethyl group of the monomer (M) e⁴dT.

5.3.3.3.A The O4-Ethyl Group of the d(e⁴TpPY) Dimers: If it is assumed that PY-PY dimers stack with a similar base-base overlap, then the data suggests that for the d(e⁴TpPY) molecules, there is more base-stacking with PY equal to T than to C for the following reasons. First, the α-methylene Δδ of the O4-ethyl group of the d(e⁴TpPY) dimers at 20°C is slightly larger with PY equal to T (0.028 ppm) than with PY equal to C (0.015 ppm). If Δδ is due primarily to the conformation with the α-methylene protons straddling the base (Figure 5.4A) and if PY-PY bases overlap similarly, then an equal population of stacked states for the two d(e⁴TpPY) dimers should result in a larger Δδ for d(e⁴TpC), which is not observed, suggesting that a greater population of stacked states exists d(e⁴TpT). Second, the Δδ° of the O4-methyl resonance of d(m⁴TpT) is 0.025 ppm, in d(m⁴TpC) it is 0.020 ppm, a small difference, but opposite to what would be expected if C stacked with r⁴T to an equal or greater extent than with T. Last, the e⁴Tp Me5 and H1' profiles of d(e⁴TpT) are upfield relative to those of d(e⁴TpC) (Figure 5.22 and 5.23), even though the ring current effects of C are larger than those of T.

5.3.3.3.B The O4-Ethyl Group of the d(e⁴TpPU) Dimers: The behaviour of the α-methylene resonances of the O4-ethyl group of the d(e⁴TpPU) dimers is more difficult to interpret because the low temperature Δδ is larger with PU equal to G (0.051 ppm) than with PU equal to A (0.023 ppm). If it is assumed that both PY-PU stacks are similar and the major orientation of the O4-ethyl group upon base-stacking is the one with the α-methylene protons straddling the base (Figure 5.4A), then one is lead to conclude on the basis of the different Δδs alone that there is more base-stacking in d(e⁴TpG) than in d(e⁴TpA). However, the smaller Δδ observed in d(e⁴TpA) appears to be due to the upfield shift of the downfield α-methylene profile (B) relative to the downfield (B) α-methylene profile in d(e⁴TpG) (Figure 5.19). This upfield movement of the B α-methylene profile of d(e⁴TpA) could be due to many things: 1) local differences in the ring current effects of A relative to G; 2) different base-base overlap geometries between d(e⁴TpG) and d(e⁴TpA); 3) different populations of

*the O4-ethyl group in conformations B and C (Figure 5.4) between d(e⁴TpG) and d(e⁴TpA); and 4) different contributions of conformations B and C (Figure 5.4) to the observed α-methylene profiles between d(e⁴TpG) and d(e⁴TpA). While the explanation for the different α-methylene Δδs between d(e⁴TpG) and d(e⁴TpA) is not obvious, especially in the absence of information that would define the favoured ethyl group orientation about the base in solution (eg., NOEs), the upfield shifts do support the formation of a right handed/χ-*anti *stack upon lowering the temperature because the Δδ°s of the α-methylene resonances are larger (0.05 - 0.08 ppm) than the Δδ°s of the neighbouring Me5 of the e⁴Tp units (< 0.03 ppm). In fact, the latter observation also supports the postulated* syn*-periplanar orientation of the O4-alkyl group about the base because in this position the α-methylene protons are more over the base of the pX unit than they would be in the* anti*-periplanar position, where they would be in a magnetic environment more similar to that of Me5.*

5.3.3.3.C The Methyl Resonance of the O4-Ethyl Group: *Figure 5.20 is a variable temperature plot of the methyl resonance of the O4-ethyl function of the d(e⁴TpX) molecules. These methyl resonances move downfield less than 0.01 ppm with decreasing temperature and their profile positions are practically identical. The relative insensitivity of these methyl δs to temperature suggests that base-stacking is not having an effect, consistent with a right handed/χ-*anti *stack with the O4-ethyl group orientated as depicted in Figure 5.4A. In such an orientation the methyl of the O4-ethyl group is distant from any ring current influences of the base of the pX unit.*

5.3.3.4 The O4-Isopropyl Group: *Figure 5.21 is a variable temperature plot of the methyl resonances of the O4-isopropyl group of the d(i⁴TpX) dimers. In all four molecules the methyl groups of the isopropyl function are magnetically non-equivalent in the ¹H NMR spectra. Their Δδs are observed to increase with decreasing temperature with the effect greater when X is a purine instead of a pyrimidine. Note that the upfield O4-isopropyl methyl resonance of the dimers follows the profile of the methyl resonances of the O4-*

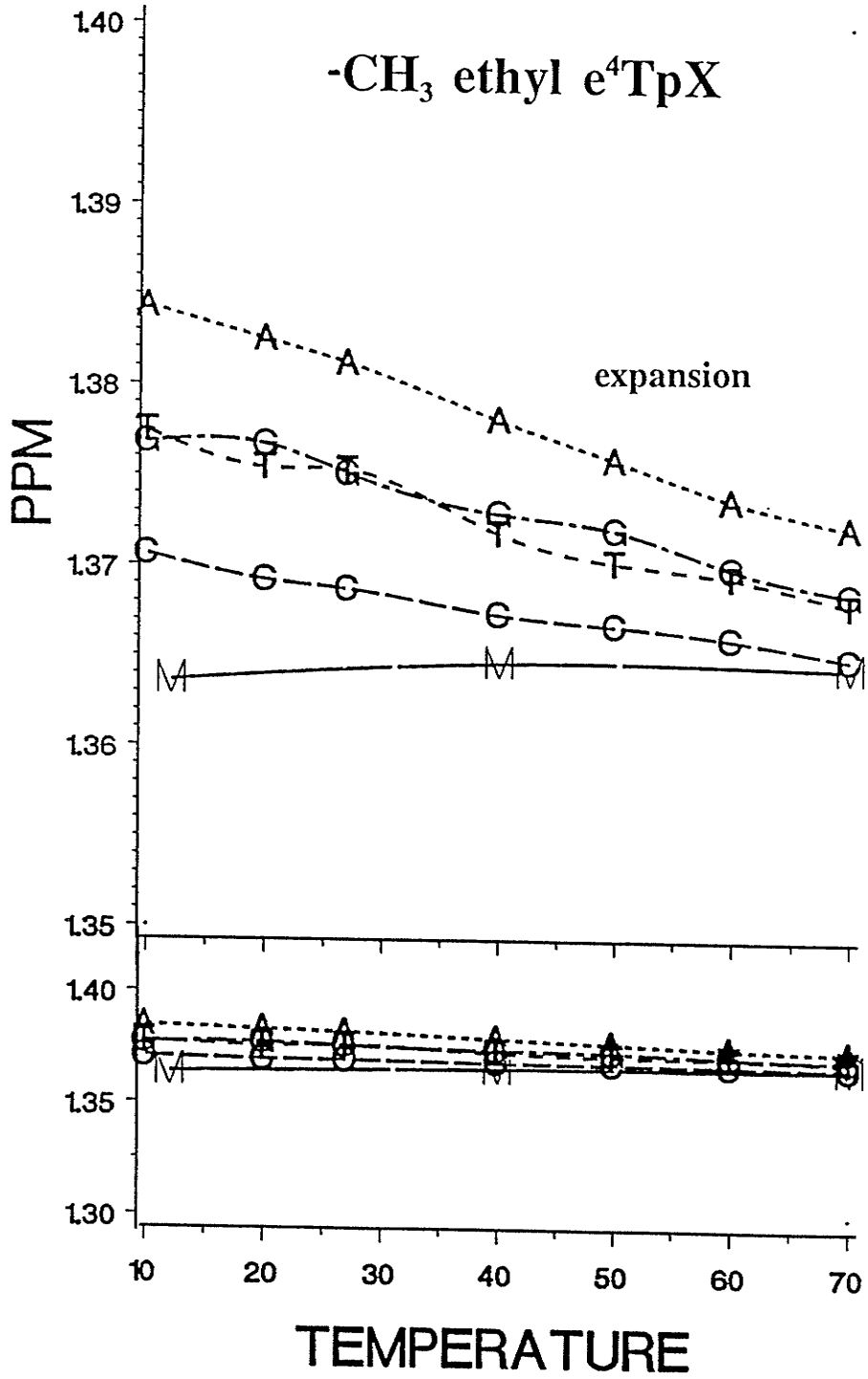

Figure 5.20: Temperature (C°) profiles of the chemical shifts (δ) of the O4-ethyl methyl protons of d(e⁴TpX) with X equal to adenine (A), guanine (G), cytosine (C), and thymine (T). Also included are the methyl proton profiles of the O4-ethyl group of the monomer (M) e⁴dT. Note that the plot at the top is an expansion of the profiles plotted in the standard scale on the bottom.

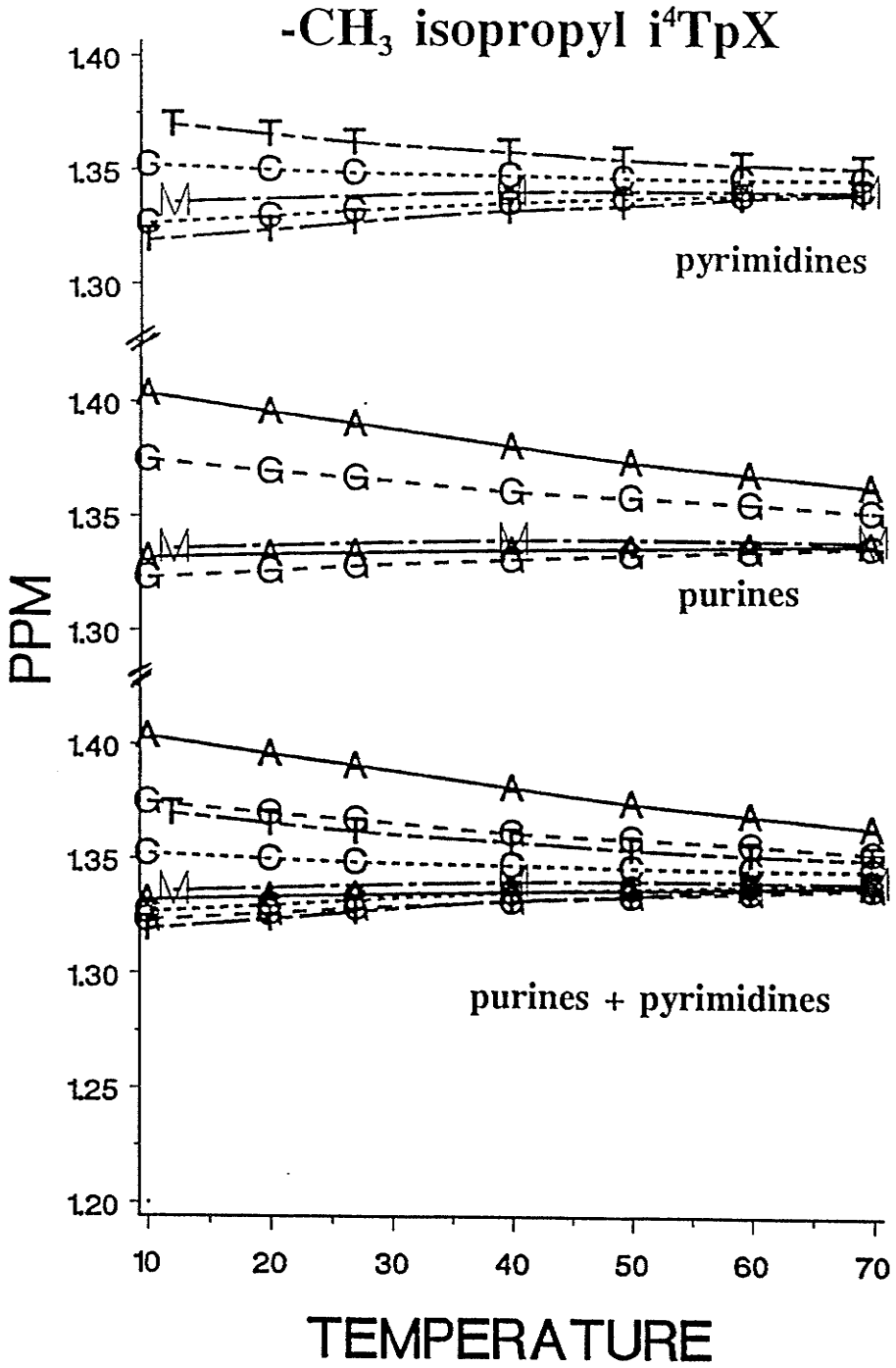

Figure 5.21: Temperature (C°) profiles of the chemical shifts (δ) of the methyl protons of the O4-isopropyl groups of d(i⁴TpX) the X equal to adenine (A), guanine (G), cytosine (C), and thymine (T). Also included are the methyl proton profiles of the O4-isopropyl group of the monomer (M) i⁴dT.

*isopropyl group of the monomer, **i⁴dT**, moving upfield marginally with decreasing temperature. On the other hand, the downfield O4-isopropyl methyl resonance of the dimers moves in the opposite direction with decreasing temperature relative to the methyl resonances of the O4-isopropyl group of **i⁴dT** and to a greater degree. This magnetic non-equivalence may be attributed to base-stacking interactions, as discussed for **d(i⁴TpT)** (Section 5.2.2.4).*

*The size of the O4-isopropyl Δδ depends on the X base, A > G > T > C. This order more closely follows the order of decreasing ring current influences, A > G > C > T (Giessner-Prettre and Pullman, 1988) than the Δδs of the α-methylene resonances of the **d(e⁴TpX)** set of molecules (G > A > T > C). Note that the observed order of increasing O4-isopropyl Δδs for various X bases follows the relative positions of the r⁴Tp H1' and Me5 temperature profiles (Figures 5.22 - 5.24). Hence, C is inducing smaller shifts in the resonances of the base and H1' protons of the i⁴Tp unit than T, as observed in the **d(e⁴TpPY)** dimers and presumably, for the same reason, less base-stacking with C (Section 5.3.3.3.A).*

*The methine resonances of the O4-isopropyl group of the **d(i⁴TpX)** dimers are plotted as a function of temperature in Figure 5.25. All the methine profiles are upfield relative to that of **i⁴dT**. Furthermore, the methine resonances move upfield with decreasing temperature. Both observations suggest that base-stacking is occurring as the temperature is lowered.*

***5.3.3.5 The H6 and H8 Profiles**: The H6 and H8 resonances of the pX fragments of the **d(NpX)** dimers are plotted as a function of temperature in Figure 5.13. These resonances all move downfield with decreasing temperature.*

***5.3.3.5.A The pPY H6 Profiles**: In the **d(NpT)** dimers there was no difference in the pPY H6 profiles with N equal to r⁴T or T, as these profiles fell on top of each other. The d(TpC) H6 variable temperature profile is not available for comparison, but the pC H6 profiles of all the **d(r⁴TpC)** dimers are coincident. Note that the pX H6 Δδ°s are larger with PY equal to T (-0.04 - -0.05 ppm) than with C (-0.01 - -0.02 ppm) which may be due to more base-stacking in the **d(NpT)** dimers relative to the **d(NpC)** dimers as previously suggested, although*

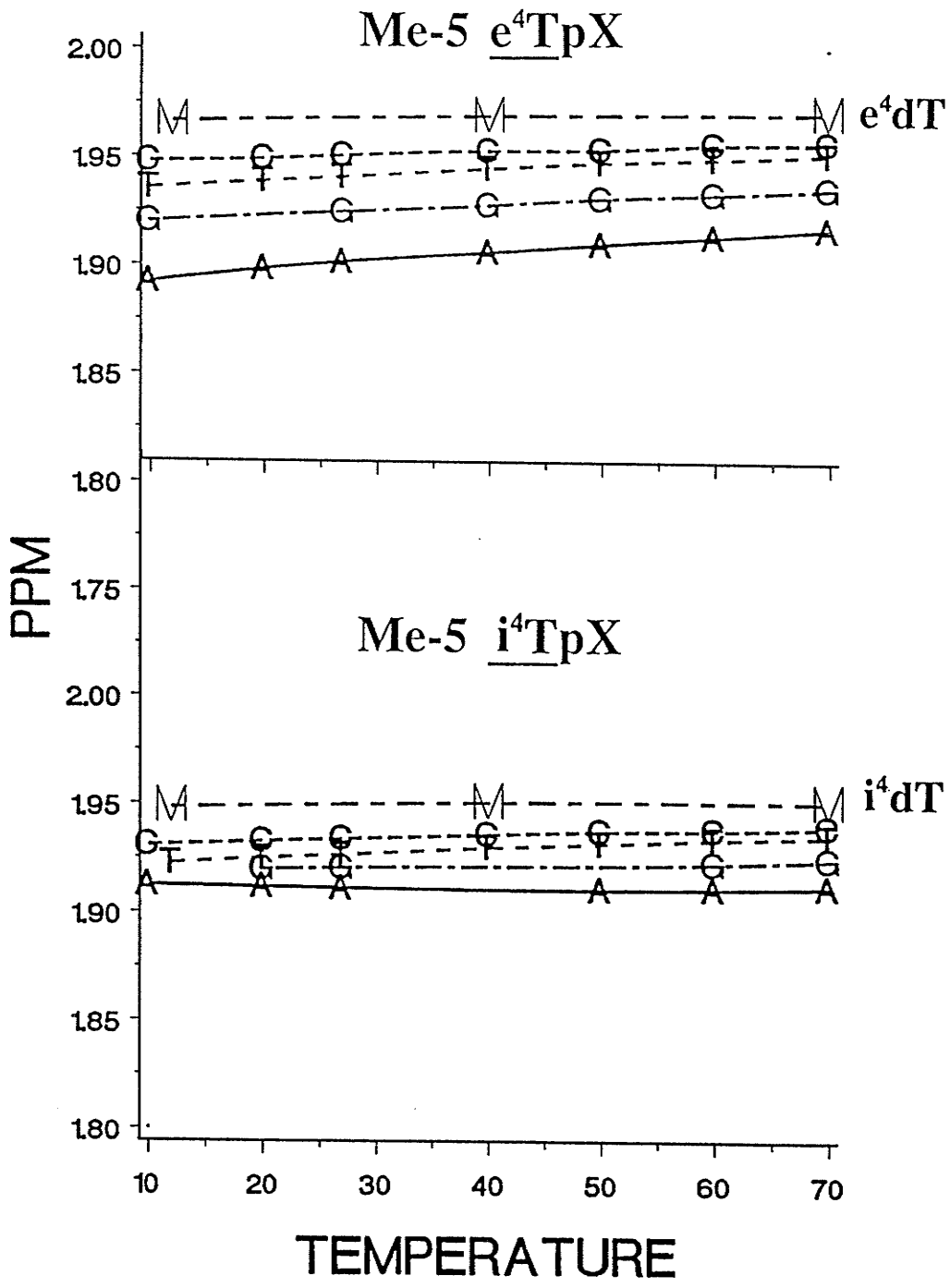

Figure 5.22: Temperature (C°) profiles of the chemical shifts (δ) of the e⁴T and i⁴T Me5 base protons of d(e⁴TpX) (top) and d(i⁴TpX) (bottom) with X equal to adenine (A), guanine (G), cytosine (C), and thymine (T). Also included are the Me5 profiles of the monomers (M) e⁴dT and i⁴dT.

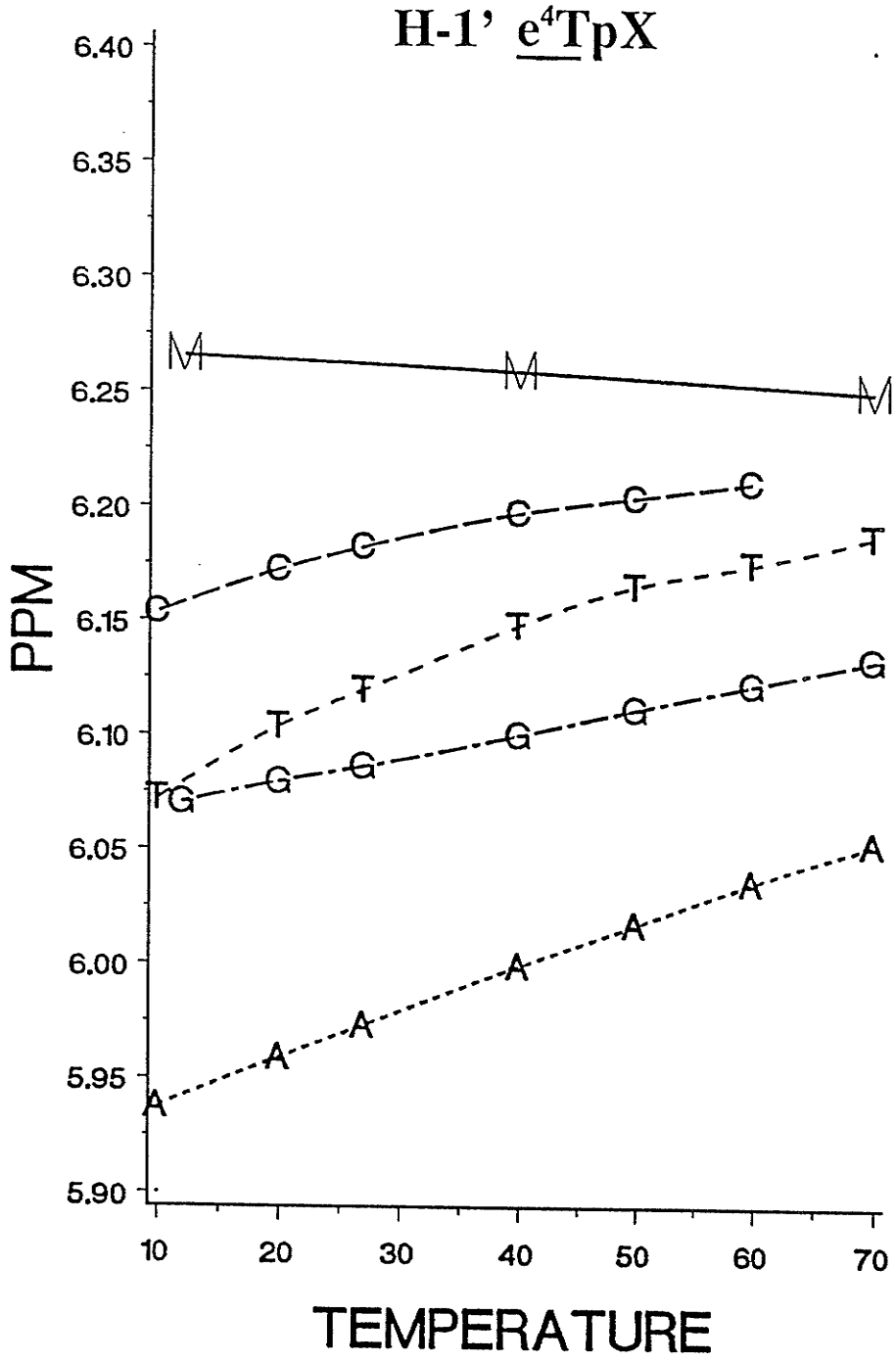

Figure 5.23: Temperature (C°) profiles of the chemical shifts (δ) of the e⁴Tp H1' sugar protons of d(e⁴TpX) with X equal to adenine (A), guanine (G), cytosine (C), and thymine (T). Also included is the H1' profile of the monomer (M) e⁴dT.

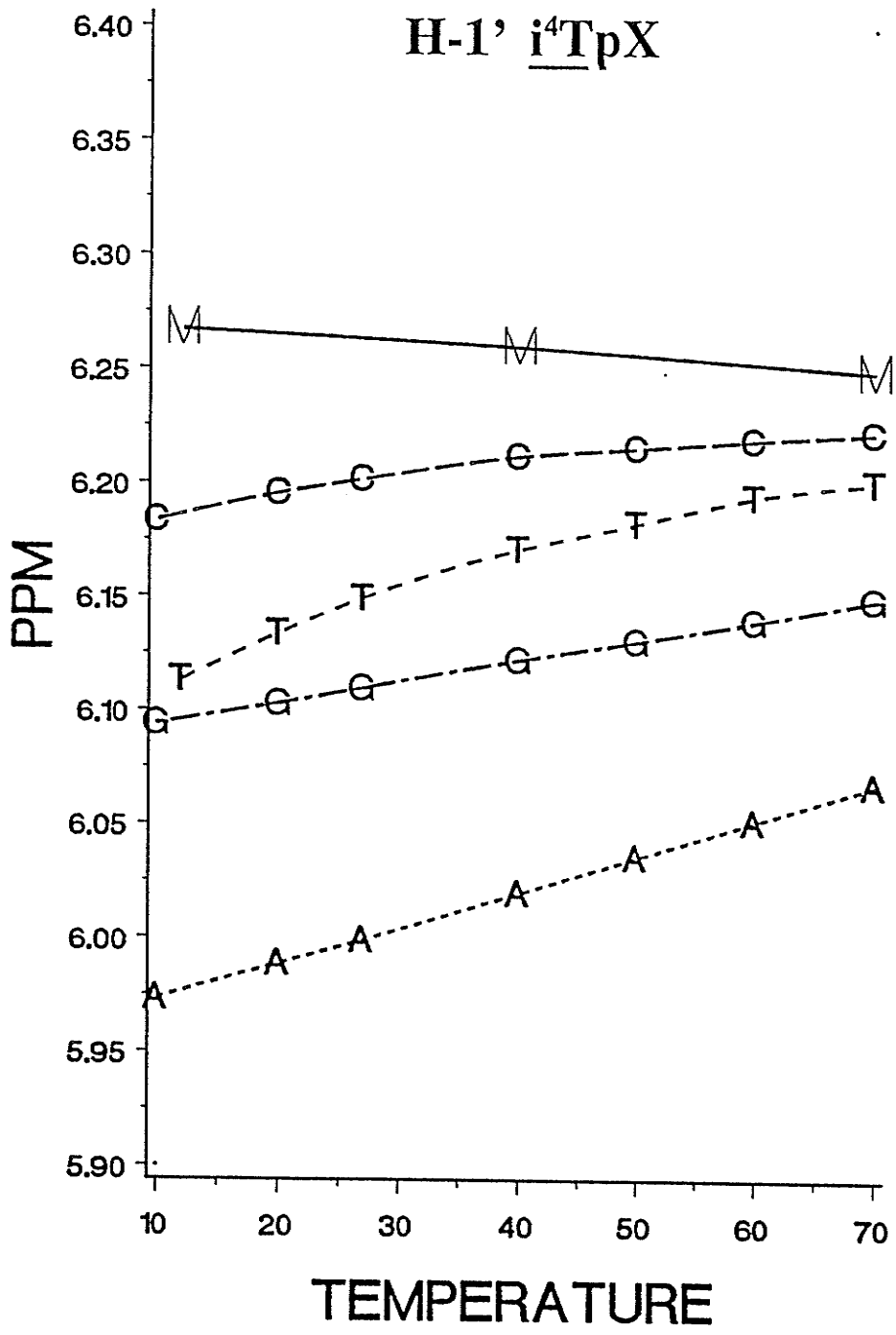

Figure 5.24: Temperature (C°) profiles of the chemical shifts (δ) of the i⁴Tp H1' sugar protons of d(i⁴TpX) with X equal to adenine (A), guanine (G), cytosine (C), and thymine (T). Also included is the H1' profile of the monomer (M) i⁴dT.

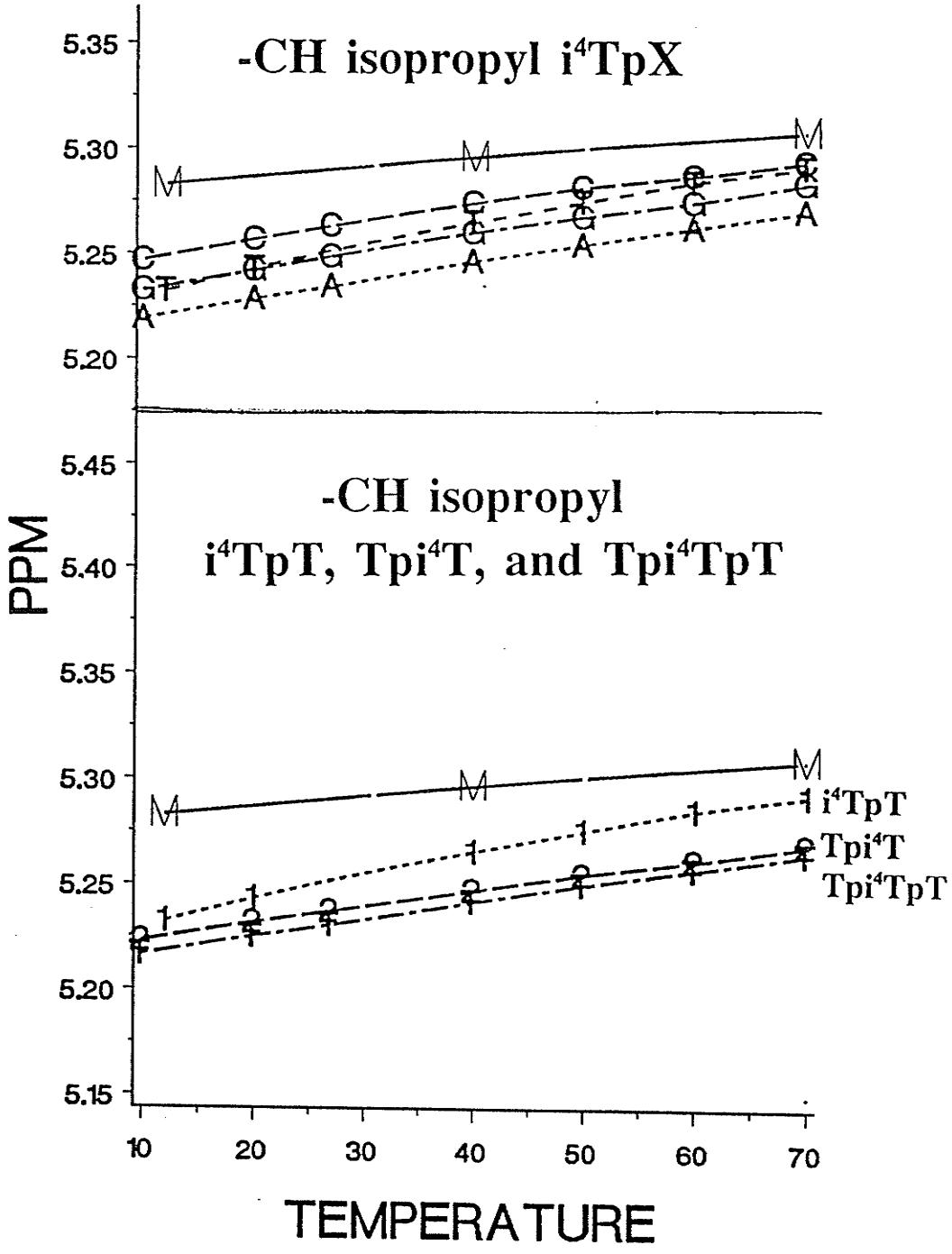

Figure 5.25: TOP) Temperature (C°) profiles of the chemical shifts (δ) of the methine proton of the O4-isopropyl groups of d(i⁴TpX) with X equal to adenine (A), guanine (G), cytosine (C), and thymine (T). Also included is the methine proton profile of the O4-isopropyl group of the monomer (M) i⁴dT. BOTTOM) Temperature (C°) profiles of the chemical shifts (δ) of the methine proton of the O4-isopropyl groups of d(i⁴TpT), d(Tpi⁴T), and d(Tpi⁴TpT). Also included is the methine proton profile of the O4-isopropyl group of the monomer (M) i⁴dT.

other factors may be involved as discussed in Section 5.2.3.2.

***5.3.3.5.B The pPU H8 Profiles**: The pPU H8 profiles of the d(NpPU) molecules vary a little, in contrast to the pPY H6 profiles which were all identical. The pG H8 profiles of the d(r⁴TpG) dimers are upfield relative to that of d(TpG), perhaps due to the larger ring current effects of r⁴T relative to T or more base-stacking in the alkylated dimers. However, the pA H8 profile of d(i⁴TpA) is identical to that of d(TpA), with the pA H8 profile of d(e⁴TpA) upfield to both of these. The pA H8 observations in the d(NpA) dimers are corroborated in the pA H2 Δδ°s and variable temperature profiles. The pA H2 Δδ°s are identical with i⁴Tp and Tp (0.11 ppm) while with e⁴Tp it is larger (0.14 ppm). Furthermore, the pA H2 profile position with i⁴Tp is in between the profiles with e⁴Tp and Tp, laying closer to that with Tp (Figure 5.11). Unfortunately, the H8 profiles, like the H6 profiles, are often difficult to interpret because of the number of influences on their δs (Lee and Tinoco, 1980). Whatever the reason(s) for the observed differences in H8 and H2 profiles of the d(r⁴TpA) dimers, the fact they do not exist in the d(r⁴TpG) dimers point to a sequence dependent conformational effect contingent on the O4-alkyl substituent.*

***5.3.4 SUMMARY**:*

***5.3.4.1 d(NpPY)**: The major conformational effect of O4-alkylation is an increase in the 3'-*endo *population of the r⁴Tp sugar relative to that of the Tp sugar. Furthermore, the 3'-*endo *population of the r⁴Tp sugars increases with decreasing temperature while the conformation of the Tp sugar remains fixed. A small increase in the 3'-*endo *conformation of the pT sugar is also observed with decreasing temperature. However, the effect with pC is not as distinct as with pT.*

Except for the sugar conformations, O4-alkylation does not appear to significantly alter the conformation of the d(r⁴TpPY) dimers relative to the analogous d(TpPY) dimers. First, there are no major distortions in the sugar-phosphate backbone as monitored by the γ *and* β *populations. Second, an O4-alkyl group does not appear to effect the base-stacking*

geometry of the ***d(r⁴TpPY)*** *dimers; right handed/*χ-anti *stacks still appear to form. Furthermore, the size of the O4-alkyl group has virtually no effect on the conformation of the* ***d(r⁴TpPY)*** *dimers.*

5.3.4.2 ***d(TpPU)****: For the* ***d(r⁴TpPU)*** *dimers it appears as if r⁴T has a smaller effect on the conformation of these molecules than in the* ***d(r⁴TpPY)*** *set. However, the largest effect is still in the sugar conformations. There is a decrease in the S conformation of the r⁴Tp sugars relative to Tp. However, with decreasing temperature the S population of both the r⁴Tp and Tp sugars increase, with the r⁴Tp S conformation not increasing by an as large an amount. There are smaller changes in the conformation of the pPU sugars relative to the pPY sugars due to O4-alkylation, with only the pG unit of* ***d(e⁴TpG)*** *showing a substantial increase in the N conformation with decreasing temperature.*

Again, except for the small differences in the sugar puckers, O4-alkylation does not seem to drastically alter the conformation of the ***d(r⁴TpPU)*** *dimers relative to the analogous* ***d(TpPU)*** *dimer, as summarized for the* ***d(NpPY)*** *dimers. However, the base proton variable temperature profiles of the* ***d(i⁴TpA)*** *and* ***d(e⁴TpA)*** *dimers differ somewhat, unlike those for the* ***d(i⁴TpG)*** *and* ***d(e⁴TpG)*** *dimers, which suggest that the size of the O4-alkyl group is subtly altering the conformation of these molecules in a sequence dependent manner.*

5.3.4.3 ***d(r⁴TpX)****: Perhaps the most noteworthy feature of these alkylated molecules is the magnetic non-equivalence of the* α*-methylene resonances of the O4-ethyl group and the methyl resonances of the O4-isopropyl group. These resonances are sensitive to temperature and the X base and hence, serve as monitors of conformational changes in these molecules (Buchko* et al., *1987).*

5.4 d(XpN):

The dimers d(Tpe^{4}T), d(Tpi^{4}T), and d(Ape^{4}T) were synthesised to compare sequence dependent conformational effects of O4-alkylation.

5.4.1 SUGAR CONFORMATIONS:

5.4.1.1 d(Tpr^{4}T):

5.4.1.1.A The pr^{4}T Sugars: *The sugar conformations of the pT and pr^{4}T sugars are only weakly affected by temperature (Table 5.3, Figure 5.28). This is reflected in the temperature dependent trends of the $^3J_{1'-2'}$s and $^3J_{3'-4'}$s, which change less than 0.2 Hz with decreasing temperature (Tables 3.3 and 3.5). At 20°C the 2'-*endo *conformation of the pr^{4}T sugars is about 10% smaller than that of the pT sugar, which is a little larger than the difference observed in the dT and e^{4}T monomers (Figure 5.28). The 10% difference in sugar conformations at 20°C between the pr^{4}T and pT units is weakly reflected in the pN $^3J_{1'-2'}$s and $^3J_{3'-4'}$s which are, respectively, 0.3 Hz smaller and 0.5 - 0.6 Hz larger for the pr^{4}T sugars relative to the pT sugar.*

5.4.1.1.B The Tp Sugars: *The Tp sugars essentially do not change conformation with decreasing temperature as the %S numbers in Table 5.3 vary by less than 3%. The absence of any temperature dependent conformational changes of the Tp sugar of the d(TpN) dimers is reflected in: 1) $^3J_{1'-2'}$ and $^3J_{3'-4'}$ trends which change by < 0.4 Hz with decreasing temperature; and 2) H2' and H2" profiles for the Np units, whose Δδ°s fall in the narrow range of -0.03 to 0.01 ppm (Tables 3.2 and 3.5).*

5.4.1.1.C Comparisons to d(NpT): *In comparing the sugar conformations of both sets of d(NpT) and d(TpN) dimers, the major finding is that for the d(NpT) dimers, at 20°C, the 3'-*endo *conformation of the r^{4}Tp sugars are up to 30% larger than that of the Tp sugar (Table 5.1). Meanwhile, the 3'-*endo *difference between the pr^{4}T and pT sugars of the d(TpN) dimers at 20°C is only 10%, which is similar to that observed in the monomers dT and e^{4}dT. Furthermore, the d(TpT) sugar conformations are essentially invariant to temperature, as are*

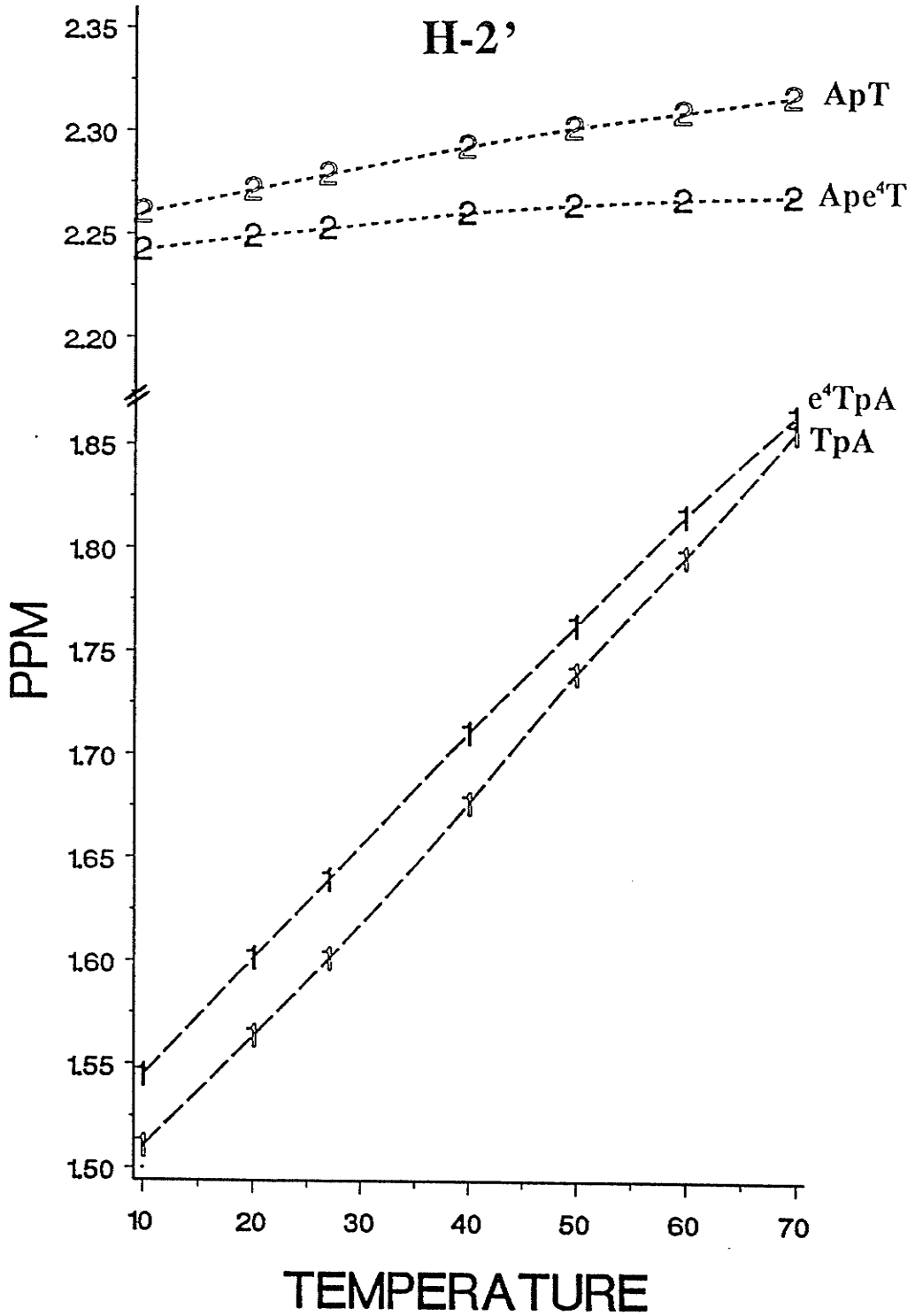

Figure 5.26: Temperature (C°) profiles of the chemical shifts (δ) of the Np (1) and pN (2) H2' sugar protons of d(NpA) and d(ApN). Bold numbers: N = e⁴T, hollow numbers: N = T.

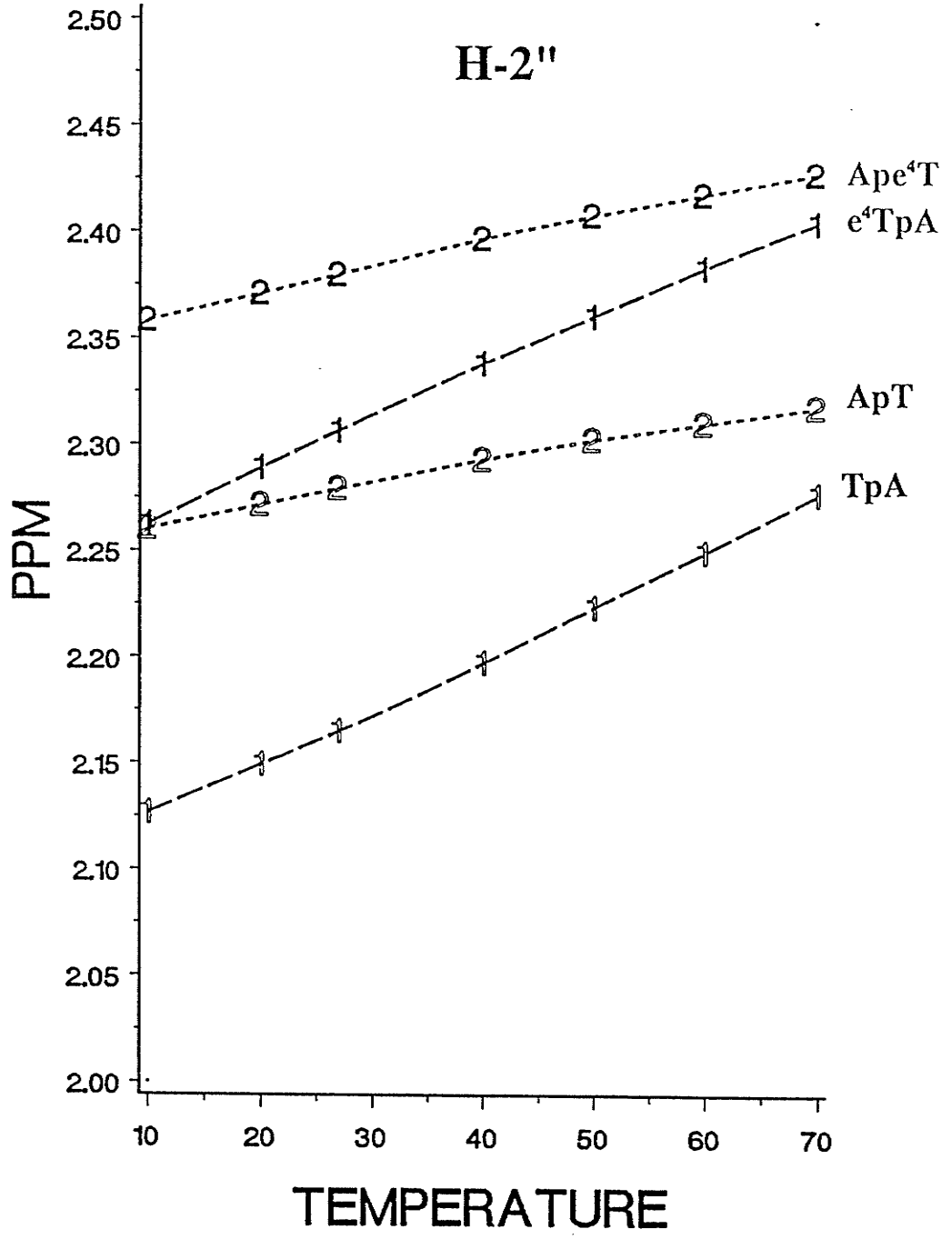

Figure 5.27: Temperature (C°) profiles of the chemical shifts (δ) of the Np (1) and pN (2) H2" sugar protons of d(NpA) and d(ApN). Bold numbers: N = e⁴T, hollow numbers: N = T.

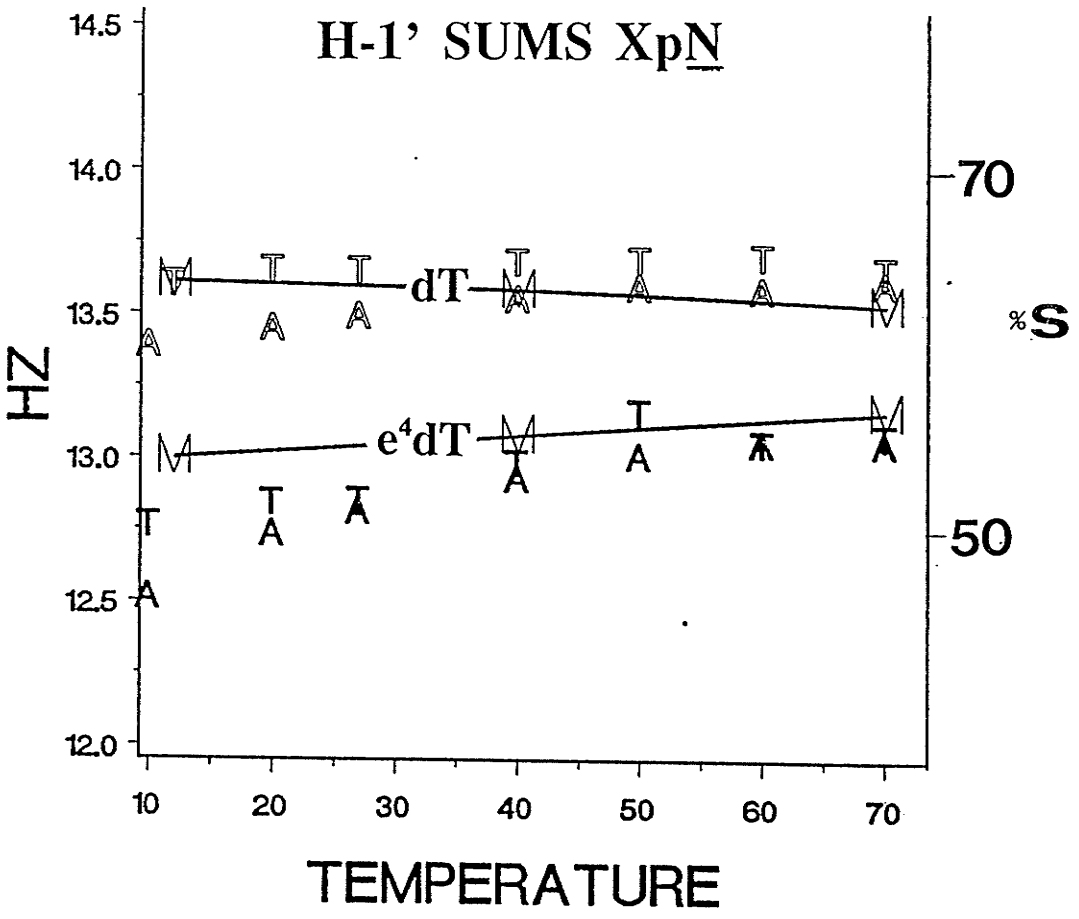

Figure 5.28: Temperature (C°) profiles of ΣI' in Hz for the pe⁴T unit of the d(XpN) dimers with X equal to adenine (A) and thymine (T). Bold letters: N = e⁴T, hollow letters: N = T. Also included are the ΣI' profiles for the monomers (M) e⁴dT and dT. The vertical axis at the right provides the %S (2'-endo) conformation of the sugar ring calculated according to equation I.

*the sugars of the d(TpN) dimers. On the other hand, the 3'-*endo *conformation of both the r^4Tp and pT units of the $d(r^4TpT)$ dimers appears to increase with decreasing temperature, with the largest temperature dependent changes for the r^4Tp units (Table 5.1). The observation that a r^4T affects the $d(r^4TpT)$ and $d(Tpr^4T)$ sugar conformations differently points to sequence dependent effects of O4-alkylation. The reason for these sequence dependent differences in the sugar conformation upon lowering the temperature are unclear. However, possible explanations are: 1) a larger population of stacked states in the $d(r^4TpT)$ dimers relative to the $d(Tpr^4T)$ dimers; and 2) different base-stacking geometries which dictate larger pucker shifts in the $d(r^4TpT)$ dimers than in the $d(Tpr^4T)$ dimers to best accommodate stacking.*

5.4.1.2 d(Ape⁴T):

*5.4.1.2.A The pN Sugars: In the d(ApN) dimers both pN sugars move towards larger 3'-*endo *populations to different extents upon lowering the temperature (Table 5.3, Figure 5.28). Hence, at 10°C there is approximately 15% more 3'-*endo *character in the pe^4T sugar than in the pT sugar. In $d(Ape^4T)$ the pe^4T N sugar pucker shift is reflected in the temperature dependence of $^3J_{1'-2'}$, which decreases 0.9 Hz, and in $^3J_{3'-4'}$, which increases 0.8 Hz (Table 3.14). Meanwhile, for the pT unit of d(ApT), there is a negligible temperature dependence in $^3J_{1'-2'}$, which decreases only 0.2 Hz, and in $^3J_{3'-4'}$, which does not change at all.*

Variable temperature profiles of the pN H2' and H2" resonances of the d(ApN) dimers are plotted in Figures 5.26 and 5.27. The pN H2' and H2" Δδ°s vary from 0.03 to 0.06 ppm for the d(ApN) dimers (Table 3.14) which are larger than those observed for the pN units of the d(TpN) molecules (-0.03 - 0.01 ppm). These differences are perhaps a reflection of the larger pN sugar pucker changes in the d(ApN) set of molecules and the larger ring current effects of an A relative to T.

5.4.1.2.B The Ap Sugars: In the d(ApN) dimers, the conformation of the Ap sugar is the same with e^4T and with T. Both Ap sugar conformations show a 10% increase in the 3'-

endo *conformation upon lowering the temperature (Table 5.3). The increase in the 3'*-endo *conformation of the Ap sugar of* ***d(ApT)*** *and* ***d(Ape^{4}T)*** *with decreasing temperature is reflected in their* $^3J_{1'-2'}S$*, which decreases 1.0 - 0.7 Hz.*

<u>5.4.1.2.C Comparisons to d(NpA)</u>: In the ***d(NpA)*** *dimers there is a smaller proportion of r^{A}Tp sugars in the S conformation relative to the Tp sugar at all temperatures. Furthermore, the S conformation of both Np sugars increases with decreasing temperature. In the d(ApN) dimers, there is also a reduction in the S conformation of the pe^{4}T sugar relative to the pT sugar. However, the S conformation of both pN sugars decreases with decreasing temperature with a larger decrease for the pe^{4}T sugar. With regards to the sugar conformation of the e^{4}dT nucleotidyl neighbour, it appears that the conformation of the Ap and the pA sugars are the same in the alkylated and non-alkylated dimers. Hence, the effects of r^{A}T on the sugar conformations of the* ***d(Ape^{4}T)*** *and* ***d(r^{A}TpA)*** *dimers appear to be sequence dependent, but to a weaker extent than observed in the* ***d(NpT)*** *and* ***d(TpN)*** *dimers.*

<u>5.4.2 THE SUGAR-PHOSPHATE BACKBONE</u>:

<u>5.4.2.1 d(TpN)</u>: Any differences in the γ *and* β *populations of the* ***d(TpN)*** *dimers are small. For the pN units, at low temperature, the* γ^+ *state is most populated, at 74 - 80 %, with the* γ^t *state containing the majority of the remaining population, at 22 - 25%. On the other hand, the Tp fragments are shifted more towards* γ^- *(10 - 11%) and* γ^t *(32 - 33%) at the expense of* γ^+ *(56 - 58%) which is typical at the 5'-end of short DNA oligomers (Mellema* et al., *1984). Meanwhile the* β^t *populations between the* ***d(TpT)*** *and* ***d(Tpr^{4}T)*** *dimers do not differ by more than 1% at low temperature due to O4-alkylation. Additionally, note that the* γ^+ *and* β^t *populations increase in all the* ***d(TpN)*** *dimers with decreasing temperature, in line with an increase in base-stacking with decreasing temperature (Altona, 1982).*

From the ^{13}C *spectra of* ***d(Tpi^{4}T)*** *and* ***d(TpT)*** *at 27°C it is possible to obtain estimates of the* ε^t *and* ε^- *populations. Such an analysis shows that the C3'-O3' torsion angle of*

Table 5.3. Furanose conformations and exocyclic bonds rotamer distributions for d(Xpr^{4}T)[a]

Molecule	%S	%γ^-	%γ^t	%γ^+	%β^t	%ε^t/%ε^-
Tp	64(61)	11(12)	33(36)	56(52)	-------	80/18
pT	64(64)	-2(1)	22(34)	80(64)	81(76)	-------
Tp	56(59)	10(12)	32(37)	58(51)	-------	-------
pe^{4}T	54(58)	0(4)	22(34)	78(62)	81(77)	-------
Tp	63(66)	11(13)	32(34)	57(52)	-------	77/23
pi^{4}T	54(58)	1(2)	25(34)	74(63)	80(75)	-------
Ap	51(61)	4(9)	25(30)	71(61)	-------	-------
pT	61(68)	-6(5)	9(26)	86(69)	91(80)	-------
Ap	51(61)	4(11)	25(27)	71(61)	-------	-------
pe^{4}T	44(58)	-1(-1)	20(28)	81(70)	91(80)	-------

[a] %S calculated according to equation I, %γ according to equations II, III, and IV, %β according to equation V, and %ε according to equations VI and VII. Coupling constants used in these equations were taken from Tables 3.3, 3.5, 3.14, and 3.24. The first number is at 10 (d(ApN)) or 20 (d(TpN)) ^{o}C, the number in brackets is at 60 (d(ApN)) or 70 (d(TpN)) ^{o}C.

d(TpN) is not altered by an i⁴T (Table 5.3). These ε observations, together with the γ and β rotamer populations, suggest that O4-alkylation does not produce any large changes in the sugar-phosphate backbone of the d(Tpr⁴T) dimers relative to d(TpT).

*5.4.2.2 d(ApN): The γ⁺ state is most populated at low temperature for the pN unit (pe⁴T: 81%, pT: 86%) than for the Ap unit (both 71%). Again, the γ⁺ population of the e⁴dT unit is smaller than that of the dT unit, as observed in all our dimers and this may be due to a preference for γ⁺ in the 3'-*endo *sugar conformation (Hruska, 1973). Note that the Ap conformer populations of d(ApN) are practically identical across Table 5.3, reflecting little conformational changes in the Ap unit upon exchanging T for e⁴T. In fact, the changes that exist for the pN unit are not major either, which, together with the observations for the Ap fragment, suggest that the sugar-phosphate backbone of the d(ApT) and d(Ape⁴T) dimers are similar. This is also reflected in the β' populations for the d(ApN) dimers which are the same at low temperature.*

5.4.3 THE BASE δs:

Parts 1 - 5 of this section will deal only with the O4-ethylated dimers, with a part introduced at the end discussing d(Tpi⁴T).

5.4.3.1 The Me5 Profiles: The Me5 resonances of d(ApN), d(NpA), d(TpT), and the O4-alkylthymidine fragment of d(e⁴TpT) and d(Tpe⁴T) are plotted as a function of temperature in Figure 5.29. These resonances all move upfield to various degrees with decreasing temperature. Note that the Me5 profiles of e⁴T are downfield of those of T, as observed in the e⁴dT and dT monomers, due to the different electronic conjugation of the two bases.

The Np Me5 Δδ°s of d(e⁴TpT), d(Tpe⁴T), and d(TpT) are small, < 0.02 ppm. These Np Me5 Δδ°s are similar to those observed in the d(NpX) dimers, where the X base also had little effect on the Me5 temperature profiles (Figure 5.22). These observations suggest that the Np Me5 is not over the X base of the pX unit when stacked, but projected outwards from the stack and is not significantly influenced by the ring currents of the base of the pX

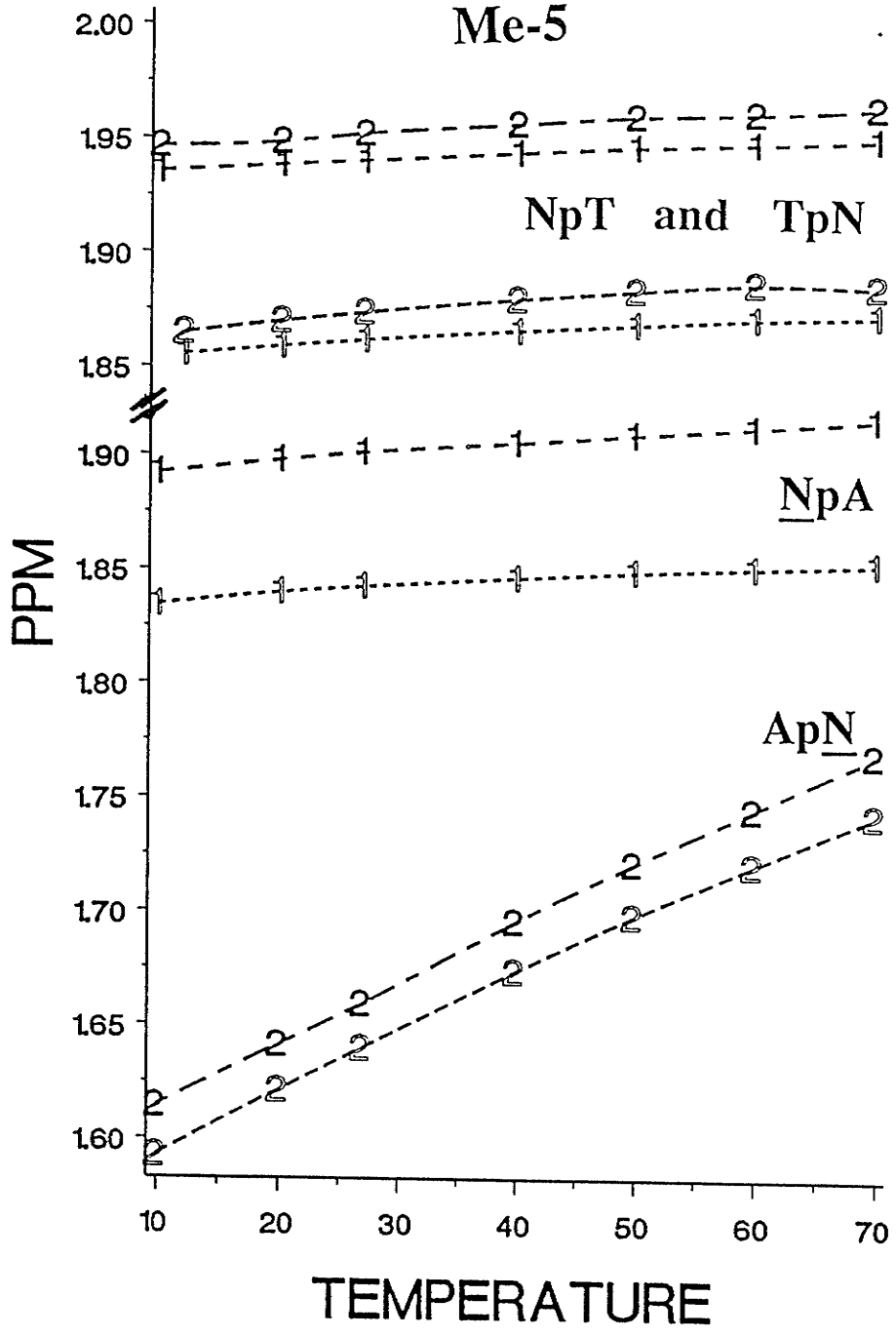

Figure 5.29: Temperature (C°) profiles of the chemical shifts (δ) of the Np (1) and pN (2) Me5 base protons of d(NpT), d(TpN), d(NpA) and d(ApN). Bold numbers: N = e^4T, hollow numbers: N = T.

unit. On the other hand, the pN fragments of ***d(Tpe⁴T)*** *and* ***d(TpT)*** *also have small Me5* $\Delta\delta$*°s, < 0.02 ppm. However, the Me5* $\Delta\delta$*° of the pT unit of* ***d(e⁴TpT)*** *is 0.05 ppm, presumably due to the larger ring current effects of* e^4*T relative to T. Furthermore, the pN Me5* $\Delta\delta$*°s of the* ***d(ApN)*** *dimers are large, 0.11 - 0.13 ppm, relative to those of the Np units of all the* ***d(NpX)*** *dimers. The larger Me5* $\Delta\delta$*°s of the pN units relative to the Np units of similar dimers (****d(XpN)*** *versus* ***d(NpX)****) concurs with a right handed/*χ-anti *stack as concluded by Kan* et al. *(1973) in their NMR studies of* ***d(TpA)*** *and* ***d(ApT)****. In such a stack the pN Me5 is more over the plane of the base of the Xp unit than the Np Me5 is over the plane of the base of the pX unit.*

5.4.3.2 The α*-Methylene Profiles of the O4-Ethyl Group:*

5.4.3.2.A ***d(Tpe⁴T)****: The conclusions made on the basis of the Me5 profiles are corroborated with the observations on the profiles of the* α*-methylene resonances of the O4-ethyl group. The* α*-methylene resonances of the O4-ethyl group of* ***d(e⁴TpT)****,* ***d(Tpe⁴T)****, and* ***e⁴dT*** *are plotted as a function of temperature in Figure 5.30. The* α*-methylene resonances of* ***d(Tpe⁴T)*** *are upfield of those of* ***d(e⁴TpT)*** *which suggests that these protons of the former dimer are more over the plane of the neighbouring base than those of the latter dimer.*

The α*-methylene* $\Delta\delta$*s at 20°C are almost identical for* ***d(e⁴TpT)*** *and* ***d(Tpe⁴T)****, with little difference in their* $\Delta\delta$*°s, at 0.05 - 0.06 ppm for the upfield signal (A) and 0.03 - 0.04 ppm for the downfield signal (B) (Table 3.2). It is likely that the* α*-methylene* $\Delta\delta$ *for* ***d(Tpe⁴T)*** *is due to temperature dependent base-stacking, as concluded for* ***d(e⁴TpT)****. However, note that this conclusion dictates that there will be a reversal of the prochiral proton that is orientated towards the inside of the stack. In* ***d(e⁴TpT)****,* H_R *is projected closer to the plane of the neighbouring base (pX) in the O4-ethyl conformation described in Figure 5.4A. On the other hand, in* ***d(Tpe⁴T)****, the base is under* H_S *and therefore, this* α*-methylene proton will be closer to the plane of the neighbouring base (Xp). Consequently,* H_S *will experience the greater ring current effects and hence, the upfield resonance, A, is assigned to* H_S *in the*

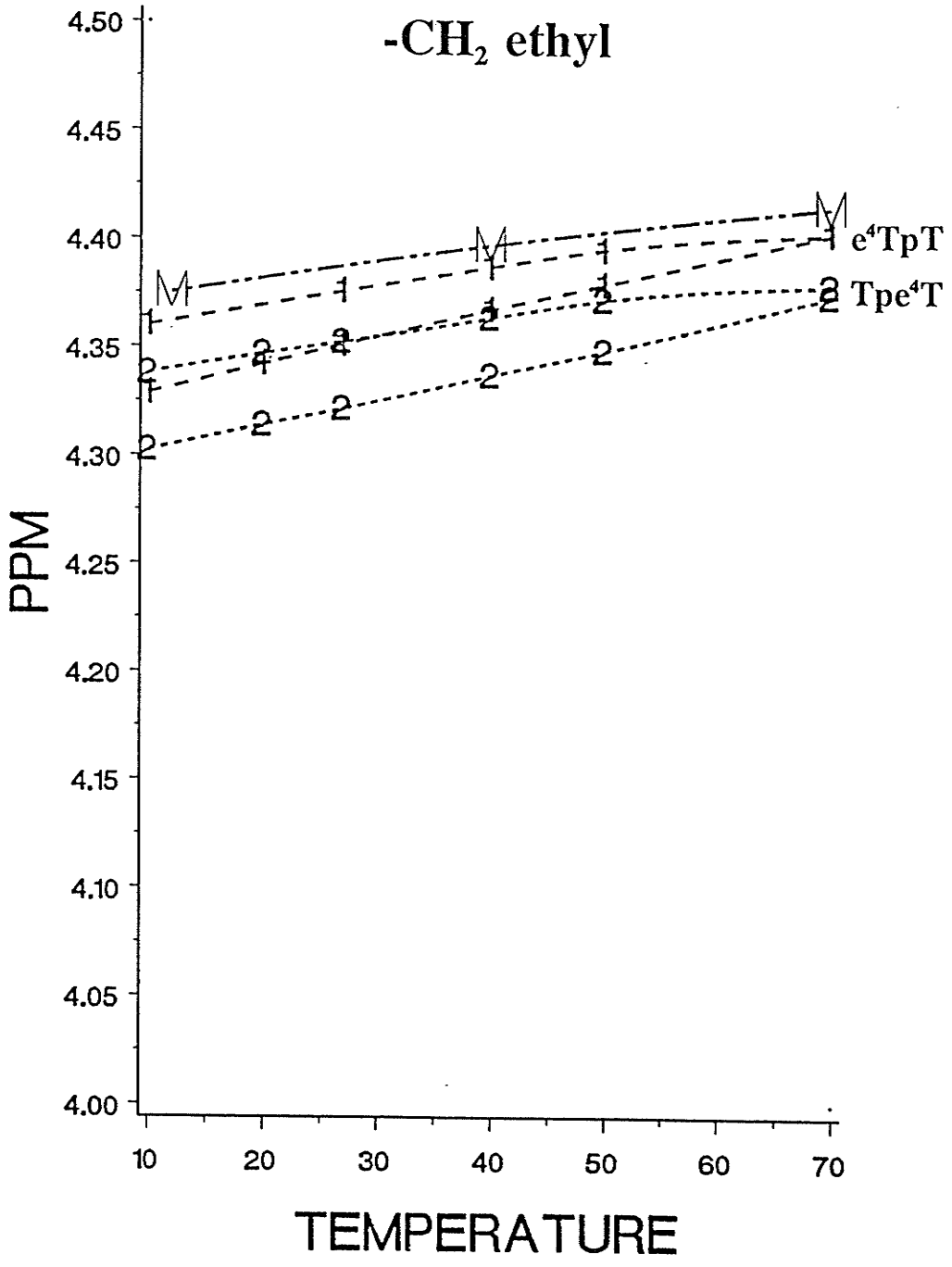

Figure 5.30: Temperature (C°) profiles of the chemical shifts (δ) of the O4-ethyl α-methylene protons of d(e⁴TpT) and d(Tpe⁴T). Also included is the α-methylene protons profile of the O4-ethyl group of the monomer (M) e⁴dT.

d(Xpe⁴T) dimers. Note that the α-methylene Δδ between d(e⁴TpT) and d(Tpe⁴T) could be correlated to the population of the dimers in a base-stacked state if the base-base geometry was equivalent in both sequences, which is not the case, as illustrated in the discussion of the Me5 resonances of the Np and pN bases. Hence, the similar Δδ observed for the α-methylene resonances of the O4-ethyl groups of d(e⁴TpT) and d(Tpe⁴T) do not mean an equivalent amount of base-stacking. Therefore, the conclusions to be drawn from the profiles in Figure 5.30 are: 1) the overall upfield position of the α-methylene temperature profiles of d(Tpe⁴T) relative to those of d(e⁴TpT) suggest better overlap of the neighbouring base over the O4-C_α region in the former dimer; and 2) there is an increase in base-stacking with the lowering of the temperature in both dimers because the α-methylene signals move upfield.

5.4.3.2.B (Ape⁴T): The conclusions drawn from the α-methylene resonances of the O4-ethyl group of d(e⁴TpT) and d(Tpe⁴T) can be made for the same resonances of d(Ape⁴T) and d(e⁴TpA) which are plotted as a function of temperature in Figure 5.31. The α-methylene resonances of d(Ape⁴T) are upfield of those of d(e⁴TpA) which suggests that the O4-C_α region of e⁴T feels the ring current effects of the base of the Ap unit more than the base of the pA unit, consistent a right handed/χ-anti stack. Furthermore, the α-methylene profiles of the d(Xpe⁴T) and d(e⁴TpX) dimers with X equal to A are upfield of the analogous molecule with X equal to T, in line with the greater ring current effects of a purine base.

Note that the α-methylene Δδ of the O4-ethyl group increases slightly for d(e⁴TpA) with decreasing temperature while for d(e⁴TpA) Δδ is decreasing, from 0.03 ppm at 60°C to an undetectable amount at 10°C. Also, the Δδ° of the α-methylene resonances of d(e⁴TpA) (0.08 ppm) are larger than those of d(Ape⁴T) (0.03 - 0.06 ppm) (Tables 3.12 and 3.14). The reason for these observations are unclear but, the obvious can be stated: 1) the positive α-methylene Δδ°s for both dimers indicate base-stacking is occurring as the temperature is lowered; and 2) the different α-methylene Δδ°s and Δδs for the O4-ethyl group of the d(e⁴TpA) and d(Ape⁴T) dimers reflect different base-stacking geometries in the

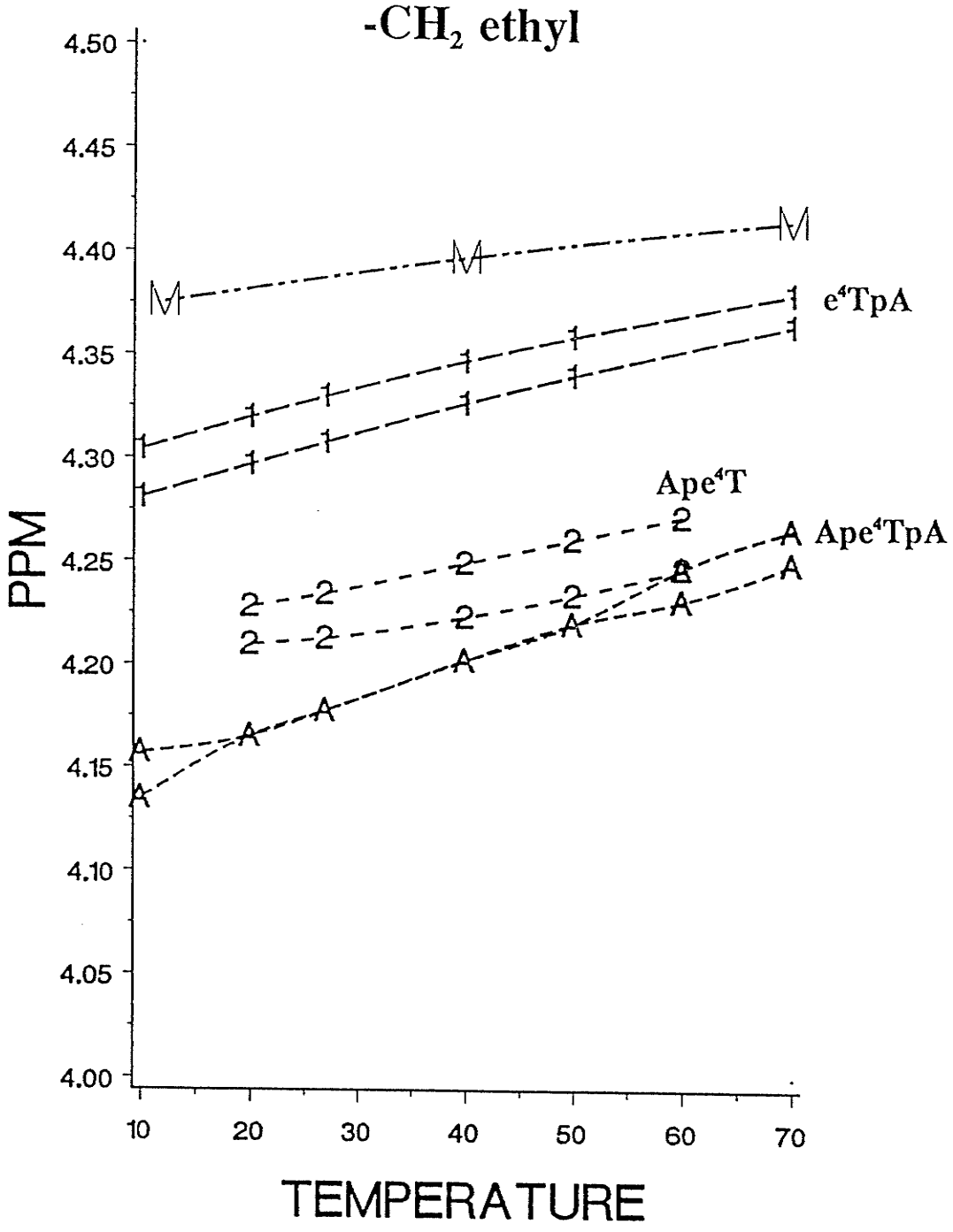

Figure 5.31: Temperature (C°) profiles of the chemical shifts (δ) of the O4-ethyl α-methylene protons of d(e⁴TpA), d(Ape⁴T) and d(Ape⁴TpA). Also included is the α-methylene protons profile of the O4-ethyl group of the monomer (M) e⁴dT.

two molecules.

***5.4.3.3 The Methyl Profiles of the O4-Ethyl Group**: Variable temperature profiles of the methyl resonance of the O4-ethyl group of d(Ape^{4}T), d(e^{4}TpA), d(e^{4}TpT), and d(Tpe^{4}T) are included in Figure 5.32. The methyl profile of the O4-ethyl group of d(Xpe^{4}T) is upfield relative to that of d(e^{4}TpX) and the difference is greater when X is A rather than T. These observations are in line with a right handed/*χ*-anti stack and imply that the O4-C*α* region of e^{4}T is more over the base of a Xp unit than the base of a pX unit.*

***5.4.3.4 The H2 Profiles**: The H2 Δδ°s of the d(ApN) dimers are between 0.09 and 0.11 ppm and are similar to those observed in the d(NpA) dimers, 0.11 to 0.14 ppm (Table 3.12 and 3.14). In both sets of dimers, slightly larger H2 Δδ°s are observed with r^{4}T relative to T, perhaps because of larger ring current effects or more base-stacking. Note that the H2 resonances move upfield with decreasing temperature in the d(ApN) and d(NpA) dimers which suggests that base-stacking is occurring. The similar characteristics of the H2 resonances of the d(ApN) and d(NpA) dimers supports a right handed/*χ*-anti base-stacking orientation because space-filling molecular models indicate that H2 in both oligomers is in a similar position relative to the neighbouring base.*

***5.4.3.5 The H6 and H8 Profiles**: The variable temperature profiles of the H6 resonances of d(TpT) and the O4-ethylthymine of d(e^{4}TpT) and d(Tpe^{4}T) are produced in Figure 5.33. The H6 variable temperature profiles of the d(ApN) and d(NpA) dimers are plotted in Figure 5.34. Both Figures show that the H6 signals of the O4-alkylated base are downfield of their non-alkylated counterpart, consistent with trends observed in the monomers, e^{4}dT and dT, due to the different electronic conjugation of the two bases (Birnbaum* et al., *1988). Because of the difficulty in interpreting H6 temperature profiles (Section 5.2.3.2) the major point to note in these two Figures is that in the presence of A, the H6 profiles move upfield with decreasing temperature, while in the presence of T, these profiles move downfield, concurrent with the larger ring current effects of purines.*

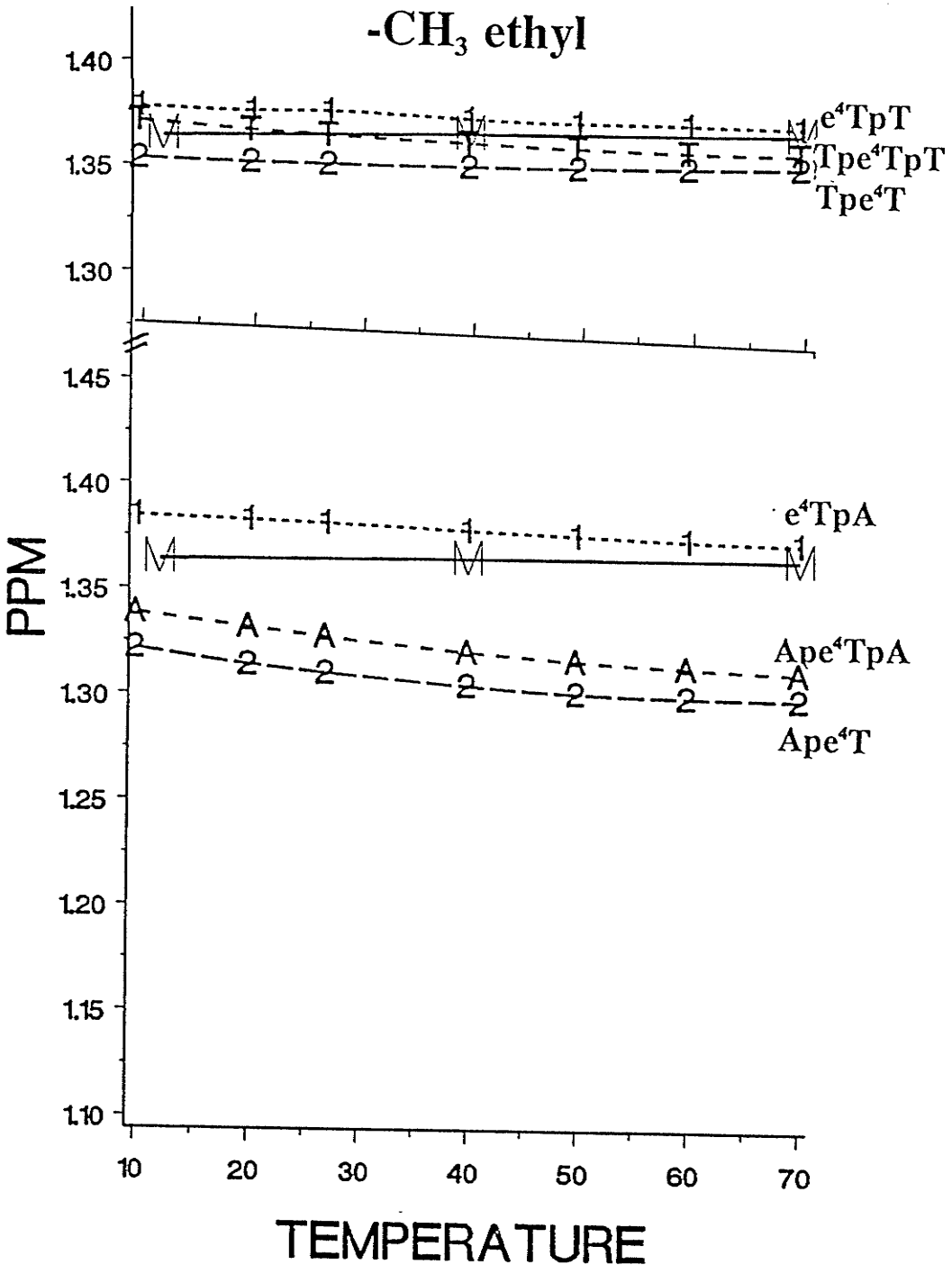

Figure 5.32: TOP) Temperature (C°) profiles of the chemical shifts (δ) of the methyl protons of the O4-ethyl groups of d(e⁴TpT) (1), d(Tpe⁴T) (2), and d(Tpe⁴TpT) (T). Also included is the methyl protons profile of the O4-ethyl group of the monomer (M) e⁴dT. BOTTOM) Temperature (C°) profiles of the chemical shifts (δ) of the methyl protons of the O4-ethyl groups of d(e⁴TpA) (1), d(Ape⁴T) (2) and d(Ape⁴TpA) (A). Also included is the methyl protons profile of the O4-ethyl group of the monomer (M) e⁴dT.

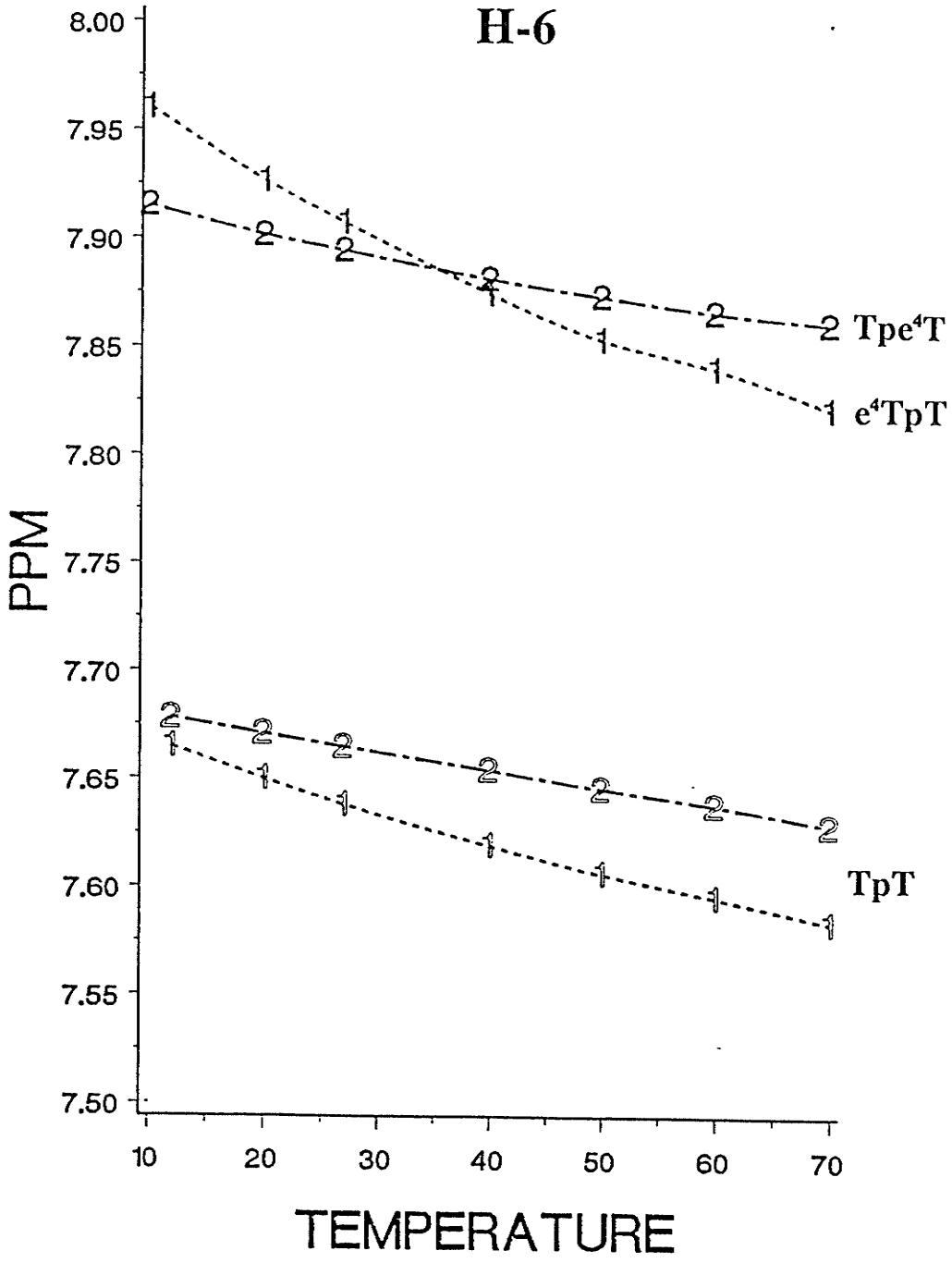

Figure 5.33: Temperature (C°) profiles of the chemical shifts (δ) of the Np (1) and pN (2) H6 base protons of d(NpT) and d(TpN). Bold numbers: N = e⁴T, hollow numbers: N = T.

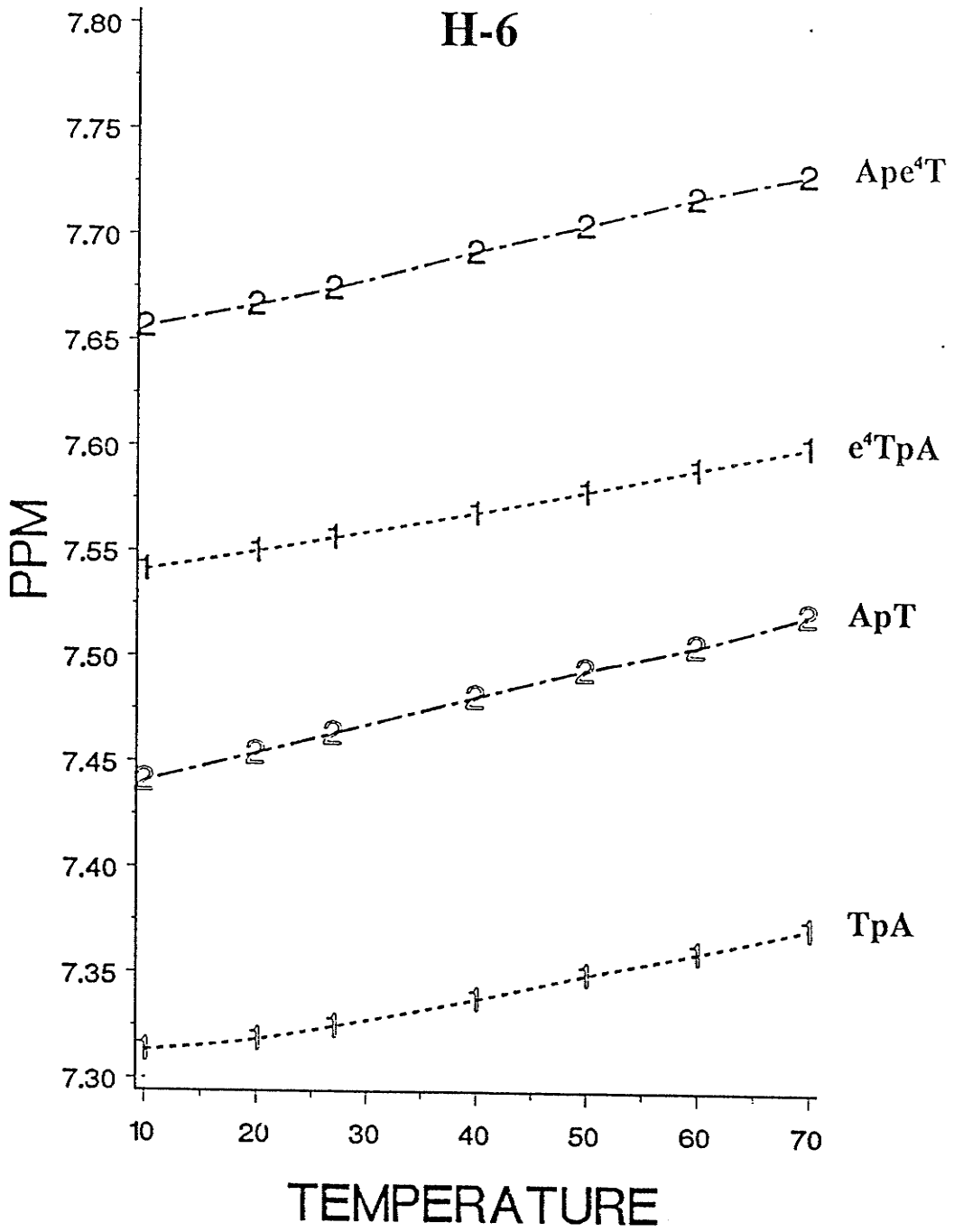

Figure 5.34: Temperature (C°) profiles of the chemical shifts (δ) of the Np (1) and pN (2) H6 base protons of d(NpA) and d(ApN). Bold numbers: N = e⁴T, hollow numbers: N = T.

The H8 Δδ°s of the d(NpA) and d(ApN) dimers vary little over temperature, at -0.02 - -0.03 ppm (Table 3.12 and 3.14). The H8 temperature profiles with e^4T are upfield of those with T, probably due to the larger ring current effects of the former base or more base-stacking in the O-alkylated dimers.

***5.4.3.6 d(Tpi^{4}T): The O4-Isopropyl Group**: The only dimer whose base protons have not yet been discussed are those of d(Tpi^{4}T). Comparison of the d(Tpe^{4}T) and d(Tpi^{4}T) data in Tables 3.2, 3.4, and 5.3 reveal small differences in the δs, Js, and rotamer populations upon changing the O4-ethyl group to an O4-isopropyl in d(Tpr^{4}T) which suggests that the size of the O4-alkyl group is not altering the conformation of these two dimers. Therefore, the only feature of d(Tpi^{4}T) to be discussed will be the ^{1}H NMR spectra of the O4-isopropyl group.*

A comparison of the methyl resonances of the O4-isopropyl function of d(Tpi^{4}T) and d(i^{4}TpT) (Figure 5.10) show that the Δδ between the prochiral methyl groups increases with decreasing temperature and the effect is larger in d(i^{4}TpT) (0.04 ppm, 20°C) than in d(Tpi^{4}T) (0.02 ppm, 20°C) (Buchko et al., *1989b). Furthermore, both methyl profiles of the O4-isopropyl group of d(Tpi^{4}T) are upfield of the corresponding profiles of d(i^{4}TpT), which suggests that the O4-C_α region of the O4-isopropyl group is over the neighbouring base in d(Tpi^{4}T) more than it is in d(i^{4}TpT), as suggested for α-methylene protons of the O4-ethyl group of the d(e^{4}TpX) and d(Xpe^{4}T) dimers. For d(i^{4}TpT), the pro-S methyl was always nearer the pT base in a right handed/χ-*anti *helix (Figure 5.4D and E), but with d(Tpi^{4}T), the Tp base will be below the O4-isopropylated base in Figure 5.4D - 5.4F and the pro-R methyl will now always be positioned closer to the neighbouring base. Hence, for d(Tpi^{4}T), there will be a reversal in relation to d(i^{4}TpT) of the prochiral O4-isopropyl methyl group that is closer to the neighbouring base, as was the case for the prochiral α-methylene protons of the ethyl function of d(Tpe^{4}T) and d(e^{4}TpT). Unfortunately, it is not possible to assign the pro-S or pro-R methyls of d(Tpi^{4}T) from the chemical shift trends because of the same reason given for d(i^{4}TpT) (Section 5.1.2.4).*

The methine resonances of the O4-isopropyl function of ***d(Tpi^{4}T)*** *and* ***d(i^{4}TpT)*** *show similar upfield movements with decreasing temperature, 0.05 and 0.04 ppm, respectively. Note that the methine isopropyl profile of* ***d(Tpi^{4}T)*** *is upfield relative to that of* ***d(i^{4}TpT)*** *(Figure 5.25), as was the case for the O4-isopropyl methyl profiles, and reflects different base-stacking geometries of the neighbouring base over the O4-C_α region of r^{4}T which is consistent with a right handed/*χ-anti *stack for both dimers.*

5.4.4 SUMMARY:

The major effect of O4-alkylation on the conformation of the ***d(XpN)*** *dimers is an increase in the 3'-*endo *conformation of the pr^{4}T sugar relative to the pT sugar. In contrast to the* ***d(NpX)*** *dimers, the effect is greater when X is an A rather than a T. There is essentially no effect of O4-alkylation on the sugar conformation of the neighbouring nucleotide in the* ***d(XpN)*** *dimers which differs with the small changes induced by e^{4}T on the neighbouring sugar conformation in some of the* ***d(NpX)*** *dimers. Together, these observations suggest that the effects of O4-alkylation of T on sugar conformations are sequence dependent.*

From the variable temperature profiles of the base protons it appears as if O4-alkylated dimers still form right handed/χ-anti *stacks. This conclusion agrees with the estimations of the sugar-phosphate backbone rotamer populations, which are similar for the alkylated and non-alkylated dimers. The only comparison of the size of the O4-alkyl group on the conformation of the* ***d(Xpr^{4}T)*** *dimers, between* ***d(Tpe^{4}T)*** *and* ***d(Tpi^{4}T)****, indicates that the alkyl group does not have any influence. Finally, as observed in the* ***d(r^{4}TpX)*** *dimers, the* α*-methylene resonances of the O4-ethyl group and the methyl resonances of the O4-isopropyl group display a temperature dependent magnetic non-equivalence that appears to be related to base-stacking.*

5.5. TRIMERS:

The molecule ***d(TpTpT)*** *and a set of* ***d(Tpr^{4}TpT)*** *trimers were synthesised with r equal to methyl, ethyl, and isopropyl to: 1) compare the effect of O4-alkylation on the conformation of* ***d(TpTpT)****; and 2) to compare the effect of different O4-alkyl groups on the conformation of the* ***d(Tpr^{4}TpT)*** *molecules. The trimers* ***d(ApTpA)*** *and* ***d(Ape^{4}TpA)*** *were made, not only to compare the effect of O4-ethylation on* ***d(ApTpA)****, but with the additional intent of comparing the pNp unit of these* ***d(ApNpA)*** *trimers to those of the* ***d(TpNpT)*** *trimers.*

5.5.1 SUGAR CONFORMATIONS:

5.5.1.1 d(TpNpT):

5.5.1.1.A The pNp Sugars: *The sugar populations of the* ***d(TpNpT)*** *trimers are listed in Table 5.4 with a variable temperature plot of the Σ1' of* ***d(TpTpT)*** *and* ***d(Tpe^{4}TpT)*** *presented in Figure 5.35. The greatest difference between the sugar puckers of* ***d(TpTpT)*** *and* ***d(Tpr^{4}TpT)*** *is for the pNp unit, where, at 20°C, the S conformation between the pr^{4}p and pTp sugars differ by over 20%. This is reflected in the magnitude of $J_{1'-2'}$ which is smaller for pr^{4}Tp (6.5 - 6.6 Hz, 10°C) than for pTp (8.1 Hz, 30°C) while the magnitude of $J_{3'-4'}$ is greater for pr^{4}Tp (3.3 - 4.2 Hz, 10°C) than for pTp (3.0 Hz, 30°C) (Tables 3.16 - 3.19). Furthermore, there is approximately a 10% shift towards 3'*-endo *for the pr^{4}Tp sugars in moving from 70 to 10°C, which contrasts to the 2'*endo *movement observed for the pTp sugar over the same temperature range. The temperature dependent increase in the 3'*-endo *conformation of the pr^{4}Tp sugars is reflected in $J_{1'-2'}$s and $J_{3'-4'}$s. Upon lowering the temperature, the pr^{4}Tp $J_{1'-2'}$ decreases 0.6 - 0.9 Hz in all three alkylated trimers and the $J_{3'-4'}$ increases 0.8 Hz when r is an ethyl or methyl (with no change when r = isopropyl).*

The H2' and H2" variable temperature profiles of the pNp sugars of ***d(TpTpT)*** *and* ***d(Tpe^{4}TpT)*** *are included in Figures 5.36 and 5.37, respectively, and reveal only a small temperature dependence for both C2' protons. The H2" profile of pe^{4}Tp is downfield relative*

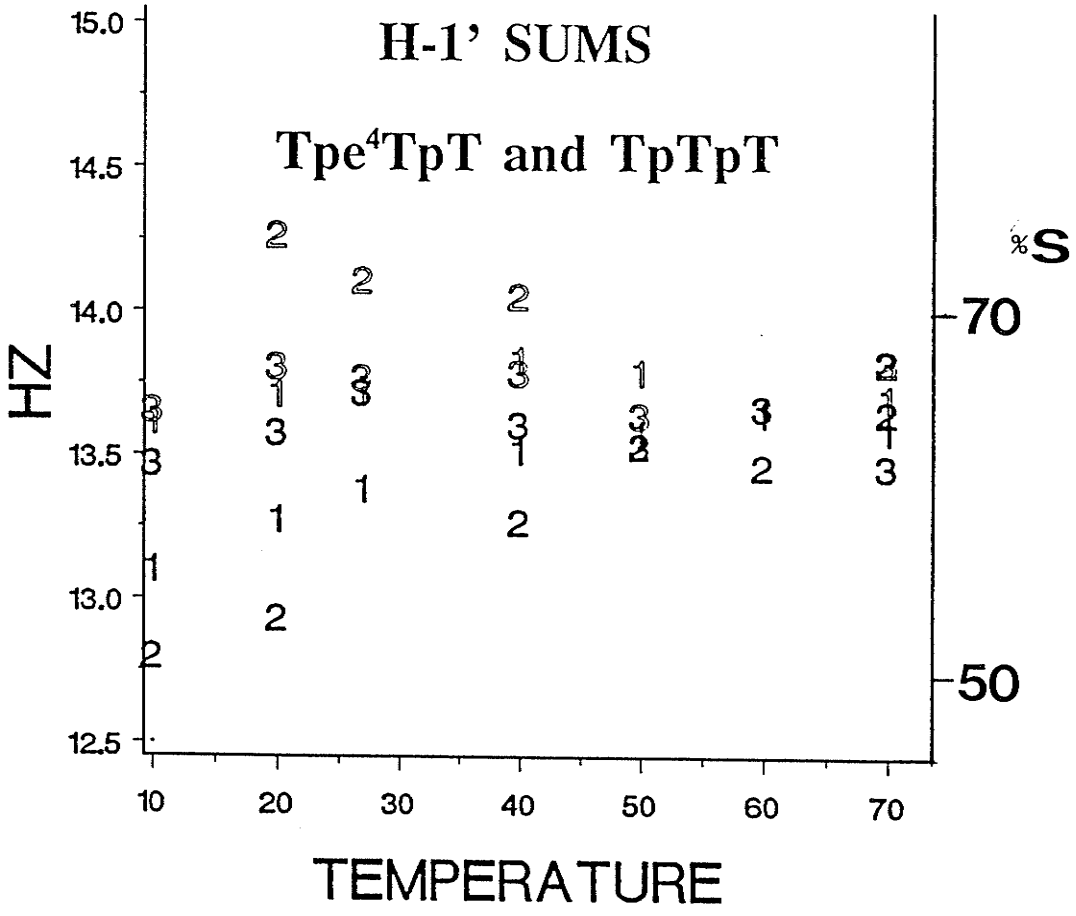

Figure 5.35: Temperature (C°) profiles of Σ1' in Hz for the Tp (1), pNp (2), and pT (3) sugars of d(TpNpT). Bold numbers: d(Tpe⁴TpT), hollow numbers: d(TpTpT). The vertical axis at the right provides the %S (2'-endo) conformation of the sugar ring calculated according to equation I.

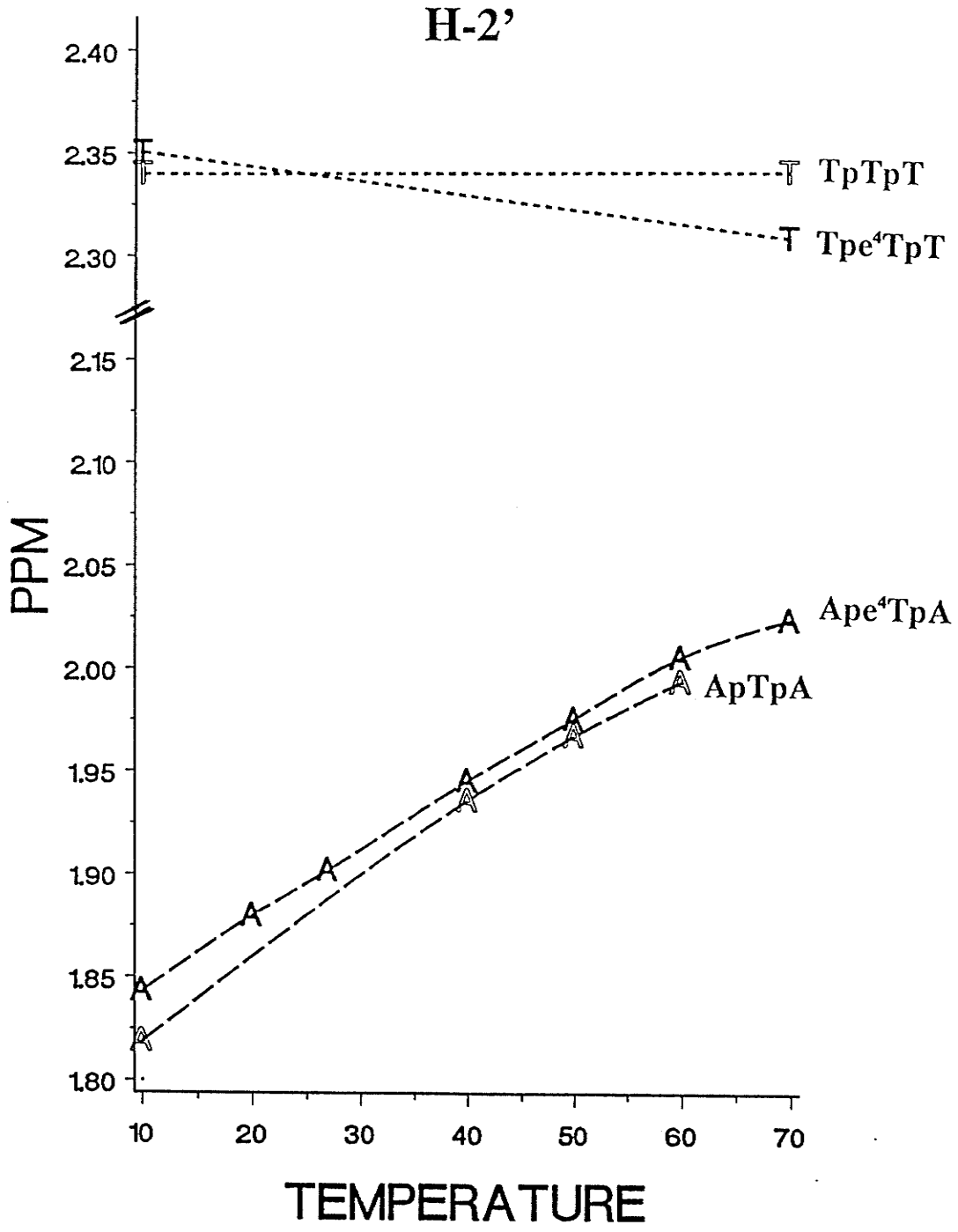

Figure 5.36: Temperature (C°) profiles of the chemical shifts (δ) of the pNp H2' sugar protons of d(ApNpA) (A) and d(TpNpT) (T). Bold letters: N = e⁴T, hollow letters: N = T.

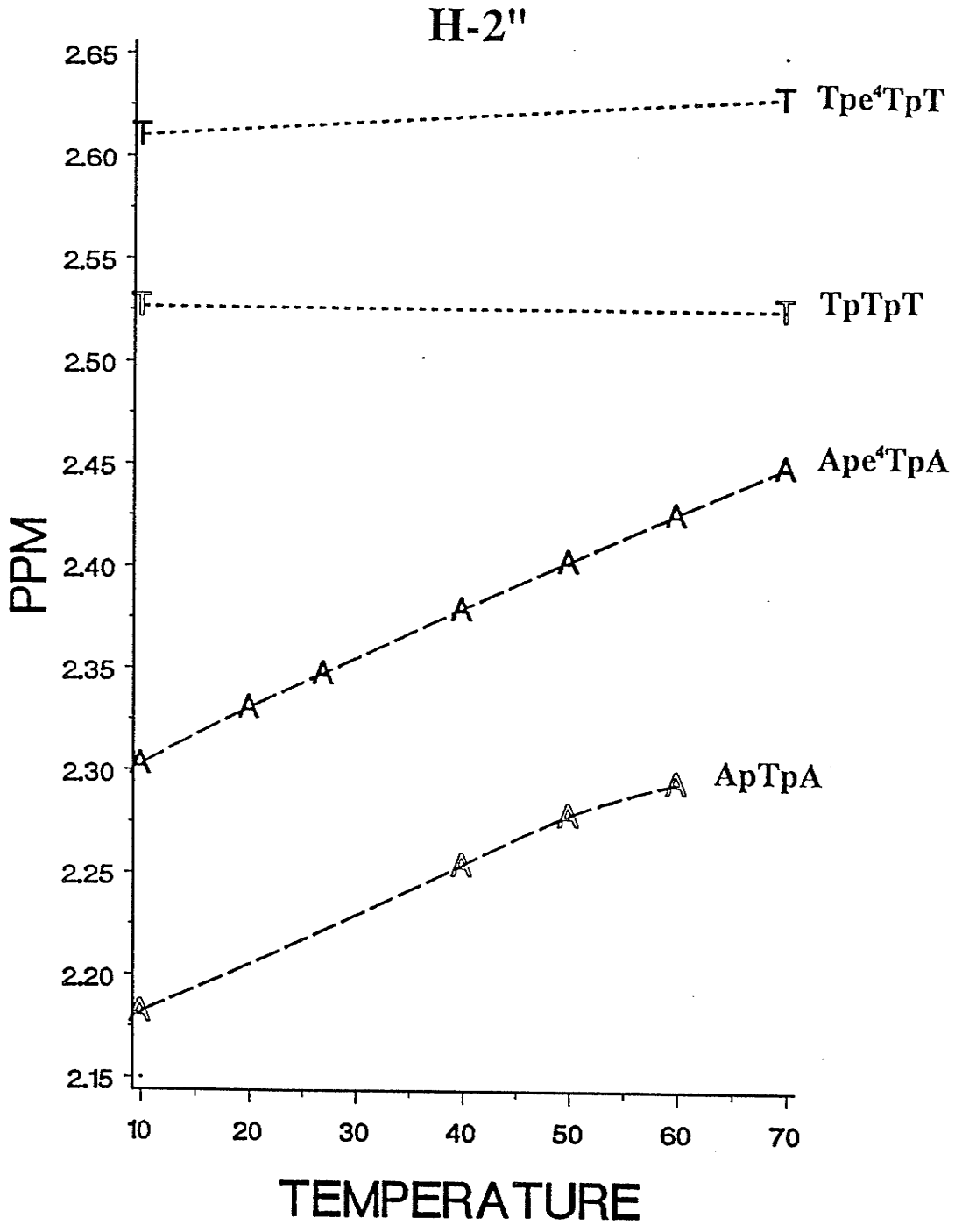

Figure 5.37: Temperature (C°) profiles of the chemical shifts (δ) of the pNp H2" sugar protons of d(ApNpA) (A) and d(TpNpT) (T). Bold letters: N = e⁴T, hollow letters: N = T.

to the H2" profile of pTp, as observed in the monomers (Figure 5.16), the Np units of the ***d(NpT)*** *dimers (Figure 5.16), and the pN units of the* ***d(TpN)*** *dimers (Table 3.2 and 3.4). On the other hand, the H2' profiles of* pe^4Tp *and pTp (Figure 5.36) are almost identical, especially at low temperature, which contrasts to: 1) the upfield position of the H2' profile of* e^4dT *relative to* ***dT*** *(Figure 5.14); 2) the upfield position of the H2' profile of the* pe^4T *unit of* ***d(Tpe^{4}T)*** *relative to the pT unit of* ***d(TpT)*** *(Table 3.2 and 3.4); and 3) the largely downfield position of the H2' profile of the* e^4Tp *unit of* ***d(e^{4}TpT)*** *relative to that of the Tp unit of* ***d(TpT)*** *(Figure 5.14). Unfortunately, due to the many variables influencing the sugar resonances (Section 5.1.5.1) it is not possible to explain these observations.*

5.5.1.1.B The Tp Sugars*: The sugar conformation of the neighbouring nucleotides of the* pr^4Tp *unit of the* ***d(Tpr^{4}TpT)*** *trimers appears influenced at the 5'-end, but not the 3'-end, as observed in Table 5.4 and Figure 5.35. In* ***d(Tpm^{4}TpT)*** *and* ***d(Tpe^{4}TpT)*** *the 3'-*endo *sugar conformation of the Tp unit increases approximately 10% with decreasing temperature while in* ***d(TpTpT)*** *the Tp sugar conformation does not change over the same temperature range. This Tp temperature dependent 3'-*endo *shift in* ***d(Tpm^{4}TpT)*** *and* ***d(Tpe^{4}TpT)*** *is reflected in the temperature dependence of its* $^3J_{1'-2'}$*, which decreases 0.7 - 0.8 Hz, and in its* $^3J_{3'-4'}$*, which increases 0.3 Hz. Coupling constants are available for* ***d(TpTpT)*** *only at 30°C and therefore, it is not possible to look at temperature dependent trends in* $J_{1'-2'}$ *and* $^3J_{3'-4'}$*. However, the magnitude of the Tp* $J_{1'-2'}$ *of* ***d(TpTpT)*** *is larger (7.7 Hz, 30°C) than those of* ***d(Tpm^{4}TpT)*** *and* ***d(Tpe^{4}TpT)*** *(6.6 Hz, 10°C) with a corresponding reversal in* $J_{3'-4'}$ *(3.2 and 3.8 - 3.9 Hz, respectively, 10°C). Note that for* ***d(Tpi^{4}TpT)****, the Tp* $J_{1'-2'}$ *and* $J_{3'-4'}$ *values at low temperature are similar to those of* ***d(TpTpT)*** *at 30°C, differing by less than 0.2 Hz, and hence, it appears as if the* pi^4Tp *unit is having a different influence on the sugar conformation of its 5'-nucleotidyl neighbour than* pm^4Tp *or* pe^4Tp*.*

5.5.1.1.C The pT Sugars*: The conformation of the pT sugar conformation is not influenced by the base of a* pr^4Tp *unit, as observed in Figure 5.35, where the* $\Sigma 1'$ *values for the pT*

units of ***d(TpTpT)*** *and* ***d(Tpe^{4}TpT)*** *never differ by more than 0.3 Hz. Furthermore, the conformation of the pT sugar of the three alkylated trimers does not vary significantly with temperature (Table 5.4) and at 10°C they are all between 61 - 66 %S, which is near the 68 %S observed in the pT unit of* ***d(TpTpT)*** *at 30°C. The absence of major conformational changes in the pT sugar of the* ***d(Tpr^{4}TpT)*** *trimers is reflected in $J_{1'-2'}$ and $J_{3'-4'}$, which vary less than 0.3 Hz upon altering the temperature, and in the H2' and H2" Δδ°s, which move upfield less than 0.03 ppm.*

5.5.1.1.D Comparisons to the Constituent Dimers: *In comparing the temperature dependence of the conformation of the pT sugars of* ***d(Tpr^{4}TpT)*** *to the pT sugars of* ***d(r^{4}TpT)****, the dimers are affected to a greater extent, showing an increase in the 3'-*endo *conformation with decreasing temperature while in the trimer the pT sugar conformation does not change. In contrast, when comparing the temperature dependence of the conformation of the Tp sugars of* ***d(Tpr^{4}TpT)*** *to the Tp sugars of* ***d(Tpr^{4}T)****, the trimer is affected to a greater extent, showing an increase in the 3'-*endo *conformation upon lowering the temperature while the conformation of the Tp sugars of the dimers do not change. If any of the temperature dependent increases in the 3'-*endo *conformations observed in the* ***d(Tpr^{4}T)*** *and* ***d(r^{4}TpT)*** *sugars are necessary to allow for the best base-stacking interactions, as previously suggested, then in the* ***d(Tpr^{4}TpT)*** *trimer the base-base interactions are probably not identical to those of the constituent dimers since the trimer sugar conformations behave differently with temperature.*

5.5.1.2 d(ApNpA): *The only differences in the sugar conformations between the* ***d(ApNpA)*** *trimers are for the pNp unit, as observed in Table 5.4 and in the variable temperature Σ1' plot (Figure 5.38). Both the pTp and pe^{4}Tp sugar puckers do not vary with temperature. At 10°C the 2'-*endo *population of pTp is approximately 10% larger than that of pe^{4}Tp. The small changes in the pNp sugar conformations of* ***d(ApNpA)*** *over temperature are reflected in small temperature dependent variations in $J_{1'-2'}$, less than 0.3 Hz.*

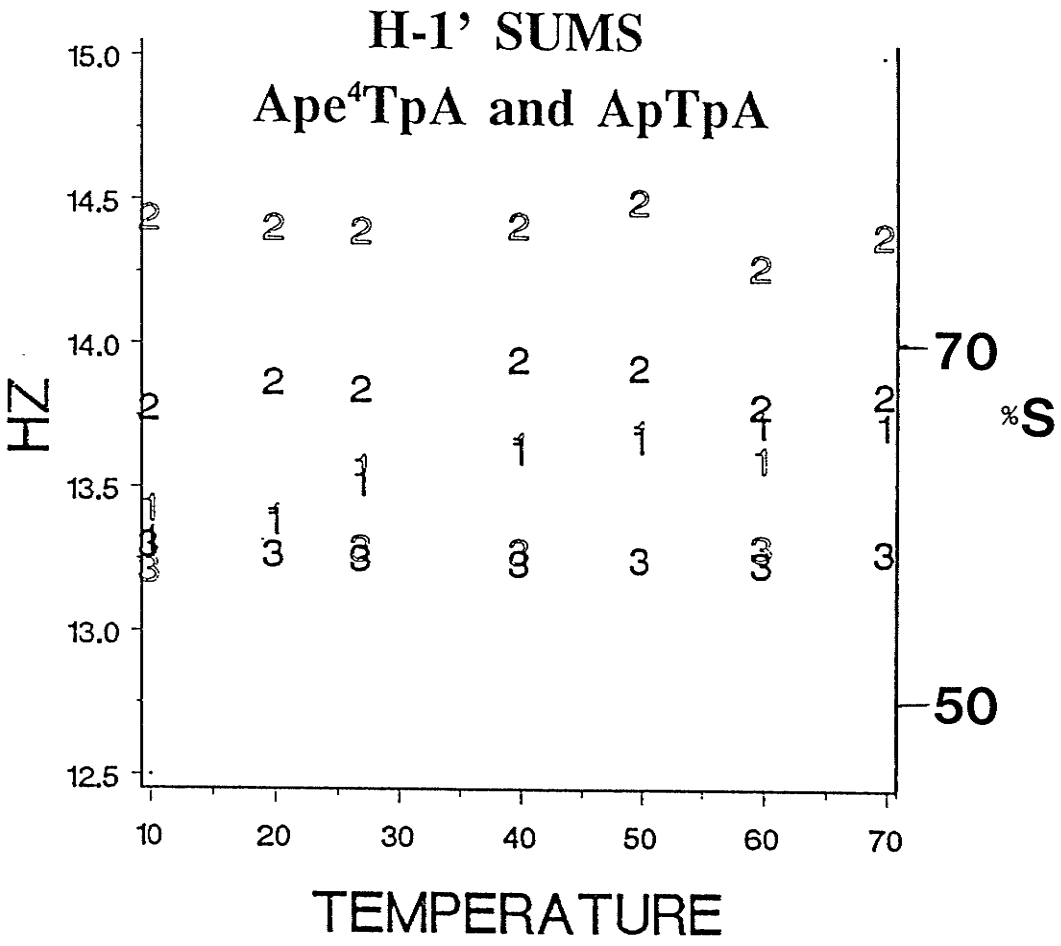

Figure 5.38: Temperature (C°) profiles of ΣI' in Hz for the Ap (1), pNp (2), and pA (3) sugars of d(ApNpA). Bold numbers: d(Ape⁴TpA), hollow numbers: d(ApTpA). The vertical axis at the right provides the %S (2'-endo) conformation of the sugar ring calculated according to equation I.

While the pNp sugar conformations do not vary with temperature, the H2' and H2" resonances do, which suggests that other aspects of the trimer conformation are changing with temperature. The H2" Δδ°s of the pNp units of the ***d(ApNpA)*** *trimers are identical, 0.11 ppm (Tables 3.20 and 3.21). The H2" profile of* pe^4Tp *is downfield relative to the profile of pTp (Figure 5.37) which is analogous to the positions of the H2" profiles of the monomers,* e^4dT *and* ***dT*** *(Figure 5.16). The pNp H2' Δδ°s are even larger than those for H2", at 0.15 and 0.18 ppm (Tables 3.30 and 3.21). These large upfield movements with decreasing temperature of the pNp H2' and H2" resonances suggest that there is an increase in base-stacking. Note that the pNp H2' Δδ°s of* ***d(ApNpA)*** *are smaller than the Np H2' Δδ°s of d(NpA) (0.32 - 0.35 ppm) but larger than the pN H2' Δδ°s of d(NpA) (0.03 - 0.05 ppm) which suggest that the base-base geometry of the dimers is not the same as the trimers.*

As mentioned, the conformation of the Ap and pA sugars of $d(Ape^4TpA)$ *is not influenced by* e^4T*, as observed in Figure 5.38, where the ΣI' profiles for Ap and pA vary less than 0.2 Hz from those of* ***d(ApTpA)***. *There is a small increase in the 3'*-endo *conformation of the Ap sugar of the* ***d(ApNpA)*** *trimers when the temperature is lowered that is reflected in their* $J_{1'\text{-}2'}$*s, which decrease 1.0 -1.1 Hz. On the other hand, the sugar conformation of the pA unit of the* ***d(ApNpA)*** *trimers is invariant to temperature, an observation reflected in their* $J_{1'\text{-}2'}$*s which remain constant. Note that the Ap sugar of the* ***d(ApNpA)*** *trimers and the Ap sugar of the* ***d(ApN)*** *dimers show an increase in the 3'*-endo *conformation with decreasing temperature. Additionally, the pA sugar of the* ***d(ApNpA)*** *trimers and the pA sugar of the* ***d(NpA)*** *dimers do not change conformation with temperature. Hence, it appears as if the temperature dependence of the conformation of the Ap and pA sugars of the* ***d(ApNpA)*** *trimers more closely follows those of their respective moieties in the* ***d(ApN)*** *and* ***d(NpA)*** *dimers, regardless of N, than the Tp and pT sugars of* ***d(TpNpT)*** *follows those of their respective moieties in the* ***d(TpN)*** *and* ***d(NpT)*** *dimers, which depend on N. This reflects sequence dependent differences in the effects of the O4-alkylation of thymine.*

*The H2' and H2" Δδ°s of the Ap and pA units of **d(ApNpA)** are all between -0.03 and 0.030 ppm (Table 3.20 and 3.21). A comparison of the Ap and pA H2' and H2" Δδ°s of **d(ApNpA)** to the corresponding values in the **d(ApN)** and **d(NpA)** dimers would be difficult to interpret because the Δδ°s are small and many factors influence them (Section 5.1.5.1).*

5.5.2 THE SUGAR-PHOSPHATE BACKBONE:

5.5.2.1 d(TpNpT): *An analysis of the γ and β populations of the **d(Tpr^{4}TpT)** trimers suggests that there are no major conformational changes dependent on the size of the O4-alkyl group (Table 5.4). Unfortunately, it is not possible to compare the rotamer populations of the **d(Tpr^{4}TpT)** trimers to **d(TpTpT)** at a high and low temperature because the data presented for **d(TpTpT)** in Table 3.16 is only at 30°C.*

*In all the units of the **d(Tpr^{4}TpT)** trimers the γ^+ state is most heavily populated and its population increases with decreasing temperature, an observation associated with base-stacking (Altona, 1982). The 5'-end of the **d(Tpr^{4}TpT)** trimers have the smallest γ^+ populations at low temperature, 58 - 60%, with the pr^{4}Tp and pT populations larger, 76 - 83%, as is typical of small DNA oligomers (Mellema* et al., *1984). The γ populations for **d(TpTpT)**, obtained at 30°C, follow the trends observed in the **d(Tpr^{4}TpT)** molecules.*

*In the three **d(Tpr^{4}TpT)** trimers, the β' populations increase 6 - 10% with decreasing temperature which is indicative of an increase in the population of base-stacked states (Altona, 1982). Furthermore, the β' populations of both the pr^{4}Tp and pT units are almost equally populated at low temperature, 83 - 86%, suggesting the size of the O4-alkyl group is not altering the sugar-phosphate backbone. The β' populations for d(TpTpT), obtained at 30°C, follows the trends observed in the **d(Tpr^{4}TpT)** trimers.*

*Carbon-13 spectra were obtained for **d(TpTpT)** and **d(Tpi^{4}TpT)** at 27°C and allow estimations of the ε' and ε⁻ populations. There is little change in ε' for the two Tp fragments, 80%, **d(TpTpT)** and 76%, **d(Tpi^{4}TpT)**. At first glance, there appears to be a difference in the ε' population of the pNp fragments, 89%, pTp, and 76%, pi^{4}Tp. However,*

Table 5.4. Furanose conformations and exocyclic bonds rotamer distributions for d(Xpr^{4}TpX)[a]

Molecule	%S	%γ^-	%γ^t	%γ^+	%β^t	%ε^t/%ε^-
Tp	68	11	33	56	---	80/23
pTp	75	2	19	79	79	89/22
pT	68	3	24	73	78	-------
Tp	51(64)	11(12)	28(35)	60(53)	-------	-------
pm^{4}Tp	51(64)	2(3)	16(26)	82(71)	86(77)	-------
pT	64(61)	0(5)	20(30)	79(65)	85(75)	-------
Tp	53(66)	10(12)	30(34)	60(54)	-------	-------
pe^{4}Tp	54(64)	-3(4)	20(24)	83(72)	86(76)	-------
pT	64(66)	0(5)	19(32)	80(62)	85(76)	-------
Tp	66(66)	11(12)	31(36)	58(52)	-------	76/16
pi^{4}Tp	53(63)	4(4)	19(28)	76(68)	84(78)	76/22
pT	64(64)	3(5)	19(28)	78(67)	83(73)	-------
Ap	61(66)	6(7)	21(29)	72(63)	-------	-------
pTp	81(78)	-6(1)	20(28)	85(70)	89(84)	-------
pA	56(58)	8(3)	17(30)	75(67)	---(86)	-------
Ap	61(68)	4(4)	23(29)	73(63)	-------	-------
pe^{4}Tp	69(69)	--(0)	---(28)	---(71)	---(81)	-------
pA	56(58)	-------	-------	-------	-------	-------

[a] %S calculated according to equation I, %γ according to equations II, III, and IV, %β according to equation V, and %ε according to equations VI and VII. Coupling constants used in these equations were taken from Tables 3.16 - 3.21 and 3.25. The first number is at 10°C, the number in brackets is at 60 (d(ApNpA)) or 70 (d(TpNpT)) °C. Populations for d(TpTpT) calculated with the Js from Rycyna *et al.* (1988) at 30°C.

note that the ε populations, calculated from $^3J_{P3'-C2'}$, are identical for both pTp and pi^{4}Tp, at 22%. Hence, the difference observed in ε' may be due to uncertainties in the pTp $^3J_{P3'-C4'}$ since this coupling is obtained from a relatively more congested part of the ^{13}C spectrum (Figure 3.26). Consequently, the pTp and pi^{4}Tp ε populations are likely very similar and this suggests, together with the γ and β data, that there are no major distortions in the sugar-phosphate backbone of d(Tpi^{4}TpT) relative to d(TpTpT), as observed for d(Tpi^{4}T) and d(i^{4}TpT) relative to d(TpT).

5.5.2.2 d(ApNpA): Js involving the C4' and C5' protons of d(Ape^{4}TpA) were only obtained at 10 and 60°C for the Ap unit and at 60°C for the pe^{4}Tp unit and hence, a full comparison to d(ApTpA) is not possible. From the data in Table 5.4 the γ $^+$ populations are observed to increase with decreasing temperature, consistent with an increase in the population of base-stacked states. For d(ApTpA), the nucleotide at the 5'-end has the smallest γ $^+$ population at low temperature, 72%, with the pTp unit highest, 85%, and the pT fragment intermediate, 75%. In comparing the available γ population data of d(Ape^{4}TpA) to d(ApTpA) it is observed that the conformer populations for the Ap and pe^{4}Tp units do not vary by more than 2% which suggests that e^{4}T is not altering the γ populations.

Phosphorus coupling constants to the C5' protons are only available for the pTp fragment of d(ApTpA) at low temperature. Therefore it is not possible to comment on any possible effects of O4-alkylation on the β' population of the d(ApNpA) trimers. However, for the pTp unit of d(ApTpA), the β' population is observed to increase with decreasing temperature which suggests that base-stacking is occurring (Altona, 1982).

5.5.3 THE BASE AND H1' δs:

5.5.3.1 The Me5 Profiles:

5.5.3.1.A d(TpNpT): The Me5 variable temperature profiles of the d(TpNpT) molecules are presented in Figure 5.39 where it can be seen that the Me5 profiles of the d(Tpr^{4}TpT)

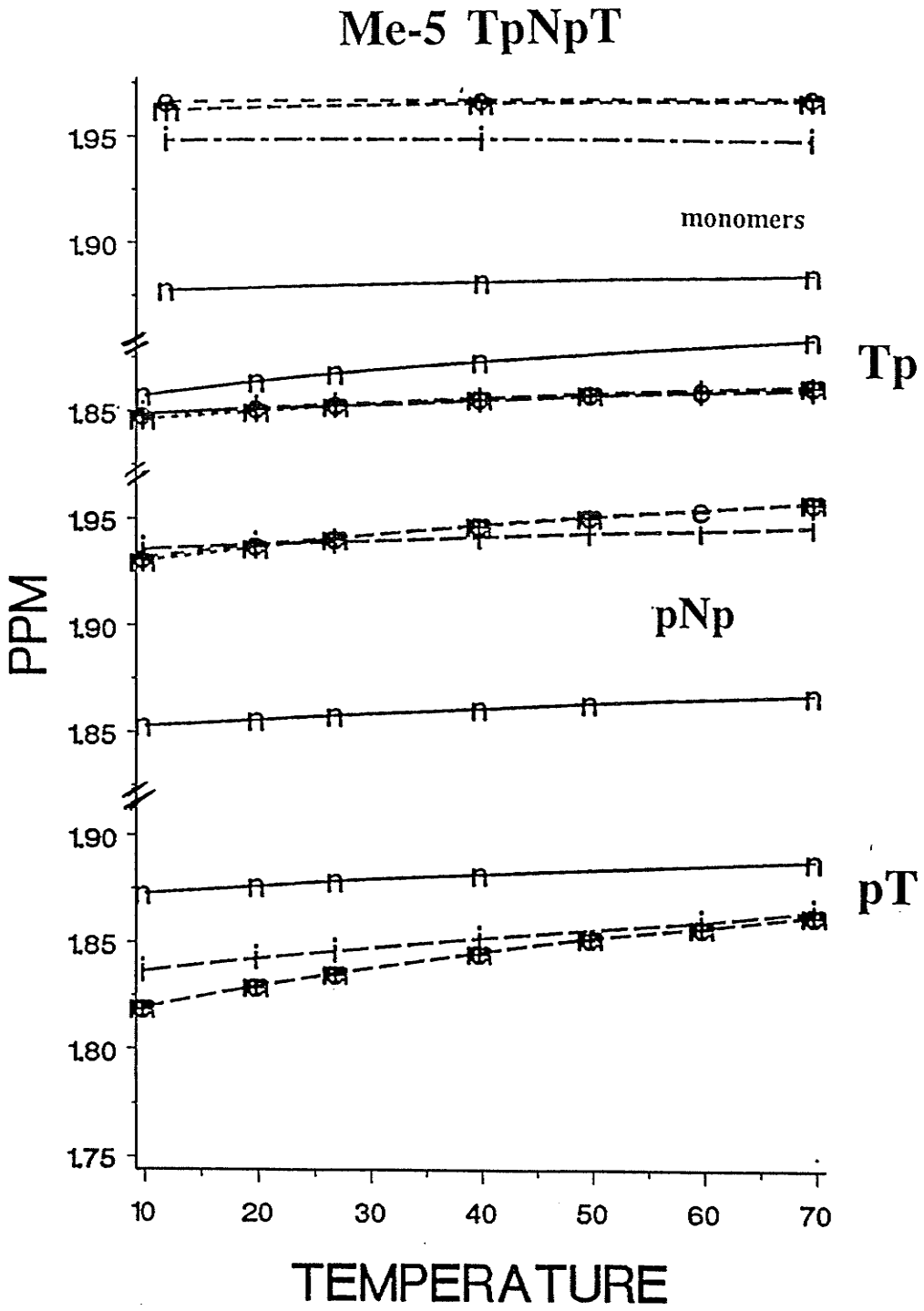

Figure 5.39: Temperature (C°) profiles of the chemical shifts (δ) of the Tp, pNp, and pT Me5 base protons of the d(TpNpT) trimers with N equal to T (n), m^4T (m), e^4T (e), and i^4T (i). Also included at the top of the plot are the Me5 profiles for the monomers dT (n), m^4dT (m), e^4dT (e) and i^4dT (i).

trimers do not depend on the size of the O4-alkyl group. Note that the Tp and pT Me5 profiles with N equal to r⁴T are upfield relative to those with N equal to T, probably reflecting the larger ring current effects of r⁴T relative to T. On the other hand, the Me5 profiles of the pr⁴Tp fragments are downfield relative to that of pTp, with the difference almost equivalent to that observed between ***r⁴dT*** *and* ***dT****, due to the altered electronic configuration of T brought about by O4-alkylation (Birnbaum* et al., *1988).*

The Δδ° for the Me5s of the ***d(Tpr⁴TpT)*** *trimers are small and therefore, suggest that little base-stacking is occurring in these molecules: pT (0.03 - 0.04 ppm) > pr⁴Tp (0.01 - 0.03 ppm) > Tp (0.01 ppm) with the Δδ°s for the isopropylated trimer at the low end of each range (Table 3.17 - 3.19). The slightly larger Me5 Δδ°s for the pr⁴Tp and pT units relative to the Tp units are consistent with a right handed/*χ-anti *stack where the Tp Me5 of these trimers are not over any base while the pr⁴Tp and pT Me5s are, and therefore, experience additional shielding.*

5.5.3.1.B d(ApNpA): The pNp Me variable temperature profiles of ***d(ApTpA)*** *and* ***d(Ape⁴TpA)*** *are compared with those of* ***d(TpTpT)*** *and* ***d(Tpe⁴TpT)*** *and the monomers* ***e⁴dT*** *and* ***dT*** *in Figure 5.40. The pNp Me5 profiles of the* ***d(ApNpA)*** *trimers move upfield with decreasing temperature to a greater extent (0.10 - 0.11 ppm) than those for the* ***d(TpNpT)*** *trimers (0.02 - 0.03 ppm) or the monomers (< 0.01 ppm) which implies that the pNp base of the* ***d(ApNpA)*** *trimers is stacking in between the two As and is not looped out as reported for some PU-PY-PU ribonucleotide trimers (Lee and Tinoco, 1980). The stacked orientation of the pNp unit within the* ***d(ApNpA)*** *trimers is supported by the α-methylene profiles of the O4-ethyl group of* ***d(Ape⁴TpA)****, to be discussed shortly, which are upfield of those for* ***e⁴dT*** *and the* ***d(Ape⁴T)*** *and* ***d(e⁴TpA)*** *dimers (Figure 5.31). Note that the separation of the pTp and pe⁴Tp Me5 profiles of the* ***d(TpNpT)*** *trimers in Figure 5.40 is similar to that of the monomers,* ***e⁴dT*** *and* ***dT****, presumably because of the different electronic ring conjugation of e⁴T and T (Birnbaum* et al., *1988). However, the separation between pTp and pe⁴Tp Me5*

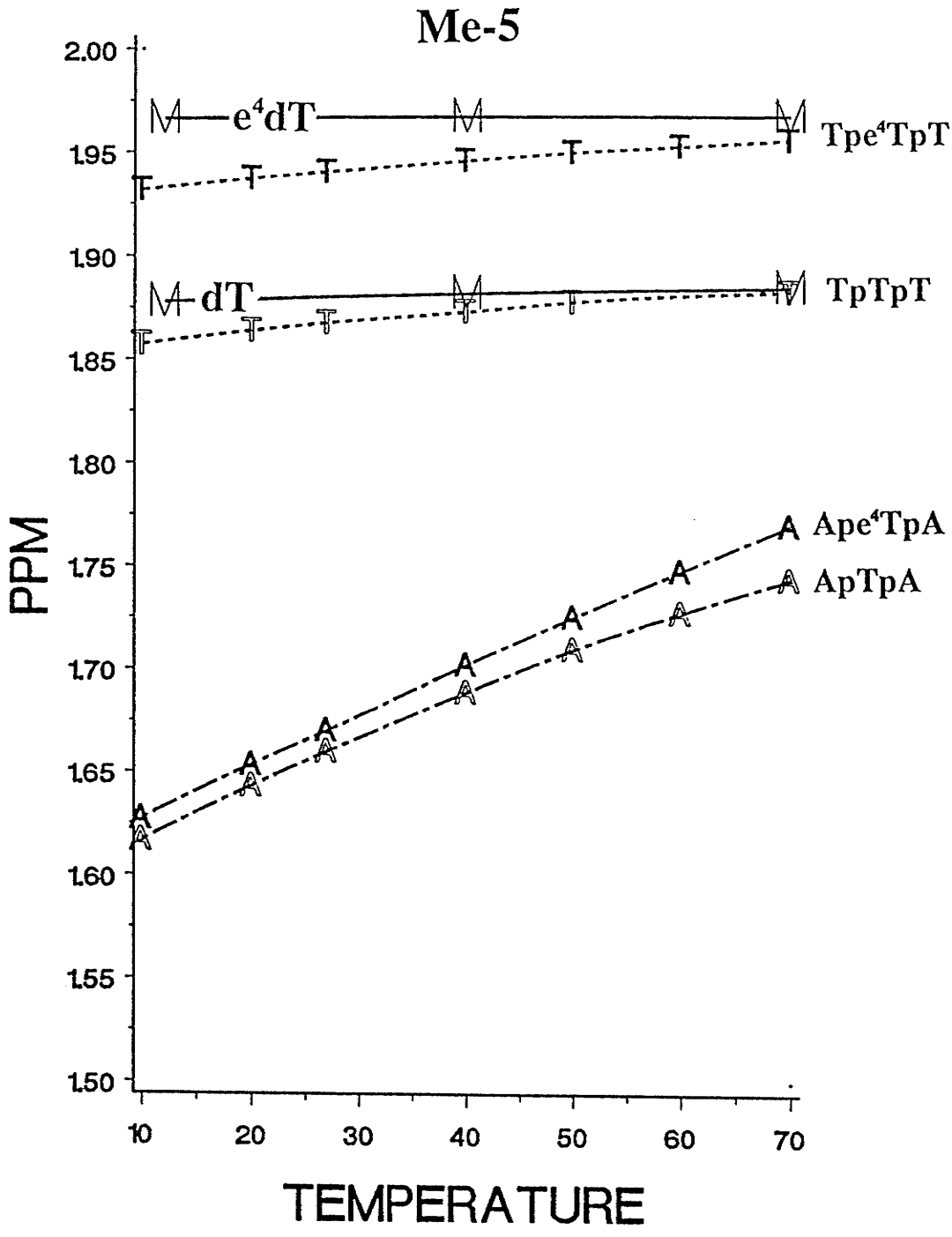

Figure 5.40: Temperature (C°) profiles of the chemical shifts (δ) of the pNp Me5 base protons of d(TpNpT) (T) and d(ApNpA) (A). Bold letters: N = e⁴T, hollow letters: N = T. Also included are the Me5 profiles of the monomers (M) e⁴dT and dT.

profiles of the d(ApNpA) trimers are unlike those of the monomers (e⁴dT and dT) and the d(TpNpT) trimers, with the Me5 profile of pe⁴Tp almost "catching" the profile of pTp at 10°C. This observation in the pNp Me5 profiles of the d(ApNpA) trimers most likely results from a different amount of base-stacking in d(Ape⁴TpA) relative to d(ApTpA) or slightly different base-stacking geometries in the two trimers.

5.5.3.2 The O4-Alkyl Group:

5.5.3.2.A d(Tpm⁴TpT): Figure 5.8 contains the variable temperature profiles of the O4-methyl group of m⁴dT, d(m⁴TpT), and d(Tpm⁴TpT). Unlike the other O4-alkyl groups, there should be no preference for any of the three possible staggered conformations about O4-C_α. Since a single resonance is observed for the O4-methyl group of m⁴dT, d(m⁴TpT), and d(Tpm⁴TpT) at all temperatures, interchange between the three staggered conformations must also be rapid on the NMR time scale. Because the O4-methyl profiles of m⁴dT, d(m⁴TpT), and d(Tpm⁴TpT) are almost coincident and their Δδ°s are identical, the average effect of the neighbouring base(s) is very weak. However, these very weak ring current effects do show up in the α-methylene profiles of the O4-ethyl, -propyl, -butyl, and -isobutyl groups and the methyl profiles of the O4-isopropyl group, which suggests that these latter resonances are highly sensitive monitors of base-stacking (Buchko, et al., *1987).*

5.5.3.2.B d(Tpe⁴TpT) and d(Ape⁴TpA): The α-methylene resonances of the O4-ethyl group of d(Tpe⁴TpT) are plotted as a function of temperature in Figure 5.41. In comparison to the same resonances in d(e⁴TpT) and d(Tpe⁴T) (Figure 5.30) the d(Tpe⁴TpT) α-methylene profiles more closely resemble those of d(Tpe⁴T). Furthermore, the α-methylene Δδ is smaller for the trimer at 10°C (0.023 ppm) than for either of the d(e⁴TpT) and d(Tpe⁴T) dimers (0.028 and 0.033 ppm, respectively, 20°C).

The α-methylene profiles of d(Ape⁴TpA), d(Ape⁴T), and d(e⁴TpA) are compared in Figure 5.31 where the profiles of d(Ape⁴TpA) are clearly upfield of those of d(Ape⁴T) and d(e⁴TpA). Note that at high temperature, the α-methylene Δδ for d(Ape⁴TpA) is 0.015 ppm,

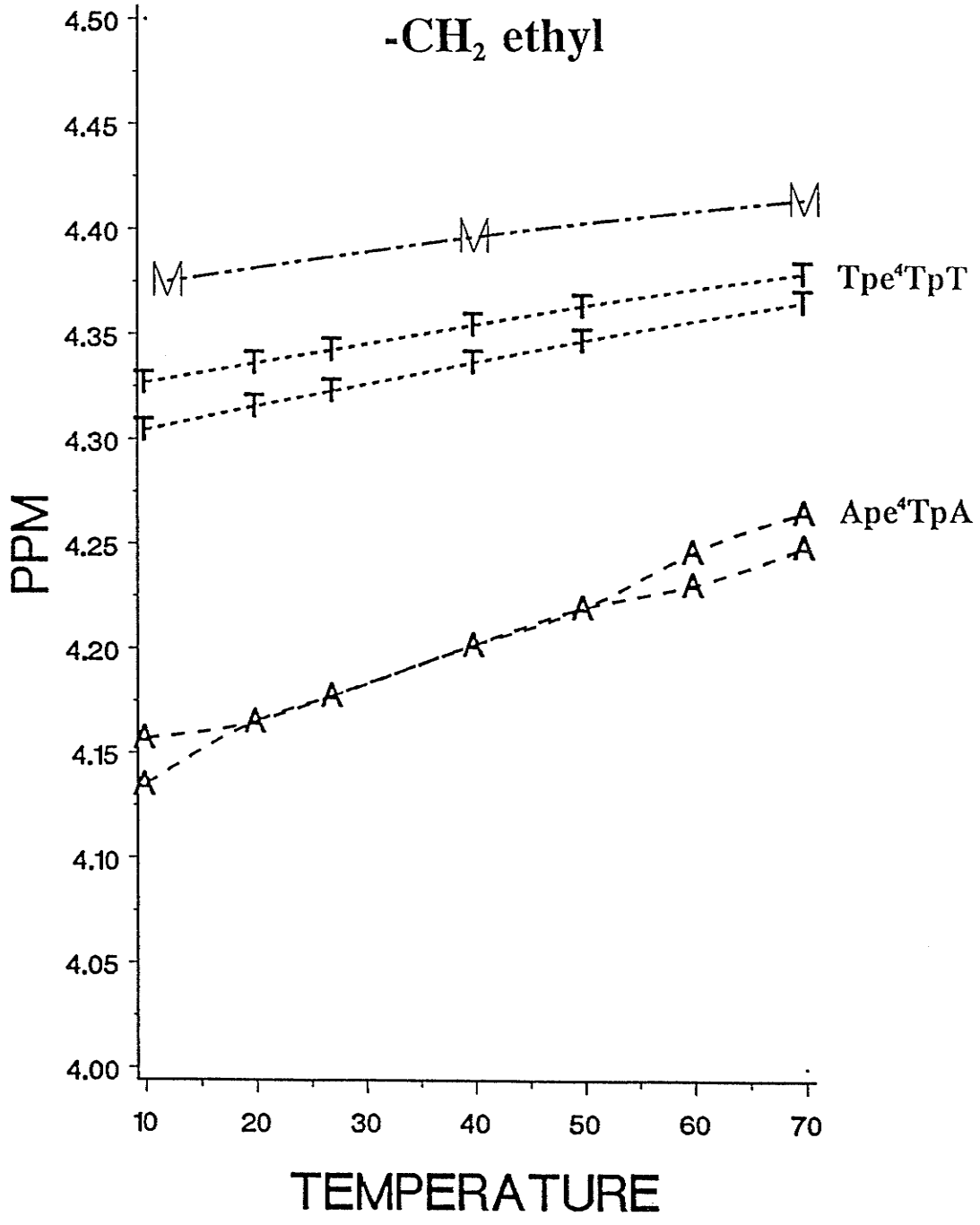

Figure 5.41: Temperature (C°) profiles of the chemical shifts (δ) of the O4-ethyl α-methylene protons of d(Tpe⁴TpT) (T) and d(Ape⁴TpA) (A). Also included is the α-methylene protons profile of the O4-ethyl group of the monomer (M) e⁴dT.

at 50°C it goes to zero and it remains there until 10°C, where it increases to 0.021 ppm, with the upfield resonance at high temperature apparently becoming the downfield resonance at 10°C. The magnetic equivalence of the α-methylene protons between 20 to 50°C mean that the sum of the influences on the O4-C_α region of e^4T are equal for both of these protons over this temperature range. If two principal states exist for the trimers, fully stacked and unstacked, then the observed α-methylene Δδ at 10°C is likely due to an increase in the population of stacked states and magnetically non-equivalent environments of the α-methylene protons in the stacked state for otherwise an increase in Δδ should not be observed at low temperature.

*The α-methylene profiles of the **d(Xpe⁴TpX)** trimers are not the sum of the α-methylene profiles of the **d(Xpe⁴T)** and **d(e⁴TpX)** dimers and there are at least two possible explanations for this. First, the chemical shift non-equivalence of the α-methylene resonances of **d(e⁴TpX)** and **d(Xpe⁴T)** were attributed to these protons straddling its base (Figure 5.4A) and feeling different ring current effects from the neighbouring base. The straddling orientation does not mean that these α-methylene protons are an equal distance away from the plane of its own base, at a 60° angle. Perhaps the adjacent nucleotide induces a skew in the straddle which twists one proton closer to its own base while the other is sent further away. If there is such a skewing by the neighbouring base, the effects on e^4T will depend on the location of the neighbouring base (5' or 3') and the type of base (A, G, C, or T). Such a skewing would make it more difficult to compare the profiles of the α-methylene resonances of the **d(e⁴TpX)** and **d(Xpe⁴T)** molecules and conversely, to compare the profiles of these dimers to the **d(Xpe⁴TpX)** trimers, because a different skew would place protons in different magnetic environments where they would feel different ring current effects. Second, the addition of pX to the 3'-end of **d(Xpe⁴T)** or a Xp to the 5'-end of **d(e⁴TpX)** will probably alter the base-stacking geometry of the original dimer and hence, comparison of the trimers to the dimers will be hampered.*

The variable temperature profiles of the methyl group of the O4-ethyl function of ***d(Tpe^{4}TpT)*** *and* ***d(Ape^{4}TpA)*** *are compared to those of their respective* ***d(e^{4}TpX)*** *and* ***d(Xpe^{4}T)*** *dimers and the* ***e^{4}dT*** *monomer in Figure 5.32. In these cases, relative to* ***e^{4}dT****, the profiles of the methyl group of the O4-ethyl function of both trimers are close to the sum of the profiles of their respective* ***d(e^{4}TpX)*** *and* ***d(Xpe^{4}T)*** *dimers. However, except for the monomers, these profiles all move downfield with decreasing temperature which suggests this group is projected away from the adjacent base(s) in the stacked state.*

5.5.3.3.C ***d(Tpi^{4}TpT)****: The methyl resonances of the O4-isopropyl group of* ***d(Tpi^{4}TpT)*** *are plotted as a function of temperature in Figure 5.10. There is no detectable magnetic non-equivalence of the methyl resonances of the O4-isopropyl function of* ***d(Tpi^{4}TpT)****; they are like those of* ***i^{4}dT****. In the* ***d(i^{4}TpT)*** *and* ***d(Tpi^{4}T)*** *dimers the methyl* $\Delta\delta$ *of the O4-isopropyl group was postulated to arise from a preference of the O4-isopropyl group to adopt conformation D or E in Figure 5.4 when in a stacked state. However, in the* ***d(Tpi^{4}TpT)*** *trimer, there may not be a strong preference for the O4-isopropyl group to adopt either of conformations D or E and hence, the observed O4-isopropyl methyl profiles of* ***d(Tpi^{4}TpT)*** *are the average of these two possible O4-isopropyl conformations, whose net effect on the O4-isopropyl methyl* δ*s is nearly identical. It is nearly identical because the* ^{13}C *spectrum at 27°C reveals a small magnetic non-equivalence between the methyl carbons of the O4-isopropyl group (0.02 ppm) (Figure 3.26) and hence, there probably is a magnetic non-equivalence between the protons of these methyl groups that is hidden within the* ^1H *NMR linewidths.*

The methine resonance of the O4-isopropyl function moves upfield almost 0.05 ppm with decreasing temperature (Table 3.19) which suggests that some base-stacking is occurring in ***d(Tpi^{4}TpT)****. Furthermore, the methine isopropyl profile of* ***d(Tpi^{4}TpT)*** *is upfield of those of the* ***d(i^{4}TpT)*** *and* ***d(Tpi^{4}T)*** *dimers (Figure 5.25) which is in line with a stacked state involving all three bases of* ***d(Tpi^{4}TpT)****.*

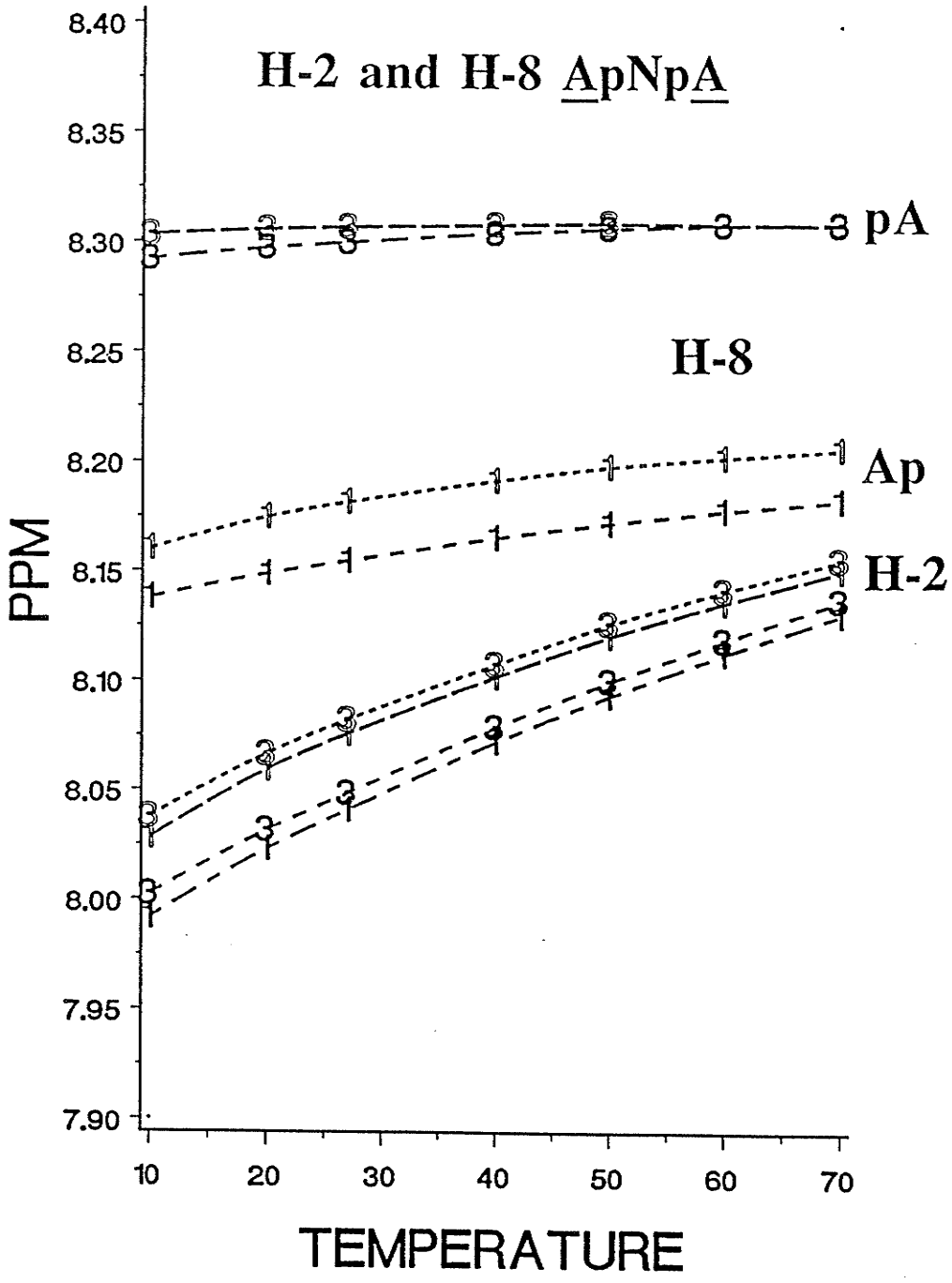

Figure 5.42: Temperature (C°) profiles of the chemical shifts (δ) of the Ap (1) and pA (3) H2 and H8 base protons of d(ApNpA). Bold numbers: N = e'T, hollow numbers: N = T.

5.5.3.4 The H2 and H8 Profiles: The H2 and H8 variable temperature profiles of the d(ApNpA) oligomers are presented in Figure 5.42. The upfield movement with decreasing temperature of all the H2 resonances (0.09 - 0.11 ppm) indicate that the adenines are involved in base-stacking. The H2 profiles of the trimers are upfield of those of both dimers, d(ApN) and d(NpA) (Table 3.12 and 3.14), which may be due to different base-stacking geometries in the trimer, more base-stacking in the trimers, or some next nearest neighbour ring current effects. On the other hand, none of the H8 resonances of d(ApNpA) are significantly altered by temperature, as observed in the d(ApN) and d(NpA) dimers. Note that most of the H8 and H2 profiles of d(Ape^{4}TpA) are upfield of the corresponding profiles of d(ApTpA) probably because of the larger ring currents effects of e^{4}T relative to T. The only exception are the H8 profiles of the pA unit which are both identical.

5.5.3.5 The H1' and H6 Profiles: Figures 5.43 and 5.44 contain the variable temperature profiles of all the H1' and H6 resonances, respectively, of the d(TpNpT) trimers. The methylated and ethylated d(Tpr^{4}TpT) trimer H1' and H6 profiles are all practically identical with small differences in some of the analogous isopropylated trimer profiles. Perhaps the small differences in the d(Tpi^{4}TpT) H1' and H6 profiles relative to those of the d(Tpe^{4}TpT) and d(Tpm^{4}TpT) trimers are related to the sugar conformational differences noted between these molecules (Section 5.1.1.1).

The d(TpNpT) trimer H1' resonances vary only slightly with temperature and those that vary least are for the pT unit, possibly because in a right handed/χ-anti *stack these H1's do not have a base over them.*

The d(TpNpT) trimer H6 resonances all move downfield with decreasing temperature with the largest $\Delta\delta$*'s for the Tp units of the d(Tpr^{4}TpT) molecules. The behaviour of the pT H6 profiles of these trimers are almost identical to those of the pT unit of the d(NpT) dimers (Figure 5.13). Also, the behaviour of the Tp H6 profiles of these trimers are identical to those of the Tp unit of the d(TpN) dimers (Tables 3.2 and 3.4). These observations might*

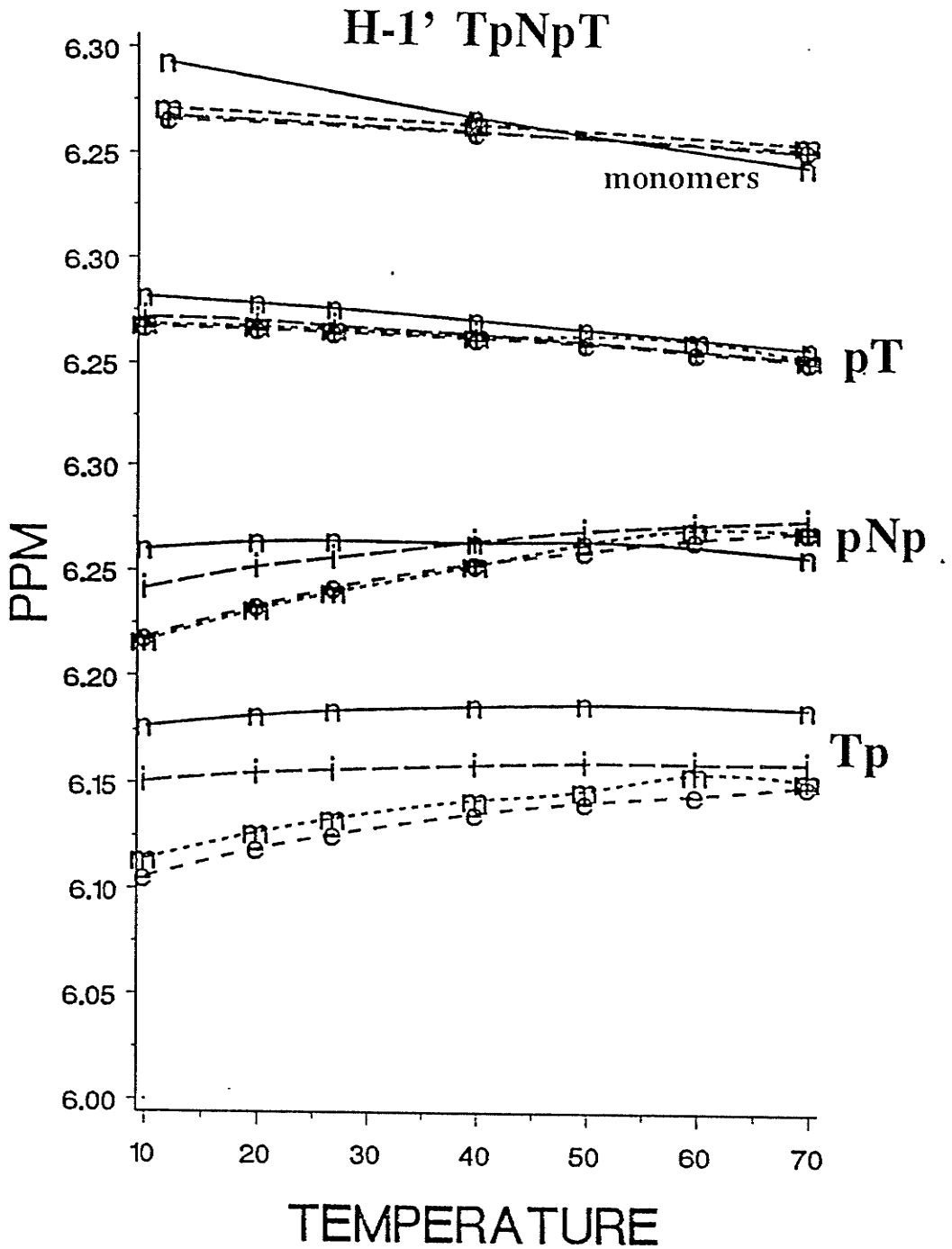

Figure 5.43: Temperature (C°) profiles of the chemical shifts (δ) of the Tp, pNp, and pT H1' sugar protons of the d(TpNpT) trimers with N equal to T (n), m⁴T (m), e⁴T (e), and i⁴T (i). Also included at the top of the plot are the H1' profiles for the monomers dT (n), m⁴dT (m), e⁴dT (e) and i⁴dT (i).

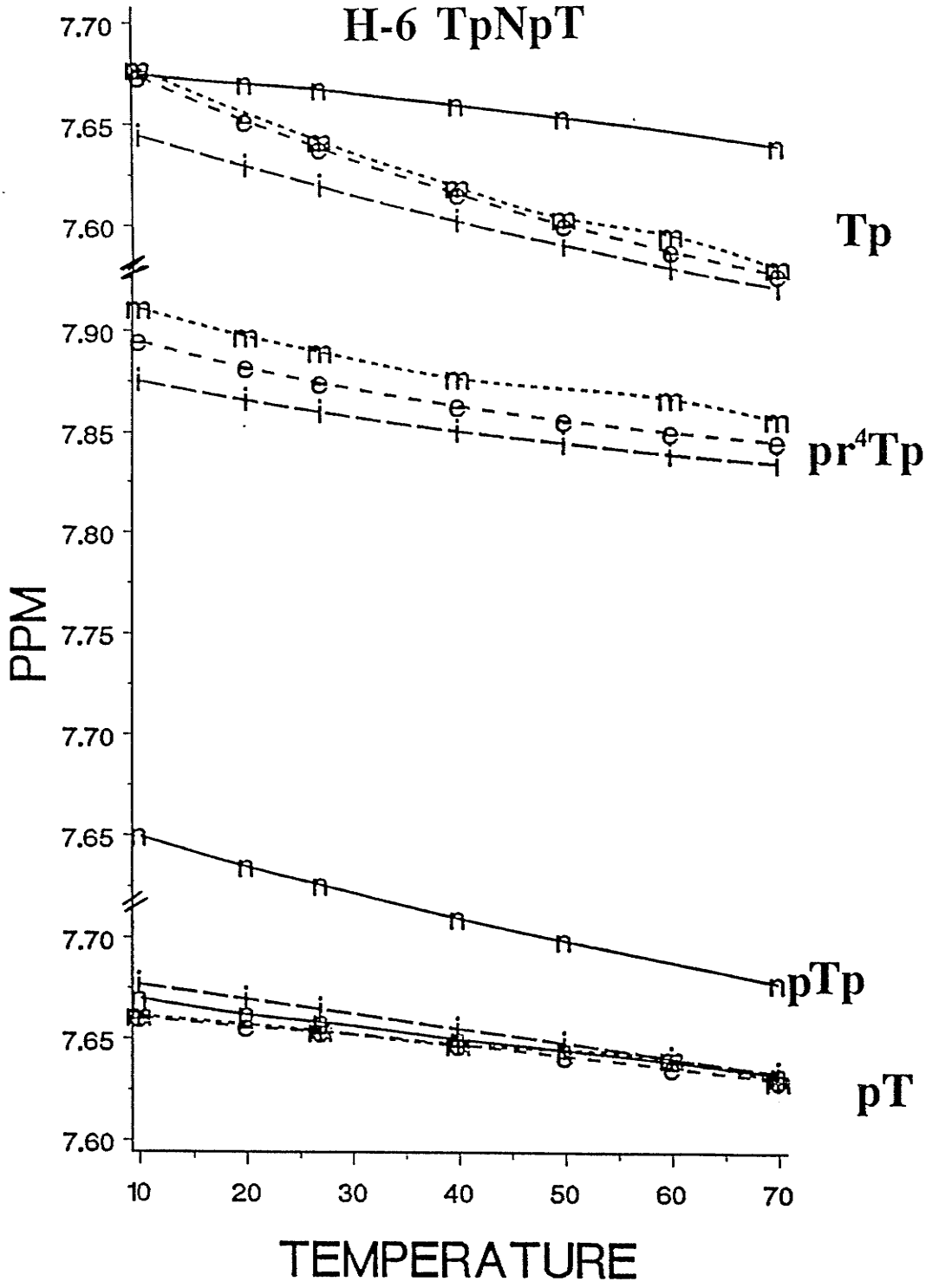

Figure 5.44: Temperature (C°) profiles of the chemical shifts (δ) of the Tp, pNp, and pT H6 base protons of the d(TpNpT) trimers with N equal to T (n), m⁴T (m), e⁴T (e), and i⁴T (i).

be expected because neither the ***d(TpN)*** *and* ***d(NpT)*** *dimers, nor these trimers, stack significantly with decreasing temperature. Note that the H6 profile of the pTp unit is upfield of those of the pr⁴Tp units to an extent seen in the* ***r⁴dT*** *and* ***dT*** *monomers, presumably due to the altered electronic conjugation of e⁴T relative to T.*

The H6 variable temperature profiles for the pNp unit of ***d(TpTpT)***, ***d(Tpe⁴TpT)***, ***d(ApTpA)***, *and* ***d(Ape⁴TpA)*** *are compared in Figure 5.45. The pNp H6 resonances of* ***d(TpNpT)*** *move downfield with decreasing temperature while those of* ***d(ApNpA)*** *move upfield. A likely cause for these observations are the larger ring current effects of two As relative to two Ts and more base-stacking in the* ***d(ApNpA)*** *trimers.*

The variable temperature profiles of the H1' resonances of ***d(ApNpA)*** *are presented in Figure 5.46. The pA and Ap H1' resonances of the two trimers move upfield almost equally with decreasing temperature, between 0.04 - 0.06 ppm, while the pNp H1' resonances move upfield approximately 0.09 ppm (Tables 3.20 and 3.21). The largest H1' Δδ° for the pNp unit would be expected in a right handed/*χ-anti *stack since this H1' is over the base of the pA unit. The similar sizes of the Ap and pA H1' Δδ° are more difficult to rationalize. This is because in a right handed/*χ-anti *stack the H1' Δδ° is expected to be smaller for the pA unit, with no base on its 3'-side, than for the Ap unit, with a base on its 3'-side. However, H1' δs are typically difficult to interpret because of the greater number of influences on them (Section 5.1.5.1). Note that changing the pNp base from T to e⁴T alters the positions of the Ap H1' profiles, moving the e⁴T influenced profile approximately 0.06 ppm upfield relative to the T influenced profile, presumably due to the greater shielding influences of e⁴T relative to T. Conversely, the larger shielding influences of e⁴T relative to T is only weakly apparent at low temperature for the pA H1' profiles, which suggests that the ring currents of the pNp base is having a small influence on the pA H1' profiles, as is expected in a right handed/*χ-anti *stack because the neighbouring base is not over the pA H1'.*

5.5.4 SUMMARY:

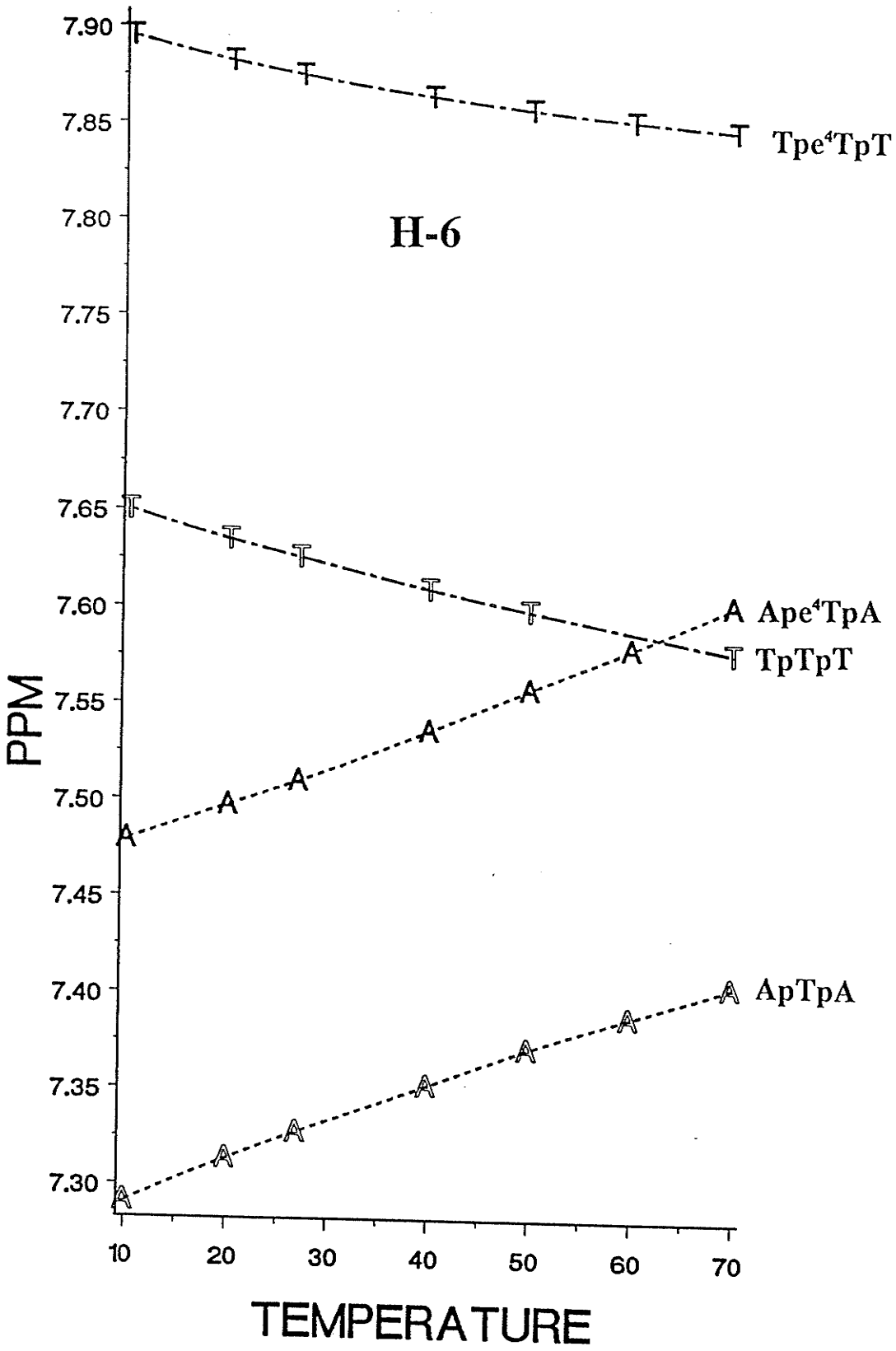

Figure 5.45: Temperature (C°) profiles of the chemical shifts (δ) of the pNp Me5 base protons of d(TpNpT) (T) and d(ApNpA) (A). Bold letters: N = e⁴T, hollow letters: N = T.

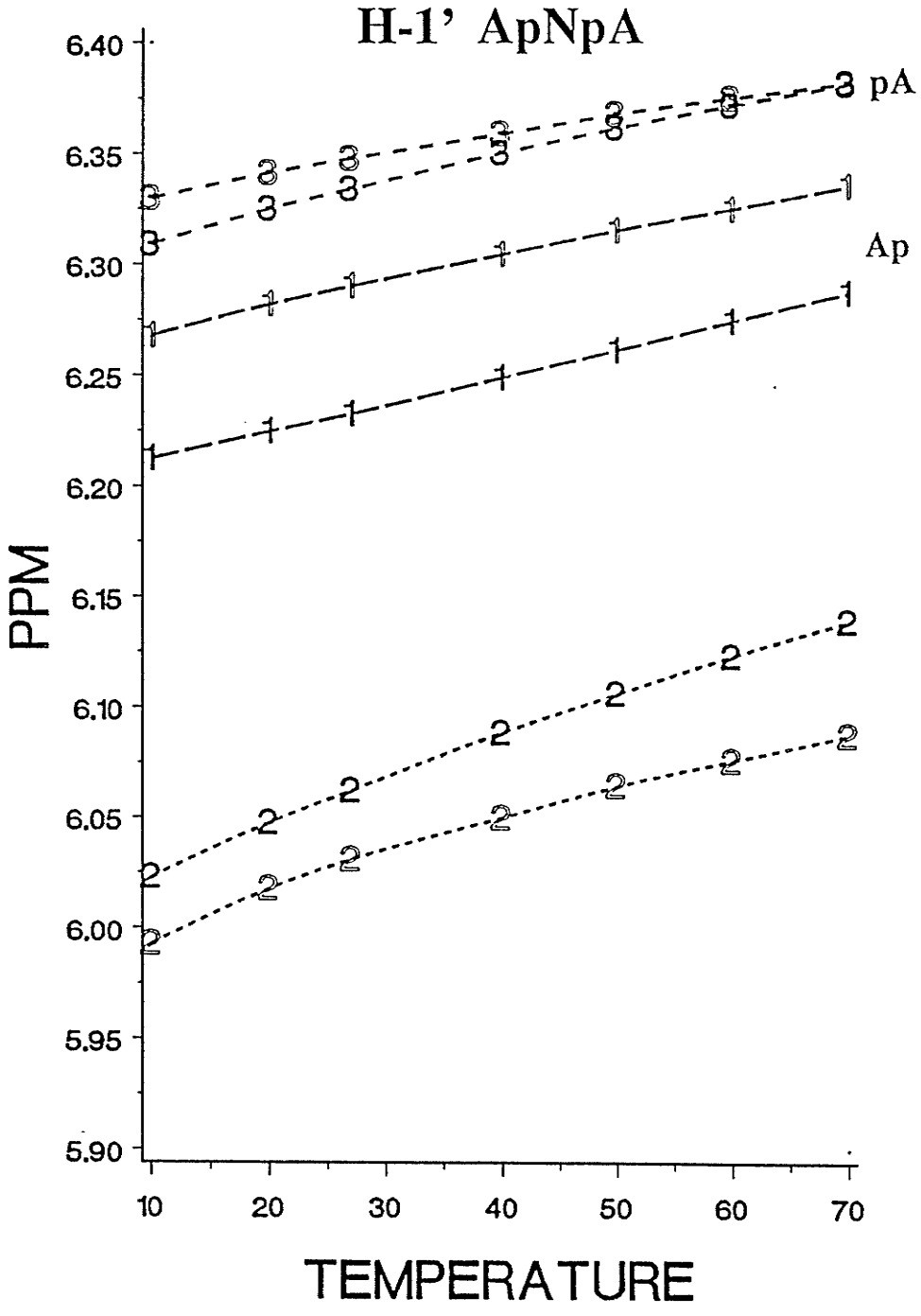

Figure 5.46: Temperature (C°) profiles of the chemical shifts (δ) of the Ap (1), pNp (2), and pA (3) H1' sugars protons of d(ApNpA). Bold numbers: N = e^4T, hollow numbers: N = T.

The ^1H NMR data suggests that the ***d(ApNpA)*** *and* ***d(TpNpT)*** *trimers stack with decreasing temperature, with considerable more stacking in the former set of trimers. The pyrimidine of the pNp unit is not looped out as confirmed by the proton profiles of the O-alkyl groups. The major conformational change due to O4-alkylation appears to be in the sugar pucker of the alkylated nucleotide, where larger 3'*endo *populations are observed relative to the non-alkylated nucleotide. The N populations of the* ***pr^{4}Tp*** *sugars increase with decreasing temperature for the* ***d(Tpr^{4}TpT)*** *trimers while it remains constant in* ***d(Ape^{4}TpA)****. Furthermore, the sugar conformations of the nucleotidyl neighbours of* ***e^{4}dT*** *are influenced slightly in* ***d(Tpr^{4}TpT)*** *but not in* ***d(Ape^{4}TpA)****. Together these last two observations suggests some sequence dependent O4-alkylation effects. Otherwise, it seems as if* ***r^{4}T*** *does not alter the conformation of the* ***d(Tpr^{4}TpT)*** *and* ***d(Ape^{4}TpA)*** *trimers relative to their non-alkylated analogues to any great extent with the possible exception of more base-stacking in* ***d(Ape^{4}TpA)*** *relative to* ***d(ApTpA)****. With respect to the effects of the size of the O4-alkyl group on the conformation of the* ***d(Tpr^{4}TpT)*** *trimers, there appears to be no difference between the methylated and ethylated molecules with minor differences in the isopropylated trimer.*

5.6 TETRAMERS:

The tetramers d(e⁴TpApe⁴TpA), d(e⁴TpApTpA), and d(TpApe⁴TpA) were synthesised and compared to each other and the non-alkylated tetramer d(TpApTpA), the latter of which has been characterized by Mellema et al. *(1984). Spectra were obtained at 500 MHz for d(e⁴TpApe⁴TpA) at 30, 55, and 70°C. Unfortunately, even at 500 MHz, the computer simulation of the d(e⁴TpApe⁴TpA) spectra was difficult due to the degree of resonance overlap, as exemplified by the number of blank spots in Tables 3.22 and 3.23. Hence, without access to larger amounts of 500 MHz spectrometer time, only the base and H1' protons of our three tetramers were studied.*

5.6.1 SUGAR CONFORMATIONS:

5.6.1.1 The pA and pAp Sugars: *The sugar conformations of the three tetramers can only be compared to each other via Σ1' variable temperature profiles because of the lack of computer simulated J data. Figure 5.47 contains such Σ1' profiles of the pA and pAp sugars of the three tetramers where it is observed that the pA Σ1's are generally smaller than those of the pAp unit which indicates a smaller* 2'-endo *population for the pA sugars. The approximate %S population of the pA sugar of the tetramers at low temperature is 55%, which is near the values observed for the pA unit of d(ApNpA) (56%) and d(NpA) (58%). On the other hand, at 10°C, the %S population of the pAp sugar of the tetramers is approximately 70%. Using the Σ1's from Mellema* et al. *(1984) and equation I a value of 78% S (8°C) is obtained for the pAp sugar of d(TpApTpA) which is quite close to the values observed for our tetramers, especially since the solvent conditions are different and our tetramers contain at least one e⁴T.*

5.6.1.2 The Np and pNp Sugars:

5.6.1.2.A d(e⁴TpApe⁴TpA) and d(TpApe⁴TpA): *Figure 5.48 contains the variable temperature Σ1' profiles for these Np and pNp sugars. The Tp sugar of d(TpApe⁴TpA) is moving towards* 2'-endo *with decreasing temperature (≅ 80% at 10°C) while the e⁴Tp sugar of*

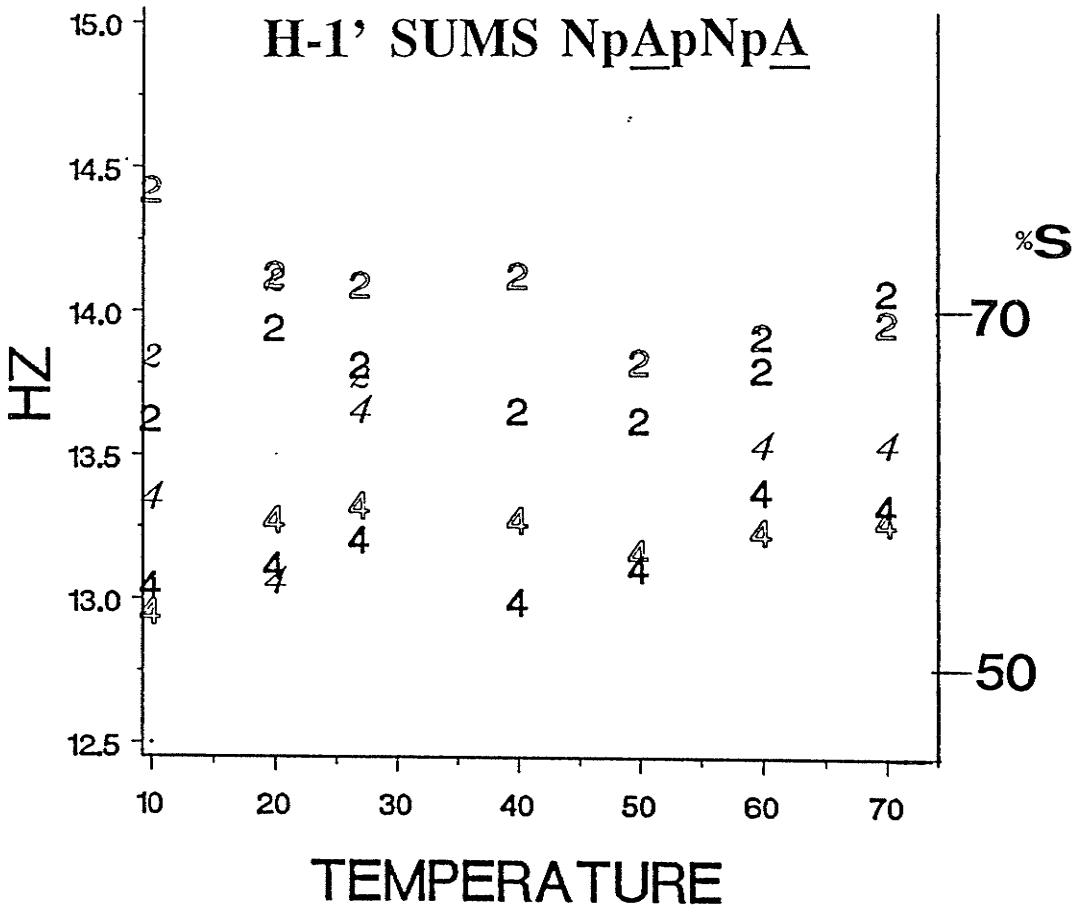

Figure 5.47: Temperature (C°) profiles of Σ1' in Hz for the pAp (2) and pA (4) sugars of the d(NpApNpA) tetramers. Bold numbers: d(e⁴TpApe⁴TpA), hollow numbers: d(TpApe⁴TpA), italic numbers: d(e⁴TpApTpA). The vertical axis at the right provides the %S (2'-endo) conformation of the sugar ring calculated according to equation I.

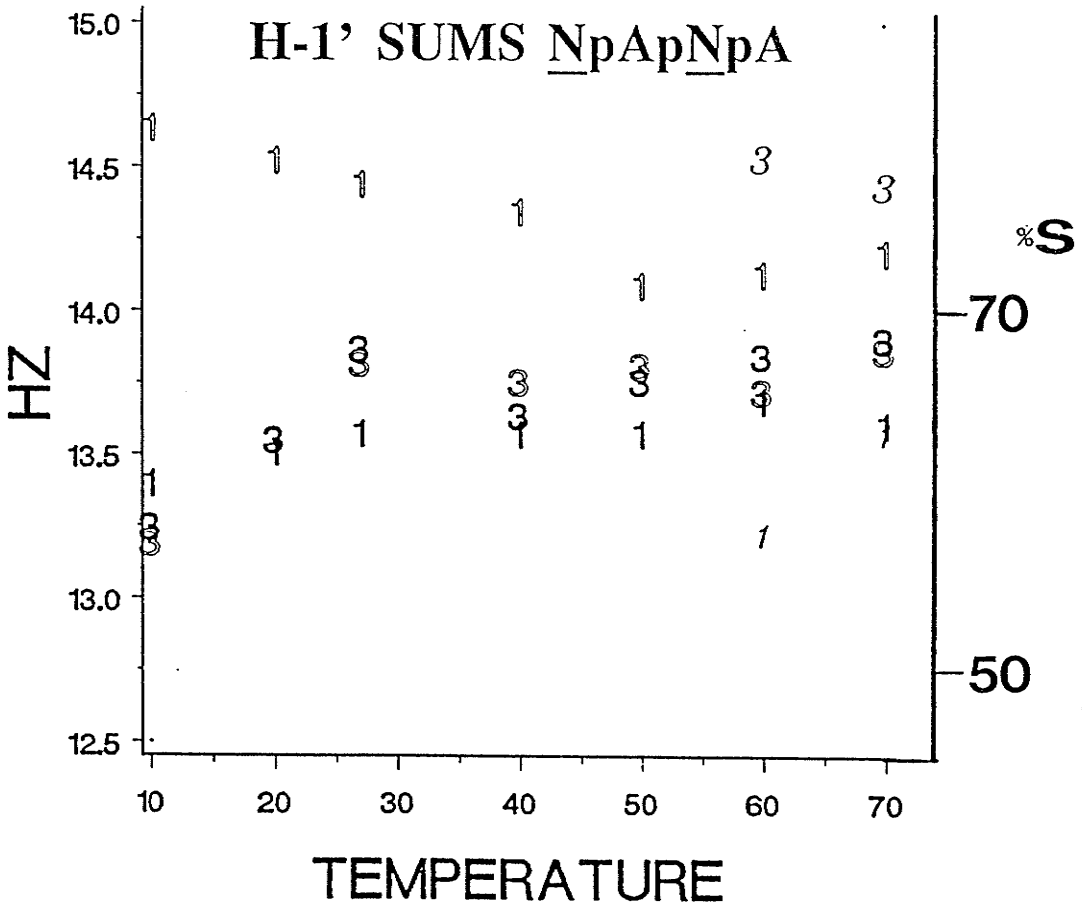

Figure 5.48: Temperature (C°) profiles of ΣI' in Hz for the Np (1) and pNp (3) sugars of the d(NpApNpA) tetramers. Bold numbers: d(e⁴TpApe⁴TpA), hollow numbers: d(TpApe⁴TpA), italic numbers: d(e⁴TpApTpA). The vertical axis at the right provides the %S (2'-endo) conformation of the sugar ring calculated according to equation I.

d(e⁴TpApe⁴TpA) is moving towards 3'-endo (≃ *60% S at 10°C). A small 3'*-endo *shift with decreasing temperature is also observed for the pe⁴Tp sugars of d(e⁴TpApe⁴TpA) and d(TpApe⁴TpA) where the %S populations are approximately 60% at low temperature, which are lower than the 69% S population reported for the pe⁴Tp sugar of d(Ape⁴TpA) (Table 5.4) and may reflect more base-stacking in the larger oligomers. Note that the presence of e⁴dT at the 5'-end, as opposed to dT, does not appear to influence the conformation of the third pe⁴Tp sugar. While these are the only sequences where the effect of e⁴dT on the next nearest sugar conformation can be studied, it appears that the conformation of the third sugar is not affected that far away from the site of alkylation.*

5.6.1.2.B d(e⁴TpApTpA): Reliable Σ1' for the e⁴Tp and pTp sugars of d(e⁴TpApTpA) were only obtained at 60 and 70°C and therefore, a detailed discussion of their conformations is not possible. However, on the basis of trends observed for the Σ1's of d(e⁴TpApe⁴TpA), d(TpApe⁴TpA), and d(ApTpA), the few Σ1' values for d(e⁴TpApTpA) appear to adhere to a pattern. The %S population of the pTp sugar of d(e⁴TpApTpA) is approximately the same as that of the pTp sugar of d(ApTpA), at 78% (70°C). On the other hand, the e⁴Tp unit of d(e⁴TpApe⁴TpA) and d(e⁴TpApTpA) have nearly identical Σ1's at 70°C which indicates that both sugar conformations are about 60% S at this temperature which are smaller than the approximately 70% S population observed for the Tp sugar of d(TpApe⁴TpA).

5.6.2 THE BASE AND H1' δs:

In discussing the base proton profiles of the d(ApNpA) trimers it was concluded (Section 5.5.4) that the conformation of both oligomers were similar, independent of whether N was e⁴T or T, with the N base stacked in between the two As. Any differences in the base proton profiles could usually be attributed to the larger ring current effects of e⁴T relative to T or to increases in the amount of base-stacking due to O4-alkylation. No one in the literature, to our knowledge, has analyzed d(ApTpA). However, Mellema et al. *(1984) have studied d(TpApTpA). Not only do their proton profiles suggest that their tetramer is*

predominately stacked at low temperature but, they have obtained NOE data that is best explained with the pTp base stacked in between the two As. If the e^4dTs in our tetramers are not drastically affecting the base-stacking geometries, as observed for the d(ApNpA) trimers, similar conclusions made by Mellema et al. *(1984) regarding d(TpApTpA) may be extended into our tetramers if analogous base proton profiles of d(TpApTpA) and of our tetramers behave similarly. Then by comparing the NpA end of our tetramers to the NpA end of d(ApNpA), it may indirectly be shown that the trimers are in a single helical stacked state with the pyrimidine inserted in between the As.*

5.6.2.1 The Me5 Profiles: Figure 5.49 contains the variable temperature profiles of the Me5 resonances of our tetramers and e^4dT. At the Np end, the Me5 resonances of all the tetramers move only slightly upfield with decreasing temperature, less than 0.03 ppm, consistent with a right handed/χ-anti *stack that projects this Me5 away from the plane of the adjacent base, as observed for the Me5 Np $\Delta\delta$°s of the d(NpX) dimers. The Me5 profiles of the e^4Tp units are downfield of those of the Tp unit, presumably due to the different electronic conjugation of e^4T relative to T. On the other hand, the Me5 $\Delta\delta$°s of the tetramer pNp units (0.08 - 0.10 ppm) are larger than those of the Np units (< 0.03 ppm), which suggests the N base of the pNp unit is feeling greater ring current effects from the adjacent As. Note that the pNp Me5 $\Delta\delta$°s of the d(ApNpA) trimers (0.10 - 0.11 ppm) and the d(NpApNpA) tetramers (0.08 -0.10 ppm) are similar and suggest comparable environments of the pNp units in both sets of molecules.*

5.6.2.2 The O4-Ethyl Group: Variable temperature profiles of the α*-methylene resonances of the O4-ethyl group of the tetramers are presented in Figure 5.50 where it is observed that a second e^4T within the oligomer has no influence on the other* α*-methylene resonances: the e^4Tp* α*-methylene profiles of d(e^4TpApe^{4}TpA) and d(e^4TpApTpA) are coincident, as are the pe^{4}Tp profiles of d(e^4TpApe^{4}TpA) and d(TpApe^{4}TpA). Both e^4Tp* α*-methylene $\Delta\delta$s increase with decreasing temperature while those of pe^{4}Tp decrease and approach zero at*

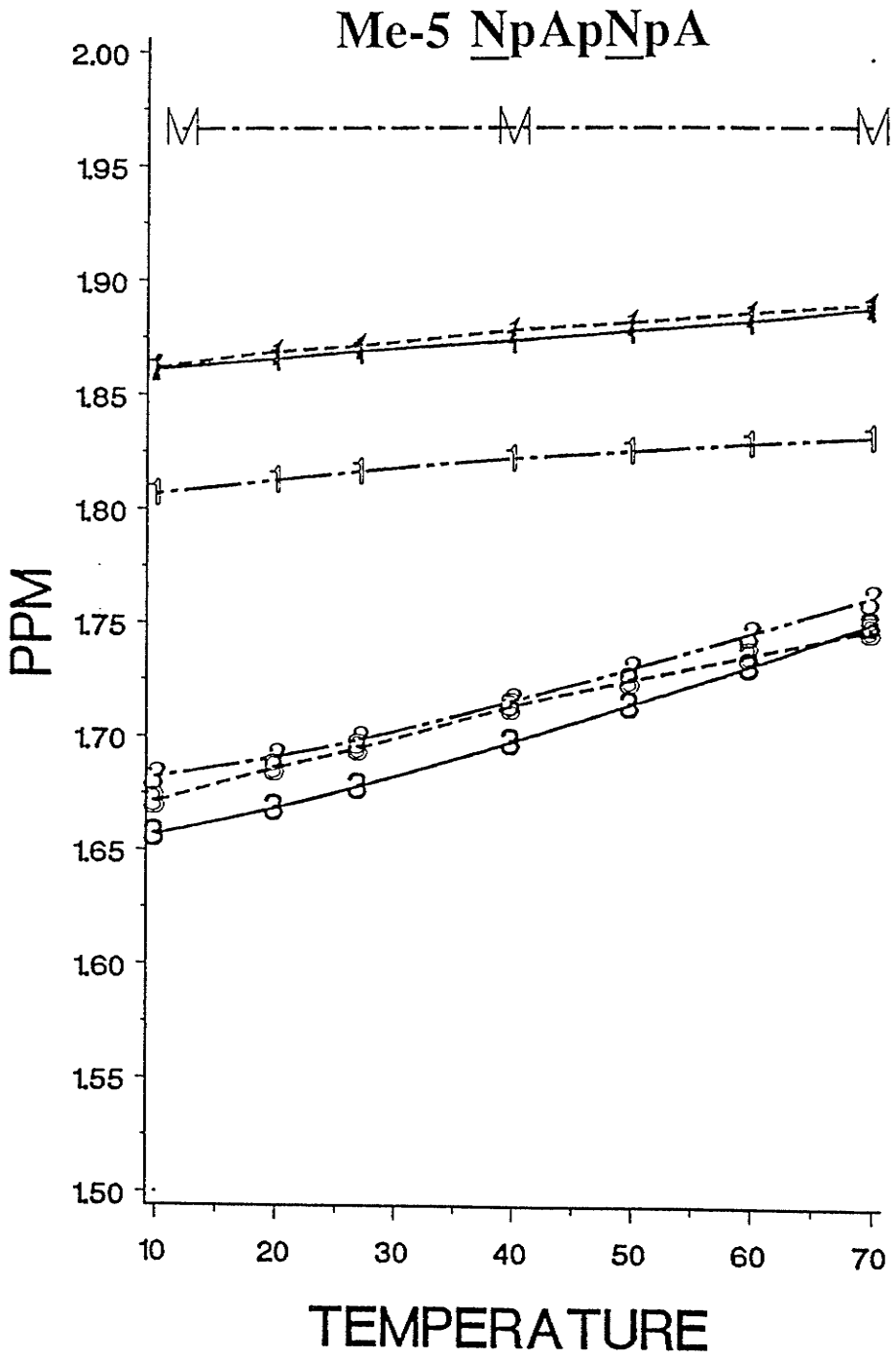

Figure 5.49: Temperature (C°) profiles of the chemical shifts (δ) of the Np (1) and pNp (3) Me5 base protons of the d(NpApNpA) tetramers. Bold numbers: d(e⁴TpApe⁴TpA), hollow numbers: d(TpApe⁴TpA), italic numbers: d(e⁴TpApTpA). Also included is the Me5 profile of the monomer (M) e⁴dT.

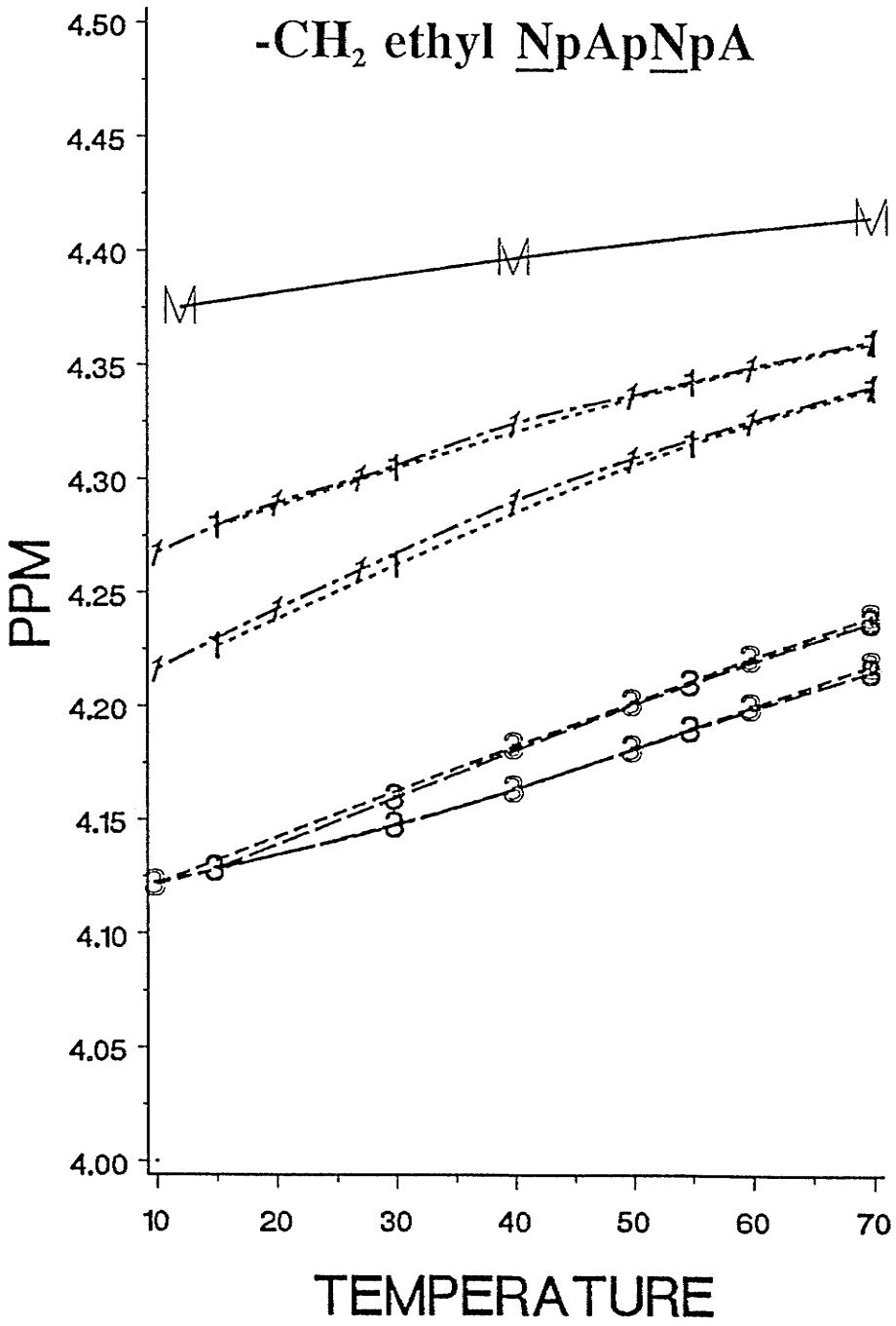

Figure 5.50: Temperature (C°) profiles of the chemical shifts (δ) of the Np (1) and pNp (3) α-methylene base protons of the O4-ethyl group of the d(NpApNpA) tetramers. Bold numbers: d(e⁴TpApe⁴TpA), hollow numbers: d(TpApe⁴TpA), italic numbers: d(e⁴TpApTpA). Also included is the α-methylene profile of the O4-ethyl group of the monomer (M) e⁴dT.

10°C. The behaviour of the tetramer e⁴Tp α-methylene profiles is analogous to that observed for the e⁴Tp unit of d(e⁴TpA) except that the tetramer Δδs are larger and their overall profile positions are upfield, perhaps because of more base-stacking in the tetramers than in the dimer or some next nearest neighbour ring current effects.

Figure 5.51 compares the α-methylene temperature profiles of the pe⁴Tp units of d(Ape⁴TpA) and d(e⁴TpApe⁴TpA) where the resonances of the tetramer are upfield of those of the trimer. However, the difference is slight and there are a number of possible explanations, such as the next nearest neighbour ring current effects, slightly different base-stacking geometries in the tetramer and trimer, or more base-stacking in the tetramer. Recall that the Me5 profiles of the pNp units of the tetramers are downfield of those of the pNp units of the d(ApNpA) trimers, opposite to the observations in the nearby α-methylene protons, which suggests that different base-stacking geometries is the best explanation for the differences in the α-methylene resonances of the pe⁴Tp unit of the tetramers relative to the pe⁴Tp unit of the d(Ape⁴TpA) trimer. However, the Me5 protons of the pNp unit of the tetramers could conceivably be in the same orientation in both the tetramers and the trimers but, not orientated properly relative to the α-methylene protons to feel the next nearest neighbour ring current influences or the effects of more base-stacking. Hence, instead of trying to interpret these small differences, which could be due to many things, the similarities should be noted because they indicate the α-methylene protons of the O4-ethyl group are in essentially the same type of environment.

The variable temperature profiles of the methyl resonance of the O4-ethyl group of the pe⁴Tp units of the tetramers and the d(Ape⁴TpA) trimer are plotted in Figure 5.52. The methyl profiles of the O4-ethyl group of the pe⁴Tp units of the tetramers are identical and slightly upfield of that of the d(Ape⁴TpA) trimer, as observed for their α-methylene profiles and probably for the same reasons. These observations, in both the α-methylene and methyl profiles of the O4-ethyl group of the tetramers and the d(Ape⁴TpA) trimer, suggests that the

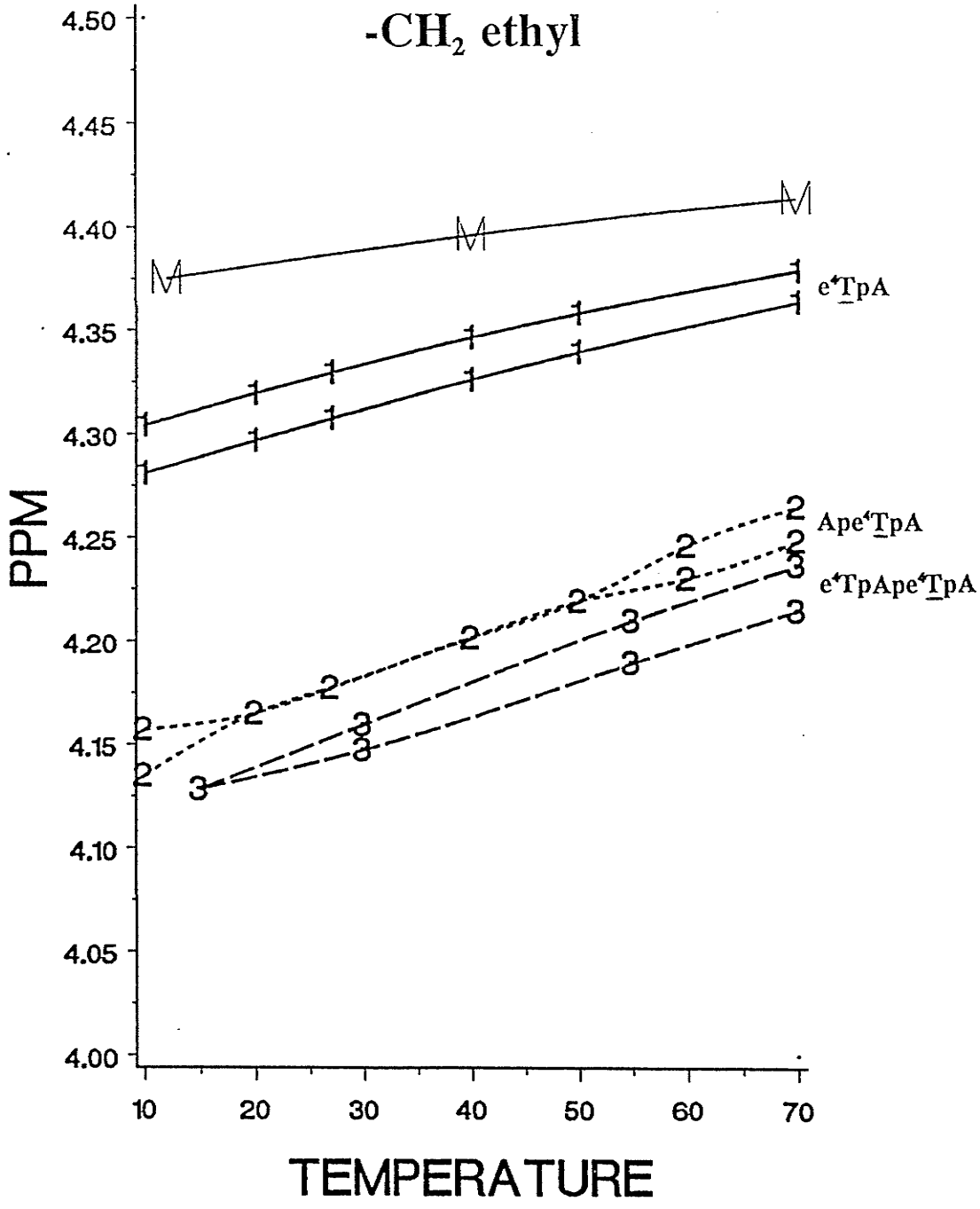

Figure 5.51: Temperature (C°) profiles of the chemical shifts (δ) of the α-methylene base protons of the O4-ethyl group of d(e⁴TpA) (1), d(Ape⁴TpA) (2), and d(e⁴TpApe⁴TpA) (3 pe⁴Tp). Also included is the α-methylene profile of the O4-ethyl group of the monomer (M) e⁴dT.

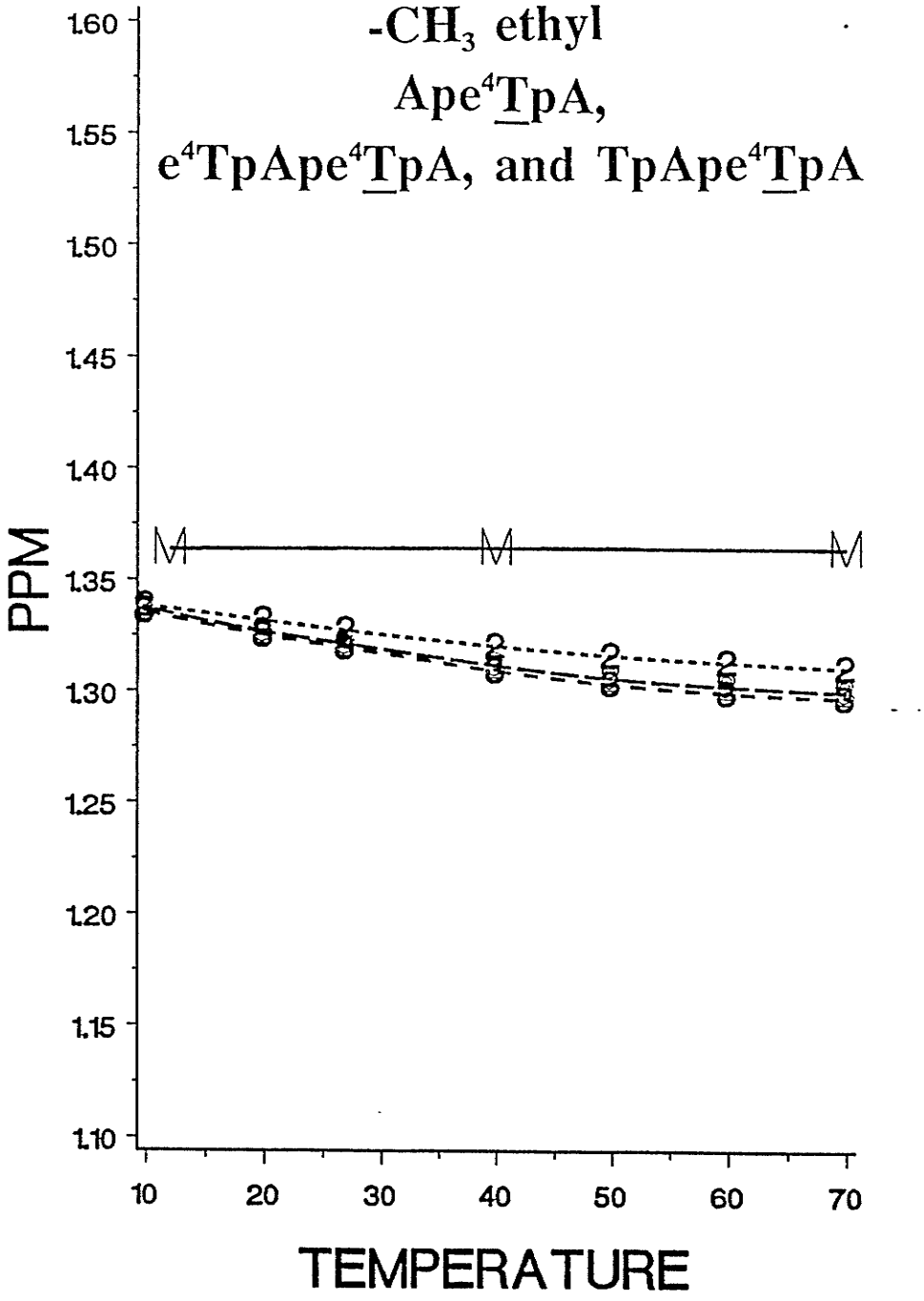

Figure 5.52: Temperature (C°) profiles of the chemical shifts (δ) of the methyl protons of the O4-ethyl group of d(Ape⁴TpA) (2), d(e⁴TpApe⁴TpA) (3, solid numbers) and d(TpApe⁴TpA) (3, hollow numbers). Also included is the methyl profile of the O4-ethyl group of the monomer (M) e⁴dT.

pe⁴Tp unit is in a similar environment in these molecules.

5.6.2.3 The H8 and H2 Profiles: Variable temperature profiles of the H8 and H2 resonances of the three tetramers are plotted in Figure 5.53. The pA H2 profiles of ***d(e⁴TpApe⁴TpA)*** *and* ***d(TpApe⁴TpA)*** *are identical and slightly upfield of the pA H2 profile of* ***d(e⁴TpApTpA)*** *as observed for the H2 profiles of the pA unit of the* ***d(NpA)*** *dimers (Figure 5.11) and the* ***d(ApNpA)*** *trimers (Figure 5.42). These small differences in the pA H2 profiles may be attributed to the weaker ring current effects of T relative to e⁴T. The variable temperature profiles of the H2 resonances of the pA unit of* ***d(e⁴TpA)***, ***d(Ape⁴TpA)***, *and* ***d(e⁴TpApe⁴TpA)*** *are plotted in Figure 5.54. Note that the profiles of the trimer and tetramer overlap which suggests that the pe⁴TpA unit in both molecules is orientated similarly.*

The H2 pAp profiles of the tetramers are dissimilar in terms of relative positions. However, these resonances all move upfield an equal amount with decreasing temperature and this suggests that base-stacking is taking place. The ***d(e⁴TpApe⁴TpA)*** *pAp H2 profile is the most upfield of the three tetramers, presumably due to the greater ring current influences of two e⁴Ts relative to one. When the pAp unit has only one e⁴T neighbour, slightly greater ring current effects are felt when it is on the 3'-side of pAp than on the 5'-side which suggests that in the stacked state the Np base is not as directly over the pAp H2 as is the pNp base. However, the differences between the pAp H2 profiles of* ***d(TpApe⁴TpA)*** *and* ***d(e⁴TpApTpA)*** *are small, like the differences observed in the H2 profiles of* ***d(NpA)*** *and* ***d(ApN)***.

The H8 temperature profiles of the pA base of the three tetramers are unaffected by the nature of the neighbouring pNp base, as these profiles overlap (Figure 5.53). The behaviour of the pA H8 profile of the tetramers is identical to that of the ***d(ApNpA)*** *trimers, as illustrated for* ***d(e⁴TpApe⁴TpA)*** *and* ***d(Ape⁴TpA)*** *in Figure 5.54. This is further support for the bases of the pNpA unit of the* ***d(ApNpA)*** *trimers and the tetramers being similarly orientated.*

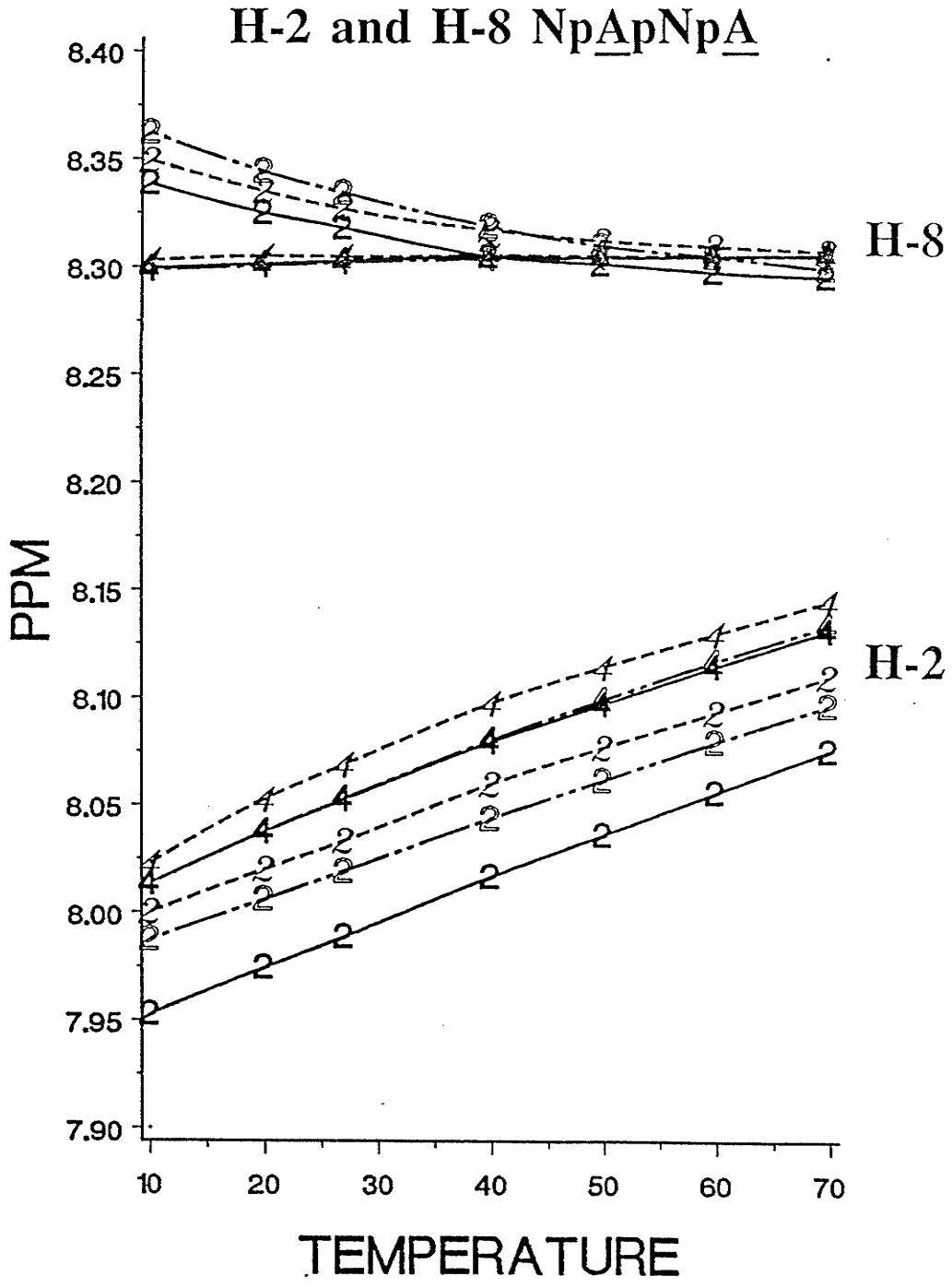

Figure 5.53: Temperature (C°) profiles of the chemical shifts (δ) for the pAp (2) and pA (4) H2 and H8 base protons of the d(NpApNpA) tetramers. Bold numbers: d(e⁴TpApe⁴TpA), hollow numbers: d(TpApe⁴TpA), italic numbers: d(e⁴TpApTpA).

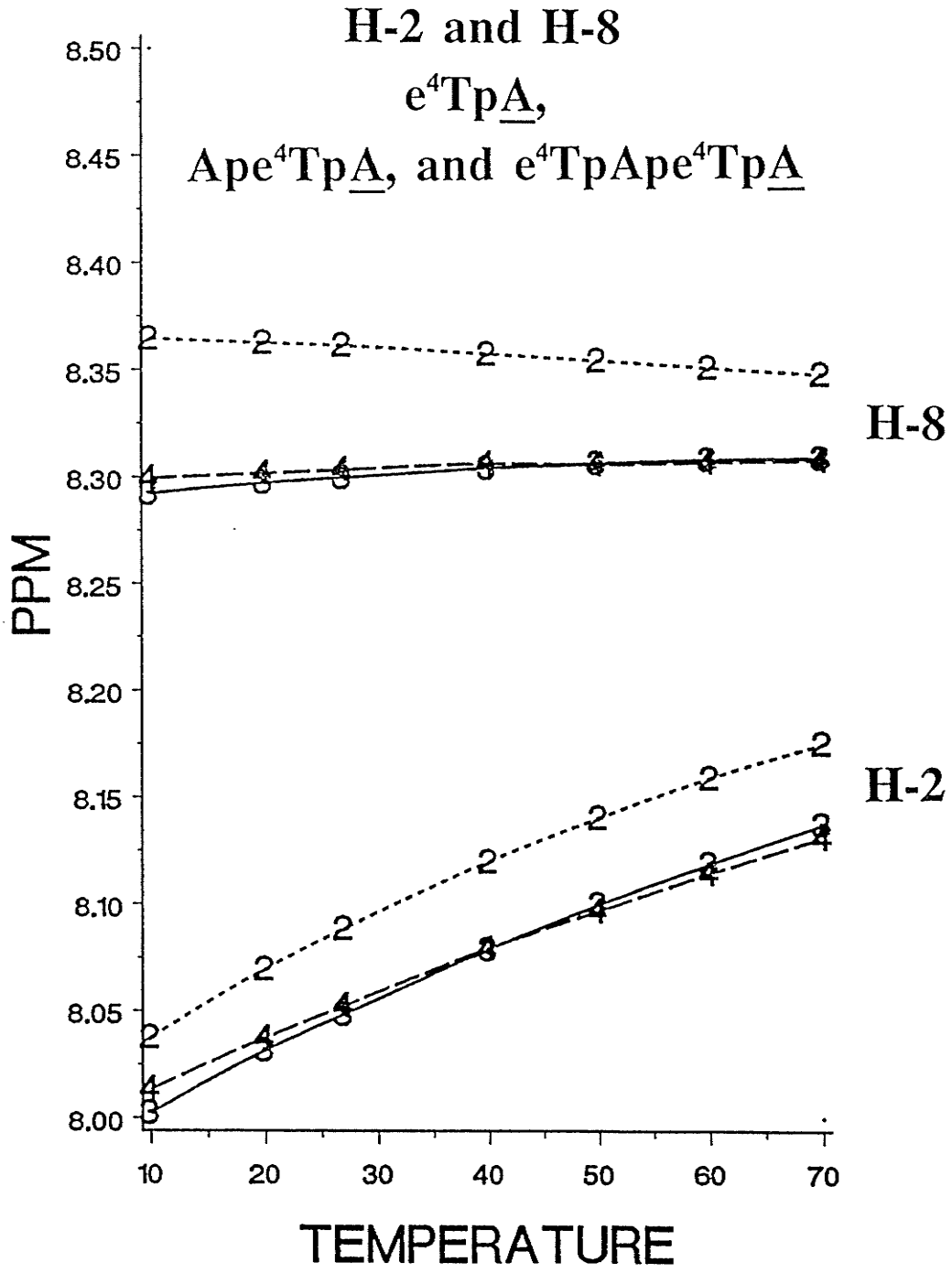

Figure 5.54: Temperature (C°) profiles of the chemical shifts (δ) of the pA H2 and H8 base protons of d(e⁴TpA) (2), d(Ape⁴TpA) (3), and d(e⁴TpApe⁴TpA) (4).

The H8 pAp temperature profiles of the tetramers are also all essentially the same (Figure 5.53). The pAp H8 profile of d(e⁴TpApe⁴TpA) is the most upfield, probably due to the greater ring current effects of two e⁴Ts relative to the one in the other two tetramers.

5.6.2.4 The H6 Profiles: The Np and pNp H6 resonances are plotted as a function of temperature for the three tetramers in Figure 5.55. The H6 profiles of e⁴T are downfield of those of T, as observed in the monomers, dT and e⁴T, due to the different electronic conjugation of these bases. The H6 profiles of the pNp units move upfield in the tetramers with decreasing temperature, as they do in d(ApNpA), which suggests that the pNp unit is stacking in between the two As. On the other hand, the H6 resonances of the Np units of the tetramers move upfield only slightly with decreasing temperature, counter to the downfield movement observed in the Tp units of all the d(NpX) dimers (Figure 5.13) and d(TpNpT) trimers (Figure 5.44). Because of the difficulties often encountered in interpreting H6 temperature profiles (Section 5.2.3.2) we can only note these differences since they may be due to a number of factors (more base-stacking, next nearest neighbour effects, changes in χ, and so on).

5.6.2.5 The H1' Profiles: The H1' δs are plotted as a function of temperature for all three tetramers in Figure 5.56. All the resonances move upfield with decreasing temperature to various degrees which generally indicates that base-stacking is taking place.

*The pA H1' profiles of the tetramers are downfield of the other tetramer H1' profiles which is consistent with a right handed/χ-*anti *stack because in such a stack the pA H1' will not be over the plane of any base. This is corroborated by the observation that there are no differences in the pA H1' profiles when e⁴T is exchanged for T in the pNp unit next to pA. These observations in the pA H1' profiles of the tetramers were also observed in the pA H1' profiles of the d(ApNpA) trimers (Figure 5.46) which again suggest that the pNpA unit is behaving similarly in both the tetramers and the d(ApNpA) trimers.*

The H1' profiles of the Np and pNp units of the tetramers are upfield of those of pAp

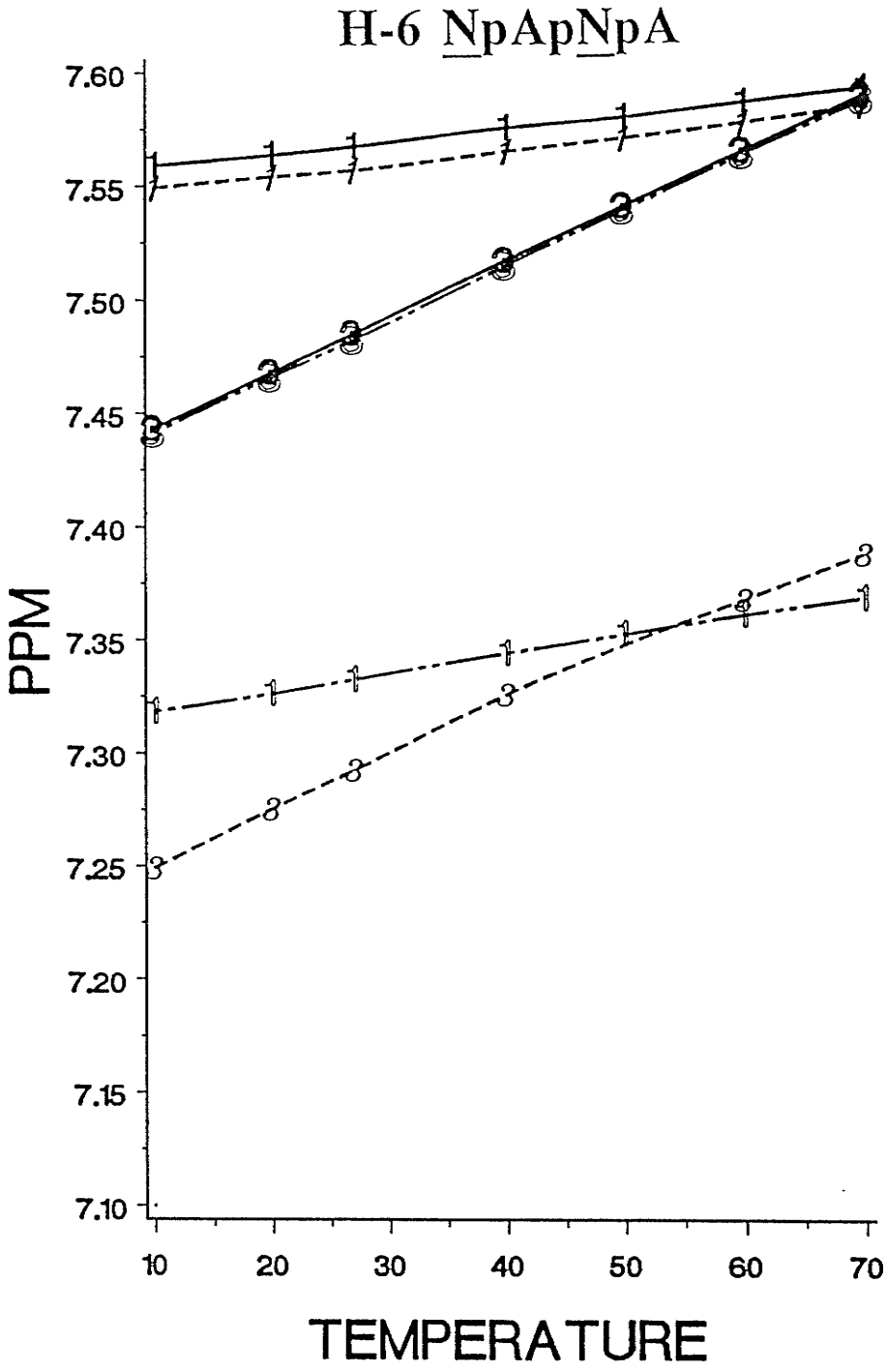

Figure 5.55: Temperature (C°) profiles of the chemical shifts (δ) of the Np (1) and pNp (3) H6 base protons of the d(NpApNpA) tetramers. Bold numbers: d(e⁴TpApe⁴TpA), hollow numbers for d(TpApe⁴TpA), italic numbers: d(e⁴TpApTpA).

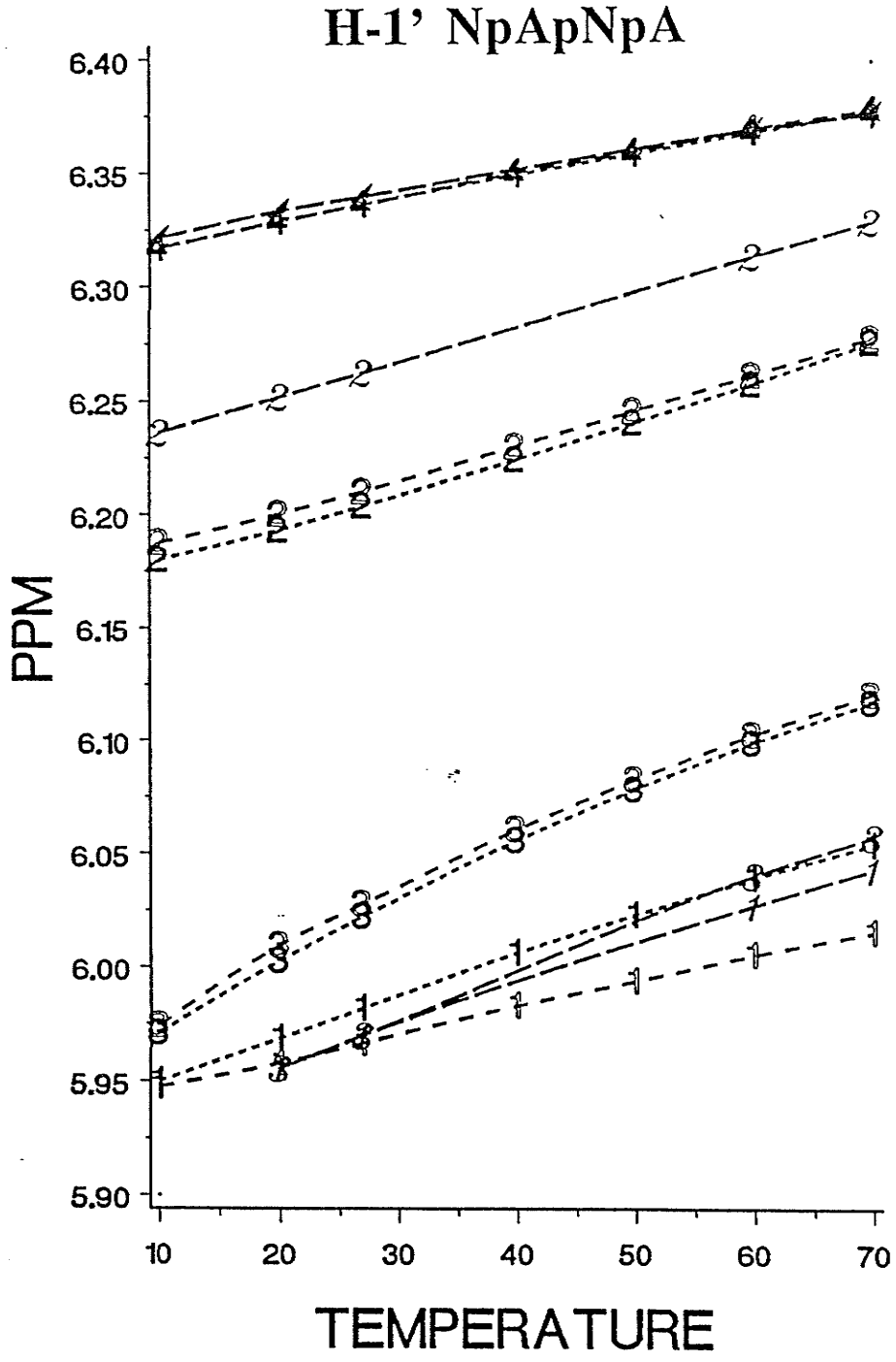

Figure 5.56: Temperature (C°) profiles of the chemical shifts (δ) of the Np (1), pAp (2), pNp (3), and pA (4) H1' sugar protons of the d(NpApNpA) tetramers. Bold numbers: d(e⁴TpApe⁴TpA), hollow numbers: d(TpApe⁴TpA), italic numbers: d(e⁴TpApTpA).

*and pA, presumably due to the larger ring current influences that the Np and pNp H1's experience in a right handed/*χ-anti *stack with an A on their 3'-side. Note that the pe⁴Tp H1' profile of* ***d(e⁴TpApe⁴TpA)*** *and* ***d(TpApe⁴TpA)*** *are nearly coincident while that for the pTp unit of* ***d(e⁴TpApTpA)*** *is more upfield. A similar, but smaller, effect is observed for the e⁴Tp H1' profiles of* ***d(e⁴TpApe⁴TpA)*** *and* ***d(e⁴TpApTpA)****, which are downfield of the Tp H1' profile of* ***d(TpApe⁴TpA)****. The effect appears to be related to the presence of e⁴T, as it was also observed for the pNp units of the* ***d(ApNpA)*** *trimers, with the pe⁴Tp H1' profile downfield of the pTp profile (Figure 5.46). Such an effect is not evident in the H1' profiles of the dT and e⁴dT monomers, which suggests that the downfield position of the H1' profiles of e⁴dT units relative to dT units is related to polymerization. However, because of the number of influences on the sugar* δ*s (Section 5.1.5.1) due to polymerization we can only make note of these observations while not being able to explain their occurrence.*

*The H1' profiles of the pAp units of the tetramers behave as expected in a right handed/*χ-anti *stack, with the profile influenced primarily by the base on its 3'-side (pNp). When the pNp base is e⁴T, as in* ***d(e⁴TpApe⁴TpA)*** *and* ***d(TpApe⁴TpA)****, the pAp H1' profiles are nearly identical. When the pNp base is T, as in* ***d(e⁴TpApTpA)****, the pAp H1' profile is downfield of the pAp H1' profiles of* ***d(e⁴TpApe⁴TpA)*** *and* ***d(TpApe⁴TpA)****, presumably due to the weaker ring current effects of T relative to e⁴T.*

5.6.2.6 Duplex Formation*: Mellema* et al. *(1984) have suggested that a small amount of duplex formation might be taking place in d(TpApTpA) at 8°C on the basis of concentration studies of internal base proton resonances of the (pApTp) section. Concentration studies were not carried out on our tetramers. However, at 10°C, the spectra for* ***d(e⁴TpApTpA)*** *and* ***d(TpApe⁴TpA)*** *were generally broader than the spectrum for* ***d(e⁴TpApe⁴TpA)****. Such observations suggest that perhaps some duplex formations may be occurring in* ***d(e⁴TpApTpA)*** *and* ***d(TpApe⁴TpA)*** *but, when both Ts are alkylated as in* ***d(e⁴TpApe⁴TpA)****, there is even less tendency to duplex and hence, the latter spectrum was sharper. These observations suggest*

that O4-alkylation of T hampers the formation of duplexes.

5.6.3 SUMMARY:

*The ^1H NMR data suggests that the three tetramers form right handed/*χ-anti *single helices whose population increases with decreasing temperature. There is little difference in the base and H1' variable temperature proton profiles of these tetramers that cannot be explained by the different ring current effects of e^4T relative to T and hence, O4-alkylation does not appear to be altering the base-stacked conformation. Base and H1' profiles of our tetramers that can be compared to those observed for d(TpApTpA) by Mellema* et al. *(1984) are similar. Mellema* et al. *(1984) interpreted their variable temperature data as we have, in terms of the formation of right handed/*χ-anti *single helices whose population increases with decreasing temperature. Their conclusions were also supported by NOE data. Note that the N base of the pNp unit of our tetramers and d(TpApTpA) appears to be stacked in between the two A. Because the base and H1' profiles of the pNpA unit of our tetramers are similar to those of the pNpA unit d(TpApTpA) and the pNpA unit of the* ***d(ApNpA)*** *trimers, it seems logical to conclude that the pNp base is also stacked in between the two As in the* ***d(ApNpA)*** *trimers. There are some changes in the sugar conformation of the e^4dT units relative to dT units in the tetramers, with e^4dT showing less of a preference for the* 2'-endo *conformation. However, this effect on sugar conformation does not appear to extend into the neighbouring nucleotides, counter to oberservations in some of our dimers and the* ***d(TpNpT)*** *trimers. It is again suggested that the e^4dT sugar might have to adopt a* 3'-endo *conformation to allow for the most favourable base-stacking interactions to take place and, depending on the sequence, the neighbouring nucleotide sugars are similarly effected to a smaller extent.*

5.7 CONCLUSIONS:

The NMR data of a large number of O4-alkylated molecules have just been discussed. A few patterns are evident and it would be convenient to briefly list them.

The first, and perhaps the most significant feature of these molecules, is the non-equivalence of the α*-methylene protons of the O4-ethyl, -propyl, -butyl, and -isobutyl groups and the methyl protons of the O4-isopropyl group in the NMR spectra. In most sequences the chemical shift difference of these resonances,* Δδ*, increases with decreasing temperature. This feature can be related to intramolecular base stacking and may be an especially useful monitor of base stacking, and double helical formation, in longer oligomers (Buchko* et al., *1987).*

Second, relative to the non-alkylated oligomers, O4-alkylation did not change the conformation along the sugar phosphate backbone. The β, γ, *and* ε *rotamer populations were essentially identicle for alkylated and non-alkylated sequences as monitored by* ^{13}C-^{31}P *and* ^{1}H-^{31}P *coupling constants.*

Third, O4-alkylation did not prevent base-stacking from occurring in these oligomers with the degree of base-stacking similar to the non-alkylated analogues. The ring current effects of an O4-alkythymine appear greater than that of thymine, as the variable temperature profiles of the protons of neighbouring bases were usually shifted upfield. This larger ring current effect of r^4T *makes it difficult to assess any changes in the base-base geometries due to alkylation. However, a right handed/*χ-anti *stack is suggested for both the alkylated and non-alkylated sequences.*

*Fourth, the major difference between alkylated and non-alkylated oligomers is an increase in the 3'-*endo *population of the* r^4dT *sugar relative to dT. In some O-alkylated oligomers there is an increase in the 3'-*endo *population of the* r^4dT *unit with decreasing temperature, with the magnitude dependent on the sequence. Furthermore, in a few sequences there is an increase in the 3'-*endo *population of the neighbouring nucleotidyl*

sugar(s), with such changes only seen with neighbouring pyrimidines. Perhaps these sequence dependent shifts in sugar conformation are necessary to allow the most favourable base-stacking interactions to take place with a r^4T.

Fifth, changing the size of the O4-alkyl group did not produce any major changes in the conformations of any of the O-alkylated oligomers. However, in some sequences there are indications of some small differences, most noticeably between the ethylated and isopropylated ***d(Tpr^{4}TpT)*** *and* ***d(r^{4}TpA)*** *molecules. This suggests that the size of the O4-alkyl group may have different conformational effects that depend on the sequence.*

In conclusion, O4-alkylation does not disrupt base-stacking (it may even enhance it). These observations are in line with those noticed by Kalnik et al. *(1988a; 1988b) in self-complementary dodecamers containing a* m^4T*:G and* m^4T*:A base pair (see Introduction). In both sequences the alkylated base is observed to stack within the double helix even though there is no evidence for base pairing, with at most one hydrogen bond theoretically possible between the two bases. Hence, in the dodecamers, stacking interactions are involved in holding the O-alkylated base within the double helix and our data indicates that base stacking is not disrupted due to O4-alkylation. The major change observed in our single stranded alkylated oligomers is in the sugar conformation of the O-alkylated nucleoside which may be significant biologically in terms of protein-DNA interactions involving repair and regulatory proteins (Barton, 1988).*

APPENDIX

```
------ FILE: PRESAT  .AU

;  PRESAT.AUR
;HOMO-NUCLEAR PRESATURATION (SOLVENT SUPPRESSION)

1 ZE              ;ZERO MEMORY
2 D1 HG S3        ;APPLY CW DEC. AT FREQ. O2, POWER S3, DURING D1
3 GO=2 DO         ;GATE DEC. OFF DURING AQ.
4 EXIT            ;EXIT WITH DEC. OFF

;RD=0
;D1 TYPICALLY 1-3 TIMES T1
;S3 TYP. 20-30L
```

PW=4.0 usec

SW=3000 Hz

SI=16K zero filled to 32K

Hz/pt=0.183

D1=1.0-2.0 sec

S3=35-40L

The FIDs were processed with a Lorentz to Gaussian lineshape transformation function (GM) prior to zero filling (normally LB=-2.0, GB=0.2. When different the GB was always -(0.1)(LB)).

```
------ FILE: POWGATE .AU

;  POWGATE.AUR
;POWER GATED HET.-NUCLEAR CPD DECOUPLING
;TO MINIMIZE DIELECTRIC HEATING

1 ZE              ;ZERO MEMORY
2 D1 CPD S1       ;BB DEC. WITH POWER S1 DURING D1
3 D2 S2           ;SWITCH TO POWER S2
4 GO=2            ;AQ. WITH DEC. POWER S2
5 D2 S1           ;LEAVE DEC. AT POWER S1 FOR NOE
6 EXIT

;S1 CA. 0.5 WATT OR AS NEEDED FOR NOE GENERATION
;S2 SET AS NEEDED FOR GOOD DECOUPLING
;D1 TYP. 1-5 TIMES AQ. AS DESIRED TO MINIMIZE AVERAGE POWER
;D2 TYP. 5-10 MSEC TO ALLOW POWER SWITCHING
;RD=0
;OPTIMUM EFFICIENCY: PW=90 DEG, D1+AQ=1.25*T1

;P9 DEFINES 90 DEG. DEC. PULSE FOR POWER S2 (SEE CPDCHECK.AU)
;S2 = CA. 1 W AND P9= CA. 100 USEC ARE TYPICAL (10MM).
```

D1=3.0-5.0 sec

S1=18 H, S3=16 H

PW=5.0 usec

SW=9800 Hz

SI=32K zero filled to 64 K

Hz/pt=0.151

The FIDs were processed with a Lorentz to Gaussian lineshape transformation function (GM) prior to zero-filling (maximum: LB=-1.0, GB=0.1).

```
------ FILE: RCT


1  ZE
2  D1 HG
3  P1 PH1
4  D0
5  P1 PH2
6  D2
7  P2 PH3
8  D2
9  P1 PH3
10 GO=2 PH4 D0
11 WR #1
12 IF #1
13 IN=1
14 EXIT

PH1=A0
PH2=A0 A0 A2 A2 A0 A0 A2 A2 A1 A1 A3 A3 A1 A1 A3 A3
PH3=A0 A2 A0 A2 A0 A2 A0 A2 A1 A3 A1 A3 A1 A3 A1 A3
PH4=R1 R1 R1 R1 R1 R1 R1 R1 R3 R3 R3 R3 R3 R3 R3 R3
```

512 x 512: F1=256 zero filled to 512, F2=1K

1K x 1K: F1=512 zero filled to 1K, F2=2K

NE=256 FIDS, SW=2200 Hz

P1=90^{o}=12.2 usec, P2=180^{o}=20.4 usec

DS=2, NS=32-64 scans

D1=1.0 sec, D2=0.0458 sec

The data were processed with a sine bell transformation in both dimensions followed by symmetrization.

```
------- FILE: COSY     .AU

;  COSY.AUR
; HOMONUCLEAR SHIFT-CORRELATED 2-D NMR (JEENER)
; W.P.AUE, E.BARTHOLDI, R.R.ERNST, J.CHEM.PHYS. 64, 2229 (1976)
; K.NAGAYAMA ET AL, J.MAGN.RES. 40, 321 (1980)

;  D1 - 90 - D0 - 90 OR 45 - FID

; SYMMETRIC MATRIX WITH SHIFTS AND COUPLINGS IN F1, F2
; OFF-DIAGONAL PEAKS CORRELATE SPINS WHICH SHARE A
; SCALAR COUPLING J.

1 ZE
2 D1              ;RELAXATION
3 P1 PH1          ;90 DEG EXCITATION PULSE
4 D0              ;EVOLUTION OF SHIFTS AND COUPLINGS
5 P2 PH2          ;MIXING PULSE, 90 OR 45 DEG
6 GO=2 PH3        ;ACQUIRE FID
7 WR #1           ;STORE FID
8 IF #1           ;INCREMENT FILE NUMBER
9 IN=1            ;INCREMENT D0 AND LOOP FOR NEXT EXPER.
10 EXIT

PH1=A0 A0 A0 A0 A1 A1 A1 A1      ;PHASE PROGRAMS CANCEL AXIAL
    A2 A2 A2 A2 A3 A3 A3 A3      ;PEAKS (SCANS 1-2), SELECT N-TYPE
                                 ;PEAKS (SCANS 3-4), SUPPRESS F2
PH2=A0 A2 A1 A3 A1 A3 A2 A0      ;QUAD IMAGES (SCANS 5-8), AND CANCEL
    A1 A3 A2 A0 A2 A0 A3 A1      ;ARTEFACTS FROM P1 (SCANS 9-16).

PH3=R0 R0 R2 R2 R1 R1 R3 R3

;PROGRAM REQUESTS FILENAME WITH .SER EXTENSION
;NE DEFINES NUMBER OF FIDS = TD1
;NS = 4,8, OR 16 (COMPLETE PHASE CYCLE)
;DS = 2 OR 4
;RD=PW=0
;D1 = 1-5*T1
;P1 = 90 DEG
;P2 = 90 DEG FOR MAX. SENSITIVITY
;   = 45 DEG FOR MINIMAL DIAGONAL (GOOD FOR TIGHT AB SYSTEMS)
;        AND 'TILTED' CORREL. PEAKS (SIGNS OF COUPLINGS).
;D0 = 3E-6 INITIAL DELAY
;IN = 0.5/SW1 = 2*DW
;ND0 = 1
;I2D = 1, SW1=SW/2

;CHOOSE SW AND SI SO THAT HZ/PT = CA. 2-6 HZ
;TYPICALLY USE TD = SI, NO ZERO-FILLING IN F2
;              NE = SI/4, ZERO-FILL IN F1
;MATRIX CAN BE SYMMETRIZED ABOUT DIAGONAL
```

512 x 512: F1=256 zero filled to 512, F2=1K

NE=256 FIDS, SW=2200 Hz

P1=90°=10.2 usec, P2=45°=5.1 usec

D1=1.0-2.0 sec,

DS=2, NS=32-64 scans

The data were processed with a sine bell transformation in both dimensions followed by symmetrization.

```
------ FILE: NOEDIFF .AU

;  NOEDIFF.AUR
; NOE DIFFERENCE SPECTROSCOPY
; USING ONE FREQ. LIST TO DEFINE A SERIES OF IRRADIATION POINTS
; (ON-RESONANCE) AND ONE CONTROL (OFF-RESONANCE)
; THE INDIVIDUAL FIDS ARE STORED.
; FOR LONG-TERM AVERAGING THE ROUTINE CYCLES THROUGH THE
; FREQ. LIST AND FIDS SEVERAL TIMES.
; ALSO CAN BE USED FOR PSEUDO-INDOR.

1 ZE
2 WR #1          /DEFINE FID
                 ;PREPARE A SET OF ZEROED FILES ON DISK
3 IF #1
4 LO TO 2 TIMES C  ;C= NO. OF FIDS TO BE STORED
  FL #2          /DEFINE FREQ. LIST
                 ;READ IN DESIRED FREQ. LIST
5 RF #1.001      ;RESET FILE EXTENSION TO .001, BEGIN CYCLE
6 RE #1          ;READ CURRENT FID FILE
7 D3 D2 S3       ;SET DEC. FREQ. D2 FROM CURRENT FL LIST
8 D1 DO          ;RELAX. TIME WITH DEC. GATED OFF
9 D2 HG          ;IRRAD. TIME (CA. T1) USING POWER S3
10 GO=8 DO       ;ACQUIRE DATA WITH DEC. OFF, LOOP TO 8
11 WR #1         ;STORE CURRENT ACCUMULATED FID
12 IF #1         ;INCREMENT FID EXTENSION
13 LO TO 6 TIMES C      ;LOOP TO 6 FOR EACH FREQ. IN FL LIST
14 IN=5          ;LOOP FOR ANOTHER CYCLE
                 ;NE=NUMBER OF CYCLES THROUGH LIST
15 EXIT

;PROGRAM REQUESTS FILENAME #1 FOR FIDS, #2 FOR FREQ. LIST.
;A FREQ. LIST MUST BE DEFINED WHICH CONTAINS ONE D2
;ENTRY FOR EACH DESIRED IRRAD. POINT PLUS ONE OFF-RES. CONTROL
;VALUE FOR D2 WHICH SHOULD BE WITHIN THE SW REGION (E.G. AT ONE
;EDGE OF THE SPECTRUM). THE NUMBER OF FREQ. IN THE LIST MUST BE
;DEFINED BY AN ENTRY IN A 'VC' LIST, WHICH ALSO DEFINES THE
;NUMBER OF FIDS TO BE STORED.

;NS DEFINES THE NO. OF TRANSIENTS PER CYCLE FOR EACH D2 VALUE
;AND SHOULD BE A MULTIPLE OF 8.

;NE DEFINES THE NO. OF CYCLES TO BE MADE THROUGH COMPLETE LIST.
;TOTAL TRANSIENTS PER FID = NE*NS.
;USE 2-4 DUMMY SCANS FOR STEADY-STATE!
;RD=0
;D3 = 0.1 SEC TO SET D2
;D1+AQ = 2-4*T1 FOR TRUNCATED NOE APPLICATIONS WHERE NO SECONDARY
;  OR STEADY-STATE EFFECTS (SPIN-DIFFUSION) ARE DESIRED.
;D2 = CA. T1 FOR SMALL MOLECULES (EXTREME NARROWING LIMIT)
;   = 50-200 MSEC FOR LARGE MOLECULES (CROSS-RELAXATION).

;S3 DEFINES DEC. POWER TYPICALLY 35-55L DEPENDING ON REQUIRED
;IRRAD. BANDWIDTH.
```

Performed under similar conditions as described for PRESAT.AU.

D1=1.0 sec, D3=3.0 sec or D1=4.0 sec, D3=5.0 sec

An exponential lineshape transformation (EM) was performed prior to zero filling (LB$\leq$1.0, GB=0.0).

REFERENCES

*Abbott, P.J. and Saffhill, R. (1979) Biochem. Biophys. Acta, **562**, 51.*

*Alderfer, J.L. and Ts'O P.O.P. (1977) Biochemistry **16**, 2410.*

*Allore, B.D., Queen, A., Blonski, W.J. and Hruska, F.E. (1983) Can. J. Chem., **61**, 2397.*

*Altona, C. and Sundaralingam, M. (1972) J. Amer. Chem. Soc. **94**, 8205.*

*Altona, C. (1982) Recl. Trav. Chim. Pays-Bas **101**, 413.*

*Aue, W.P., Bartholdi, E., and Ernst, R.R. (1976) J. Chem. Phys. **64**, 2229.*

Barton, J.K. (1988) Chem. Engineering News, Sept., 30.

*Bartsch, H. and Montesano, R. (1984) Carcinogenesis **5**, 1381.*

*Behe, M. and Felsenfeld, G. (1981) Proc. Natl. Acad. Sci. U.S.A. **78**, 1619.*

*Bell, R.A., Everett, J.R., Hughes, D.W., Alkema, D., Hader, P., Neilson, T. and Romaniuk, P.J. (1981) Biopolymers **20**, 1383.*

*Birnbaum, G.I., Sadana, K.L., Blonski, W.J.P. and Hruska, F.E. (1986) J. Amer. Chem. Soc. **108**, 1181.*

*Birnbaum, G.I., Sadana, K.L., Razi, M.T., Lee, T., Sebastian, R., Buchko, G.W., and Hruska, F.E. (1988) Can. J. Chem. **66**, 1628.*

*Bolton, P.H., (1982) J. Magn. Reson. **48**, 336.*

*Bolton, P.H., Bodenhausen, G. (1982) Chem. Phys. Lett. **89**, 139.*

Borer, P.N., (1975) CRC Handbook of Biochemistry and Molecular Biology, 3rd ed., Nucleic Acid, Vol. I, G.D. Fasman editor, CRC Press, Inc., Cleveland, Ohio. 589.

*Borowy-Borowski, H. and Chambers, R.W. (1989) Biochemistry **28**, 1471.*

*Brahms, J., Maurizot, J.C. and Michelson, A.M. (1967) J. Mol. Biol. **25**, 481.*

*Braunschweiler, L. and Ernst, R.R. (1983) J. Magn. Reson. **53**, 521.*

*Brennan, R.G., Pyzalska, D., Blonski, W.J.P., Hruska, F.E. and Sundaralingam, M. (1986) Biochemistry **25**, 1181.*

*Brent, T.P., Dolan, M.E., Fraenkel-Conrat, H., Hall, J., Karran, P., Laval, F., Margison, G.P., Montesano, R., Pegg, A.E., Potter, P.M., Singer, B., Swenberg, J.A. and Yarosh, D.B. (1988) Proc. Natl. Aced. Sci. U.S.A. **85**, 1759.*

Buchko, G.W. (1986) M.Sc. thesis, McMaster University, Hamilton, Ontario.

Buchko, G.W., Hruska, F.E., Razi, M.T. and Sadana, K.L. (1987) Book of Abstracts: Fifth Conversation in Biomolecular Sterodynamics, Adenine Press, Guilderland, N.Y., 83.

*Buchko, G.W., Hruska, F.E. and Sadana, K.L. (1989a) Can. J. Chem. **67**, 109.*

*Buchko, G.W., Hruska, F.E. and Sadana, K.L. (1989b) Can. J. Chem. **67**, 1344.*

Buchko, G.W., Hruska, F.E., Razi, M.T. and Sadana, K.L. (1989c) Book of Abstracts Sixth Conversation in Biomolecular Sterodynamics, Adenine Press, Guilderland, N.Y., .

Bush, C.A. and Brahms, J. (1973) Physio-Chemical Properties of Nucleic Acids, J. Duschesne editor, Academic Press, New York, 147.

*Cantor, C.R., Warshaw, M.M. and Shapiro, H. (1970) Biopolymers **9**, 1059.*

*Caruthers, M.H. (1985) Science **230**, 281.*

*Cheng, D.M. and Sarma, R.H. (1977) J. Amer. Chem. Soc. **99**, 7333.*

*Cheng, D.M., Dhingra, M.M. and Sarma, R.H. (1978) Nucl. Acids Res. **5**, 4399.*

*Cheng, D.M., Kan, L.-S., Lentzinger, E.E., Jayaraman, K., Miller, P.S. and Ts'O, P.O.P. (1982) Biochemistry **21**, 621.*

*Corey, E.J. and Venkateswarlu, A. (1972) J. Amer. Chem. Soc. **94**, 6190.*

*Crockett, G.C. (1983) Aldrichimica Acta **16**, 47.*

*Davies, D.B. (1978) Prog. NMR Spect. **12**, 135.*

*Davies, D.B. and Danyluk, S.S. (1974) Biochemistry **13**, 4417.*

*Den Engelse, L. Menkveld, G.J., De Brij, J. and Tates, A.D.(1986) Carcinogenesis (London) **7**, 393.*

Divakar, K.J. and Reese, C.B. (1982) J.C.S. Perkin I, 1171.

*Drew, H., Takano, T., Tanaka, S., Itakura, K. and Dickerson, R.E. (1980) Nature **286**, 567.*

*Eich, G., Bodenhausen, G. and Ernst, R.R. (1982) J. Amer. Chem. Soc. **104**, 3731.*

*Eritja, R., Horowitz, D.M., Walker, P.A., Ziehler-Martin, J.P., Boosalis, M.S., Goodman, M.S., Itakura, K. and Kaplan, B.E. (1986) Nucl. Acids Res. **14**, 5641.*

*Fairall, L., Martin, S. and Rhodes, D. (1989) EMBO J. **8**, 1809.*

*Fazakerley, G.V., Sowers, L.C., Eritja, R., Kaplan, B.E. and Goodman, M.F. (1987) Biochemistry **26**, 5641.*

*Feigon, J., Leupin, W., Denny, W.A. and Kearns, D.R. (1983) Biochemistry **22**, 5943.*

*Flynn, P.F., Kintanar, A., Reid, B.R. and Drobny, G. (1988) Biochemistry **27**, 1191.*

*Friedman, O.M., Mahapatra, G.N., Dash, B. and Stevenson, R. (1965) BBA **103**, 286.*

Gaffney, B.L., Marky, L.A. and Jones, R.A. (1984) Biochemistry **23**, *5686.*

Gaffney, B.L. and Jones, R.A. (1989) Biochemistry **28**, *5881.*

Gerchman, L.L. and Ludlum, D.B. (1973) Biochim. Biophys. Acta **308**, *310.*

Giessner-Prettre, C. and Pullman, B. (1987) Quarterly Rev. Biophys. **20**, *113.*

Haasnoot, C.A.G. and Altona, C. (1979) Nucl. Acids Res. **6**, *1135.*

Hare, D., Shapiro, L. and Patel, D.J. (1986) Biochemistry **25**, *7456.*

Harris, R.K. (1983) Nuclear Magnetic Resonance Spectroscopy. Pitman Publishing Inc., Toronto, 105.

Harwood, L.M. (1985) Aldrichimica Acta **18**, *25.*

Hruska, F.E. (1973) Jerusalem Symp. on Quantum Chem., 345.

Hruska, F.E., Bell, C.L., Victor, T.A. and Danyluk, S.S. (1968) Biochemistry **7**, *3721.*

Hruska, F.E. and Blonski, W.J.P. (1982) Can. J. Chem. **60**, *3026.*

Hughes, D.W., Bell, R.A., Neilson, T. and Bain, A.D. (1985) Can. J. Chem. **63**, *3133.*

Hunter, W.N., Brown, T., Anand, N.N., and Kennard, O. (1986) Nature **320**, *552.*

IUPAC-IUB (1970) Eur. J. Biochem. **15**, *203.*

Ivanov, V.I., Minchenkova, L.E., Schyolkina, A.K. and Poletayev, A.I. (1973) Biopolymers **12**, *89.*

Jaskunas, S.R., Cantor, C.R. and Tinoco, I., Jr. (1968) Biochemistry **7**, *3164.*

Jensen, D.E. (1986) unpublished results.

Johnson, B.B., Dahl, K.S., Tinoco, I., Ivanov, V.I. and Zhurkin, V.B. (1981) Biochemistry, **20**, *73.*

Kalnik, M.W., Kouchakdjian, M. Li, B.F.L., Swann, P.F. and Patel, D.J. (1988a) Biochemistry **27**, *100.*

Kalnik, M.W., Kouchakdjian, M. Li, B.F.L., Swann, P.F. and Patel, D.J. (1988b) Biochemistry **27**, *108.*

Kalnik, M.W., Li, B.F.L., Swann, P.F. and Patel, D.J. (1989a) Biochemistry **28**, *6170.*

Kalnik, M.W., Li, B.F.L., Swann, P.F. and Patel, D.J. (1989b) Biochemistry **28**, *6170.*

Kan, L.-S., Barrett, J.C. and Ts'o, P.O.P (1973) Biopolymers **12**, *2409.*

Kan, L.-S., Ts'o, P.O.P., Haar, F.v.d., Sprinzl, M. and Cramer, F. (1974) Biochem. Biophys. Res. Comm. **59**, *22.*

*Kan, L.-S., Cheng, D.M., Chandrasegaran, S., Pramanik, P. and Miller, P.S. (1987) J. Molec. Struct. Dynm. **4**, 785.*

*Kearns, D.R. (1984) CRC Crit. Rev. Biochem. **15**, 237.*

*Kierzek, R., Ito, H., Bhatt, R. and Itakura, K. (1981) Tett. Let. **22**, 3761.*

*Klevit, R.E., Wemmer, D.E., and Reid, B.R. (1986) Biochemistry **25**, 3296.*

*Klyne, W. and Prelog, V. (1960) Experientia **16**, 521.*

*Kondo, N.S., Holmes, H.M., Stempel, L.M. and T'so, P.O.P. (1970) Biochemistry **9**, 3479.*

*Kusmierek, J.T., and Singer B. (1976) Biochim. Biophys. Acta, **442**, 420.*

*Lankhorst, P.P., Haasnoot, C.A.G., Erkelens, C. and Altona, C. (1984) J. Biomol. Struct. Dyn. **1**, 1387.*

*Lankhorst, P.P., Haasnoot, C.A.G., Erkelens, C., Westerink, H.P., van der Marel, G.A., van Boom, J.H. and Altona, C. (1985) Nucl. Acids Res. **13**, 925.*

*Lawley, P.D., Orr, D.J., Shah, S.A., Farmer, P.B. and Jarman, M. (1973) Biochem. J., **135**, 193.*

*Lawrence, D.P., Wenqiuo, C., Zon, G., Wojiech, J.S., Uznanski, B. and Briodo, M.S. (1987) J. Molec. Struct. Dynm. **4**, 757.*

*Lee, C.-H., Ezra, F.S., Kondo, N.S., Sarma, R.H. and Danyluk, S.S. (1976) Biochemistry **15**, 3627.*

*Lee, C.-H. and Tinoco, I., Jr. (1980) Biophys. Chem. **11**, 283.*

*Li, B.F.L., Reese, C.B. and Swann, P.F. (1987) Biochemistry **26**, 1086.*

*Lindahl, T., Sedgwick, B., Sekiguchi, M. and Nakabeppu, Y. (1988) Ann. Rev. Biochem. **57**, 133.*

*Loeb, L.A. and Kunkel, T.A. (1982) Annu. Rev. Biochem. **51**, 429.*

*Loeb, L.A., Liu, P.K. and Fry, M. (1986) Prog. Nucl. Acid Res. Mol. Biol. **33**, 57.*

*Loveless, A. (1969) Nature **223**, 206.*

*Mellema, J.-R., Pieters, J.M.L., van der Marel, G.A., van Boom, J.H., Haasnoot, C.A.G. and Altona, C. (1984) Eur. J. Biochem. **143**, 285.*

*Miller, P.S., Chandrasegaran, S., Dow, D.L., Pulford, S.M. and Kan, L.-S. (1982) Biochemistry **21**, 5468.*

*Nishimura, Y., Torigoe, C. and Tsuboi, M. (1986) Nucl. Acids Res. **14**, 2737.*

Noggle, J.H. and Schirmer, R.F. (1971) The Nuclear Overhauser Effect, Academic Press, N.Y., 1.

*Ogilvie, K.K. (1973) Can. J. Chem. **51**, 3799.*

*Olsthoorn, C.S.M., Bostelaar, J.F.M. and Altona, C. (1980) Eur. J. Biochem. **106**, 85.*

*Parthasarathy, R. and Fridey, S.M. (1986) Carcinogenesis **7**, 221.*

*Patel, D.J., Pardi, A. and Itakura, K. (1982) Science (Washington, D.C.) **216**, 581.*

*Patel, D.J., Kozlowski, S.A., Ikuta, S., and Itakura, K. (1984) Biochemistry **23**, 3218.*

*Patel, D.J., Shapiro, L., Kozlowski, S.A., Gaffney, B.L., and Jones, R.A. (1986) Biochemistry **25**, 1027.*

Perrin, D.D., Armarego, W.L.F. and Perrin, D.R. (1980) Purification of Laboratory Chemicals, Pargamon Press Ltd., Great Britain.

*Petruska, J. Goodman, M.F., Boosalis, M.S., Sowers, L.C., Cheong, C. and Tinoco, I., Jr. (1988) Proc. Natl. Acad. Sci. U.S.A. **85**, 6252.*

*Pohl, F.M. and Jovin, T.M. (1972) J. Mol. Biol. **67**, 375.*

*Powell, J.T., Richards, E.G. and Gratzer, W.B. (1973) Biopolymers **11**, 235.*

*Pramanik, P. and Kan, L.-S. (1987) Biochemistry **26**, 3807.*

*Preston, B.D., Singer, B. and Loeb, L.A. (1986) Proc. Natl. Acad. Sci. USA **83**, 8501.*

*Quirt, A.R. and Martin, J.S. (1971) J. Magn. Reson. **5**, 318.*

*Reese, C.B. (1978) Tett. **34**, 3143.*

*Reich, C. and Tinoco, I. Jr. (1980) Biopolymers **19**, 833.*

*Remin, M. and Shugar, D.S. (1972) Biochem. Biophys. Res. Commun. **48**, 636.*

*Rich, A., Nordheim, A. and Wang, A.H.J. (1984) Ann. Rev. Biochem. **53**, 791.*

*Richardson, K.K., Richardson, F.C., Crosby, R.M., Swenberg, J.A. and Skopek, T.R. (1987) Proc. Natl. Aced. Sci. U.S.A. **84**, 344.*

*Rinkel, L.J., Mellema, J.-R., Van der Marcel, G.A., Van Boom, J.H. and Altona, C. (1986) Eur. J. Biochem. **154**, 259.*

*Rinkel, L.J. and Altona, C. (1987) J. Biomol. Struct. Dyn. **4**, 621.*

*Rycyna, R.E. and Alderfer, J.L. (1985) Nucl. Acids Res. **13**, 5949.*

*Rycyna, R.E., Wallace, J.C., Sharma, M. and Alderfer, J.L. (1988) Biochemistry **27**, 3152.*

Saenger, W. (1984) Principles of Nucleic Acid Structure, Springer-Verlag New York Inc., N.Y., 135.

Saffhill, R., Margison, G.P., and O'Connor, P.J. (1985) Biochim. Biophys. Acta, 823, 111.

Sanders, J.K.M. and Mersh, J.D. (1982) Prog. NMR Spec. 15, 353.

Schaller, H., Weimann, G., Lerch, B. and Khorana, H.G. (1963) J. Amer. Chem. Soc. 85, 3821.

Singer, B. (1975) Progr. Nucl. Acids Res. Molec. Biol. 15, 219, 330.

Singer, B. (1976) Nature 264, 333.

Singer, B., Sun, L. and Fraenkel-Conrat, H. (1975) Biochemistry 14, 772.

Singer, B., Kroger, M. and Carrano, M. (1978) Biochemistry 17, 1246.

Singer, B. and Grunberger, D. (1983) Molecular Biology of Muatagenes and Carcinogenes, Plenum, New York, 1.

Singer, B., Sagi, J. and Kusmierek, J.T. (1983) Proc. Natl. Acad. Sci. USA 80, 4584.

Singer, B., Spengler, S.J., Fraenkel-Conrat, H. and Kusmierek, J.T. (1986) Proc. Natl. Acad. Sci. USA 83, 28.

Singer, B., Chavez, F., Spengler, S.J., Kusmierek, J.T., Mendelman, L., and Goodman, M.F. (1989) Biochemistry 28, 1478.

Sun, L. and Singer, B. (1975) Biochemistry 14, 1795.

Sundaralingam, M. (1969) Biopolymers 7, 821.

Sundaralingam, M. (1973) Conformations of Biological Molecules and Polymers. Bergmann, E.D. and Pullman, B. editors. Academic Press, N.Y. 417.

Tinoco, I. Jr. and Bustamante, C. (1980) Ann. Rev. Biophys. Bioeng. 9, 107.

Topal, M.D. and Warshaw, M.M. (1976) Biopolymers 15, 1775.

Topal, M.D., Eadie, J.S., and Conrad, M. (1986) J. Biol. Chem. 261, 9879.

Tunis-Schneider, M.J.B. and Maestre, M.F. (1970) J. Mol. Biol. 52, 521.

van de Ven, F.J.M. and Hilbers, C.W. (1988) Eur. J. Biochem. 178, 1.

Wemmer, D.E. and Reid, B.R. (1985) Ann. Rev. Phys. Chem. 36, 105.

Wood, D.J., Hruska, F.E. and Ogilvie, K.K. (1974) Can. J. Chem. ??, 3353.

Yamagata, Y., Kohda, K. and Tomita, K. (1988) Nucl. Acids Res. 16, 9307.

Yokoyama, S., Inagaki, F. and Miyazawa, T. (1981) Biochemistry **20**, *2981.*

Young, M.A. and Krugh, T.R. (1975) Biochemistry **14**, *4841.*

Zhdanov, R.I. and Zhenodarova, S.M. (1975) Synthesis 222.